JET PROPULSION

Journal of the
AMERICAN ROCKET SOCIETY

Rocketry . . . . Jet Propulsion Sciences . . . . Astronautics

VOL. . . . OCTOBER 1956 (In Two Parts) NUMBER 10, PART 1

Japan's first post-war military missile . . . p. 893

ARS ESTABLISHES TECHNICAL COMMITTEES—SEE PAGE 908

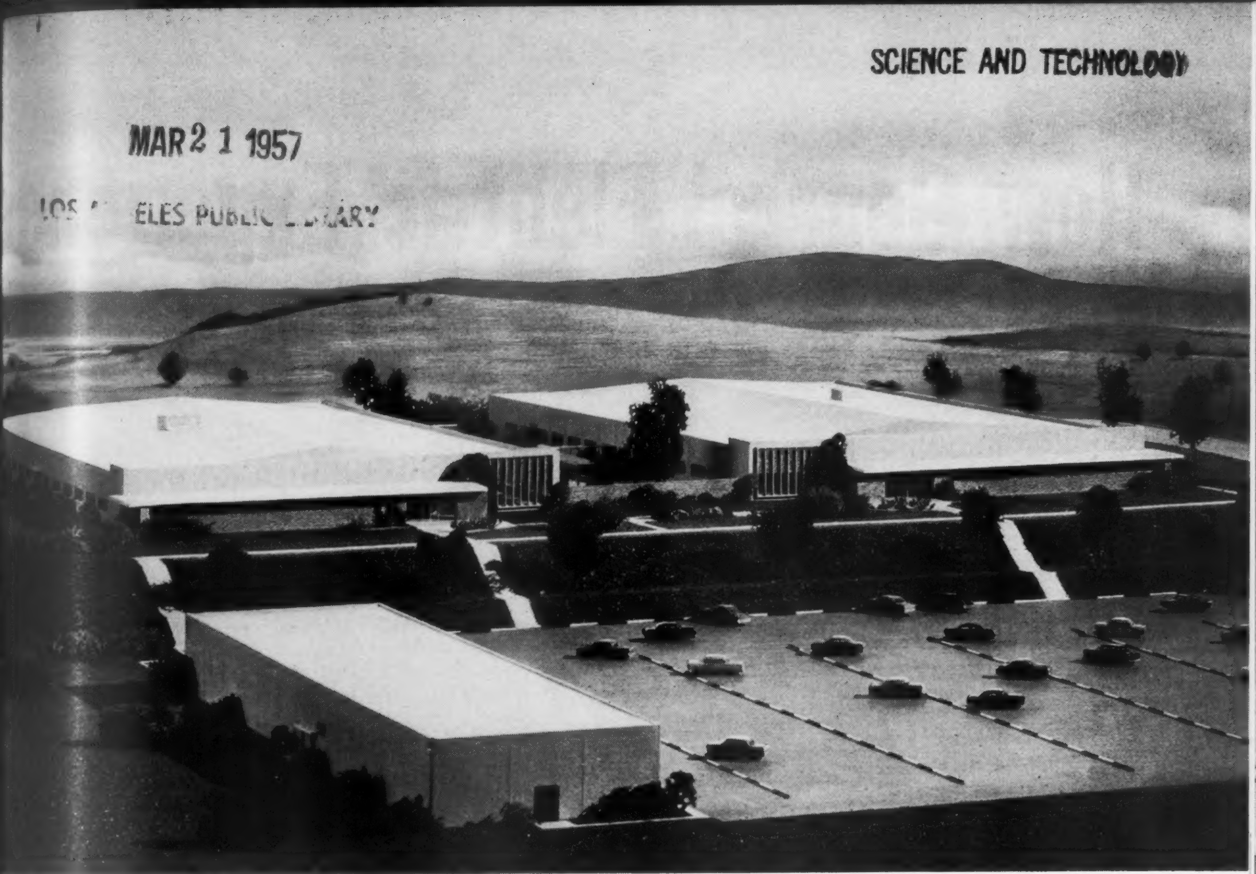

SCALE MODEL, NEW LOCKHEED RESEARCH CENTER AT PALO ALTO, CALIFORI
Here scientists and engineers are now working in modern laboratories on a number of highly significant projects.

LOCKHEED DEDICATES NEW RESEARCH CENTER

Scientists and engineers are now performing advanced research and development in their new Lockheed Research Center at Stanford University's Industrial Park, Palo Alto, California. In recent ceremonies marking its completion, the Research Center was dedicated to scientific progress.

First step in a $20,000,000 expansion program, it provides the most modern facilities for scientific work related to missiles and space flight. Significant activities are already being carried on in more than 40 areas, including upper-atmosphere problems, nuclear physics, hypersonic aerodynamics, use of new and rare materials, propulsion and advanced electronics.

Lockheed's expansion program has created positions on all levels for scientists and engineers in virtually every field of missile technology. Inquiries are invited from those possessing a high order of ability.

Lockheed

MISSILE SYSTEMS DIVISION

research and engineering staff

LOCKHEED AIRCRAFT CORPORATION

VAN NUYS • PALO ALTO • SUNNYVALE

CALIFORNIA

How General Electric Experienc

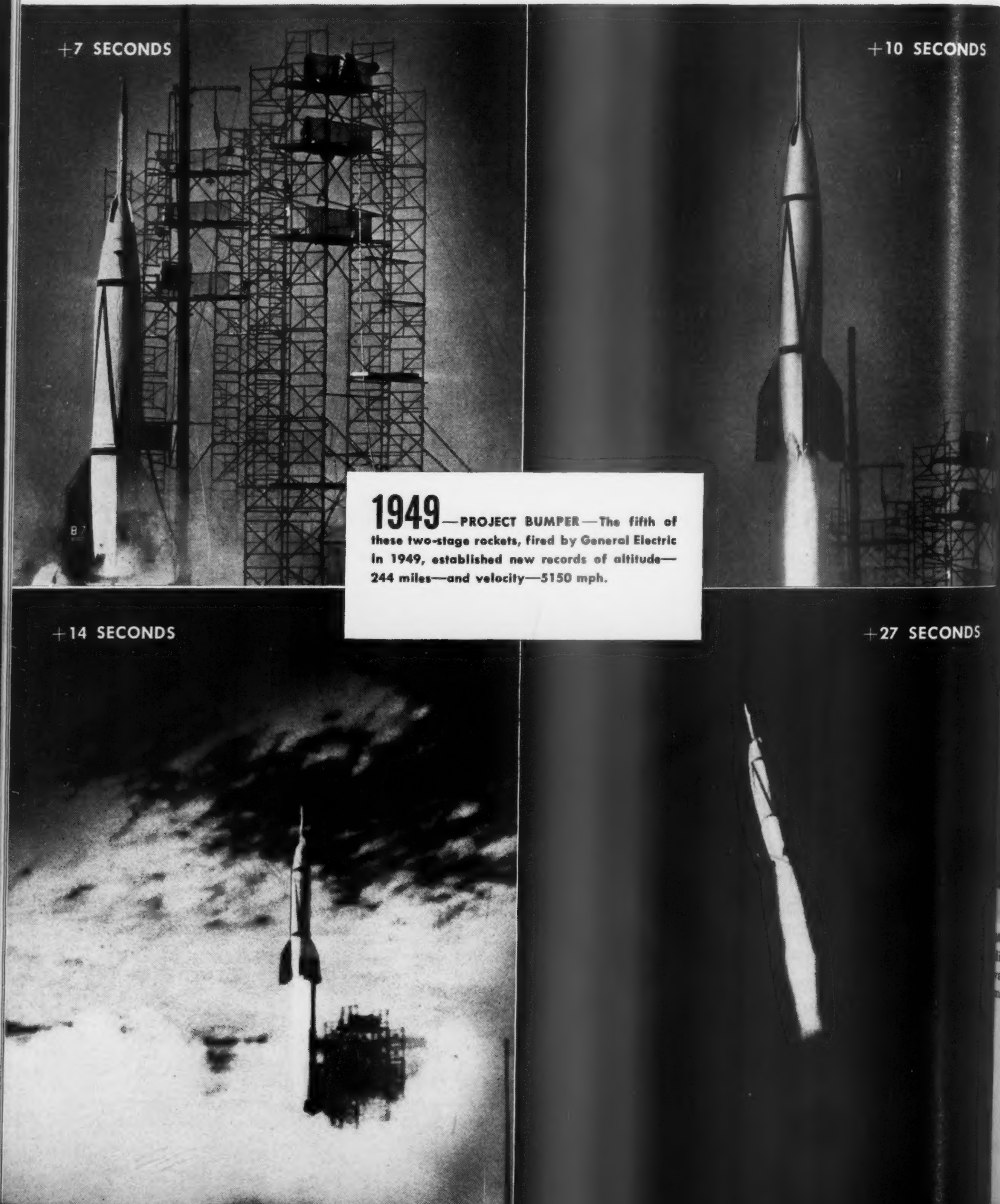

1949—PROJECT BUMPER—The fifth of these two-stage rockets, fired by General Electric in 1949, established new records of altitude—244 miles—and velocity—5150 mph.

P6M

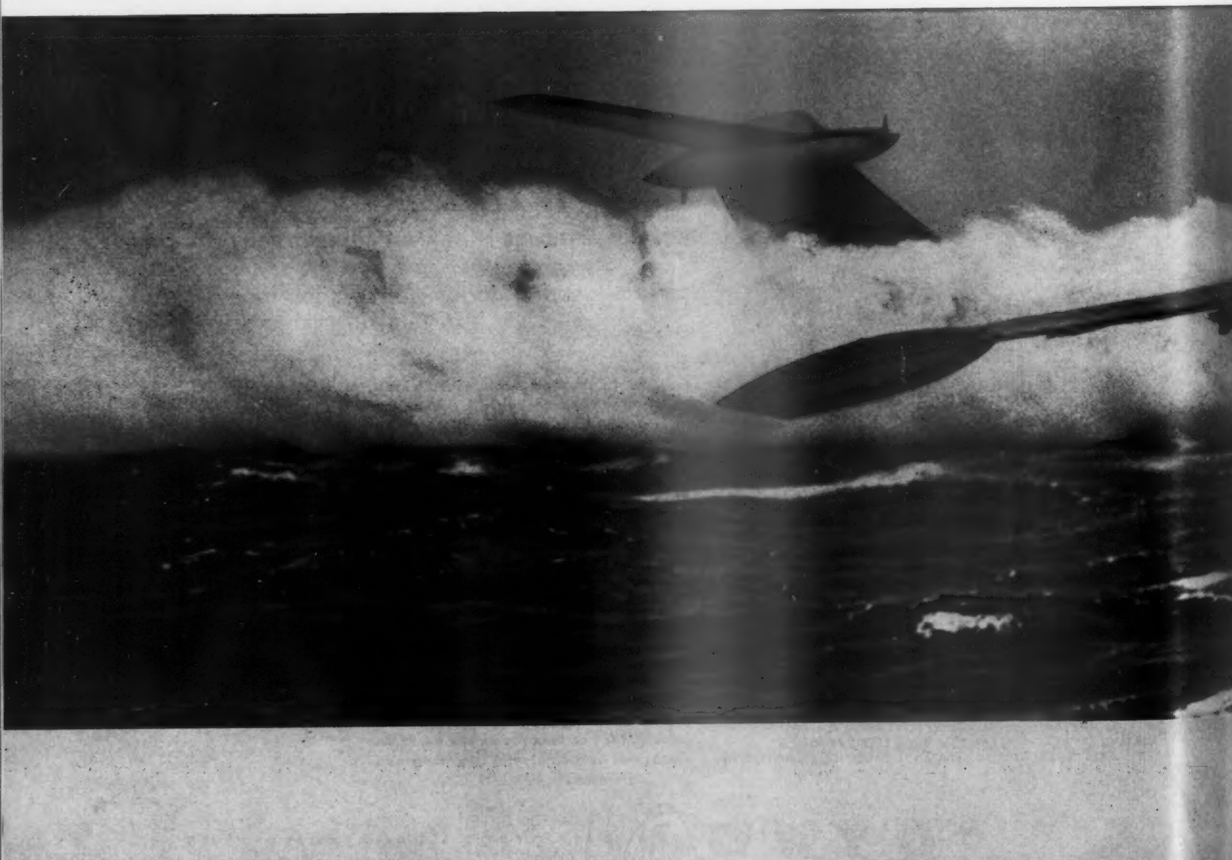

ROKIDE* spray coatings solve critical high temperature problems

Norton oxide coatings provide valuable protection against heat and abrasion

The three Norton Rokide spray coatings — Rokide "A" aluminum oxide, Rokide "ZS" zirconium silicate and Rokide "Z" stabilized zirconia—are proving themselves in such critical applications as reaction motors and in AEC projects. These hard, crystalline refractory oxides offer the following important advantages:

They are both thermally and electrically insulating. Their hardness, chemical inertness and stability in combustion temperatures provide high resistance to excessive heat, abrasion, erosion and corrosion. Their high melting points and low thermal conductivities reduce the temperatures of the underlying materials and permit higher operating temperatures.

Rokide Coatings vs. Stainless Steel

	ROKIDE "A"	ROKIDE "ZS"	ROKIDE "Z"	STAINLESS STEEL
Thermal Expansion (X107/°F. from 70° to 2550°F.)	43.	23.	64.	122.
Thermal Conductivity (BTU/hr./sq. ft.; in./°F. mean temp. of 1500°F.)	19.	15.	8.	185.
Density (grams per cc.)	3.2	3.8	5.	7.8
Melting Point (°F.)	3600	3000	4500	2600
Hardness (Knoop)**	2000	1000	750	400

**Determinations made on monolithic products of zero porosity (to give intrinsic crystal hardness) and not on coatings themselves.

Licensing Policy

Licenses for the use of the Rokide coating process can be obtained from Norton Company.

Let Norton Help

Norton high melting, fusion-stabilized materials are the basic ingredients of the famous Norton ℞'s — refractories *engineered and prescribed* for the widest range of uses. Take advantage of the broad experience of Norton Engineers in the use of these materials for jet propulsion and other modern high temperature applications. For further facts on Rokide coatings, write, mentioning your requirements, to Norton Company, New Products Division, 641 New Bond Street, Worcester 6, Massachusetts.

†Manufactured by Metallizing Company of America, Chicago 24, Illinois

*Trade-Mark Reg. U. S. Pat. Off. and Foreign Countries

NORTON
REFRACTORIES
Engineered ... ℞ ... Prescribed
Making better products ... to make your products better

A Rocket Chamber Nozzle coated with Norton Rokide "A" coating on entrance and exit components. Rokide coatings are applied in molten state with Rokide Spraying equipment†, in thicknesses generally ranging from .005″ to .05″.

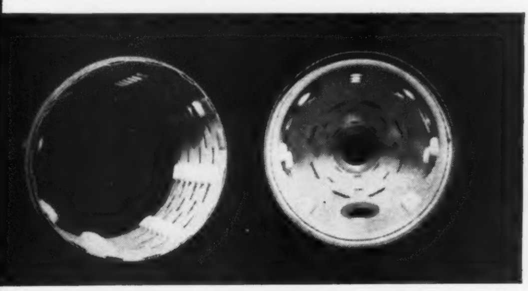

Jet Engine Combustion Chamber Parts coated with Norton Rokide "Z" coating. Rokide coatings may be applied to parts of a wide variety of sizes and shapes.

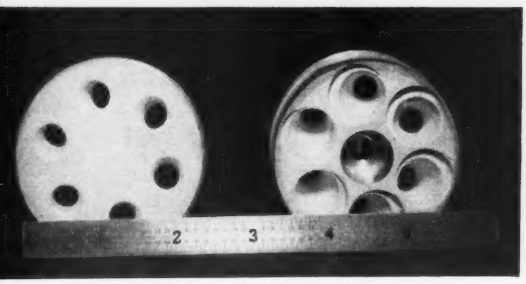

Rocket Nozzle Plates of aluminum, coated with Norton Rokide "A" coating. While Rokide coatings are commonly applied to metals, they are also effective on various other materials.

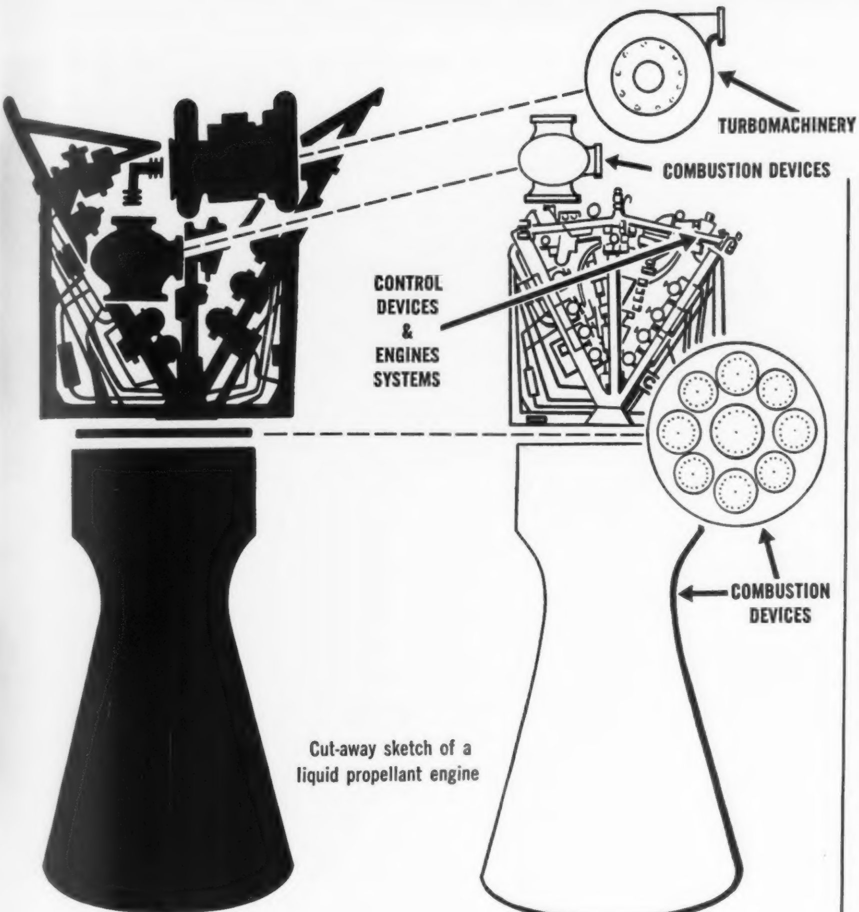

Cut-away sketch of a liquid propellant engine

Turbomachinery
Thermodynamics
Hydrodynamics
Aerodynamics
Stress Analysis
Pump Design
Turbine Design
Compressor Design
High speed gearing and bearing design

Control Devices
Servo Systems
Electrical Design
Pneumatic Design
Hydraulics Design
Electro Mechanical Design

Combustion Devices
Thermodynamics
Heat Transfer
Hydrodynamics
Aerodynamics
Aerothermodynamics
High Temperature Design
High Pressure Design
Ignition

Engine Systems
Engine Installation
Systems Design
Structural Design
Pneumatic Systems
Electrical Systems

Several select positions are also available for analytical and theoretical engineers in the following activities (which are concerned with the complete rocket engine):

APPLIED MECHANICS – Senior dynamicists and stress analysts with advanced abilities.

SYSTEMS ANALYSIS – for performance and numerical analysis, and reliability. Also design analysis involving complex systems engineering concepts combining gas dynamics, heat transfer, thermodynamics and fluid flow.

R & D Engineers: can you fit into this picture?

Chances are that one of the areas of engineering listed at the right will fit you like a glove! All you need be is a research, development or design engineer with a desire for challenging work and pertinent background experience.

ROCKETDYNE needs men with special talents to help design and develop rocket engines for long-range and intercontinental missiles. Its Propulsion Field Laboratory – located on a 1700-acre site in the Santa Susana Mountains a few miles west of Los Angeles, California – is the largest rocket engine testing facility in the Free World. Here, and also at our new design, development and engineering facility in Canoga Park, you will find the rewards of leadership – good salary, personal and professional recognition, exciting work and secure future. ROCKETDYNE offers many different areas of opportunity. For example: as an Engines System engineer at ROCKETDYNE, you may direct construction on full-scale mock-ups of engine assemblies. You may design laboratory testing machinery to evaluate engine components or Ground Handling Systems and packaging for complete engines. You may be responsible for the programming of engine testing schedules and the preparation of specifications for instrument procedures. Or, you may be responsible for evaluating engine test data in terms of overall engine development. At ROCKETDYNE you can go as far as your abilities can carry you. Check these ROCKETDYNE opportunities today!

Write to A. W. Jamieson,
Rocketdyne Engineering
Personnel Dept. 10-JP
6633 Canoga Avenue,
Canoga Park, California

Please send me a copy of "The Big Challenge" – fact-filled booklet explaining rocket engines and engineering.

Name ______________

Home Address ______________

Degree ______________ Year ______________

School ______________

ROCKETDYNE
A Division of North American Aviation, Inc.

BUILDERS OF POWER FOR OUTER SPACE

A section of the Nike guided missile system. Western Electric Co., Prime Contractor.

CRUSADER 1096
Crusader.....1956 A.D.
His weapon—Chance Vought's supersonic interceptor—while infinitely more complex, it must be just as reliable as his forebearer's sword.
Sub-systems such as this Servomechanisms, Inc., Angle of Attack and Mach computer do their part in assuring that American Military Aircraft maintain their leadership in performance and reliability.
SERVOMECHANISMS INC.
WESTERN DIVISION Hawthorne, California
EASTERN DIVISION Westbury, L.I., New York
MECHATROL DIVISION Westbury, L.I., New York
MECHAPONENTS DIVISION El Segundo, California

OCTOBER 1956

VOLUME 26 NUMBER 10

JET PROPULSION

Journal of the AMERICAN ROCKET SOCIETY

Editor-in-Chief

MARTIN SUMMERFIELD

Reliability of Combustion Efficiency Evaluation for Jet Propulsion Based Upon Aerodynamic Measurement of Combustion Temperature

GILBERT S. BAHN[1]

Marquardt Aircraft Co., Van Nuys, Calif.

Aerodynamic measurement of combustion temperature relies upon measurement of the total-to-static pressure ratio across the combustor exhaust nozzle, and simultaneous measurement of the weight flow. Combustion efficiency computed from this temperature expresses jet propulsion performance characteristics of the combustor, subject to both systematic and random errors. The sources and magnitudes of these errors are examined, as a key to estimation of reliability of combustion efficiency values. Care must be taken to avoid certain potential systematic errors, but in most instances corrections can be made which themselves do not introduce appreciable random errors. With such care and with reasonably refined instrumentation, the major source of random error is the evaluation of nozzle exit Mach number. The resulting probable error in combustion efficiency, expressed as either a temperature rise ratio or a ratio of fuel/air ratios to compare theoretical and actual performance, is in the neighborhood of ±5 per cent. When development of thrust for jet propulsion is the point of interest, this is reasonable reliability, considerably less doubtful than offhand estimates which are often made to provide conservative views.

Nomenclature

A = flow cross-sectional area (effective)
C_A = area coefficient
C_M = Mach number coefficient
C_v = velocity coefficient
c_p = heat capacity at constant pressure
F/A = fuel/air ratio
g = acceleration of gravity
M = Mach number
P = static pressure
P_t = total pressure
R = gas constant
T = static temperature
T_t = total temperature
T_v = velocity temperature, total temperature minus static temperature
v = velocity
v_c = critical (sonic) velocity
W = weight flow
γ = heat capacity ratio
γ_{avg} = heat capacity ratio at average temperature
γ_s = heat capacity ratio at static temperature
η_c = combustion efficiency
ρ = density

Presented at the ARS 25th Anniversary Annual Meeting, Chicago, Ill., Nov. 14–18, 1955.

[1] Senior Thermodynamics Engineer. Mem. ARS.

Introduction

CONSIDERABLE data scatter is normally encountered in combustion efficiency values derived from aerodynamic measurements of combustion temperature. Consequently, there is generally a tendency to allow a fairly large margin of error in interpreting the efficiency data. The purpose of this paper is to examine the factors which tend to limit reliability of the combustion efficiency values, so as to enable the test engineer to minimize his errors and so as to define for the reviewer of test data the degree of reliability prevailing. In so far as possible, requisite corrections are indicated and probable errors are assigned, to serve at least as tentative standards. While attention is directed to combustion of normal hydrocarbons in air, the general considerations apply to combustion of other fuels with other oxidants.

Two basic ratios are considered, that of temperature rise and that of fuel/air ratio. Either of these might be used as a measure of combustion efficiency from a general power plant standpoint; both may logically be related to the aerodynamic combustion temperature. If the purpose of combustion is solely to increase the temperature of the air, then the ratio of actual temperature rise to ideal temperature rise for the same fuel/air ratio is a correct measure of combustion efficiency. If the fuel requirements of the combustor are of primary interest, the theoretical fuel/air ratio to obtain the actual temperature rise may be divided by the actual fuel/air ratio employed for this purpose. Because they are so intimately related by definition, selection between these two efficiency bases is mainly a matter of expositional convenience.

In considering the reliability of combustion efficiency values, one must account for both random and systematic errors. When an approximation, however gross, is made to correct for and eliminate a systematic error, it is claimed hereby that such approximation carries with it a random error. The need for correction arises in regard to both measured test data and theoretical properties. Some corrections are major and some are practically insignificant. It is the intention here to consider all which come to mind, because a correct assessment of degree of significance may depend upon the particular combustion process being evaluated.

First attention below is devoted to the implications of measuring a single integrated combustion temperature by aerodynamic means, when in reality there likely is nonuniformity of temperature over the flow cross section. Next, consideration is given to the effects of a number of variables upon the theoretical properties (e.g., temperature rise) involved in combustion efficiency calculation. Attention is then directed to the several bases of calculation which might be

used in conjunction with the aerodynamic combustion temperature. and the ones of significance to jet propulsion are indicated. Finally, probable errors of the aerodynamic temperature and of the corresponding combustion efficiency are estimated.

As the presentation develops, only one source of error appears to be appreciable, and the magnitude of the error is approximated by reference to the literature. The other errors presented come from the author's general experience. They are, of course, each subject to argument as either too liberal or too conservative. This depends upon what one may consider to be reasonable refinement of instrumentation. The treatment is such that one might substitute as desired at any points of serious disagreement, and then re-evaluate the probable error in combustion efficiency.

Aerodynamic Measurement of Combustion Temperature

The crux of the approach considered here is the measurement of combustion temperature by the aerodynamic method, several original expositions of which were made about the same time ((1, 2, and 3)[2] are examples). In this method there is simultaneous measurement of gas weight flow before combustion, by means of an air metering nozzle and fuel flow meters, and of sufficient parameters other than combustion gas temperature for definition of the gas weight flow after combustion. Obviously, then, the continuity equation can be solved for temperature. The method has the advantages that it is automatically integrating for temperature, provides a value of temperature at a specific position (namely, the throat of the combustor exhaust nozzle) which has special significance in jet propulsion, and depends upon durable hardware. It still does not provide a perfect gas temperature for combustion efficiency evaluation, but, as is shown below, there is no *one* such temperature.

An alternative technique in applying the aerodynamic method of temperature measurement is to measure thrust developed by the gas as it emerges from the combustor exhaust nozzle. This scheme has not been as thoroughly developed as use of the continuity equation. It can be shown that, barring instrumentation errors, it provides the same combustion temperature and same combustion efficiency as the continuity equation.

Jet propulsion combustors very rarely, if ever, experience complete uniformity of flow parameters over the flow cross section. Instead, some stratification of total pressure and pronounced stratification of total temperature is usually the rule. The result of stratification (4, 5, 6) is to produce less thrust than if profiles of all flow parameters were uniform and one-dimensional flow prevailed. When the combustion efficiency measurement reflects the loss in potential thrust attributable to stratification, it is a useful measure of over-all combustor performance, allowing for the consequence of inferior fuel distribution as well as deficient combustion.

By far the more significant instance of stratification is that of temperature and on this basis it is possible to approximate combustor analysis with one-dimensional flow treatment. A reasonable number of point values of total pressure measured at the exhaust nozzle entrance is used to provide an average value, and it is assumed that this value is constant over the flow cross section. Analysis of the effects of temperature stratification is then possible.

When the continuity equation is employed, the measured gas flow may be thought of as the summation of flow through a number of stream tubes

$$W = \Sigma\Delta W = \Sigma\Delta(\rho A v) = \Sigma\Delta\left(\frac{PAM\sqrt{\gamma}}{\sqrt{RT}}\right) \quad \text{[1a]}$$

[2] Numbers in parentheses indicate References at end of paper.

Assume for the present that not only P and M but also γ and R are constant for all stream tubes

$$W = \frac{PM\sqrt{\gamma g}}{\sqrt{R}}\Sigma\Delta\left(\frac{A}{\sqrt{T}}\right) = \frac{PM\sqrt{\gamma g}}{\sqrt{R}}\frac{A}{\sqrt{T_{comb}}} \quad \text{[1b]}$$

Therefore, when T_{comb} is evaluated by solution of the continuity equation, it is a representation of the equation

$$\sqrt{T_{comb}} = \frac{1}{\Sigma\left(\frac{\Delta A/A}{\sqrt{T}}\right)} \quad \text{[2]}$$

The performance parameters required for combustion efficiency calculation are fuel flow, air flow, inlet fuel and air temperatures, and combustion gas temperature. When Equation [1] is solved for T_{comb}, values of γ and R must be substituted. These are both functions of temperature and composition. Actually

$$W = PM\sqrt{g}\,\Sigma\Delta\left(\frac{\sqrt{\gamma}A}{\sqrt{RT}}\right) = PM\sqrt{g}\,A\left(\sqrt{\frac{\gamma}{RT}}\right)_{comb} \quad \text{[1c]}$$

In order to resolve $(\sqrt{\gamma/RT})_{comb}$ for the value of T_{comb}, some assumption is required. Both γ_{comb} and R_{comb} might be desired on the basis of complete destratification to correspond to the destratified gas temperature. It is customary, however, for this purpose to assume that T_{comb} is itself the gas temperature resulting from complete destratification, and so to assign γ_{comb} and R_{comb} as the theoretical values obtaining at T_{comb}. Now with γ and R expressed as graphical functions of T, $(\sqrt{\gamma/RT})_{comb}$ can be resolved for T_{comb} by iteration.

Theoretical Properties Required

These parameters affect the theoretical (or ideal) properties needed in combustion efficiency evaluation: (a) fuel/air ratio, (b) fuel composition, (c) fuel heating value, (d) inlet fuel temperature, (e) inlet air temperature, (f) air composition (including humidity, prior combustion products, etc.), (g) fundamental thermodynamic properties of combustion gas constituents, (h) system static pressure, and (i) system static temperature. The inlet fuel temperature may be removed from consideration by adjusting the fuel heating value to correspond to the inlet air temperature.

Given a presumably reliable set of fundamental thermodynamic properties of the combustion gas constituents, equilibrium equations are ordained as functions of pressure and temperature. Thus when a given gross composition is defined by the fuel composition, the air composition, and the fuel/air ratio, the exact theoretical composition according to equilibrium requirements can be established as a function of pressure and temperature. Furthermore, the theoretical enthalpy and the theoretical gas constant can also be established as a function of (gross) composition, pressure, and temperature. The theoretical heat capacity ratio can be derived from the theoretical enthalpy and gas constant. If equilibrium is to be assumed at all times when theoretical properties are concerned, the enthalpy must include the heat of dissociation, and values of γ will reflect the heat of dissociation (7). Finally, from the appropriate enthalpy-temperature relationship and the appropriate heating value, theoretical combustion temperature can be established as a function of fuel/air ratio.

Theoretical combustion gas properties are available in a number of references, including (7–24). Theoretical combustion temperature or temperature rise data are most widely employed. Those which ignore dissociation where it is significant will be excluded from consideration. Allowance for variation in inlet air temperature is a prime requirement. Usually allowance is made for variation in system static pressure. Frequently there is no allowance made for variation in

the following: fuel composition, fuel heating value, inlet fuel temperature, and air composition. Fuel properties may be estimated by means of (25–30). Estimated reliabilities for the preceding parameters appear in the Appendix.

Whether the discrepancies are important between actual values and the bases employed in construction of theoretical data will depend upon too many particulars for exposition here. The person wishing to evaluate the precise reliability of his combustion efficiency calculations should perform at least sample calculations with theoretical data which account for all variables. For example, (8) does this on a correction factor basis, and (7) presents families of graphs for the same purpose. After a number of sample calculations are performed precisely, they may be repeated with theoretical data less precisely defined as to the minor variables, such as fuel composition. The individual systematic errors thus revealed may be generalized into a random error of application of the less precise approach, or perhaps to a systematic as well as a random error.

Bases of Calculation

Calculation of combustion efficiency on either a temperature rise basis or a fuel/air ratio basis is now straightforward. The fault in the temperature rise basis is that it hides the variation of heat capacity with temperature and neglects the endothermic nature of dissociation. On the other hand, it is a measure of how efficiently the combustor managed simply to create temperature rise with the fuel actually supplied for that purpose

$$\eta_c = \frac{\Delta T_{\text{actual}}}{\Delta T_{\text{ideal}}} = \frac{T_{\text{comb}} - T_{\text{inlet}}}{f(F/A)_{\text{actual}}} \qquad [3]$$

where ΔT_{ideal} corresponds to the actual fuel/air ratio.

One may either account for or ignore any heat losses from the walls of the combustor which may occur. In evaluating a combustor where these losses are likely to be fixed, it is best to forget them; they do not contribute to performance. In evaluating a combustor from which the losses may later be eliminated, it is best to correct for them, still keeping in mind that the resultant combustion efficiency arose under operating conditions, such as wall temperature, corresponding to the losses. Where correction is desired, presumably the loss is itself so small (say, 1 per cent) as to make error in the correction be of negligible magnitude.

The fuel/air ratio basis of efficiency is very similar to the temperature rise basis

$$\eta_c = \frac{(F/A)_{\text{ideal}}}{(F/A)_{\text{actual}}} = \frac{f(\Delta T_{\text{actual}})}{(F/A)_{\text{actual}}} \qquad [4]$$

where $(F/A)_{\text{ideal}}$ corresponds to the actual temperature rise. Near stoichiometric conditions this efficiency tends to emphasize the large waste of fuel accompanying a relatively small loss in potential temperature rise, and thus is somewhat more appropriate for performance evaluation.

When the inlet fuel/air ratio is greater than stoichiometric, the proper approach in computing combustion efficiency depends upon the particular situation. Actually our concern now is for the region richer than that corresponding to the maximum theoretical temperature rise; mixtures just slightly richer than stoichiometric continue to show increase of theoretical combustion temperature with increase of fuel flow since the added fuel can burn with the oxygen liberated by dissociation. Thus the peak of the theoretical temperature rise graph occurs with a slightly over-rich mixture.

As soon as the theoretical temperature rise diminishes, it is apparent that less heat per pound of products is being effectively liberated than at the peak point. Since the object of the combustion process is to elevate the gas temperature, under certain circumstances some inefficiency of reaction might be advantageous, meaning a higher combustion temperature than a completely reacted mixture at equilibrium would attain. For example (9), a fuel/air ratio of 0.0667 results in an ideal combustion temperature of 4045 R (with inlet temperature of 600 R) and a fuel/air ratio of 0.1000 results in an ideal value of 3625 R, a drop of 420 R. On the other hand, if somehow 0.0333 lb of unreacted fuel were brought to temperature equilibrium with the equilibrium combustion products of 1 lb of air and 0.0667 lb of fuel, the ideal temperature would be about 3900 R, a drop of only about 145 R from the peak. (This figure is based, even so, upon a rather liberal allowance for heat of decomposition of the uncombusted 0.0333 lb of fuel.) The explanation for the improvement is that the reaction of carbon with carbon dioxide to form carbon monoxide is endothermic. Thus, actually less heat is liberated when rich mixtures are allowed to reach chemical equilibrium than if the excess fuel is merely present as a sensible heat absorber.

If the efficiency is poor enough throughout the rich region so that the actual temperature rise graph always lies underneath the ideal temperature rise graph all the way out to rich blowout, the ratio of actual to ideal temperature rise can serve as a convenient measure of combustion efficiency in the rich as well as in the lean region of operation.

A ratio of fuel/air ratios might be used to measure combustion efficiency of rich mixtures. Here there would seem to be no need for anomaly. The minimum theoretical fuel/air ratio to attain the actual combustion temperature would be divided by the actual fuel/air ratio. The minimum theoretical value would, of course, be leaner than stoichiometric, so the efficiency would always be less than unity.

Evaluation of Combustion Temperature and Combustion Efficiency

Equation [1] must now be evaluated from an error standpoint

$$T_{\text{comb}} = \frac{P^2A^2M^2\gamma g}{W^2R} \qquad [1d]$$

It should be noted that g is the local value; it can be known precisely. For assessment of γ and R, which have been discussed previously, and for later use as well, the actual fuel/air ratio is needed. Reasonable errors from the author's experience, with the latter value verified by (31), are ± 1 per cent in fuel flow and ± 1 per cent cent in air flow, leading to ± 1.4 per cent in fuel/air ratio. Obviously, greater or lesser precision is possible, depending upon the installation. An error analysis is easily performed; in particular this is advisable for free jet or wind tunnel testing, where the error in air flow may range from ± 2 to ± 3 per cent. Parenthetically, it should be noted that this error may be minimized by measuring at a choked-flow station.

With an error in fuel/air ratio of ± 1.4 per cent, and with the other appropriate errors (in inlet air temperature, fuel composition, etc.) allowed for, the probable error in the theoretical ratio γ/R can be established by examination of the effect of the individual errors at the calculated temperature T_{comb}. As suggested earlier, corrections for minor variables might be eliminated by effectively randomizing the systematic errors about mean graphs, but this would somewhat decrease the over-all reliability. In most cases γ and R are chiefly sensitive to temperature and pressure. Thus it should be possible to assign the theoretical value of γ/R with insignificant error if the minor variables are allowed for, provided the requisite theoretical relationships are at hand and are employed. If the potential systematic errors are randomized, the theoretical ratio γ/R still should be correct within no more than $\pm {}^1/_2$ per cent. Of course, a definitely fixed systematic error might derive from use of a falacious theoretical graph, and this should be avoided.

Based upon the values of ± 1 per cent for air flow and ± 1

per cent for fuel flow, the probable error in W^2 is roughly ± 2 per cent, the fuel flow being practically negligible.

The symbols P, A, and M apply to the vena contracta of the exhaust nozzle; P should be measurable to $\pm ^1/_2$ per cent, and P^2 to ± 1 per cent. Based upon physical measurement of the nozzle exit area, cold flow evaluation of the area coefficient (32), and correction where necessary for thermal expansion of the nozzle. A should be reliable to $\pm ^1/_2$ per cent and A^2 to ± 1 per cent.

The only remaining term to be accounted for is M^2, pertaining to the vena contracta of the exhaust nozzle. M is calculated according to isentropic flow theory (one-dimensional flow) from the nozzle pressure ratio by applying an experimentally determined correction factor, the Mach number coefficient, which is analogous to a nozzle velocity coefficient, although not quite identical. (The distinction is indicated subsequently.)

M will be in error by the following: errors in physical measurement of pressures contributing to the nozzle pressure ratio; error in representation of the appropriate average pressure ratio for one-dimensional flow calculation according to the average values of a limited number of physical measurements of pressures; error in determination of the Mach number coefficient by calibration runs; and such other errors as are discussed below. With a sufficient number of data taken during calibration, the Mach number coefficient should be procurable without significant error. On this basis, the principal source of error lies in the reliability of the measured nozzle pressure ratio which is to be used to compute M. To evaluate this reliability, recourse is made to (32).

In the subject reference, it was assumed that all other parameters were known except the effective nozzle velocity coefficient, and the continuity equation was then solved for the latter. Based on the presumption that this coefficient in truth *had* a real value, data scatter in the resultant calculated values actually represents data scatter in the computed isentropic Mach numbers. This in turn is attributable to inadequacy of the measured nozzle pressure ratio to comply reliably with one-dimensional flow theory. In the subject reference only two total pressure tubes and two static pressure tubes were employed to evaluate the nozzle pressure ratio. For pressure ratios between 1.2 and 2.8, 96 values of effective nozzle velocity coefficient are reported, deriving from among 15 different nozzles.

Although engineering-wise there appears to have been a slight falling off of the coefficient at pressure ratios above 2.0, it does not appear that this could be effectively proved statistically. Thus it is quite fair to treat the 96 data points as scattered about a mean effective nozzle velocity coefficient and to call this mean the real value of the coefficient, according to the earlier presumption. The calculated standard deviation of the 96 points about the mean value (which was 0.944) is ± 1.55 per cent, and the corresponding probable error is ± 1.05 per cent. This then appears to be the probable error of a calculated value of v, attributable to imprecision of the nozzle pressure ratio.

It remains to be shown that C_M is closely equivalent to C_v, so that the error of presentation of C_v can be taken as the error in C_M when calculations are to be made with the perspective that the nozzle pressure ratio is exact and the error lies in the coefficient. In the equations which follow, primes indicate actual values and asterisks indicate the theoretical results of isentropic expansion; γ and R are assumed constant between T' and T^*, and the same total temperature applies in both cases

$$C_v = \frac{v'}{v^*} = \frac{M'v_c'}{M^*v_c^*} = C_M \frac{v_c'}{v_c^*} = C_M \sqrt{\frac{T'}{T^*}} = \frac{M'}{M^*} \sqrt{\frac{T'}{T^*}} \quad \text{[5a]}$$

Also

$$c_p(T' - T^*) = \frac{\gamma}{\gamma - 1} R(T' - T^*) = \frac{v^{*2} - v'^2}{2g}$$

which by substitution and rearrangement leads to

$$\frac{T'}{T^*} = 1 + \frac{\gamma - 1}{2}(1 - C_v^2)M^{*2}$$

Therefore

$$C_M = \frac{C_v}{\sqrt{1 + \frac{\gamma - 1}{2}(1 - C_v^2)M^{*2}}} \quad \text{[5b]}$$

It is now readily apparent that, even when $M^* = 1$, values of C_v and C_M are very nearly the same, so that ± 1.05 per cent probable error in C_v serves as a good estimate of the probable error in C_M.

In proceeding from the cold flow case of (32) to a hot flow case of interest, somewhat greater nonuniformity of pressure profiles may be expected, and need for several pressure measurements to yield a satisfactory average may be anticipated. Allowance may be made for somewhat insufficient provision, therefore, and the probable error assigned to C_M (but referable back to the nozzle pressure ratio) may thus be increased to ± 1.5 per cent.

During hot gas flow from the nozzle, change in physical properties of the gas (neglecting thermodynamic properties) may influence the values of C_M slightly. Although the effect would be systematic, the proper correction would carry a random error. Without knowing the magnitude or sign of the correction, its random error may be assumed to have been accounted for by the increase just previously made in the probable error of C_M.

If total pressure measurements are made ahead of the nozzle vena contracta, another correction to account for is total pressure loss because of continuing combustion as the gas passes through the exhaust nozzle. This loss, which is entirely distinct from random error in total pressure, is due to the requirements of conservation of momentum. Actually, it applies from the point where total pressure was measured ahead of the nozzle entrance. Once some combustion efficiency data are at hand, one should be able to estimate, reasonably well, first the degree of combustion of interest and then the corresponding total pressure loss. If carefully estimated, the resulting correction (in C_M or in nozzle pressure ratio, as desired) need not amplify the probable error otherwise established.

Cold-flow nozzle calibrations are based upon precisely defined gas properties (usually of air). If the probable error so far assigned to C_M is to stand during hot flow conditions, hot gas properties involved in isentropic flow equations must also be precisely defined. Specifically, this means that a precise and appropriate value of γ is required to give M for isentropic expansion down to the nozzle throat.

First of all, what is meant by isentropic expansion must be defined. Strictly speaking, the total entropy of a gas mixture includes a term to account for the increased disorder of the system attributable to its being a mixture rather than a pure gas (7). If there were no dissociation, the entropy of mixing would be constant and could be neglected. Likewise this term could be ignored if dissociated mixtures at high static temperature did not reassociate upon expanding and cooling to lower static temperature. When the composition changes upon expansion, the entropy of mixing changes too. Therefore an isentropic expansion with reassociation is different from an isentropic expansion without it, and the final Mach numbers and static temperatures for a given pressure ratio are different. Clearly the isentropic reference case employed should represent the actual situation regarding recombination.

Penner has estimated (33) that in relatively long nozzles equilibrium will prevail through to the exhaust, while in relatively short nozzles the original dissociation will be frozen. It is assumed here that relatively large combustors with relatively long nozzles are under consideration. Thus one desires isentropic expansion with reassociation according to equi-

librium demands (although Daniels has reported (34), in so far as nitric oxide is concerned, that cooling at the rate of 20,000 C per sec will forestall reconversion, and this corresponds to a fairly long nozzle residence time). The exact way to compute the pertinent expansion graphically is presented in (7). An approximate approach is to employ a value of γ derived from heat capacity which in turn is derived from enthalpy which contains the enthalpy of dissociation. Where dissociation is pronounced, such values are considerably less than corresponding values which ignore dissociation. Values of γ for dissociated air at high temperatures appear in (35).

Let us assume that the appropriate expansion process is employed, as closely as it can be approximated based on assumption as to degrees of reassociation or frozen dissociation in the nozzle. Isentropic expansion is then calculated according to the equation

$$\left(\frac{P_t}{P}\right)^{(\gamma-1)/\gamma} = \frac{T_t}{T} = 1 + \frac{\gamma - 1}{2} M^2 \qquad [6]$$

One must account for variation of γ with temperature during the course of the expansion process. The total temperature is the sum of static and velocity temperatures

$$T_t = T + T_v = T + \frac{v^2}{2gc_p} = T + \frac{M^2\gamma g R T}{2g\dfrac{\gamma}{\gamma - 1}R}$$
$$= T\left(1 + \frac{\gamma}{\gamma}\frac{\gamma - 1}{2} M^2\right) \simeq T\left(1 + \frac{\gamma - 1}{2} M^2\right) \qquad [7]$$

In the numerator of the next to the last expression, γ is the value applying to T, the static temperature; γ in the denominator and $\gamma - 1$ in the numerator derive from c_p, which is the mean value between T and T_t. (It must always be remembered that T_t is merely the stagnation value of static temperature, and in all of the Mach number functions one theoretically is dealing with change between $M = 0$, $T = T_t$ and $M = M$, $T = T_t - T_v$.)

The only pertinent instance where γ appears as the point value is where it is used to compute sonic velocity. All other appearances are somehow related to a mean heat capacity, and γ representative of the effective heat capacity should be used. For this the arithmetic mean of the two end values of γ is usually approximated, and γ_s/γ_{avg} is taken equal to unity.

When one is solving Equation [6] for Mach number by graphs or tables, or algebraically, starting with the nozzle pressure ratio and T_t, it is necessary to iterate for T in order to establish a suitable mean value between T_t and T, and thus to solve correctly for M. Given γ as a function of T, however, such solution can be made without significant error. References [36] and [37] allow tabular and graphical solutions, respectively, allowing for variation in γ.

It is seen that in so far as the chosen isentropic expansion providing the theoretical value of M is concerned, there is no need for significant random error. Let us lump together (a) uncertainty as to the exact nozzle process and (b) the fact that Equation [6] is less precise when reassociation prevails than is graphical allowance for entropy of mixing. Then somewhat under ± 1 per cent appears to be a reasonable probable error in γ, and the corresponding probable error in M falls appreciably below $\pm ^1/_2$ per cent and can be neglected. It should be noted, however, that the systematic error in M can be really appreciable (up to 4 per cent, conceivably) if reassociation occurs but is ignored for convenience so as to employ thermodynamic functions which exclude the enthalpy of dissociation.

Now we can sum up to indicate the probable error in T_{comb}, according to Equation [1d]. Any compensating effects will be ignored as too deeply hidden for apparency or significance. Summarizing, we have $\pm ^1/_2$ per cent in γ/R, ± 2 per cent in W^2, ± 1 per cent in P^2, and ± 1 per cent in A^2. In addition, we have negligible error in the theoretical (isentropic) value of M, but ± 1.5 per cent in C_M, and thus ± 3 per cent in the effective value of M^2, representing error in the pressure ratio determining M as well as actual random error of calibration. The other errors are nearly inconsequential with respect to that introduced by C_M, the combined probable error amounting to to ± 4 per cent when rounded off. (Rounding off adequately accounts for the small additional error contributed by the term $(1 + ((\gamma - 1)/2)M^2)$ when T_{comb} is converted from the static value given by [1d] to the total value desired for computation of η_c.)

Thus it is seen that the critical factor is the probable error of computing Mach number on the basis of the measured nozzle pressure ratio. Although in the preceding discussion the flow coefficient has been broken down into C_A and C_M, with the former incorporated into A by definition and with the substantial (and rather liberal) error attributed to the latter, in application a single coefficient will probably be determined. If this can be established with less than the data scatter indicated in (32), then a more reliable effective value of nozzle pressure ratio will be indicated, and there will result a two-for-one reduction in the contribution to the probable error of T_{comb}.

T_{inlet} may be taken correct to $\pm ^1/_2$ per cent. If [3] is used, the error in T_{inlet} is negligible compared to the error in T_{comb}, so ΔT_{act} is correct to slightly more than ± 4 per cent, the exact difference depending upon the ratio of ΔT_{act} to T_{act}. Previously, fuel/air ratio has been assigned ± 1.4 per cent probable error. At a fuel/air ratio of 0.05, as an example, this corresponds to a negligible ± 1 per cent in ΔT_{ideal}. Thus η_c itself bears essentially the ± 4 per cent error of T_{comb} when based upon temperature rise. When based upon fuel/air ratio, the error in η_c at 0.05 fuel/air ratio is ± 6 per cent, attributable to the ± 4 per cent error in T_{comb}.

Conclusions

Consideration has been given to sources of systematic error, in calculation of combustion efficiency by the aerodynamic method, that are attributable to the method as distinct from obvious gage corrections to basic instrumentation readings. References have been cited which permit these systematic errors to be dealt with. Where the effort is justified, corrections can be made with apparently insignificant contribution thereby to the over-all random error of representation. Where a relatively constant systematic error is anticipated in a test program, this error may be shown to be insignificant, if it is, or else a common approximate correction may be evaluated and applied thenceforth.

The sources of random error deriving from the instrumentation have also been considered, and probable values have been assigned as tentative standards. A probable error in the neighborhood of ± 5 per cent results for combustion temperature and for combustion efficiency, and this is assigned as a tentative standard for η_c based upon either temperature rise or fuel/air ratio. The error is chiefly attributable to the error in measuring the combustor exhaust nozzle total-to-static pressure ratio. The other individual random errors appear to be of minor importance. However, the presentation allows one to readily replace any of the assigned probable values as desired, and then recompute the probable error in combustion efficiency applying to a particular investigation.

Appendix

This section deals with the factors which normally have minor effects upon the theoretical properties of the combustion gases. Analysis for a particular case will indicate whether the effects are significant therein.

Actual batches of hydrocarbon fuel can vary somewhat in carbon/hydrogen ratio, in sulfur content, and in the particular congregation of constituent molecules; all of these have an influence upon the heating value. So, effectively, does the fuel feed temperature. In addition, the relative proportion of

carbon, hydrogen, sulfur, and any other elements present affects the heat capacities and dissociation effects of the combustion gases. Variations in inlet air humidity also affect the combustion gas properties. It is conceivable that some combustion performance tests might be run in industrial environments where the inlet air is in some way sufficiently contaminated for the contamination to have minor but positive significance.

There are, of course, two ways to elevate the temperature of combustor inlet air which is already at, or about, the desired inlet pressure. By means of a heat exchanger, heat can be transferred into the air without chemical effect. On the other hand, the air may be "preburned" in a "preburner" combustor, either merely to achieve temperature increase or else to simulate afterburner inlet conditions. The vitiated air issuing from the preburner is now, depending upon the viewpoint, either the product of combustion of the preburner fuel/air ratio or else a combination of pure air and stoichiometrically reacted preburner fuel and air. If the vitiation is limited, such as in simulating some ramjet inlet air temperatures, the vitiation may in practice be neglected in computation of combustion efficiency of the main combustor. Obviously some error thus is introduced into the theoretical enthalpy or temperature rise. (It really is not pertinent to the topic of this paper but it is quite pertinent to the example under discussion that if the preburner is not 100 per cent efficient, the true fuel flow to the main combustor is greater than the quantity of fuel directly injected thereinto.)

One can imagine all sorts of complications resulting from presence of unnatural material in the combustion products. Not only may the thermodynamic properties of the products be affected; there may also be influences upon the rate of reaction, which may help to explain discrepancies in interpreting reported combustion efficiencies. While vitiation and inlet air humidity are the most significant items in this regard, other possibilities are air contamination by leakage of heat exchanger fluids and fuel contamination by dissolved gases, entrained water, and the like. Finally, one should not neglect the possibility of variation in fuel composition due to evaporation losses from either ground storage or aircraft fuel tanks, which of course is at least as significant in regard to heating value as in regard to combustion gas properties.

When one is interested in defining the theoretical properties as precisely as possible, the following seem to be reasonable degrees of precision for the minor variables: ± 1 per cent in fuel heating value, ± 1 F in inlet fuel temperature, ± 2 per cent in fuel heat capacity for adjustment of heating value, insignificant error in fuel composition if heating value is independently known, $\pm 1/2$ per cent in inlet air absolute temperature, air composition correct to ± 0.1 mol per cent of each constituent, and insignificant error in system static pressure in so far as it affects equilibrium conditions. As pointed out earlier, these errors are not necessarily assigned on a hard-and-fast basis, but are subject to whatever revision the reader may believe preferable.

It should be noted that hydrocarbon fuel properties are often estimated on the basis of specific gravity, ASTM distillation data, and/or viscosity and aniline point. For this purpose (25–30) are pertinent.

There is much to be said for adhering to one given basis of data reduction for combustion efficiency so as to be as consistent as possible within the limits prescribed by the adopted assumptions. Almost every different source of thermodynamic data for the products of hydrocarbon combustion differs slightly from any other in regard to either heating value or carbon/hydrogen ratio of the fuel, or both. Frequently the compilers of the information differ in the basic data they have employed for pure constituent properties. Of late a paper has appeared (38) which casts doubt upon the equilibrium constants employed to date for the dissociation of molecular nitrogen to atomic nitrogen. Where considered in the past, this was treated as a very high temperature phenomenon; now it appears to be an extremely high temperature phenomenon of no importance whatever when air (the nitrogen source) is the oxidant. Thus those references which ignored the slight (apparent) dissociation of nitrogen in the past now appear to be on firmer ground than those which went to the trouble to consider it. This, then, is an example of the potential benefit of not converting the calculation basis to the very latest foundation. The immediately recognizable benefits are that the old performance data are still pertinent for comparisons, and re-education of the persons doing the computing is obviated.

It is well to keep in mind the difference between employing theoretical data for efficiency calculation and using them for theoretical performance calculations. In the latter case the objective usually is comparative information, and the various assumptions may well be accepted as applying to the whole range of conditions covered in the calculations. Moreover, a number of assumptions of efficiency values of one sort or another are usually involved in such performance studies, and these may make it nonsensical to quibble over minor differences in basic theoretical data. In contrast to this there is the situation where one can reduce the spread of actual test data by accounting for greater than normal humidity, or some such abnormality.

References

1 Cesaro, R. S., Koenig, R. J., and Pack, G. J., "Experimental Analysis of a Pressure-Sensitive System for Sensing Gas Temperature," NACA TN 2043, Feb. 1950. See also NACA RM E7C03, RM E7H27, RM E8C04, TN 2526, and Report 896.

2 Koffer, G. W., "Combustion Data Reduction Methods," Marquardt Aircraft Co., Report 5050 (AD 61738), July 24, 1950.

3 Bahn, G. S., and Macaulay, R. W., "XH-17 Composite Combustion Report: Temperature Measurement," General Electric Co. Report R52GL62, Part 3, Feb. 25, 1952.

4 Friedman, J., Bennet, W. J., and Zwick, E. B., "The Engineering Application of Combustion Research to Ramjet Engines," Fourth Symposium on Combustion, Williams & Wilkins, Baltimore, 1953, pp. 756–764.

5 Bjerklie, J. W., "A Combustor Analysis Method Evolved from Basic Flame Stability and Fuel Distribution Research," Jet Propulsion, vol. 25, May 1955, pp. 227–231.

6 Bahn, G. S., "Rational Prediction of Combustion Efficiency for Baffle-Type Combustors," Fifth Symposium on Combustion, Reinhold, New York, 1955, pp. 336–343.

7 Bahn, G. S., "Thermodynamic Properties of Combustion Gases," ASME Paper 53-S-39, April 1953.

8 Hall, N. A., and Mulready, R. C., "Ideal Temperature Rise from Constant Pressure Combustion of Hydrocarbon Fuels," SAE Preprint 182, April 1948.

9 Mulready, R. C., "The Ideal Temperature Rise Due to the Constant Pressure Combustion of Hydrocarbon Fuels," Meteor Report UAC-9, United Aircraft Corp. Research Dept., July 1947.

10 Wolfson, B. T., "Standard Thermodynamics Performance Data for Air Breathing Propulsion Systems," Wright Air Development Center Technical Note WCRR 52-19, Dec. 1952.

11 Topps, J. E. C., "The Thermal Properties of the Combustion Products of Kerosene Air Mixtures," National Gas Turbine Establishment Report R. 14, April 1947 (ATI 31854).

12 Fielding, D., Topps, J. E. C., and Thompson, W. R., "Thermodynamic Properties of Air and Combustion Products of Hydrocarbon Fuels," National Gas Turbine Establishment Report R. 74 (Part I), June 1950, R. 120 (Part II), July 1952, and R. 160 (Part III), June 1954.

13 Keenan, J. H., and Kaye, J., "Gas Tables," Wiley, New York, 1948.

14 Hottel, H. C., Williams, G. C., and Satterfield, C. N., "Thermodynamic Charts for Combustion Processes," Wiley, New York, 1949.

15 Turner, L. R., and Bogart, D., "Constant-Pressure Combustion Charts Including Effects of Diluent Addition," NACA Report 937, 1949.

16 Huff, V. N., Gordon, S., and Morrell, V. E., "General Method and Thermodynamic Tables for Computation of Equi-

(Continued on page 887)

Stable Cyclonic Flames of Natural Gas and Air

LYLE F. ALBRIGHT[1] and LLOYD G. ALEXANDER[2]

University of Oklahoma

An investigation was conducted to determine quantitatively the characteristics of flames stabilized by cyclonic motion in mixtures of air and natural gas. Gases flowing cyclonically from a nozzle burned stably at superficial velocities up to 100 fps (actual velocities were higher). The temperatures of the flames were sometimes higher than 2400 F. Extremely stable flames were obtained when mixtures of air and natural gas flowed cyclonically in approximately 0.5-in. ID ducts varying in length from 4 to 20 in. The flames burned mainly inside the ducts in the form of hollow cylinders, and in many cases did not touch or appreciably heat the duct wall, although flame temperatures above 2600 F were observed. Flames were stabilized at superficial velocities up to 700 fps. Combustion was frequently incomplete. Stable flames were also obtained in ducts bent through an angle of 90 deg and in a conical diverging section. Flame stabilization results from a reverse flow toward the nozzle along its axis. Hot combustion gases are recycled and act as a pilot flame for the entering gases. In some cases, air is entrained and recycled with the combustion gases.

Introduction

THE applications of cyclonic flow in combustion seem to have been restricted mainly to two-phase systems such as powdered solid fuels (6, 7, 12, 13, 16)[3] or atomized fuel oil (17) and air. The term "cyclonic flow" as used here applies to the rotational motion of a fluid around its flow axis. This type of flow apparently causes solid or liquid fuel particles to be mixed more uniformly with the air, and the centrifugal forces cause the ashes and slag to separate from the combustion gases.

Experimental and theoretical studies of cyclonic flow itself are meager. Limited results have been reported on cyclonic flow of liquids (4), cyclone dust collectors (14), cyclonic flow of air in cylinders (9), and cyclonic scrubbers (10). Several investigators, including Fulton (5) and Van Deemter (15), have studied the flow characteristics in Ranque or Hilsch tubes, and Curley and MacGee (3) present a bibliography of pertinent literature on the subject.

Alexander (2) and undergraduate students at the University of Illinois demonstrated in some exploratory investigations that cyclonic flow caused mixtures of natural gas and air to burn in uniquely stabilized manners. Preliminary indications showed that a reverse flow of hot gases occurred along the flow axis. It was conjectured that this reverse flow acted as a pilot for the entering combustible gases. Later, Hottel and Person (8) reported similar results and gave a similar explanation.

It was decided to investigate further the applications of cyclonic flow of combustible gas mixtures in emergent cyclonic free jets, ducts, and diverging sections. Flame characteristics and the stability limits of the flames were studied for mixtures of natural gas and air.

Presented at the ARS 25th Anniversary Annual Meeting, Nov. 14–18, 1955, Chicago, Ill.

[1] Associate Professor of Chemical Engineering; present address, Purdue University, Lafayette, Ind.

[2] Engineer; present address, Oak Ridge National Laboratory, Oak Ridge, Tenn.

[3] Numbers in parentheses indicate References at end of paper.

Apparatus and Procedure

The flow sheet of the apparatus used for producing cyclonically stabilized flames is shown in Fig. 1. The apparatus was constructed so that natural gas and air could be metered, by means of sharp-edge orifices, to the cyclonic nozzle (item 10). The air pressure at the orifice was regulated by means of a solenoid valve in the side of the air surge tank (item 12). Natural gas pressures up to 70 psi were obtained using a gas compressor (item 1).

Two flow arrangements could be obtained by proper manipulation of the valves. In the first, the air and natural gas streams were combined and presumably mixed as the gases

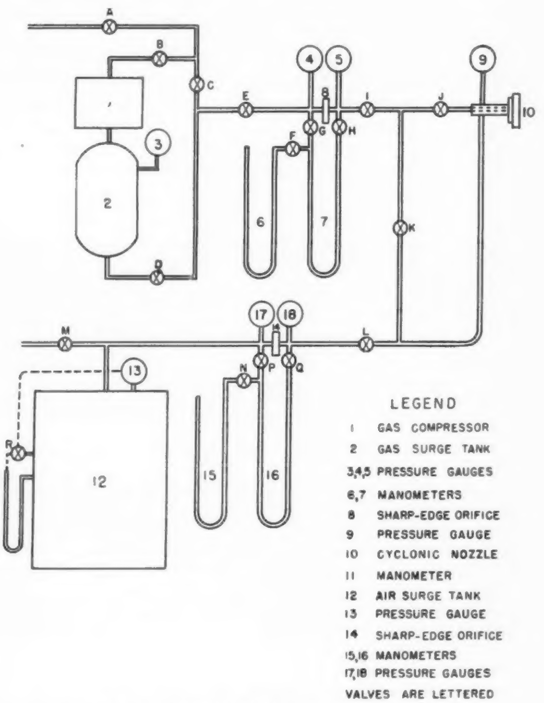

Fig. 1 Flowsheet of flame apparatus

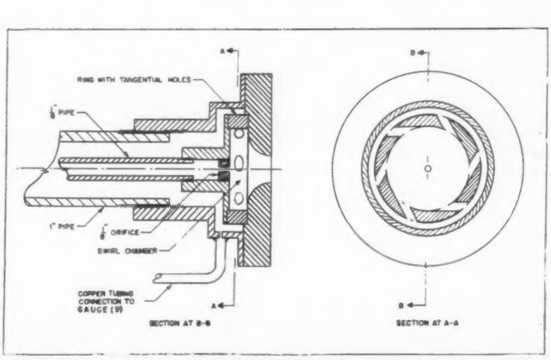

Fig. 2 Cyclonic combustion nozzle

passed through several feet of pipe. Then the gases were introduced through the outer pipe of the annulus of the cyclonic nozzle (Fig. 2). The second arrangement allowed the air only to be introduced to the outer side of the annulus and the natural gas to the inner pipe. In this case the air and natural gas did not mix until they were in the swirl chamber of the cyclonic nozzle. The gas stream entering through the outer pipe of the annulus passed into the swirl chamber through six tangential ports (0.150 in. ID). These ports were drilled 60 deg apart in a ring (1.50 in. ID, 2.00 in. OD, and 0.375 in. thick) which was pressed into a face plate containing a converging nozzle (0.50 in. throat diam). The inner pipe ($^1/_8$ in.) of the annulus opened through a $^1/_8$-in. orifice in the wall of the swirl chamber at its axis. The pressure in the annulus was measured by means of a calibrated pressure gage (item 9).

Approximate $^1/_2$-in. ID glass or metal tubes for the flame tests were attached to the face plate of the nozzle. The tubes used in the present study varied from 4 to 20 in. in length with inside diameters ranging from 0.482 to 0.535 in. In addition, several bent (60–90 deg) glass tubes about 8–12 in. long were used. Flame studies were also made with a metal conical diverging section bolted to the face plate of the cyclonic nozzle. This section was 7.25 in. long with the internal diameter 0.53 in. at the inlet and 1.375 in. at discharge.

Temperature measurements in the flames and of the exhaust gases were made using an unprotected chromel-alumel thermocouple and a potentiometer. The thermocouple was capable of recording temperatures up to 2600 F for short times, but at higher temperatures it failed. Analyses of the exhaust gases were made with a standard Hays Orsat analyzer for carbon dioxide, oxygen, and carbon monoxide. Gas samples were obtained through an uncooled stainless steel sampling tube (0.065 in. OD and 0.030 in. ID). The thermocouple and gas sampling tube were mounted on a rod, which could be positioned at all desired locations in a vertical plane passing through the axis of the nozzle. A converging nozzle machined to ASME code specifications (18) with an inlet diameter of 1.390 in. and a throat diameter of 0.500 in. was used to calibrate the sharp-edge orifices for air and natural gas at the higher flow rates. A dry gas-meter was used for calibration purposes up to about 2.0 cfm.

As the air and fuel gas rates were varied, it was noticed that the characteristics and appearance of the resulting flames changed markedly. Several series of experiments were made with cyclonic free jet flames and with cyclonic flames in various ducts attached to the cyclonic nozzle. In each case the flames were observed over a wide range of flow conditions. In these investigations, the natural gas and air flows were changed slowly, and sufficient time (at least 10–15 sec) was allowed between changes in order to insure equilibrium of all flames being studied. Whenever the flame characteristics changed or when the flame blew out, the inlet and outlet pressures on both the air and gas orifices were recorded. In addition the pressure gage (item 9) reading was recorded.

Results

Flames in Emergent Cyclonic Free Jet

Several relatively distinct types of flames were observed when natural gas and air were mixed and discharged freely from the cyclonic flow nozzle. Typical flames were obtained by setting the gas flow at a relatively low rate and increasing the air flow to produce flame types designated A, B, C, and D, respectively. Photographs of typical flames are shown in Fig. 3. Flow conditions at which each flame type occurred are presented in Fig. 4, as a plot of the mole ratio of air to natural gas versus superficial velocity. The mole ratio is defined as the volume ratio of air to natural gas entering the nozzle. The "superficial velocity" is the calculated velocity

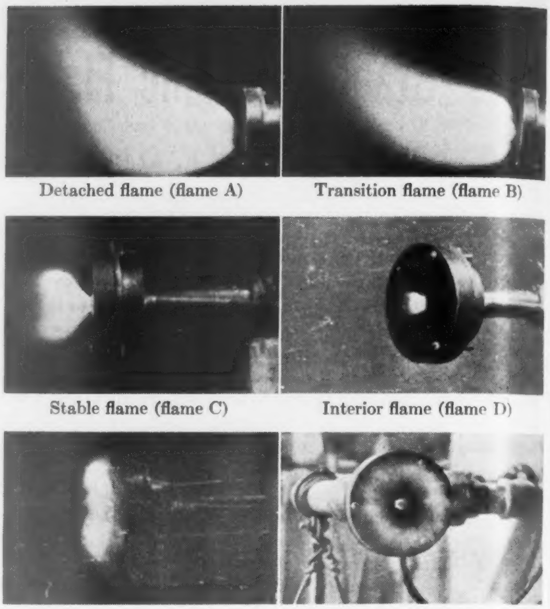

Detached flame (flame A) — Transition flame (flame B)

Stable flame (flame C) — Interior flame (flame D)

Radial flame—side view (flame E) — Radial flame—end view (flame E)

Fig. 3 Flames of cyclonic nozzle

Fig. 4 Stability limits for cyclonic free jet

in the cyclonic nozzle throat assuming the natural gas and air passed through linearly, unburned, and at room conditions.

Flame A was detached and noisy. As the air flow was increased, the flame retracted along the flow axis to produce flame B, which also burned noisily and raggedly. The transformation from flame B to flame C was gradual. Flame C was stable and burned smoothly with a high-pitched hissing sound. The flame outside the nozzle formed a hollow cone. The flame inside the nozzle was a hollow cylinder and extended to near the back wall of the swirl chamber. At superficial velocities approaching 100 fps, the flame became ragged and exhibited considerable internal disturbances. At high gas flows, flame C blew out with an increase in the air flow but, at lower gas flows, increasing air flows converted it to flame D. This flame was a hollow cylinder which burned primarily inside the nozzle. It was stable at superficial velocities up to almost 100 fps. The odors of aldehydes were detected in the exhaust gases for flames of the interior type. As the air rate increased, the interior flame blew out. Pressure drops in the cyclonic nozzle varied with

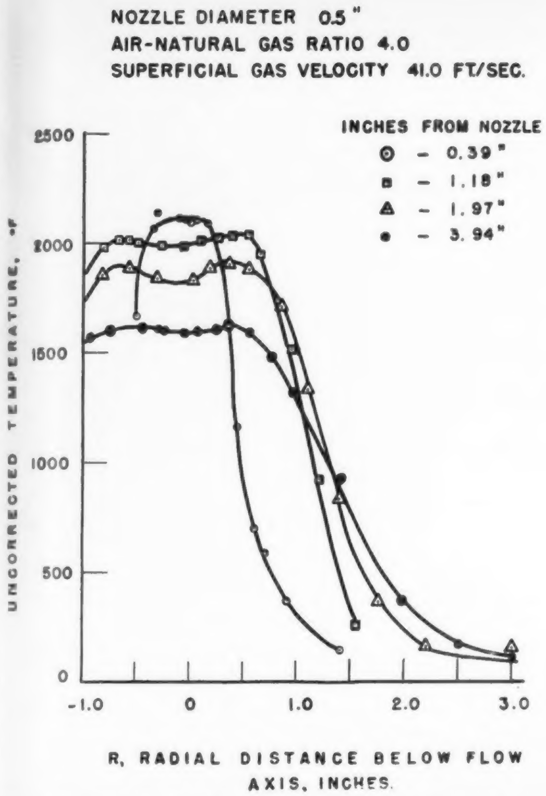

Fig. 5 Temperature distribution in flame (flame C) from cyclonic free jet

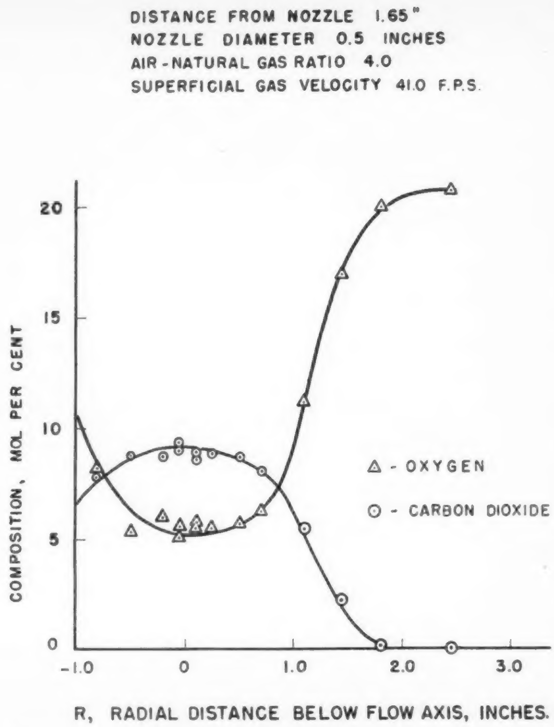

Fig. 6 Gas composition distribution in flame from cyclonic free jet

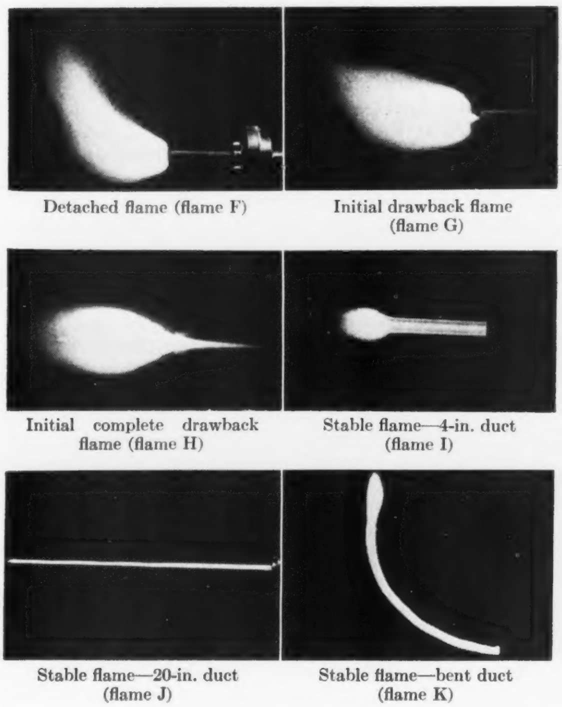

Detached flame (flame F)

Initial drawback flame (flame G)

Initial complete drawback flame (flame H)

Stable flame—4-in. duct (flame I)

Stable flame—20-in. duct (flame J)

Stable flame—bent duct (flame K)

Fig. 7 Flames in glass ducts

the superficial velocity, but they were about 3 psi at 100 fps.

It was found that flame C could sometimes be converted to another relatively stable flame (flame E, Fig. 3) by blowing air along the flow axis toward the nozzle. This latter flame burned within about $^1/_4$ in. of the face plate of the cyclonic nozzle. It appeared that the burning gases emerging from the nozzle turned approximately 90 deg as they left the nozzle and flowed radially away from the discharge. In certain cases the radial flame remained indefinitely in this shape. At other times it reverted to flame C after several seconds or else blew out.

Temperature profiles of a typical stable cyclonic free jet flame (C) are shown in Fig. 5. The temperatures along the axis are lower by several degrees than those about $^1/_4$ in. from it. The maximum uncorrected temperature in this flame was found to be over 2100 F. Results for other flames at higher flow rates indicated temperatures as high as 2400 F.

The temperatures in the interior flames (flame D) from the free cyclonic nozzle were considerably lower (maximum about 700 F) than in flame C. The maximum occurred at about 0.15 in. from the flow axis.

The exhaust gases of a stable cyclonic free jet flame were analyzed, and the results are shown in Fig. 6. Samples were taken at a horizontal distance from the nozzle slightly beyond the visible flame. No carbon monoxide was found in the samples analyzed. However, the sampling tube was uncooled, and no attempt was made to quench the reaction.

Flames in Ducted Cyclonic Streams

When air and natural gas were premixed prior to entry into the cyclonic nozzle, four distinct flame types were observed in approximate 0.5-in. ID ducts. Typical flames in a glass duct 4 in. long and 0.512 in. ID are shown in Fig. 7. The flames were obtained by setting the natural gas rate at a relatively low value and increasing the air rate to produce flames F, G, H, and I, respectively. A plot of the flow conditions at which each flame occurred is shown in Fig. 8. The mole ratio and superficial velocities were calculated in a manner similar to the one used for emergent cyclonic free jets. The only difference was that the superficial velocity

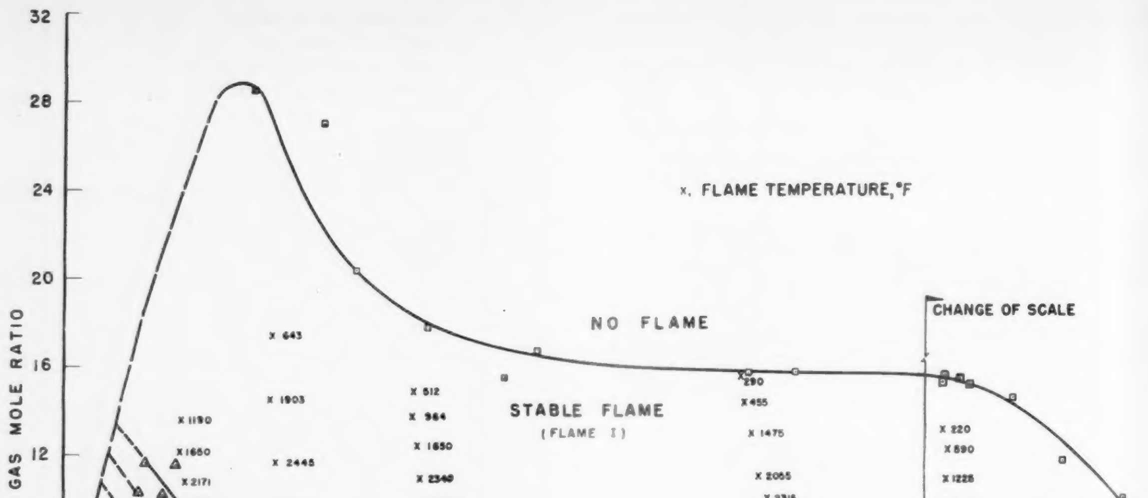

Fig. 8 Limits and temperatures of flames in 4-in. duct (0.512-in. ID) with premixed gases

was based on the accurately measured internal diameter of the duct, 0.512 in., in this case.

Flame F was a detached flame similar to flame A of Fig. 3. As the air flow increased, the flame retracted to form flame G, similar to flame B. As the air flow increased further, the flame retracted further until it extended throughout the entire length of the tube (flame H). At the duct outlet, the color of the flame was light green. With further increases of the air rate, a point was reached where flame H changed abruptly to flame I, which is hereafter referred to as the stable flame for ducted flow. This flame was light blue in color throughout It appeared to be a hollow cylinder extending into the cyclonic flow nozzle itself. In many cases the flame did not touch or appreciably heat the duct walls, although the flame itself was frequently extremely hot. The color of the flame generally was most intense at mole ratios of air to natural gas of about 8.5:1, and at these conditions an appreciable portion of the flame protruded from the duct. At higher ratios, especially near blowout conditions, the flame became less distinct and smaller in both diameter and length of protrusion from the duct. Just before blowout at the high mole ratios, the flame was so indistinct that it was hard to see, especially during the daytime, and the exhaust gases from it were relatively cool. At high gas velocities and low mole ratios, the odor of partially oxidized hydrocarbons such as aldehydes and alcohols often became strong.

Flame I was stable at superficial velocities up to about 700 fps. Up to about 500 fps and mole ratios from 8:1 to 12:1, the gases burned smoothly with a muffled roaring sound. At higher velocities the flames became ragged. Below 400 fps stable flames were obtained at mole ratios from about 15:1 to 7:1. This range narrowed as the velocity was increased. At 700 fps, the ratio for stability was 8.8:1. The intermediate flames (G and H) occurred only at velocities less than about 50 fps. The degree of detachment of flame F increased as the superficial velocity increased.

The flames obtained in an 8-in.-long duct were similar to those for the 4-in.-long duct. In 12- and 20-in. ducts, flames G and H were not observed. The stable flames were, however, similar to those obtained in 4- and 8-in. ducts. A typical stable flame in a 20-in. duct is shown as flame J in Fig. 7.

The stability limits of the stable flames were identical in the various ducts tested within probable experimental accuracy, with two exceptions. The maximum superficial velocity for stability in the 20-in. duct was slightly less than in the others. Also, at velocities up to 100 fps, the shorter the duct the higher the mole ratio obtainable before blowout was reached. In addition, it was noticed that the flames in the 20-in. duct appeared to be somewhat less stable, especially at higher velocities, than similar flames in shorter ducts.

It was found that flames could be stabilized in ducts about 8 to 12 in. long which were bent through angles of 60 and 90 deg. Flame K in Fig. 7 is a typical bent flame. The general characteristics (except for bend) and stability limits of these flames were similar to those in unbent ducts.

Flames were stabilized in an 8-in.-long duct when the natural gas was introduced noncyclonically and the air cyclonically. The appearance and general characteristics of this flame were similar to those of flames obtained when the two gas streams were premixed and introduced cyclonically. However, at lower velocities the flame did not always extend throughout the entire length of the duct. The stability limits (Fig. 9) of the flame resulting from this flow arrangement were considerably greater in regard to mole ratios of air to natural gas than the flames with premixed gases. The flames were stabilized at mole ratios of 100:1 or greater for superficial velocities up to 200 fps. The upper mole ratio limit decreased to about 34:1 as the velocity increased to about 700 fps, the maximum velocity of the stable flame. The lower limits of the mole ratios for flame stabilization were higher than those of the flame with premixed gases at all velocities greater than 200 fps.

When the diverging section was attached to the cyclonic

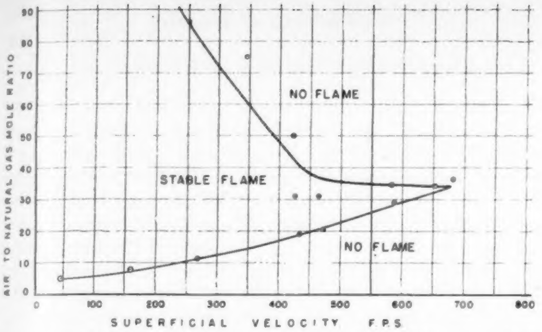

Fig. 9 Stable flame limits in 8-in.-long duct with noncyclonic gas and cyclonic air

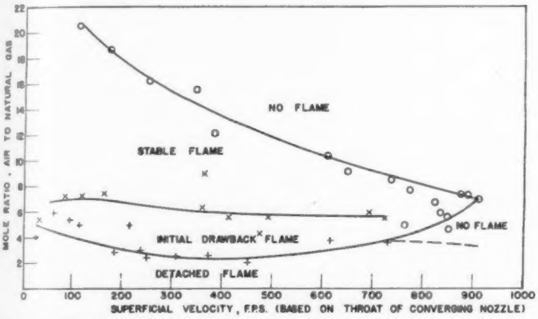

Fig. 10 Stability limits of flames in diverging section with noncyclonic natural gas and cyclonic air

nozzle and air only was introduced cyclonically, flames were stabilized at superficial velocities up to about 900 fps, as shown in Fig. 10. The superficial velocity as used here was calculated at the throat of the cyclonic nozzle. At low mole ratios the flame was detached and ragged. As the air flow increased, the flame began to draw back into the nozzle. At still higher mole ratios and with superficial velocities below about 500 fps, the so-called stable flame was formed. The flame extended, in general, throughout the diverging section and as a hollow cylinder into the cyclonic nozzle itself. The walls of the diverging section generally became heated to an appreciable extent especially near the open end. Although no temperature or gas analysis measurements were made, it was thought combustion was relatively complete. At superficial velocities above about 700 fps the flame apparently did not extend to the back wall of the swirl chamber. As the velocity increased from 700 to 900 fps the flame moved to an ever-increasing extent nearer the discharge end of the diverging section. Some preliminary tests with premixed air and natural gas in the diverging section produced flames similar to those in which the gases were unmixed and the air only was introduced cyclonically.

The process of converting a detached flame (flame F) to a stable flame (flame I) was considerably more difficult in longer ducts. If the natural gas flow was too great, the detached flame blew out as the air was increased. The maximum natural gas flow permitting a successful conversion to a stable flame became less as the duct length was increased. In the 20-in. duct, the gas flow was too small to be measured accurately. It was further found that the maximum flow decreased as the duct diameter was decreased.

Pressure drops in the cyclonic nozzle and ducts were high and varied with superficial velocities. At 700 fps the pressure drop was about 55 psi.

Maximum uncorrected flame temperatures were measured at the duct discharge for several ducted flames of premixed gases over wide ranges of air and natural gas flow rates up to an over-all superficial velocity of about 500 fps. The results for the 4-in. duct, which are typical, are shown in Fig. 8. It

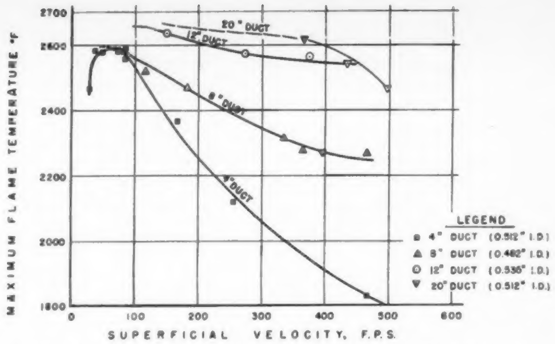

Fig. 11 Maximum flame temperature for ducted flames

was found that, at a given velocity, the highest temperature occurred at air to natural gas mole ratios of about 8.5:1. At higher mole ratios near blowout conditions the exhaust gases were relatively cool (as low as 290 F). At ratios less than 8.5:1 the temperature at a given velocity decreased several hundred degrees below the maximum. A plot of the maximum uncorrected flame temperature for a given velocity versus velocity is presented in Fig. 11. The highest temperature found with the 4-in. duct was about 2580 F at a velocity of about 50–80 fps, and the maximum temperatures decreased as the velocities increased above 80 fps.

Flame temperature measurements were also made at the discharge of 8-, 12-, and 20-inch ducts. The maximum temperatures are shown in Fig. 11. It is seen that below 500 fps longer tubes produce hotter flames at a given velocity. It was, however, not possible to obtain mole ratios of 8.5:1 at the lower velocities in the longer tubes because the tubes heated and failed. Serious heating of the 8-, 12-, and 20-in. ducts was noted at velocities from about 20–70, 20–140, and 20–300 fps, respectively.

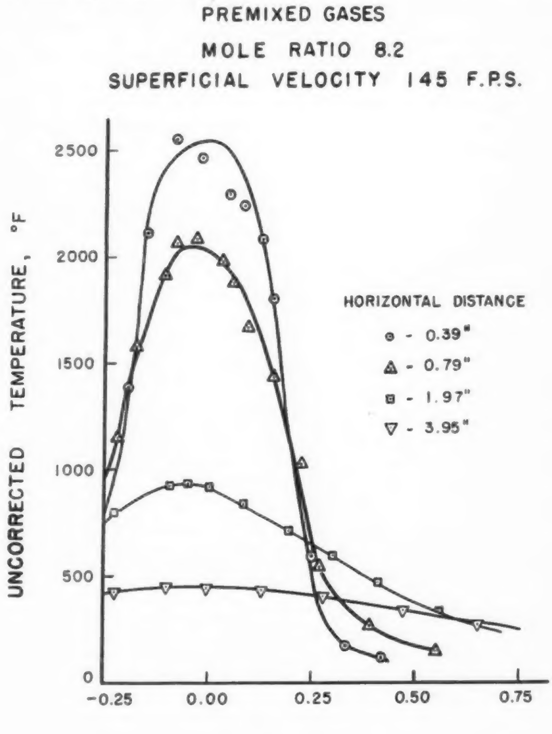

Fig. 12 Temperature distribution in stable flame from 8-in. duct

Table 1 Typical natural gas analysis

Specific gravity component	0.7228 Volume, %
O_2	1.88
CO_2	0.00
N_2	10.16
CH_4	72.07
C_2H_6	9.82
C_3H_8	4.25
i-C_4H_{10}	0.41
C_4H_{10}	0.88
i-C_5H_{12}	0.19
C_5H_{12}	0.17
C_6H_{14}	0.10
C_7H_{16}	0.07
	100.00

Temperature data for several profiles in a stable flame at the discharge of an 8-in.-long duct are presented in Fig. 12. The maximum temperature in a plane 0.39 in. from the discharge was 2545 F and occurred near the flow axis. This temperature was higher than the temperatures measured in either of the two flames in emergent cyclonic free jets at comparable distances. The temperatures in the ducted flames, however, decreased more rapidly than those in cyclonic free jet flames at increasing horizontal and radial distances, even though the superficial velocity in the duct was higher. When the air only was introduced cyclonically (and the gas noncyclonically) in an 8-in. duct, the maximum temperature observed was 2245 F.

Combustion was incomplete in stable ducted flames with premixed gases as shown in Table 2. The carbon monoxide contents were high, ranging up to 0.8 per cent and the carbon dioxide contents were considerably lower than in free jet flames. A gas sample was collected at the outlet near the inner wall of the duct while the stable flame was burning. This gas sample was found to contain only a trace of carbon monoxide, and to be essentially unburned gas. Minor changes in the mole ratio did not seem to change the combustion efficiency of the apparatus significantly. Lower superficial velocities did increase it, however, since the flame extended to the wall of the duct and no hydrocarbons passed through the duct completely unburned.

Discussion of Results

Flame Stabilization in a Cyclonic Free Jet

Cyclonic flow of a combustible gas mixture in an emergent cyclonic free jet was found to stabilize flames to an extent and in a manner impossible for linear flow. This stabilization results from the unique flow patterns which recirculate a portion of the hot combustion gases which then ignite the entering gas stream. This explanation is supported not only by the proof (1) that a reverse flow occurs toward the nozzle along the axis when air is passed through the nozzle, but also by the fact that temperatures of the flames were at minima at the axis in transverse planes. The lower temperatures were caused, no doubt, by partial cooling of the burned gases before they were recirculated and by inclusion of fresh air in the reverse flow stream.

The stable flame occurred at superficial velocities up to 100 fps. The actual velocities, however, were undoubtedly much higher since combustion increased the temperature and moles of gas and since the main outward gas flow was confined to only a portion of the cross-sectional area of the throat. Calculations based on the total and static pressure measurements (1) for air flowing through the cyclonic nozzle indicate local velocities above 200 fps when the superficial velocity was 41 fps. For the same conditions the reverse flow velocity along the axis was about 60 fps. Flames at superficial velocities of about 100 fps were quite unstable and appeared to be on the verge of blowing out. As a result, no investigation was made at higher velocities.

Temperature data and analyses of the exhaust gases from two stable flames indicate fairly high combustion temperatures and possibly complete combustion. Although the temperature measurements are uncorrected for radiation, convection, or catalytic effects, it is probable, however, that the measurements indicate fairly accurately the trend of distribution and approximate ranges of temperatures. Analyses of the samples taken with an uncooled sampling tube are open to question, since it is possible that the gases continued to react while in the tube. As a result, it may be that combustion was not complete as indicated. The analyses, however, indicate that a large excess of oxygen was available for combustion. Since the air to natural gas mole ratios for these flames were considerably below the stoichiometric ratio, there must have

Table 2 Analysis exhaust gases from stable flame in 8-in. duct (0.535 in. ID) with premixed gases

Mole ratio	Superficial velocity fps	Horizontal distance in.	Radial distance below flow axis, in.	CO_2, %	O_2, %	CO, %
8.2	119	1.97	0.0	4.8	11.4	0.6
8.2	119	3.94	0.0	2.8	16.2	0.0
8.0	124	2.36	0.0	4.0	12.5	0.2
8.0	124	2.36	0.0	4.1	12.3	0.5
8.6	170	2.36	0.34	0.9	17.5	0.5
8.6	170	2.36	0.02	2.1	15.5	0.7
8.6	170	2.36	0.00	2.2	15.4	0.6
8.6	170	2.36	−0.14	1.2	16.6	0.6
8.6	170	2.36	−0.64	0.4	19.0	0.3
8.9	174	1.58	0.87	0.1	19.6	0.1
8.9	174	1.58	0.59	0.3	18.6	0.2
8.9	174	1.58	−0.03	0.7	17.6	0.5
8.9	174	1.58	−0.47	0.5	19.0	0.3
8.9	174	1.58	−0.87	0.0	20.2	0.0
8.9	174	2.36	0.50	1.0	17.2	0.6
8.9	174	2.36	0.50	1.0	17.8	0.6
8.9	174	2.36	0.25	1.8	16.0	0.7
8.9	174	2.36	0.00	1.7	16.5	0.8
8.9	174	3.94	0.0	0.8	18.4	0.6
8.9	174	7.88	0.0	0.4	19.6	0.0
8.4	435	2.36	0.0	0.4	19.4	0.2
7.8	473	2.36	0.0	0.8	19.2	0.7
10.1	503	2.36	0.0	0.4	19.6	0.0

been considerable mixing of the burning gases with the surrounding air.

Fig. 4 indicates that the air to fuel ratio for the transition flame (flame B) and the stable flame (flame C) decreases as the superficial velocity increases. This is probably associated with the amount of ambient air entrained and recirculated with the recycling combustion gases. It should be emphasized that both the air to fuel ratio and the superficial velocity of Fig. 4 were calculated from the measured input of the burner. No attempts were made to estimate the amounts of entrained air. Since several flames of the cyclonic free jet occurred with fuel-rich mixtures, they were presumably diffusion flames.

The detached flame (flame A), the transition flame (flame B), the interior flame (flame D), and the radial flame (flame E) did not appear stable enough to be of any practical importance in regard to energy release. The radial flame characteristics, however, probably could be altered to a considerable extent by changes of the shape and size of the nozzle face plate. The stable flame, however, may be of interest as a pilot flame under severe flow conditions or as a means of producing stable flames at high rates of energy release.

Flame Stabilization in Ducts

Several types of flame were produced when combustible air and natural gas mixtures were passed cyclonically through a duct, but only the stable flames, such as flames I, J, and K, were considered to be of any practical importance. These flames were much more stable than any flame of the cyclonic free jet, and much higher superficial velocities and air to natural gas mole ratios were possible without blowout. In certain cases, the duct diameter was slightly larger than the throat of the cyclonic nozzle, so the superficial velocity in the throat was even higher. The actual gas velocities were, no doubt, much higher than the superficial velocities because of the combustion taking place and because the outflowing gases flowed mainly in a thin annulus near the duct wall with a considerable tangential velocity component (9).

It was noted that the mole ratio limits of air to natural gas for the flames with premixed gases compare rather closely, at velocities from about 100 to 400 fps, to the upper and lower combustion limits for methane in air, which are 15:1 and 5:1, respectively (11). The natural gas used was primarily methane (see Table 1). The mole ratio for the stable flame at its highest velocity was 8.9:1, which is near the stoichiometric ratio for complete combustion of methane.

When the air only was introduced cyclonically and the gas noncyclonically, stable flames occurred in some cases at mole ratios of air to natural gas far above the upper combustion limit. It can be assumed that the air and natural gas did not mix thoroughly until, at least, combustion had started. This seems to explain why the flame, in some cases, did not always extend over the entire length of the duct.

Flame stabilization in ducts with both unmixed and premixed gases was undoubtedly caused, as in cyclonic free jets, by a reverse flow (9) of hot combustion gases which acted as a pilot light for the combustible gas mixture. It would then be expected that, as with the flames in the cyclonic free jet, the flame front would start near the flow axis and travel axially and radially. Temperature measurements (Fig. 12) and gas analyses support this hypothesis. The temperature profile of the flame leaving the duct indicates that the flame front was located at about 0.05 in. from the wall. Gas analyses indicated that the gases flowing in the annular region outside the flame were essentially unburnt.

The maximum flame temperature (see Fig. 11) for a given superficial velocity always occurred at a mole ratio approximately equal to the stoichiometric ratio of the mixture. The higher temperatures for longer ducts and lower velocities are probably caused by longer residence time of the gases in the duct. Since in many cases combustion was far from complete (see Table 2), longer residence time would allow more time for the flame to travel radially toward the duct wall and hence give more complete combustion. If the combustion is to be complete, it is expected that the flame front must reach the duct wall.

The degree of stability of the so-called stable flame appeared to be relatively constant for all ducts tested except for the 20-in. duct. In this duct considerable vibrations and standing waves were noted for certain flows at higher velocities. These disturbances were probably caused by the decay of the cyclonic motion with length. As a result it did not seem necessary to study longer ducts with the present cyclonic nozzle.

The flames produced by cyclonic flow in the diverging section appear to be promising in regard to stability, large range of flow conditions possible, and relatively complete combustion. Higher superficial velocities were obtained than with cylindrical ducts. It is probable, however, that the actual velocities in the flame were no greater in the diverging section than in the ducts, since at higher velocities the flame did not extend into the smaller diameter portion of the diverging section. Stable flames in the diverging section occur over much larger ranges of flow conditions than is possible with other types of burners.

Conclusions

It has been demonstrated that highly stable flame can be obtained when mixtures of air and natural gas flow cyclonically. Apparatus tested include emergent cyclonic free jets, straight and bent ducts that are about 0.5 in. in diam and 4 to 20 in. long, and a conical diverging section. Flames produced were stabilized at superficial velocities up to 700 fps and in many cases the rate of energy release seemed to be high.

Acknowledgment

The authors wish to thank the National Advisory Committee for Aeronautics, who supported this research, for permission to publish the results.

References

1 Albright, L. F., and Alexander, L. G., "Flame Stabilization Resulting from Cyclonic Flow in Mixtures of Natural Gas," Unpublished final report to NACA, 1954.

2 Alexander, L. G., Unpublished notes, 1949–1952.

3 Curley, W., and MacGee, R., *Refrigerating Engineering*, vol. 59, 1951, p. 166.

4 Einstein, H. A., and Li, H., Heat Transfer and Fluid Mechanics Institute, Stanford University Press, Stanford, Calif., 1951.

5 Fulton, C. D., *Refrigerating Engineering*, vol. 58, 1950, p. 473.

6 Gilg, F. X., *Power Generation*, vol. 54, no. 2, 1950, p. 64.

7 Grunert, A. E., Skog, L., and Wilcoxson, L. S., *Transactions of The American Society of Mechanical Engineers*, vol. 69, 1947, p. 613.

8 Hottel, H. C., and Person, R. A., Fourth Symposium on Combustion, Williams and Wilkins, Baltimore, 1953, p. 781.

9 Iinoya, K., *Memoirs of the Faculty of Engineering, Nagoya University*, vol. 5, no. 2, 1953, p. 131.

10 Johnstone, H. F., and Silcox, H. E., *Industrial and Engineering Chemistry*, vol. 39, 1947, p. 808.

11 Lewis, B., and Von Elbe, G., "Combustion, Flames, and Explosion of Gases," Academic Press, New York, 1951.

12 Parmale, B. J., U. S. Patent 2,476,507, 1946.

13 Parmale, B. J., U. S. Patent 2,476,508, 1946.

14 Sheppard, C. B., and Lapple, C. E., *Industrial and Engineering Chemistry*, vol. 31, 1939, p. 972.

15 Van Deemter, J. J., "Applied Scientific Research," vol. A III, Central National Council for Applied Scientific Research in the Netherlands, The Hague, 1953, p. 174.

16 Vroom, R. C., U. S. Patent 2,325,442, 1941.

17 Wootring, G. H., U. S. Patent 2,300,190, 1940.

18 "Power Test Codes; Flow Measurements by Means of Standardized Nozzles and Orifice Plates," The American Society of Mechanical Engineers, New York, 1940.

The Theoretical Specific Thrust of a Rocket Motor for the C-H-N-O-F System[1]

M. S. MORGAN,[2] J. SILVERMAN,[3] and W. T. WEBBER[4]

Rocketdyne, a Division of North American Aviation, Inc., Canoga Park, Calif.

Since but seven variables determine the theoretical I_{sp} of the carbon-hydrogen-nitrogen-oxygen-fluorine system, a generalized solution of the problem using arbitary values of the variables is possible. Curves of theoretical I_{sp} based on the assumption of isentropic expansion of combustion products whose chemical composition is frozen at chamber conditions versus oxidation ratio are presented for various hypothetical compositions and heats of formation at a chamber pressure of 500 psia and a nozzle exit pressure of one atmosphere. Within the range of values of the variables chosen, the I_{sp} for any propellant combination and mixture ratio can be determined from the graphs by interpolation or, for greater accuracy, by suitable cross-plots. Some examples of such cross-plots are presented. In general, the accuracy of the results is plus or minus one per cent.

RECENT advances in large digital computing machines have modified classical approaches to the solution of many scientific and engineering problems. Since a large number of computations can be performed economically, it is sometimes feasible to make general solutions of certain problems so that specific data are readily available. This approach is particularly applicable to the computation of the theoretical specific impulse of rocket propellants, which, for a large number of propellant combinations, is a function of a small number of variables.

The specific impulse I_{sp} of a rocket propellant is defined as the thrust produced per unit rate of propellant consumption

$$I_{sp} = \frac{F}{\dot{w}} = \sqrt{\frac{2J\,(H_c - H_e)}{g}} \qquad [1]$$

where

F = thrust
$\dot{w}$ = total propellant flow rate
J = mechanical equivalent of heat
H_c = enthalpy of combustion products in combustion chamber
H_e = enthalpy of combustion products at nozzle exit

This equation neglects the (usually small) thrust resulting from any difference between the ambient and exit gas pressures. Although the ultimate choice of a propellant combination may frequently depend upon other factors in addition to specific impulse (such as storability, toxicity, logistics, etc.), accurate and reliable theoretical specific impulse data are, nevertheless, an important prerequisite for rocket design work. Unfortunately, the computation of I_{sp} is long and tedious, and a prohibitive amount of work would be involved in such computations for all of the propellant combinations of interest. The method of computing I_{sp} may be found in the literature (1, 2)[5] and will not be repeated here.

Experience to date has indicated that the majority of the useful liquid rocket propellants are made up of two or more of the elements carbon, hydrogen, nitrogen, oxygen, and fluorine. Since but seven independent variables completely determine the theoretical I_{sp} of the C-H-N-O-F system, it is possible to make a generalized solution of I_{sp} for these elements, using arbitrary values of the variables. These variables may be expressed most conveniently as C/(C + H) weight ratio, O/(O + F) weight ratio, weight percentage of nitrogen, oxidation ratio, effective heat of formation of the reactants, combustion chamber pressure, and nozzle exit pressure. Such a generalized solution was made and tabular I_{sp} data obtained for the first five of the variables. Chamber and exit pressures, which comprise the remaining variables, were not varied because the effect of these on I_{sp} can be quickly estimated from available correlation charts.

The terms "oxidation ratio" and "effective heat of formation" are used in a rather particular sense. The former is defined as the ratio of the numerical total of oxidizer gram atoms (oxygen or fluorine) in the propellant mixture to the number of these gram atoms required to burn completely one mole of the fuel. Since the following valences are assumed for the elements in the products (for complete combustion)

Oxygen = $-2(H_2O, CO_2)$
Fluorine = -1 (HF, CF_4)
Nitrogen = 0 (N_2)
Hydrogen = $+1(H_2O, HF)$
Carbon = $+4$ (CO_2, CF_4)

the oxidation ratio OR may be represented simply as

$$OR = \frac{2n_{\text{oxygen}} + n_{\text{fluorine}}}{n_{\text{hydrogen}} + 4n_{\text{carbon}}} \qquad [2]$$

where n = the number of gram atoms of a particular species.

The effective heat of formation Q_F' is defined as the total heat required to convert the reactants at their entrance temperatures to their elements in their standard states at 298.16 K. Thus, in the most general case for liquid propellant systems

$$Q_{F(m)}' = \sum_{ox,\,fl} \left[W\,(\Delta H_F - \Delta H_V + \int_T^{298} C_p dT) \right] \qquad [3]$$

where

W = weight fraction
ΔH_F = standard heat of formation, cal/g
ΔH_V = heat of evaporation at the boiling point, cal/g
C_p = heat capacity, cal g^{-1} K^{-1}
m, ox, fl = subscripts for mixture, oxidizer, fuel respectively

The sign convention for Q_F' is that of Bichowsky and Ros-

Presented at the ARS Fall Meeting, Los Angeles, Calif., Sept. 18–21, 1955.

[1] The work reported herein was carried out under Contract No. AF 33(600)-28469 with the United States Air Force.

[2] Formerly Research Engineer, Propulsion Field Laboratory, Research Section.

[3] Supervisor, Propulsion Field Laboratory, Thermodynamics and Analysis Unit, Research Section.

[4] Research Engineer, Propulsion Field Laboratory, Research Section. Mem. ARS.

[5] Numbers in parentheses indicate References at end of paper.

sini. The ΔH_V term in Equation [3] is only applicable to those propellants which are normally gaseous at 298 K, but which are injected as liquids.

The numericalization of the variables may be illustrated with the following hypothetical propellant

$$C_cH_hO_oN_nF_f\text{(fuel)} + x\ C_{c'}H_{h'}O_{o'}N_{n'}F_{f'}\ \text{(oxidizer)}$$

It is convenient to assume 1 g mole of fuel and x g moles of oxidizer for the propellant mixture. Hence

$$OR = \frac{2(o + xo') + 1(f + xf')}{4(c + xc') + 1(h + xh')} \qquad [4]$$

The mixture ratio r is evaluated for use in the determination of $Q_{F(m)}'$. Thus

$$r = \frac{x\,[C_{c'}H_{h'}O_{o'}N_{n'}F_{f'}]}{[C_cH_hO_oN_nF_f]} = \frac{\text{g}\cdot\text{oxidizer}}{\text{g}\cdot\text{fuel}} \qquad [5]$$

where brackets indicate the gram molecular weight (or gram atomic weight) of the species bracketed. Now

$$Q_{F'm)}' = \frac{Q_{F(f)}' + rQ_{F(ox)}'}{r + 1} \qquad [6]$$

$$\%\ N_{(m)} = \frac{100\ (n + xn')N}{[C_cH_hN_nO_oF_f] + x\ [C_{c'}H_{h'}N_{n'}O_{o'}F_{f'}]} \qquad [7]$$

$$\frac{C}{C + H} = \frac{[C]\ (c + xc')}{[C]\ (c + xc') + [H]\ (h + xh')} \qquad [8]$$

$$\frac{O}{O + F} = \frac{[O]\ (o + xo')}{[O]\ (o + xo') + [F]\ (f + xf')} \qquad [9]$$

The computations were performed by an IBM Type 701 digital electronic data processing machine enabling a direct tabulation of the following parameters

A Combustion chamber conditions
  1 Temperature
  2 Equilibrium composition
  3 Enthalpy of products
  4 Entropy of products

B Nozzle exit conditions
  1 Temperature
  2 Composition (identical to A2 above)
  3 Enthalpy of products
  4 Entropy of products

C Specific impulse; the assumptions and conditions may be summarized as
  1 Adiabatic combustion
  2 Equilibrium composition of combustion products frozen at chamber conditions
  3 Isentropic expansion of ideal gas
  4 Combustion chamber pressure = 500 psia
  5 Nozzle exit pressure = 14.7 psia
  6 Optimum area expansion ratio at sea level

Thermodynamic data were based, whenever possible, upon the selected values of the National Bureau of Standards and were interpolated from a tabular compilation with a 100 K temperature interval. The errors in the equilibrium composition were held to less than 0.02 per cent, enthalpy and entropy balances to less than 0.1 per cent. Twenty-one species, namely, CF_4, CF_3, CF_2, CF, CO_2, CO, HF, H_2O, OH, NO, COF_2, H_2, N_2, O_2, F_2, H, N, O, F, C (gas) and C (graphite) were considered in computing the composition. In cases where there were solid products of combustion, I_{sp} was computed for various velocities of the solid particles from zero to the velocity of gas.

The range of variables, chosen to include most of the propellant combinations of probable interest, is

$\dfrac{C}{C + H}$ (weight ratio) = 0 to 1

$\dfrac{O}{O + F}$ (weight ratio) = 0 to 1

Per cent N (weight per cent) = 0 to 45 (and in some cases to 60)

Q_F' (cal g^{-1}) = −300 to +600 (and in some cases to +900)

OR = 0.4 to 1.0 (and in some cases 0.1 to 1.0)

Discussion

From the tabular data compiled from the IBM "printouts" it is possible in principle to construct a hyperspace, either a Euclidean or non-Euclidean six-space, which would represent the dependency of I_{sp} on the five chosen independent variables. Despite the inability to visualize such a hyperspace, it is, in practice, entirely possible to handle the space mathematically. Such a representation is anticipated; however, the IBM data can be handled with equal effectiveness by the simple expedient of cross-plotting and interpolating, and this is the method of representation illustrated in Figs. 1, 2, 3, and 4. The versatility of this type of representation will be demonstrated shortly.

In general, the accuracy of I_{sp} data obtained from the generalized charts is ±0.5 per cent. Table 1 illustrates the magnitude of the differences which can be expected between I_{sp} values determined from the charts and those derived from detailed calculations. Some extrapolation is valid to determine the I_{sp} of propellant combinations (i. e., propyne-liquid-oxygen in Table 2) for which some of the variables are outside the range of this solution. Thus, a curve of I_{sp} vs. Q_F' may be extrapolated as much as 300 cal/g with reasonable accuracy (probably a total error in I_{sp} of ±1.0 per cent). The specific impulse may also be extrapolated somewhat to higher nitrogen concentrations or to higher oxidation ratios.

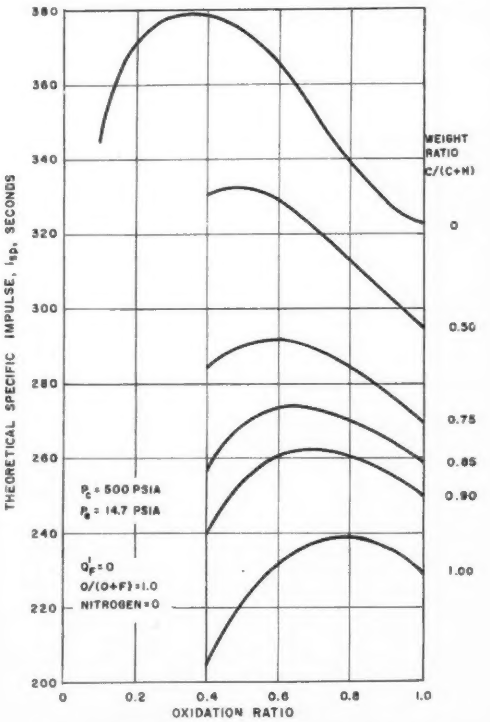

Fig. 1 I_{sp} **as a function of oxidation ratio and C/(C + H) weight ratio for C-H-O system**

However, extrapolating to oxidation ratios below 0.4 may introduce appreciable error.

Perhaps few problems are of greater interest or importance than that of quantitatively predicting the effect on performance of structural modifications in a given molecule. The generalized charts are admirably suited to yield such information in a time interval $^1/_{50}$ to $^1/_{100}$ of that normally required by detailed calculations. For example, to determine the relative effect on specific impulse of introducing unsaturation into a hydrocarbon molecule on the one hand, as opposed to substituting nitrogen for carbon on the other, as in the sequence

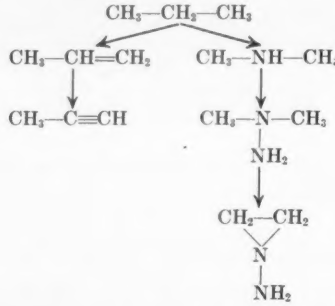

families of curves such as those given in Fig. 5 are useful. Herein, performance is plotted as a function of C/(C + H), Q_F', and per cent N, whereas the constant variables are O/(O + F) = 1 (liquid oxygen) and OR = 0.6. For the cited example, a complete tabulation of the variables, along with the performances derived from Fig. 5, is given in Table 2. In this case, for convenience, Q_F' of the fuels is assumed equal to the standard heat of formation. The significant point is that skilled interpolation from Fig. 5 permitted the determination of the I_{sp} values listed in Table 2 in 30 min compared to an estimated 35 to 50 hr required to give the same results by detailed calculations with a standard desk-top calculator. Complete performance curves for each fuel with liquid oxygen can be obtained from a series of four curves similar to Fig. 5 and covering four (or more if desired) discreet values of the oxidation ratio. Total time required would thus be only 2 hr.

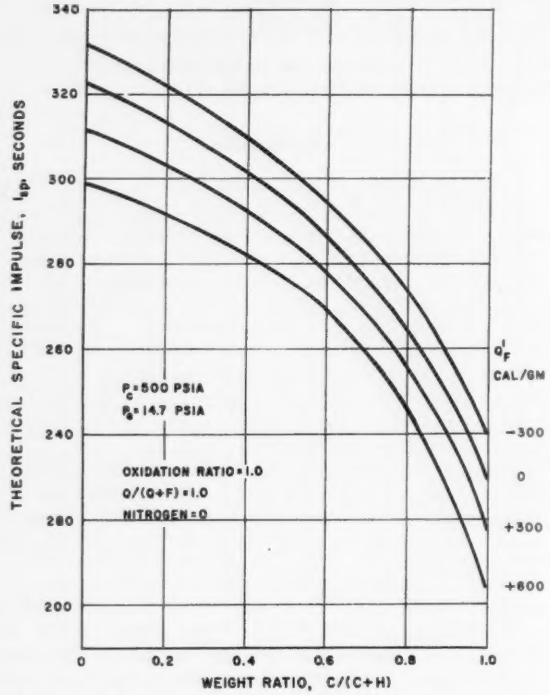

Fig. 2 I_{sp} as a function of C/(C + H) weight ratio and Q_F' for C-H-O system

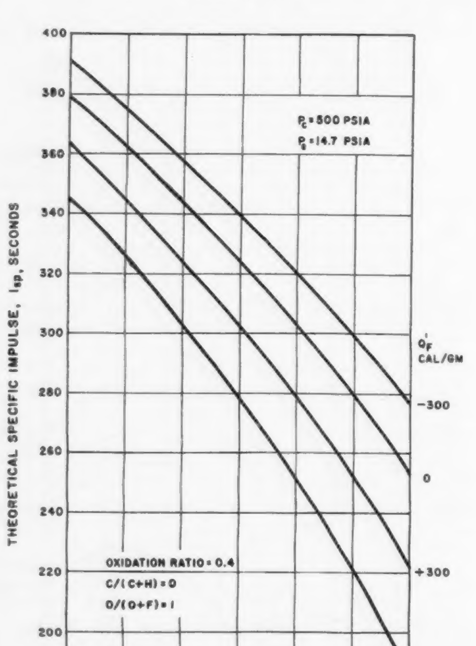

Fig. 3 I_{sp} as a function of weight per cent nitrogen and Q_F' of reactants

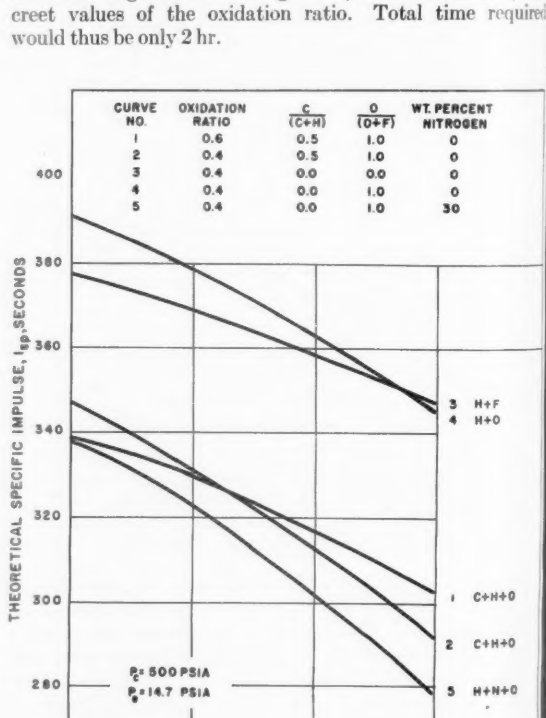

Fig. 4 I_{sp} as a function of Q_F' of reactants

It is, incidentally, apparent from Table 2 that the heat of formation, as such, is not a reliable criterion for the prediction of the performance of a given fuel.[6]

Ultimately, the generalized IBM results can be cross plotted or tabulated in every conceivable manner to give a performance manual whose utility would be limited only by the ingenuity of the user. Figs. 6 and 7, for example, illustrate solutions to other typical problems. Of course, the charts are equally applicable to problems involving solid propellant formulations. The reduction of performance to chamber and exit pressure conditions other than those given can be accomplished with reasonable accuracy from thrust coefficient curves available in the rocket literature. Thus,

(*Continued on page 891*)

[6] Tables of data permitting the derivation of performances of most propellant systems of present-day interest may be obtained from the author.

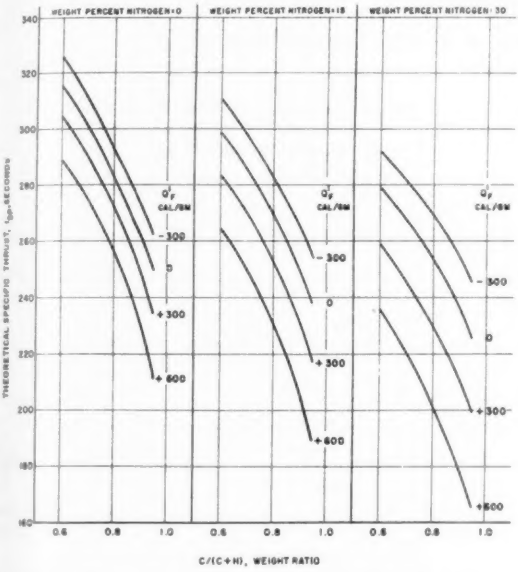

Fig. 5 Theoretical specific thrust of C-H-O-N system
Oxidation ratio = 0.6, P_c = 500 psia, P_e = 14.7 psia
Optimum expansion, frozen composition

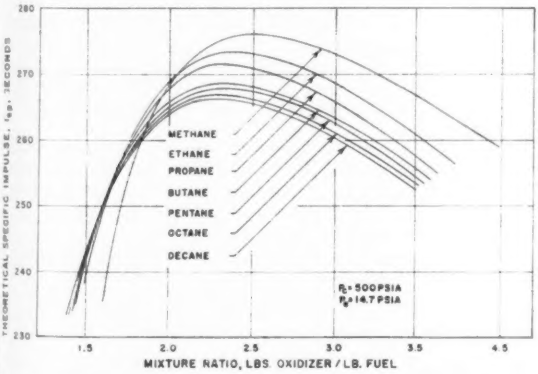

Fig. 6 Theoretical specific impulse of normal paraffins with liquid oxygen as the oxidizer

Table 1 Comparison of I_{sp} determined from generalized charts and from detailed computation

	Propellant combination	Oxidation ratio	I_{sp} from charts, sec	I_{sp} from detailed computation, sec	Difference, sec
1	Liquid oxygen Liquid hydrogen	0.4	363.0	363.4	0.4
2	Liquid oxygen Hydrazine	0.4	254.0	254.0	0.0
3	Liquid oxygen n-Octane	0.8	263.5	263.5	0.0
4	Liquid oxygen Nitropropane	1.0	248.0	247.7	0.3
5	Liquid oxygen 92.5% ethanol	1.0	247.5	248.1	0.6
6	Liquid fluorine Liquid hydrogen	0.4	363.0	363.2	0.2
7	Nitric acid Turpentine	1.0	232.0	230.0	2.0
8	Nitrogen tetraoxide Hydrazine	0.4	254.0	254.0	0.0
9	Fluorine monoxide Methylamine	0.8	298.0	298.5	0.5

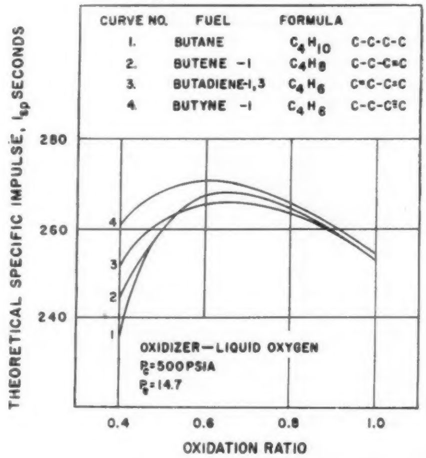

Fig. 7 Effect of double and triple carbon-carbon bonds on I_{sp}

Table 2 I_{sp} of various fuels with liquid oxygen[1]

Fuel	$Q_{F(fl)}$ cal g^{-1}	r	$Q_{F(m)}'$ cal g^{-1}	$\frac{C}{C+H}$	N, %	I_{sp}, sec
$CH_3CH_2CH_3$	+563	2.177	+243	0.8171	0	270.5
$CH_3CH{=}CH_2$	−116	2.053	+27	0.8563	0	270.5
$CH_3C{\equiv}CH$	−1106	1.917	−316	0.8994	0	274
$(CH_3)_2NH$	+182	1.597	+129	0.7729	12.0	270
$(CH_3)_2N{-}NH_2$	−201	1.278	−34	0.7487	20.5	273
CH_2 $(CH_2CH_2)N{-}NH_2$	−826	1.928	−219	0.7989	16.5	277

[1] $Q_{F(ox)} = +96.2$ cal g^{-1} and oxidation ratio $OR = 0.6$.

The Effect of Vehicle Structure on Propulsion System Dynamics and Stability[1]

ROBERT S. WICK[2]

Jet Propulsion Laboratory, California Institute of Technology, Pasadena, Calif.

In this paper, the relationship between the propulsion system and the vehicle structure is investigated. It appears that the structural behavior cannot be neglected when the propulsion system is designed. This is so because the dynamic behavior and stability of liquid propellant systems can be shown to be dependent on the structural characteristics of the vehicle it is mounted in. A general analysis of the interaction between the propulsion system and the vehicle structure is presented and also applied to a monopropellant rocket-propelled vehicle. The rocket propulsion system and the vehicle structure are analyzed by servomechanism techniques. The complete vehicle system is represented by a block diagram and appropriate transfer functions are estimated for the various portions of the system. The complete system is equivalent to a multiloop servomechanism. The Satche diagram which is analogous to a Nyquist diagram is then used to evaluate the over-all stability. The results of the stability analysis are presented in terms of the natural frequency of the vehicle structure, the combustion lag, and the distribution of mass between various portions of the vehicle.

Nomenclature

a = acceleration (ft/sec²)
A = nondimensional parameter = $2\Delta p/\bar{p}_c$
B = nondimensional parameter = $\rho\, L_l\bar{u}_3/\bar{p}\theta_g$
C = nondimensional parameter = $C' + C''$
C' = nondimensional parameter = $\rho L_l L/\bar{p}\theta_g^2$
C'' = nondimensional parameter = $\rho h L/\bar{p}_c\theta_g^2$
d = diameter of feed line or feed tank
$f(\phi)$ = some function of nondimensional time ϕ
$f(s)$ = the Laplace transform of $f(\phi)$
F = thrust of rocket motor
ΔF = variation in thrust
$\Delta F/\bar{F}$ = nondimensional variation in thrust
g = structural damping factor
G = nondimensional parameter = $L(M_1 + M_2)/F\theta_g$
h = height of propellant in feed tank
H = nondimensional parameter

$$= 1 - \frac{\rho\bar{F}L_l}{\bar{p}_c M_1}\left[\frac{1 + (h/L_l)}{1 + (M_2/M_1)}\right]$$

H' = nondimensional parameter

$$= 1 - (\rho\bar{F}L_l/\bar{p}_c M_1)$$

i = $\sqrt{-1}$
k = spring constant of vehicle structure (lb/ft)
L = arbitrary length
L_l = length of feed line between propellant feed tank and injector
L^* = characteristic chamber length
m = mass flow rate
M_1 = mass of upper portion of vehicle containing propellant feed tanks
M_2 = mass of lower portion of vehicle containing rocket motor
M_R = reduced mass of vehicle = $M_1M_2/(M_1 + M_2)$
p = pressure
Δp = pressure drop
$\bar{p}_c$ = steady-state chamber pressure
s = variable in definition of Laplace transform
t = time
$T.F.(s)$ = transfer function
$T.F._c(s)$ = transfer function of combustion chamber relating variations in chamber pressure to mass flow rate variations into the combustion chamber
$T.F._f(s)$ = transfer function of feed system relating mass flow rate variations to chamber pressure variations acting on injector face
$T.F._{f\Delta}(s)$ = transfer function relating variations in propellant flow rate to displacement of portions of the vehicle
$T.F._N(s)$ = transfer function of rocket nozzle relating variations in thrust to chamber pressure
$T.F._{P.S.}(s)$ = transfer function of rocket motor taking into account only the chamber pressure feedback loop
$T.F._{R.V.S.}(s)$ = transfer function relating variations in propellant flow rate due to chamber pressure oscillations acting through vehicle structure feedback loop
$T.F._{V.S.}(s)$ = transfer function of vehicle structure relating nondimensional displacement of the propellent feed system to nondimensional variations in thrust
u = velocity (ft/sec)
$\bar{u}_3$ = steady-state propellant flow velocity in feed line
δ = nondimensional combustion lag = τ/θ_g
Δ = displacement of a portion of the vehicle
Δ/L = nondimensional displacement of a portion of the vehicle
θ_g = gas residence time in combustion chamber
μ = nondimensional mass flow rate = $(m - \bar{m})/\bar{m}$ = nondimensional fluctuation of mass flow rate into the combustion chamber
μ_d = nondimensional mass flow rate disturbance
μ_f = nondimensional mass flow rate fluctuation due to chamber pressure acting on injector
μ_g = nondimensional fluctuation of gas rate evolution in combustion chamber
μ_i = nondimensional mass flow rate fluctuation entering combustion chamber
μ_Δ = nondimensional mass flow rate fluctuation due to displacement of a portion of the vehicle
μ'_Δ = nondimensional mass flow rate disturbance in vehicle structure feedback loop
ρ = density of propellant (slugs/cu ft)
τ = combustion lag
ϕ = nondimensional time = t/θ_g
ψ = nondimensional variation in pressure from steady state = $(p - \bar{p})/\bar{p}$

Received Oct. 20, 1955.

[1] This paper presents the results of one phase of research carried out at the Jet Propulsion Laboratory, California Institute of Technology, under Contract No. DA-04-495-Ord 18, sponsored by the Department of the Army, Ordnance Corps, and is a condensation of Jet Propulsion Laboratory Progress Report No. 20-248, listed as Reference (1) at the end of the paper. Detailed mathematical derivations and mathematical appendixes may be found therein. Subsequent Jet Propulsion Laboratory progress reports on this subject are listed as (2, 3) in the References.

[2] Research Group Supervisor; presently: Senior Scientist Atomic Power Division, Westinghouse Electric Corporation, Box 1468, Pittsburgh.

ψ_{cd} = nondimensional variation in chamber pressure from steady state due to a disturbance
ψ_{ci} = nondimensional variation from steady state in chamber pressure acting on feed system
ψ_{co} = nondimensional variation in chamber pressure from steady state due to the variation in mass flow
ω = frequency (rad/sec)
ω_n = natural frequency of vehicle structure = $\sqrt{k/M_R}$
Ω = nondimensional frequency = $\omega\theta_g$
Ω_n = nondimensional natural frequency of vehicle structure = $\omega_n\theta_g$

Superscripts

$(\bar{\ })$ = mean quantity
$(\ )^*$ = critical

Subscripts

1 = upper portion of vehicle which contains feed tanks
2 = lower portion of vehicle which contains rocket motor
T = propellant feed tank
o = injection orifice
I = case I (cf. Tables 1 and 2)
II = case II (cf. Tables 1 and 2)
III = case III (cf. Table 1)

1 Introduction

THE effect of vehicle structure on combustion stability[3] of liquid propellant rocket motors has not been considered in previous theoretical analyses (4–6).[4] The basic premise of these analyses has been that the propellant feed system is coupled to the combustion chamber only through the action of the chamber pressure on the exit of the propellant feed system. Combustion instability[5] is therefore possible since there is a time delay (the combustion lag) between the arrival of liquid propellant in the combustion chamber and the subsequent release of gaseous combustion products.

Since in the practical application of rocket motors the propellant feed system and the combustion chamber must be mounted in a vehicle, it is necessary to consider the effect of the vehicle structure on combustion stability in the rocket thrust chamber. It might be expected that motion of either the propellent feed tanks and/or the injector manifold would affect the propellant flow into the motor because of the inertia of the propellant.

In this paper the concept of combustion stability in rocket thrust chambers is expanded to include the effect of vehicle structure by use of servomechanism techniques. The over-all system consisting of vehicle structure and rocket motor is shown to be equivalent to a multiloop system. The importance of the various parameters which describe a simplified monopropellant rocket-propelled vehicle is discussed for the system type of combustion instability. The fact that some of these parameters can change during flight is also discussed.

2 General Analysis

A The Concept of a Propulsion System As a Closed-Loop Servomechanism

The concept of a propulsion system being equivalent to a closed-loop servomechanism has been discussed by several authors (7 through 11). A liquid propellant rocket propulsion system can be broken down into two components, namely, the propellant feed system and the combustion chamber, as shown in Fig. 1. If the components are assumed to be linear, conventional Laplace transform notation (12) can be used. The nondimensional mass-flow fluctuation from the feed system $\mu(s)$ is related to the nondimensiona chamber

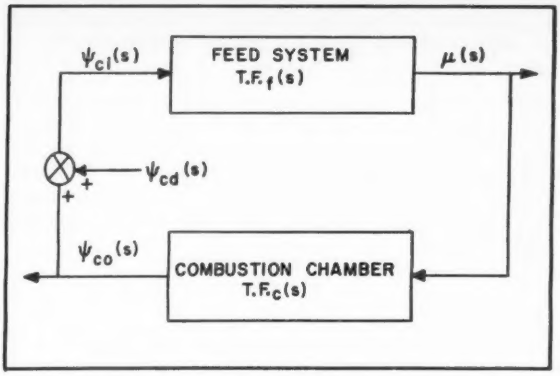

Fig. 1 Liquid propellant, rocket propulsion system

pressure oscillation $\psi_{ci}(s)$ acting on the feed system by means of the transfer function $T.F._f(s)$ of the feed system. The nondimensional chamber pressure oscillation $\psi_{co}(s)$ resulting from the variation in mass flow is related to the nondimensional mass flow into the chamber $\mu(s)$ by means of the transfer function $T.F._c(s)$ of the combustion chamber. It should be noted that no assumptions about the actual combustion and gas dynamic processes taking place in the combustion chamber need to be made in order to use this representation. The nondimensional pressure fluctuation $\psi_{ci}(s)$ acting on the injector (i.e., the feed system) is made up of two parts: the nondimensional chamber pressure fluctuation $\psi_{co}(s)$ due to combustion in the combustion chamber and a combustion chamber pressure disturbance $\psi_{cd}(s)$. The reason for this combination is subsequently made apparent. These statements can be expressed in equation form as

$$\psi_{co}(s) = T.F._c(s)\mu(s) \qquad [1]$$

$$\mu(s) = T.F._f(s)\psi_{ci}(s) \qquad [2]$$

$$\psi_{ci}(s) = \psi_{co}(s) + \psi_{cd}(s) \qquad [3]$$

Solving for the chamber pressure fluctuation $\psi_{co}(s)$ in terms of the chamber pressure disturbance $\psi_{cd}(s)$

$$\psi_{co}(s) = \frac{T.F._c(s)T.F._f(s)}{1 - T.F._c(s)T.F._f(s)}\,\psi_{cd}(s) \qquad [4]$$

The variation in chamber pressure thus depends on the nature of the disturbance $\psi_{cd}(s)$ and on the characteristics of the feed system and combustion chamber as expressed by their respective transfer functions. The significance of the disturbance $\psi_{cd}(s)$ becomes apparent as it approaches zero. If the over-all system is stable, the variation in chamber pressure approaches zero. If the over-all system is unstable, the chamber-pressure variation $\psi_{co}(s)$ increases with time. Mathematically, stability or instability is determined if the roots of the characteristic equation, obtained by equating the denominator of Equation [4] to zero, have negative or positive real parts, respectively

$$1 - T.F._c(s)T.F._f(s) = 0 \qquad [5]$$

[3] Combustion instabilities generally can be classified into two types: (a) the system type, in which flow into the combustion chamber is not steady and the pressure throughout the chamber is substantially uniform and dependent on time only, and (b) the acoustic type, in which substantial pressure waves are reflected about the chamber and the flow into the chamber may vary or be constant.

[4] Numbers in parentheses indicate References at end of paper.

[5] In theory the term instability is associated with oscillations which increase indefinitely with time, whereas in practice it is associated with oscillations of an undesirable magnitude.

B Extension of the Closed-Loop Servomechanism Concept to Include Feedback Loops Through Vehicle Structure

The extension of the block diagram representation to include the effect of vehicle structure behavior is shown in Fig. 2. The system shown is a multiloop system. The chamber pressure feedback loop is the loop just described. The second or vehicle structure feedback loop can be explained in a manner similar to that used for the chamber pressure feedback loop.

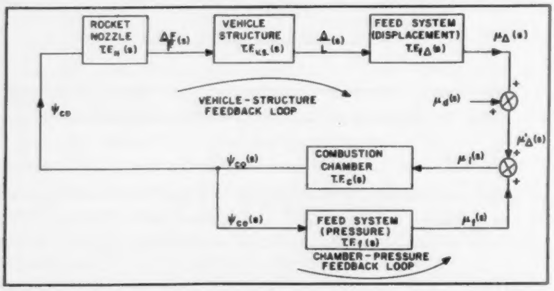

Fig. 2 Liquid propellant, rocket propulsion system mounted in vehicle structure

The nondimensional chamber pressure variation ψ_{co} acts on the rocket nozzle, described by its transfer function $T.F._N(s)$, to produce a nondimensional thrust variation $\Delta F/\bar{F}(s)$, which in turn acts on the vehicle structure, described by its transfer function $T.F._{V.S.}(s)$, to produce a nondimensional displacement of the propellant feed system and injector $\Delta/L(s)$. The nondimensional displacement $\Delta/L(s)$ acts on the propellant feed system to produce a nondimensional fluctuation $\mu_\Delta(s)$ of the propellant flow into the combustion chamber. It is tacitly assumed that the chamber pressure and feed system displacement effects on the feed system are independent of each other and combine linearly. Thus the nondimensional fluctuation of the flow rate of the propellant $\mu_i(s)$ into the combustion chamber is the sum of the flow rate fluctuation $\mu_f(s)$ resulting from chamber pressure fluctuations on the injector face (i.e., the propellant feed system), the flow rate fluctuation $\mu_\Delta(s)$ resulting from the vehicle structure displacements, and the flow rate fluctuation $\mu_d(s)$ due to the disturbance.[6] At this point the second feedback loop is complete.

It is possible to simplify the respresentation of the multiloop block diagram by replacing the chamber pressure feedback loop with an equivalent single block, as is shown schematically in Fig. 3. The transfer function $T.F._{P.S.}(s)$ of the rocket propulsion system can be calculated when the following equations relating the components of the loop are known

$$\mu_i(s) = \mu'_\Delta(s) + \mu_f(s) \qquad [6]$$

$$\mu_f(s) = T.F._f(s)\psi_{co}(s) \qquad [7]$$

$$\psi_{co}(s) = T.F._c(s)\mu_i(s) \qquad [8]$$

Solving for the chamber pressure fluctuation ψ_{co} in terms of the propellant flow rate disturbance $\mu'_\Delta(s)$

$$\psi_{co}(s) = \frac{T.F._c(s)}{1 - T.F._f(s)T.F._c(s)}\mu'_\Delta(s) \qquad [9]$$

Comparing Equation [9] with the expression for the replacement block

$$\psi_{co}(s) = T.F._{P.S.}(s)\mu'_\Delta(s) \qquad [10]$$

it is at once apparent that

$$T.F._{P.S.}(s) = \frac{T.F._c(s)}{1 - T.F._f(s)T.F._c(s)} \qquad [11]$$

It may be noted that the denominator of Equation [11] is equal to the denominator of Equation [4].

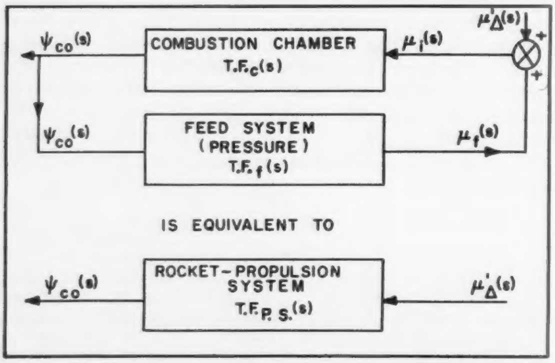

Fig. 3 Replacement of chamber pressure feedback loop by a single block

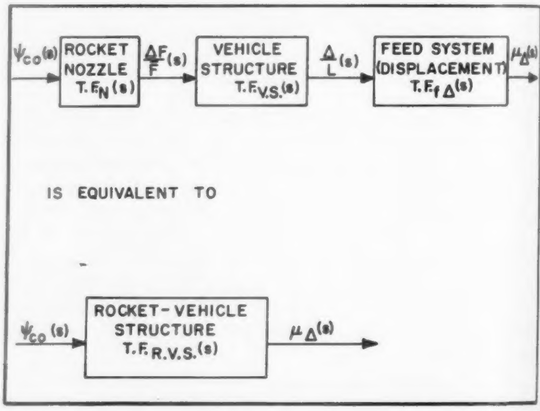

Fig. 4 Replacement of several components in the vehicle structure feedback loop by a single block

The several components making up the vehicle structure feedback loop can be replaced by a single block, as is shown in Fig. 4. The appropriate equations are

$$\frac{\Delta F}{\bar{F}}(s) = T.F._N(s)\psi_{co}(s) \qquad [12]$$

$$\frac{\Delta}{L}(s) = T.F._{V.S.}(s)\frac{\Delta F}{\bar{F}}(s) \qquad [13]$$

$$\mu_\Delta(s) = T.F._{f\Delta}(s)\frac{\Delta}{L}(s) \qquad [14]$$

and

$$\mu_\Delta(s) = T.F._{R.V.S.}(s)\psi_{co}(s) \qquad [15]$$

Thus, the rocket vehicle structure transfer function $T.F._{R.V.S.}(s)$ is

$$T.F._{R.V.S.}(s) = T.F._N(s)T.F._{V.S.}(s)T.F._{\Delta f}(s) \qquad [16]$$

The multiloop system shown in Fig. 2 can be simplified by transforming it into the equivalent single-loop system shown in Fig. 5. The appropriate equations are

$$\mu_\Delta(s) = T.F._{R.V.S.}(s)\psi_{co}(s) \qquad [17]$$

$$\psi_{co}(s) = T.F._{P.S.}(s)\mu'_\Delta(s) \qquad [18]$$

$$\mu'_\Delta(s) = \mu_d(s) + \mu_\Delta(s) \qquad [19]$$

[6] A nondimensional disturbance $\mu_d(s)$ in propellant flow rate is included instead of the chamber pressure disturbance for reasons which are subsequently made clear.

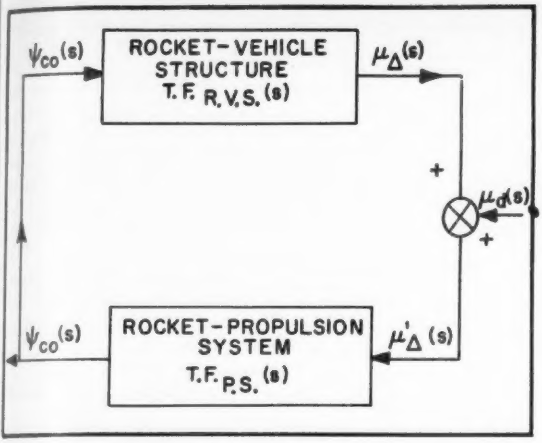

Fig. 5 Single feedback loop system equivalent to multiloop system which describes rocket motor mounted in vehicle structure

Solving for the chamber pressure fluctuation $\psi_{co}(s)$ as a function of the propellant flow-rate disturbance $\mu_d(s)$

$$\psi_{co}(s) = \frac{T.F._{P.S.}(s)}{1 - T.F._{P.S.}(s)T.F._{R.V.S.}(s)}\,\mu_d(s) \qquad [20]$$

When the expression for $T.F._{P.S.}(s)$ from Equation [11] is substituted in Equation [20], the equation for $\psi_{co}(s)$ is

$$\psi_{co}(s) = \frac{T.F._c(s)}{1 - T.F._c(s)[T.F._f(s) + T.F._{R.V.S.}(s)]}\,\mu_d(s) \qquad [21]$$

Consequently the characteristic equation is

$$1 - T.F._c(s)[T.F._f(s) + T.F._{R.V.S.}(s)] = 0 \qquad [22]$$

It may be noted that there is similarity between the characteristic equation for the multiloop system [22] and the characteristic equation for the original single-loop system. It is at once apparent that, when the transfer function $T.F._{R.V.S.}(s)$ is very small, the behavior of the multiloop system is similar to that of the single-loop system with respect to stability. It is also apparent that the additional loop can act as either a stabilizing or a destabilizing influence.

Up to this stage of the analysis, no very restrictive assumptions about the behavior of either the propulsion system or the missile structure have been made. The assumption of linear behavior is not restrictive when it is realized that, for a system indicated to be unstable by a comprehensive linear analysis, nonlinear effects invalidate this predicted instability only if they tend to limit the amplitude of the oscillations to a value acceptable from the engineering point of view. If the system were indicated to be stable by the linear analysis, instability would not result from the nonlinear effects which were neglected according to a theorem due to Liapounoff (13).

In Section 3 this analysis is applied to a simplified monopropellant rocket-propelled vehicle.

3 Application of the General Analysis to a Simplified Monopropellant Rocket-Propelled Vehicle

A Derivation of the Characteristic Equation

Most vehicles designed to be propelled by liquid propellant rocket motors are so complex structurally that it would be impossible to determine the vehicle structure transfer function $T.F._{V.S.}(s)$ by analytical methods. Consequently, in order to demonstrate the effect of vehicle structure on combustion stability, it is necessary to choose a simplified model of a vehicle.

The model chosen is shown schematically in Fig. 6. It is assumed that the mass of the vehicle can be lumped into two parts. Mass 1 consists of the rocket motor and associated

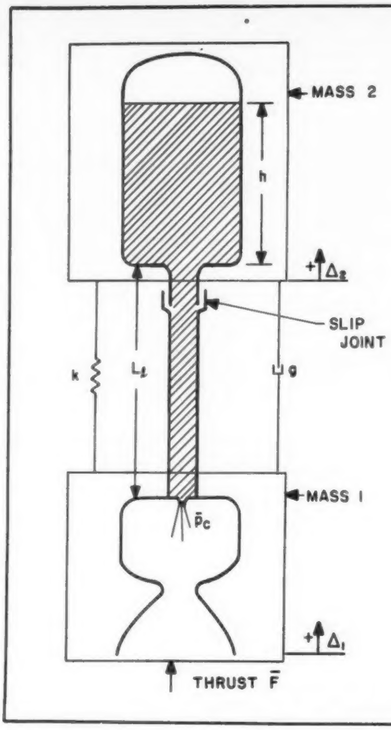

Fig. 6 Schematic diagram of simplified monopropellant rocket-propelled vehicle

mass. Mass 2 consists of the propellant feed tanks, the propellant, and the mass associated with the forward portion of the vehicle. The two masses are connected by a spring with a spring constant k which is equivalent to the structural rigidity of the vehicle. The structural damping is represented by the damping factor g. Appendix A of (1) discusses the difference between structural damping and viscous damping.

The injector manifold and the propellant feed line move with mass 1, and the feed tank moves with mass 2 because of the slip joint at the feed tank. Consequently, the propellant in the feed line and manifold is affected by the motion of mass 1, and the propellant in the feed tank, by the motion of mass 2. The block diagram representing the vehicle structure feedback loop is broken down as shown in Fig. 7. Since

$$\mu_{\Delta 1}(s) = T.F._{f\Delta 1}(s)T.F._{V.S.1}(s)T.F._N(s)\psi_{co}(s) \qquad [23]$$

$$\mu_{\Delta 2}(s) = T.F._{f\Delta 2}(s)T.F._{V.S.2}(s)T.F._N(s)\psi_{co}(s) \qquad [24]$$

$$\mu_{\Delta}(s) = \mu_{\Delta 1}(s) + \mu_{\Delta 2}(s) \qquad [25]$$

it is at once apparent that

$$T.F._{R.V.S.}(s) = T.F._N(s)[T.F._{f\Delta 1}(s)T.F._{V.S.1}(s) + T.F._{f\Delta 2}(s)T.F._{V.S.2}(s)] \qquad [26]$$

Before any further analysis can be made, it is necessary to make specific assumptions regarding the behavior of the feed system, the combustion chamber, and the nozzle. The assumptions are stated briefly; the detailed calculation of the various transfer functions can be found in Appendices A, B, C, and D of (1).

Only the system type of combustion instability is considered; consequently it is reasonable to assume that the propellant is incompressible. Summerfield's equations (5) for the combustion chamber are used as a first approximation. As is shown in Appendix D of (1), the rocket nozzle transfer function $T.F._N(s)$ can be assumed to be approximately equal to unity for the system type of instability.

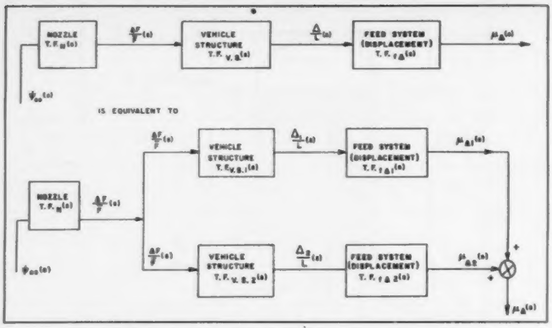

Fig. 7 Block diagram of vehicle structure feedback loop for simplified monopropellant rocket-propelled vehicle

The characteristic equation is obtained as follows by substituting Equation [26] in Equation [22]

$$1 - T.F._c(s)\{T.F._f(s) + T.F._N(s)[T.F._{f\Delta 1}(s)T.F._{V.S.1}(s) + T.F._{f\Delta 2}(s)T.F._{V.S.2}(s)]\} = 0 \qquad [27]$$

From Appendix A of (1)

$$T.F._{V.S.1}(s) = \frac{(M_2/M_R)s^2 + \Omega_n^2(1 + ig)}{s^2G[s^2 + \Omega_n^2(1 + ig)} \qquad [28]$$

$$T.F._{V.S.2}(s) = \frac{\Omega_n^2(1 + ig)}{s^2G[S^2 + \Omega_n^2(1 + ig)]} \qquad [29]$$

From Appendix B of (1)

$$T.F._c(s) = e^{-\delta s}/(1 + s) \qquad [30]$$

From Appendix C of (1)

$$T.F._f(s) = -1/(A + Bs) \qquad [31]$$

$$T.F._{f\Delta 1}(s) = C's^2/(A + Bs) \qquad [32]$$

$$T.F._{f\Delta 2}(s) = C''s^2/(A + Bs) \qquad [33]$$

From Appendix D of (1)

$$T.F._N(s) = 1.0 \qquad [34]$$

Substituting the values of the transfer function in Equation [27]

$$1 - \frac{e^{-\delta s}}{1 + s}\left\{\frac{-1}{A + Bs} + \left[\frac{\frac{C'M_2}{GM_R}s^2 + \frac{C}{G}(1 + ig)\,\Omega_n^2}{(A + Bs)[s^2 + \Omega_n^2(1 + ig)]}\right]\right\} = 0 \qquad [35]$$

where $C' + C'' = C$. This characteristic equation should be compared with that obtained for the rocket propulsion system when the effect of vehicle structure is neglected, which is

$$1 + \frac{e^{-\delta s}}{(1 + s)(A + Bs)} = 0 \qquad [36]$$

Inclusion of the vehicle structure feedback loop is responsible for an additional term which acts as a multiplication factor.

B Method for Obtaining Roots of the Characteristic Equation

The roots of the characteristic Equation [35] must be obtained in order to determine the stability of the over-all system. If the roots have positive real parts, the system is unstable; if the roots have negative real parts, the system is stable. The usual procedure is to vary one of the physical parameters in Equation [35] until roots with no real parts are obtained. This result gives the critical values of the frequency and of the parameter which was varied. The critical value is that for which disturbances neither increase nor decrease with time. Most authors have chosen the combustion lag as the variable parameter. The method of solution is discussed in detail in Appendix E of (1).

C Effect of Vehicle Structure on Combustion Stability

It is shown in Appendix E of (1) that the parameters dependent on vehicle structure are present in a single term. The nature of the vehicle structure multiplication factor depends on whether the ratio

$$\frac{H}{H'} = \frac{1 - \left(\frac{\rho\bar{F}L_l}{p_cM_1}\right)\left[\frac{1 + (h/L_l)}{1 + (M_2/M_1)}\right]}{1 - \frac{\rho\bar{F}L_l}{p_cM_1}} \qquad [37]$$

is less than, equal to, or greater than unity.

As an example, the nondimensional critical combustion lag and the nondimensional critical frequency have been calculated as a function of the structural natural frequency for H/H' greater than, equal to, and less than 1. The rocket motor parameters A and B are both equal to 0.5, and H' is equal to 0.7 for all three situations. The ratio H/H' may be varied by changing the height h of propellant in the feed tank while the masses of the two parts of the vehicle are held constant. This variation could be accomplished approximately by changing the height-to-diameter ratio of the feed tanks while the tank volume is kept constant. The values of the various parameters used in this example are listed in Table 1. It should be emphasized that there are many possible ways in which the various parameters can be varied to give different values of H/H'. In the example presented, the method chosen to vary the ratio allows the maximum number of quantities to be held constant. For the general situation, it must be remembered that the parameters H, H', Ω_n, and B are closely interrelated and that one usually cannot be varied without changing the others.

The critical combustion lag and frequency for this example are plotted vs. structural natural frequency in Figs. 8 and 9, respectively.[7] The shaded areas in Fig. 8 include values of the combustion lag for which the over-all system is stable.[8] Although the negative values of the combustion lag in Fig. 8 ($H/H' > 1.0$) are physically unreal, they represent a mathematical solution. It appears that the negative values of combustion lag are more likely to be found where $H/H' > 1.0$.

[7] The critical frequency is that frequency which corresponds to the critical combustion lag.

[8] Unstable regions in which all roots do not have positive real parts are not indicated in the figures in the main portion of the text but are discussed in Appendix E of (1).

Table 1 Values of parameters used in the example illustrating the effect of the ratio H/H' on over-all stability[1]

Case	Feed tank height	Feed tank diameter	Height-to-diam ratio	H	H'	H/H'
I	h_I	d_I	h_I/d_I	0.9	0.7	1.285
II	$3.22\,h_I$	$0.557\,d_I$	$5.78\,h_I/d_I$	0.7	0.7	1.00
III	$4.89\,h_I$	$0.452\,d_I$	$10.82\,h_I/d_I$	0.55	0.7	0.786

[1] $A = 0.5$, $B = 0.5$, and $g = 0.1$.

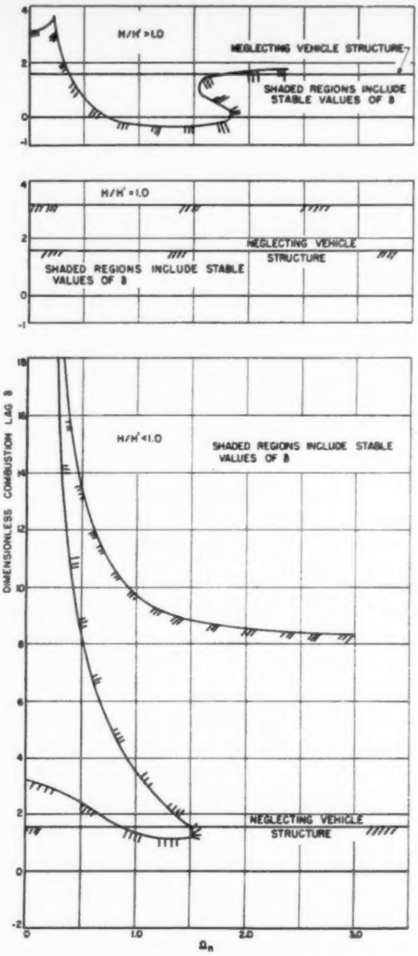

Fig. 8 Effect of vehicle structure natural frequency on the critical combustion lag for $H/H' > 1.0$, $= 1.0$, and < 1.0 ($A = 0.5$, $B = 0.5$, and $g = 0.1$)

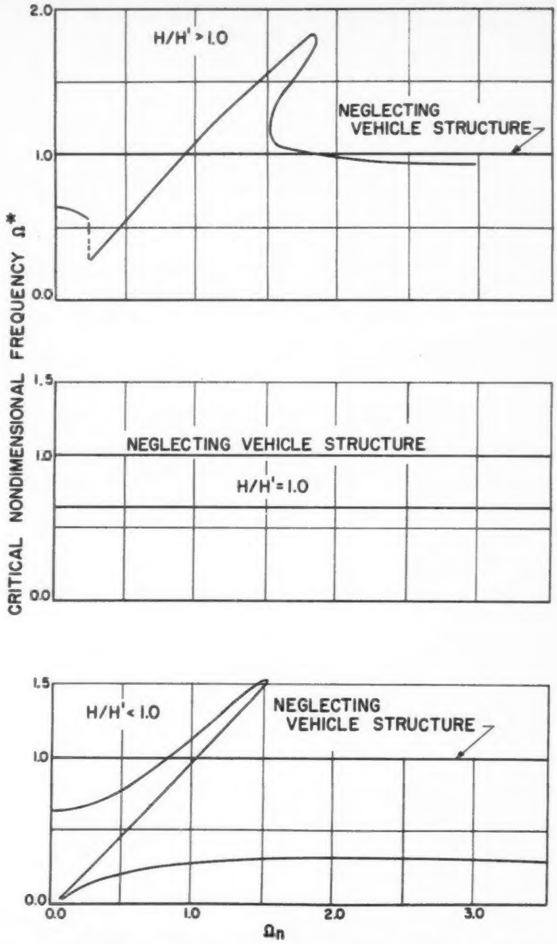

Fig. 9 Effect of vehicle structure natural frequency on the critical frequency for $H/H' > 1.0$, $= 1.0$, and < 1.0 ($A = 0.5$, $B = 0.5$, and $g = 0.1$)

It should be emphasized that the major differences in the shape of the three curves presented in Figs. 8 and 9 are due to the fact that the ratio H/H' is less than, equal to, or greater than unity rather than to the fact that the magnitude of the parameters is changed.

Several facts are at once apparent from a study of Figs. 8 and 9. First, the natural frequency of the vehicle structure has a pronounced effect on combustion stability, and there are certain ranges of vehicle structure natural frequency within which the behavior of the over-all system is dominated by the vehicle structure (in these ranges the critical frequency equals the natural frequency of the vehicle structure). Second, for a given structural natural frequency, it is possible to change the critical combustion lag and the nature of the vehicle structure vector by changing one of the physical quantities which enter into the parameters H and H'. (These parameters are interrelated, and in most instances one cannot be changed independently of other parameters.)

In the preceding and the following examples the structural damping constant g was taken to be 0.1. This value can be considered as an upper limit likely to be encountered in most conventional vehicle structures. It is instructive to consider the solution for no structural damping, i.e., $g = 0$, although it is not physically real. It is shown in Appendix E of (1) that the behavior of the vehicle structure vector depends to a great extent on whether $H/H' > 1$, $H/H' = 1$, or $H/H' < 1$ for all values of structural damping. In Figs. 10 and 11 a comparison is made between finite damping and no damping for values of $H/H' > 1.0$ and $H/H' < 1.0$, respectively. There is no difference between finite and no damping if $H/H' = 1.0$, and thus both curves are the same as that in Fig. 8 ($H/H' = 1.0$). The arrows in Figs. 10 and 11 indicate the change in position of the curves as the damping factor g is reduced to zero. In the situation where $H/H' > 1.0$, the region in which stable operation is possible at low vehicle structure natural frequencies is relatively narrow; as g approaches zero, this stable region disappears. However, for $H/H' < 1.0$, the region in which stable operation is possible at low vehicle structure natural frequencies is relatively unaffected by changes in the damping factor g.

It is possible to obtain limiting values of the vehicle structure vector at $\Omega_n = 0$ and $\Omega_n \to \infty$ for all values of damping; that is

$$\lim_{\Omega_n \to 0} \left\{ \frac{s^2 + (1 + ig)\,\Omega_n^2}{H'\left[s^2 + \dfrac{H}{H'}(1 + ig)\,\Omega_n^2\right]} \right\} = \frac{1}{H'} \qquad [38]$$

and

$$\lim_{\Omega_n \to \infty} \left\{ \frac{s^2 + (1 + ig)\,\Omega_n^2}{H'\left[s^2 + \dfrac{H}{H'}(1 + ig)\,\Omega_n^2\right]} \right\} = \frac{1}{H} \qquad [39]$$

The characteristic Equation [35] reduces to

$$1 - \frac{e^{-\delta s}}{\frac{1}{H'}(A + Bs)(1 + s)} = 0 \qquad [40]$$

as Ω_n approaches zero and to

$$1 - \frac{e^{-\delta s}}{\frac{1}{H}(A + Bs)(1 + s)} = 0 \qquad [41]$$

as Ω_n approaches infinity. These characteristic equations are identical with the one in which vehicle structure is neglected [36] except for the terms $1/H'$ and $1/H$. They can be put into identical form by letting $A' = (1/H')A$ and $B' = (1/H')B$ in Equation [40] and by letting $A'' = (1/H)A$ and $B'' = (1/H)B$ in Equation [41]. The critical time lag can be determined by assuming a pseudo rocket motor with no vehicle structure and parameters A' and B' or A'' and B'' instead of A and B.

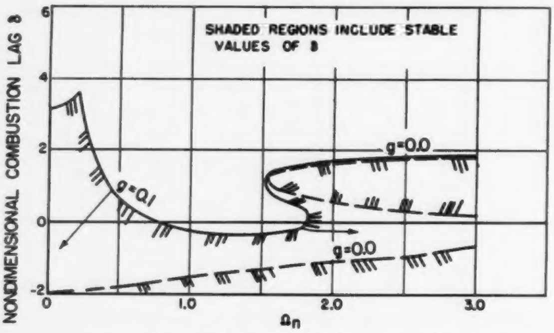

Fig. 10 Comparison of finite structural damping with no damping for $H/H' > 1.0$ ($A = 0.5$, $B = 0.5$, and $H_1 = 0.7$)

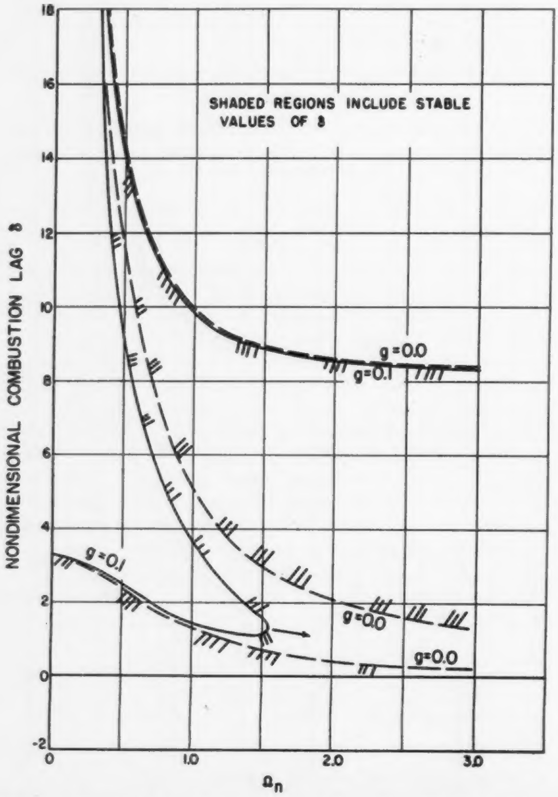

Fig. 11 Comparison of finite structural damping with no damping for $H/H' < 1.0$ ($A = 0.5$, $B = 0.5$, and $H_1 = 0.7$)

Since in most practical instances H and H' are less than unity, A' and B' and A'' and B'' are larger than A and B, and in the limiting cases $\Omega_n \to 0$ and $\Omega_n \to \infty$ the critical combustion lag is greater than the value calculated when vehicle structure is not taken into account. In other words, except in the range of vehicle structure natural frequencies where the over-all stability is extremely sensitive to vehicle structure natural frequency, the inclusion of vehicle structure has a stabilizing influence.

D Effect of Injector Pressure Drop on Combustion Stability, Taking into Account Vehicle Structure

The changes in the parameters discussed in Section 3C resulted from changing design factors outside the rocket motor and injector. According to Summerfield's theory of combustion instability, values of $A(=2\Delta p/\bar{p}_c)$ equal to or greater than unity are sufficient to assure stability for any value of combustion lag for the feed system and motor being analyzed (5). Taking into account the vehicle structure dynamics, the analysis shows that even with A equal to unity there is still a range of unstable operation. In Figs. 12 and 13 the effect of doubling the pressure drop (i.e., changing A from 0.5 to 1.0) is shown for $H/H' < 1.0$ and $H/H' > 1.0$, all other factors remaining the same. The range of possible unstable operation is limited to low vehicle structure natural frequencies. In the special instance where H/H' is equal to unity, the critical combustion lag is independent of vehicle structure natural frequency.

E Effect of Combustion Chamber Capacitance (L^* or θ_g) on Combustion Stability, Taking into Account Vehicle Structure

At this point the effect on the over-all stability of changing only the volume of the combustion chamber is considered. Increasing the volume of combustion chambers has been shown experimentally to decrease the amplitude of low-frequency oscillations (7). Moreover, the existing theories of combustion stability predict that increasing the capacitance (i.e., L^*, volume, or gas residence time θ_g) of the combustion chamber increases the critical combustion lag, all other factors being equal. For the motor and feed system characterized by $A = 0.5$ and $B = 0.5$ (neglecting the effect of vehicle structure), doubling the gas residence time θ_g by increasing the chamber volume increases the absolute value of the critical combustion lag. This fact can be appreciated only after changing the dimensionless critical combustion lag δ^* to the absolute critical time lag τ^* by multiplying δ^* by the gas residence time. Doubling the gas residence time decreases B by one half to a value of 0.25, and the dimensionless critical time lag decreases from 1.57 to 1.25. However, the decrease in δ^* is more than compensated for by the fact that the gas residence time which multiplies δ^* to obtain τ^* has doubled in value. These statements are summarized in Table 2.

The effect on the stability of the over-all system of doubling the gas residence time while holding all other parameters constant is shown in Figs. 14 and 15.[9] In these figures the same reference time $\theta_{g(B=0.5)}$ is used to nondimensionalize the combustion lag, the critical frequency, and the vehicle structure for B equal to both 0.5 and 0.25. Unlike the instance where vehicle structure is neglected, stability of the over-all system is improved only for certain values of vehicle structure natural frequency. For very low and high vehicle structure natural frequencies, there is always an improvement in the over-all system stability as the L^* is increased. It must be remembered that, if the motor mass is an extremely small portion of the total mass, any changes in L^* cause proportionate changes in motor mass and structural natural frequency.

[9] It is assumed that the percentage change in the motor and associated mass is small.

F Effect of Parameter Changes During Flight on Combustion Stability[10]

In the derivation of the preceding analytical results it was assumed that the various parameters (e.g., mass and height of propellant) in the feed tank which actually decrease during a vehicle flight are constant. It can be shown that in making a stability analysis it is perfectly reasonable to assume that quasi-steady conditions exist during any portion of the flight. Consequently the analysis for stability can be made for conditions (i.e., instantaneous values of h and M_2) corresponding to successive instants in a vehicle flight. Then it can be determined whether or not, for the existing combustion lag, instability is likely to be encountered.

[10] A detailed analysis of this topic appears in (2).

The vehicle structure natural frequency

$$\omega_n = \sqrt{\frac{k(M_1 + M_2)}{M_1 M_2}} \qquad [42]$$

increases since M_2 is diminishing at the same rate as propellant is consumed in the combustion chamber. Equation [42] can be rewritten as

$$\omega_n = \sqrt{\frac{k}{M_1}\left(1 + \frac{M_1}{M_2}\right)} \qquad [43]$$

Since the ratio M_1/M_2 is likely to be quite small even when the feed tanks are empty, it is apparent that the structural natural frequency does not increase very much during course of flight.

The ratio H/H' is likely to change during the course of a vehicle flight since H is a function of both the height h of

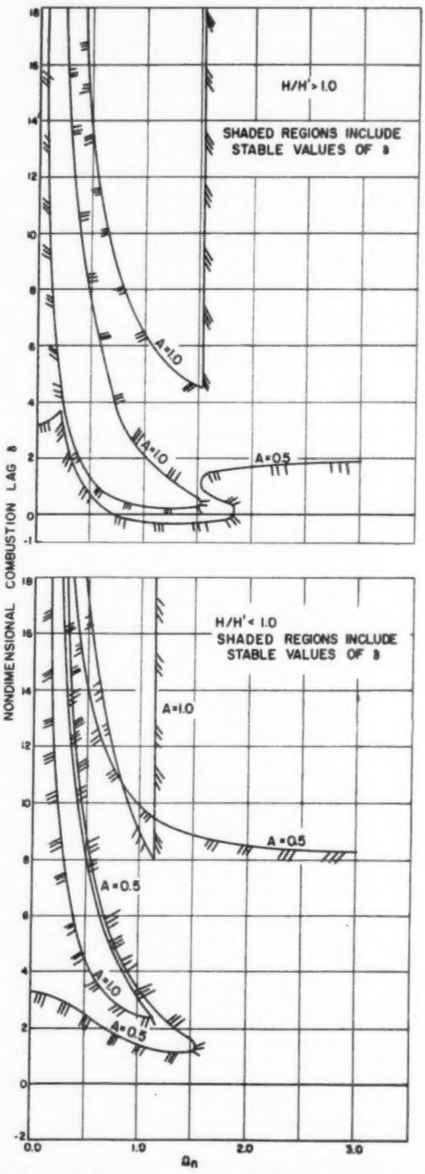

Fig. 12 Effect of injector pressure drop on curves of critical combustion lag vs. vehicle structure natural frequency for $H/H' > 1.0$ and < 1.0 ($B = 0.5$ and $g = 0.1$)

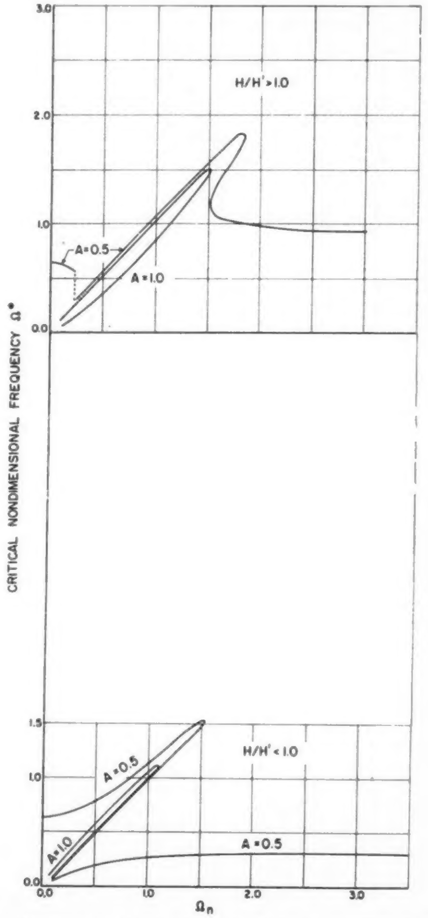

Fig. 13 Effect of injector pressure drop on curves of critical frequency vs. vehicle structure natural frequency for $H/H' > 1.0$ and < 1.0 ($B = 0.5$ and $g = 0.1$)

Table 2 Values of critical combustion lag and frequency reduced to a common time base illustrating the effect of L^* on stability

Case	A	B	θ_g	δ^*	τ^*	Ω^*	ω^*
I	0.5	0.5	θ_{g_I}	1.571	$1.571\,\theta_{g_I}$	1.000	$1.000/\theta_{g_I}$
II	0.5	0.25	$2\,\theta_{g_I}$	1.23	$2.46\,\theta_{g_I}$	1.33	$0.67/\theta_{g_I}$

propellant in the feed tank and the mass M_2 of the upper portion of the vehicle.

$$H = 1 - \frac{\rho \bar{F} L_l}{\bar{p}_c M_1}\left[\frac{1 + (h/L_l)}{1 + (M_2/M_1)}\right] \qquad [44]$$

The manner in which H changes depends entirely on how the quantity

$$\frac{1 + (h/L_l)}{1 + (M_2/M_1)}$$

changes during the course of flight. It is apparent that this ratio can either decrease, remain constant, or increase, depending on the relative magnitudes of h/L_l and M_2/M_1 at the beginning and end of the powered portion of the flight. It is quite conceivable that by proper design the ratio would remain constant.

As the result of H changing during flight, the ratio H/H' changes. It is thus possible that the ratio H/H' would change from a value less than to greater than unity, or vice versa. Whether increasing or decreasing change in H/H' is more desirable when design limitations do not allow a constant value depends on the range of vehicle structure natural frequency likely to be encountered as well as the values of the other parameters involved in the over-all stability.

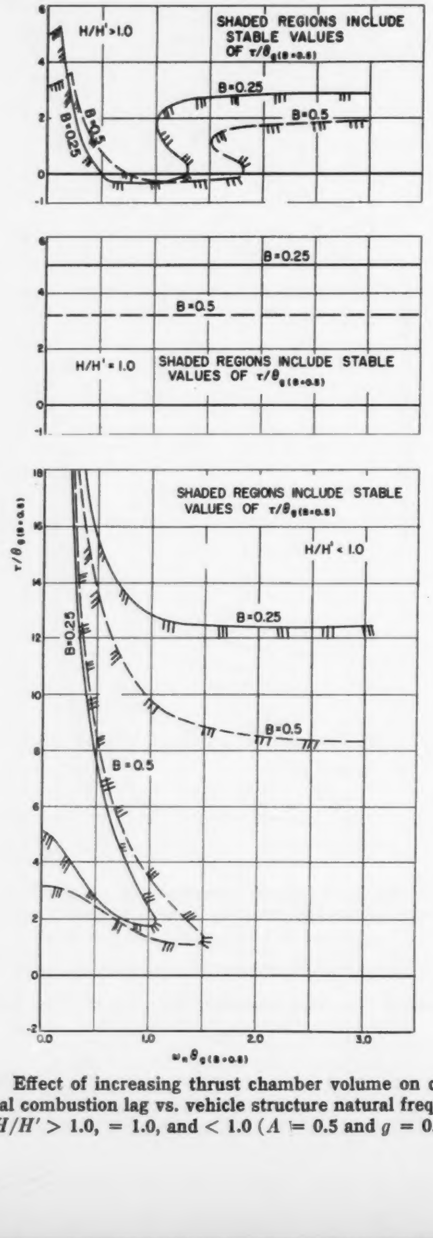

Fig. 14 Effect of increasing thrust chamber volume on curves of critical combustion lag vs. vehicle structure natural frequency for $H/H' > 1.0$, $= 1.0$, and < 1.0 ($A = 0.5$ and $g = 0.1$)

G Summary of Results for Monopropellant Vehicle

The inclusion of vehicle structure behavior in the analysis actually indicates improved stability (over the situation where vehicle structure effects are neglected) if the vehicle structure natural frequency is sufficiently high or low. In the intermediate range of vehicle structure natural frequency, the parameters which most affect combustion stability are the ratio H/H' and the vehicle structure natural frequency Ω_n.

The natural frequency of the vehicle structure analyzed depends for all practical purposes on the manner in which the thrust chamber is mounted in the vehicle. In other words, the stiffness of the thrust ring or plate which transmits the thrust to the rest of the vehicle determines the natural frequency. Consequently, the critical combustion lag is greatly influenced by the construction of the thrust ring. If a fairly flexible mounting scheme is expected (i.e., low vehicle structure natural frequencies), the analytical results show that the vehicle should be designed so that the ratio $H/H' < 1.0$; this value makes it possible to attain a stable region, even with little or no structural damping.

Whether or not the conventional methods of improving combustion stability (such as increasing the injection pressure drop and increasing the chamber volume) are effective

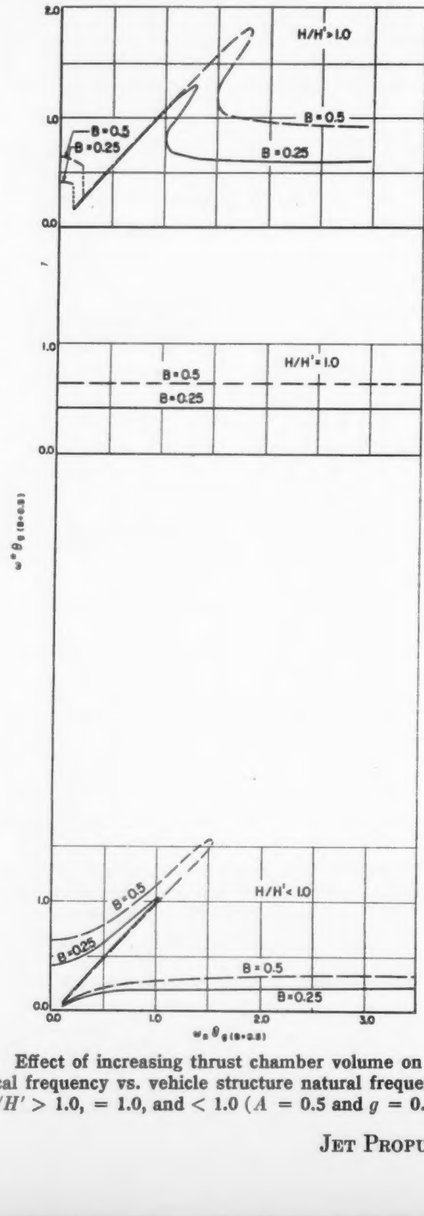

Fig. 15 Effect of increasing thrust chamber volume on curves of critical frequency vs. vehicle structure natural frequency for $H/H' > 1.0$, $= 1.0$, and < 1.0 ($A = 0.5$ and $g = 0.1$)

in improving the stability of a multiloop system depends on the entire design. These methods of improving stability appear to offer the greatest improvement if the vehicle structure natural frequency is either very high or very low.

4 Conclusions

The results obtained from the application of the general multiloop analysis to a simplified vehicle emphasize the importance of several general principles. These principles are very probably applicable to the general situation where a propulsion system is to be mounted in a flexible vehicle structure.

It has been shown that the feedback loop through the vehicle structure cannot be neglected. An extension of the analysis to include a feedback loop through static test stand structure has indicated that this feedback can not be neglected either (2). Thus, in both the development and adaptation of a propulsion system to a complete vehicle, the effect of feedback through the structural members involved cannot be neglected.

The results of the analysis of the simplified vehicle show that there are definite design criteria which can be followed to give greater assurance of stable operation. It must be emphasized that, even for the simple system analyzed as an example, the important parameters are closely interrelated, and in the actual design a number of compromises would have to be made.

Application of the analysis to actual vehicles will undoubtedly be dependent on the feasibility of obtaining experimentally most of the transfer functions required for the analysis. Theoretical studies based on the general analyses presented should give useful indications of the trends to be expected during the development of a complete vehicle.

References

1 Wick, R. S., "The Effect of Vehicle Structure on Combustion Stability in Liquid-Propellant Rockets," Progress Report 20-248, Jet Propulsion Laboratory, Pasadena, Dec. 1, 1955.

2 Wick, R. S., "The Effect of Structure of Combustion Stability on Liquid-Propellant Rockets During Flight and During Static Test-Stand Firing," Progress Report 20-274, Jet Propulsion Laboratory, Pasadena, July 29, 1955.

3 Wick, R. S., "An Analysis of the Effect of Propellant Compressibility on the Dynamic Response of Structures Containing Propellant Feed Tanks," Jet Propulsion Laboratory, Pasadena, April 1, 1955.

4 Gunder, D. F., and Friant, D. R., "Stability of Flow in a Rocket Motor," *Journal of Applied Mechanics*, vol. 17, 1950, pp. 327–333.

5 Summerfield, Martin, "A Theory of Unstable Combustion in Liquid Propellant Rocket Systems," *Journal of the American Rocket Society*, vol. 21, 1951, pp. 108–114.

6 Crocco, L., "Aspects of Combustion Stability in Liquid Propellant Rocket Motors," *Journal of the American Rocket Society*, vol. 21, 1951, pp. 163–178; vol. 22, 1952, pp. 7–16.

7 Odgers, I. L., Van de Verg, N., and Wick, R. S., "Combustion-Stability Research," Progress Report 20–203, Jet Propulsion Laboratory, Pasadena, Jan. 29, 1954.

8 Tsien, H.-S., "Servo-Stabilization of Combustion in Rocket Motors," *Journal of the American Rocket Society*, vol. 22, 1952, pp. 256–262.

9 Marble, F. E., and Cox, D. W., "Servo-Stabilization of Low-Frequency Oscillations in a Liquid Bipropellant Rocket Motor," *Journal of the American Rocket Society*, vol. 23, 1953, pp. 63–74.

10 Mullaney, G. J., and Berman, K., GET-2234, General Electric Company, Schenectady, N. Y.

11 Lee, Y. C., Gore, M. R., and Ross, C. C., "Stability and Control of Liquid Propellant Rocket Systems," *Journal of the American Rocket Society*, vol. 23, 1953, pp. 75–81.

12 Brown, G. S., and Campbell, D. P., "Principles of Servomechanism," John Wiley and Sons, New York, 1948.

13 Minorsky, N., "Introduction to Non-Linear Mechanics," Edwards Brothers, Ann Arbor, Michigan, 1947, p. 52.

Reliability of Combustion Efficiency Evaluation

(*Continued from page 866*)

librium Composition and Temperature of Chemical Reactions," NACA Report 1037, 1951.

17 Smith, R. W., Jr., Edwards, H. E., and Brinkley, S. R., Jr., "Thermodynamics of Combustion Gases: Temperatures of Methane-Air and Propane-Air Flames at Atmospheric Pressure," Bureau of Mines Report of Investigations no. 4938, Jan. 1953.

18 Smith, R. W., Jr., Manton, J., and Brinkley, S. R., Jr., "The Thermodynamics of Combustion Gases: Temperatures of Methane-Air, Propane Air, and Ethylene-Air Flames," Bureau of Mines Report of Investigations no. 4983, June 1953 (AD 15258).

19 Smith, R. W., Jr., Manton, J., and Brinkley, S. R., Jr., "The Thermodynamics of Combustion Gases: Temperature of Acetylene Air Flames," Bureau of Mines Report of Investigations no. 5035, Feb. 1954 (AD 26692).

20 Brinkley, S. R., Jr., Smith, R. W., Jr., and Sapsara, O., "Thermodynamics of the Combustion Products of Kerosene with Air," Bureau of Mines Report PX3-107/3, Feb. 1952.

21 Brinkley, S. R., Jr., Smith, R. W., Jr., Edwards, H. E., and Haben, M. A., "Thermodynamics of the Combustion Products of Kerosene with Air at Low Pressures," Bureau of Mines Report PX3-107/9, Aug. 1953.

22 Robertson, A. E., and Rogers, M., "Thermodynamic Charts for Ramjet Fuel Evaluation," Naval Ordnance Laboratory Memo 9552, 1948.

23 Rogers, M., Rhodes, M. M., and Robertson, A. E., "Fuel Thermo-Charts for Use in Ramjet Performance Analysis: Carbon Disulfide," Naval Ordnance Laboratory Memo 9674, 1948 (ATI 51474).

24 Rhodes, M. M., "Fuel Thermo-Charts for Use in Ramjet Performance Analysis, Acetylene (C_2H_2) and Benzaldehyde (C_6H_5CHO)," Naval Ordnance Laboratory Memo 9861, 1948 (ATI 59075).

25 Perry, J. H., "Chemical Engineer's Handbook," McGraw-Hill, New York, 3rd edit., 1950, pp. 564–568 (Distillation, J. S. Carey).

26 Hougen, O. A., and Watson, K. M., "Chemical Process Principles Charts," Wiley, New York, 1946, Figs. 63–69.

27 Spiers, H. M., "Technical Data on Fuel," British National Committee, World Power Conference, London, 5th edit., 1952.

28 Linden, H. R., and Othmer, D. F., "Combustion Calculations for Hydrocarbon Fuels," *Chemical Engineering*, vol. 54, 1947, no. 4, pp. 115–119; no. 5, pp. 148–153.

29 Linden, H. R., "The Relationship of Physical Properties and Ultimate Analysis for Liquid Hydrocarbons," *Oil & Gas Journal*, vol. 48, no. 9, 1949, pp. 60–62, 65.

30 Edmister, W. C., and Pollock, D. H., "Phase Relations for Petroleum Fractions," *Chemical Engineering Progress*, vol. 44, 1948, pp. 905–926.

31 "Flow Measurement by Means of Standardized Nozzles and Orifice Plates," ASME Power Test Codes, Supplement on Instruments and Apparatus, Part 5, Measurement of Quantity of Materials, Chap. 4, Sect. VI, "Tolerance," 1949.

32 Grey, R. E., Jr., and Wilsted, H. D., "Performance of Conical Jet Nozzles in Terms of Flow and Velocity Coefficients," NACA Report 933, 1949.

33 Penner, S. S., "Linearization Procedures for the Study of Chemical Reaction in Flow Systems," Discussion at Fifth Symposium on Combustion, based upon Guggenheim Jet Propulsion Center/California Institute of Technology Technical Report no. 1, Contract DA 04-495-Ord-446, May 1953.

34 Daniels, F., "Nitrogen Oxides and Development of Chemical Kinetics," *Chemical and Engineering News*, vol. 33, 1955, pp. 2370–2373.

35 "Handbook of Supersonic Aerodynamics: Properties of Gases," Aerodynamics Handbook, Staff of The Johns Hopkins University Applied Physics Labatory, NAVORD Report 1488, vol. 5, Aug. 1953.

36 Kennedy, E. C., Sonheim, D. W., and Barnes, Anna Mae, "New Mach Number Tables for Ram Jet Flow Analysis: $\gamma = 7/5$ and $\gamma = 9/7$," Consolidated Vultee Aircraft Corp. Ordnance Aerophysics Laboratory Mem. 50, April 7, 1952.

37 Bahn, G. S., Vance, Joyce F., and Howard, Sandra D., "Graphs for Reheat Performance Evaluation," General Electric Co. Data Folder DF53GL32, Jan. 5, 1953.

38 Hendrie, J. M., "Dissociation Energy of N_2," *Journal of Chemical Physics*, vol. 22, 1954, pp. 1503–1507.

Technical Notes

A Simple Method for Computing the Temperature History of a Body Entering the Atmosphere at High Supersonic Velocities

GIBSON OAKES,[1]

Boeing Airplane Co., Seattle, Wash.

A simplified method for determining the temperature history of any point on a re-entry body is presented. This method relates to atmospheric entry under any assigned values of prescribed initial conditions, such as altitude, velocity, and path angle. Derivation of velocity variation with respect to altitude leads to the transient temperature rise defined by a first order, nonlinear differential equation of the fourth degree with variable coefficients, $dT_w/dy = f(T_w, y, V, h_c, \ldots)$. A procedure for numerical integration is outlined so that a solution can be readily programmed on the IBM 701 digital computer (see Ref. 6). By appropriate transfer instructions included in the programming, it is possible to solve the case in which transition from laminar to turbulent flow takes place.

Nomenclature

A, B, D, E, F = proportionality constants
A_c = cross-sectional area (base), ft²
C = specific heat of metal skin, Btu/lb°R
C_p = specific heat at constant pressure (atmosphere), Btu/lb°R
C_D = drag coefficient
e = base of natural logarithms
G = specific heat capacity = $C\tau w$, Btu/ft²°R
g = acceleration due to gravity, ft/sec²
h_c = heat transfer coefficient, Btu/ft²hr°R
k = thermal conductivity, Btu/ft hr°R
L = body station, ft
m = mass of body, slugs
p, q, r, s = power law constants
Pr = Prandtl number
R = recovery factor
Re = Reynolds number
t = time, sec
T_{aw} = recovery temperature, °R
T_f = reference (film) temperature, °R
T_w = skin temperature, °R
T_∞ = ambient (free stream) temperature, °R
V = velocity, ft/sec
w = density of skin, lb/ft³
y = vertical distance, ft
α = power law constant
β = proportionality constant
ϵ = emissivity
ζ = parameter used in solution of dTw/dy
η = altitude increment coefficient = $50000/y$
θ = entry path angle
μ = viscosity, slug/ft sec.
ρ = density of atmosphere, slug/ft³
σ = Stefan-Boltzmann constant Btu/ft²hr°R⁴
τ = skin thickness
ψ = drag-mass parameter = $C_dA_c/2m$

Subscripts

f = mean film (boundary layer) conditions
n = ordinal index $n = 0, 1, 2, 3, \ldots$
0 = initial conditions
tr = transition from laminar to turbulent flow
∞ = free stream conditions

Introduction

IT IS generally recognized that the heating rates associated with the re-entry of a body into the atmosphere can be very severe. These heating rates are caused by the high velocity that is, in general, a consequence of flight at high altitudes. The change from kinetic to thermal energy near the body's surface brings about high boundary layer recovery temperatures. For example, at Mach 10, the temperature in the boundary layer is sufficient to vaporize diamond.

At such high speeds, however, a temperature difference will exist between the adiabatic wall and the surface. Thus the severity of the surface temperature condition is mitigated in part by the inherent thermal capacitance of the skin, a function of specific heat, density, and material thickness. Furthermore, at high speeds and high skin temperatures, materials of high surface emissivity lose heat to the atmosphere through radiative heat transfer. While the equilibrium surface temperature is influenced only by convective heat input and radiative heat output, the transient temperature rise of the re-entry body involves, in addition, consideration of thermal lag as a mechanism of temperature limitation. It is with the transient case that we shall be concerned in this paper.

The solution of the heat balance equation involved is a complicated process by virtue of its nonlinearity. It is therefore a tiresome task if a complete temperature history of the entire surface must be had. The variable coefficients require that the process be step-by-step with a large number of input parameters. Various initial velocities, body stations, path angles, etc., require many independent solutions if trends are desired.

Determination of the convective heat transfer coefficient is of primary importance since the value associated with a turbulent boundary layer can be an order of magnitude greater than that for laminar flow. Unfortunately, the factors that influence the transition from laminar to turbulent flow are only partly known.

The Reynolds' number corresponding to transition from laminar to turbulent flow is dependent on a number of variables, among which are Mach number, surface temperature to free stream temperature ratio, surface roughness, and pressure gradient (5).[2] While the qualitative effects of these variables are known, their quantitative interaction is at present open to conjecture, the validity of which rests on the outcome of future tests. To cover this current uncertainty with respect to transition Reynolds' number Re_{tr}, the solution of the differential heat transf r equation is so programmed that there is a "built-in" shift from laminar flow h_c to turbulent h_c by means of a transfer instruction executed when any assigned "input" Re_{tr}, which is fed into the program, is reached. As more reliable data on Re_{tr} is acquired, the problem can be repeated with the corrected value fed in.

The total program involves stepwise listing of density and velocity variation with respect to altitude and the placing of such information in electrostatic storage in the IBM 701 computer for use in the final solution of the differential equa-

Received July 16, 1956.
[1] Design Specialist; now with Aerophysics Development Corp., Santa Barbara, Calif.
[2] Numbers in parentheses indicate References at end of paper.

EDITOR'S NOTE: This section of JET PROPULSION is open to short manuscripts describing new developments or offering comments on papers previously published. Such manuscripts are published without editorial review, usually within two months of the date of receipt. Requirements as to style are the same as for regular contributions (see first page of this issue).

tion of temperature rise. The analysis below presents the procedure in sufficient detail so that any re-entry case can be successfully programmed.

Assumptions

1 Path angle θ is assumed to be constant throughout the entire re-entry phase.

2 Heat received by the skin due to radiation from the sun or surrounding atmosphere or from interior parts of the body is not considered.

3 Heat losses are due to Stefan-Boltzmann radiation only.

4 The skin thickness τ is sufficiently small so that the temperature gradient through it is negligible.

5 The convective heat transfer coefficient will be expressed by

$$h_c = A\,\frac{k_f}{L}\,Re_f^{\alpha}\,Pr_f^{0.33}$$

in which

Constant	Laminar flow	Turbulent flow
A	0.575	0.0296
α	0.50	0.80

Procedure

Density vs. Altitude

Although the relationship between altitude and density is given in a number of sources, e.g., NACA (1) and Newell (2), a suggested approximation is an expression such as $\rho = \rho_0 \exp\{\beta(i\Delta y - a)\}$ where $a = \eta\Delta y = 50{,}000$ ft, $0 \leq i \leq \eta$; i being any altitude increment coefficient within a given altitude range, such as those shown in Table 1.

Close agreement with (1) is shown by the density vs. altitude plot in Fig. 1.

Table 1

Altitude range, ft	ρ_0, slug/ft^3	β
0–50,000	2.5×10^{-3}	3.568×10^{-5}
50,000–100,000	4.2×10^{-4}	5.149×10^{-5}
100,000–150,000	3.2×10^{-5}	4.605×10^{-5}
150,000–200,000	3.7×10^{-5}	3.348×10^{-5}
200,000–250,000	6.0×10^{-7}	2.773×10^{-5}

Velocity History

A body of mass m in entering the atmosphere at an angle θ with respect to the earth's surface behaves in the manner shown in Fig. 2 (Ref. 7)

$$m\,\frac{dV}{dt} = mg \sin\theta - m\rho\psi V^2 \qquad [1]$$

$$mV\,\frac{d\theta}{dt} = mg\cos\theta \qquad [2]$$

When, however, V is high supersonic, of the order of 10,000 fps or greater, the relationship specified in [2] is of vanishing importance and assumption 1 is valid.

As will be seen later, it is desirable to make y the independent variable rather than t. Thus, remembering that

$$\frac{dy}{dt} = V\sin\theta \qquad [3]$$

it is seen that, by substitution of [3] into [1]

$$V\sin\theta\,\frac{dV}{dy} = g\sin\theta - \rho\,\psi V^2 \qquad [4]$$

For convenience in determination of velocity history during

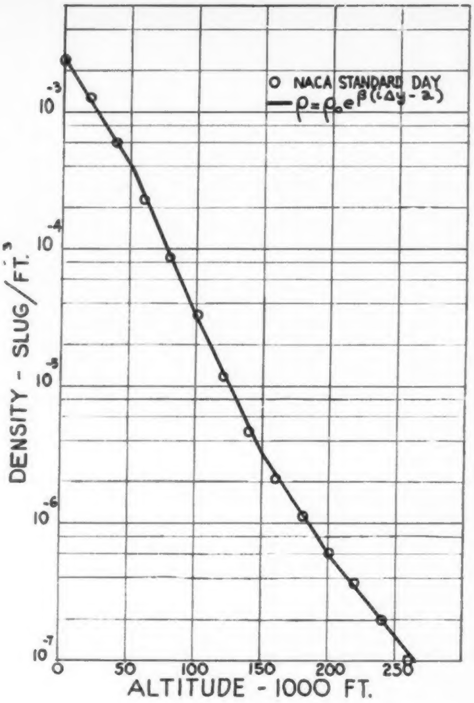

Fig. 1 Variation of density with altitude

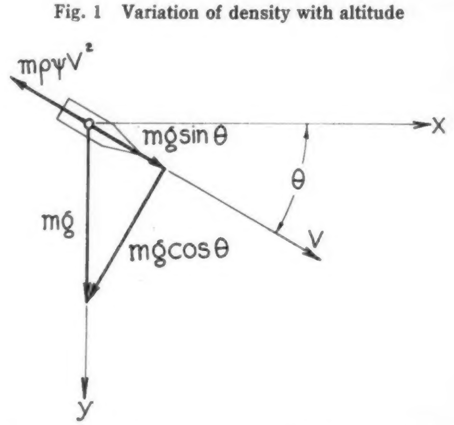

Fig. 2 Forces acting on a body entering the atmosphere

re-entry, the finite difference form [5] will be used

$$\left.\begin{aligned} V &= V_{n-1} \\ dV &= V_{n-1} - V_n \\ dy &= \Delta y \end{aligned}\right\} \qquad [5]$$

Thus

$$V_n - V_{n-1}\left[\left(1 - \frac{\rho\psi\Delta y}{\sin\theta}\right) - \frac{g\Delta y}{V_{n-1}{}^2}\right] \qquad [6]$$

Equation [6] is simple and reasonably accurate as long as the interval Δy is small.

Temperature History

The transient temperature rise of the body during descent is defined by

$$\frac{G\,dT_w}{dt} = h_c(T_{aw} - T_w) - \sigma\epsilon\,T_w^{4} \qquad [7]$$

The solution of this equation by numerical methods is best accomplished by making altitude y the independent variable rather than time t, since h_c is more readily expressible as a function of y than of t.

Remembering that

$$\frac{dy}{dt} = V \sin \theta$$

Equation [7] is rewritten as

$$\frac{dT_w}{dy} = \frac{h_c\,(T_{aw} - T_w)}{GV \sin \theta} - \frac{\sigma \epsilon T_w^4}{GV \sin \theta} \qquad [8]$$

The initial conditions are

Velocity	=	V_0
Skin temperature	=	T_{w_0}
Altitude	=	y_0
Ambient air temperature	=	T_{∞_0}

From these

$$\text{recovery temperature} \quad T_{aw_0} = T_{\infty_0} + \frac{RV_0^2}{2gJ\ C_p}$$

or

$$T_{aw_0} = T_{\infty_0} + BV_0^2 \ (C_p \text{ variable})$$

or, in general

$$T_{aw_n} = T_{\infty_0} + BV_n^2$$

We can now proceed toward the solution of dTw/dy using Runge and Kutta's numerical method, see (3 and 4).

(1) $T_{aw_n} = T_{\infty_0} + BV_n^2$ (see Fig. 5)
(2) $T_{f_n} = 0.50\ T_{w_n} + 0.28\ T_{\infty_0} + 0.22\ T_{aw_n}$
(3) $k_{f_n} = D(T_{f_n})^p$
(4) $Pr_{f_n} = E(T_{f_n})^q$
(5) $\mu_{f_n} = F(T_{f_n})^r$
determined from curves of K_f, Pr_f and μ_f vs. T_f in Figs. 3 and 4
(6) $Re_{f_n} = (\rho_n V_n L)/\mu_{f_n}$
(7) $Re_{f_n} - Re_{f_{tr}} \left\{ \begin{array}{ccc} & (-) & (+) \\ A & 0.575 & 0.0296 \\ \alpha & 0.50 & 0.80 \end{array} \right\}$
(8) $h_{c_n} = A(k_{f_n}/L)\ Re_{f_n}^{\ \alpha}\ Pr_{f_n}\ 0.33$
(9) $C_n = 0.106 + 0.000026\ T_{w_n}$
(10) $G_n = C_n \tau W$
(11) $\zeta_n = h_{c_n}\,(T_{aw_n} - T_{w_n})/(G_n\ V_n \sin \theta) - \sigma\epsilon\ T_{w_n}^{\ 4}/(G_n\ V_n \sin \theta)$

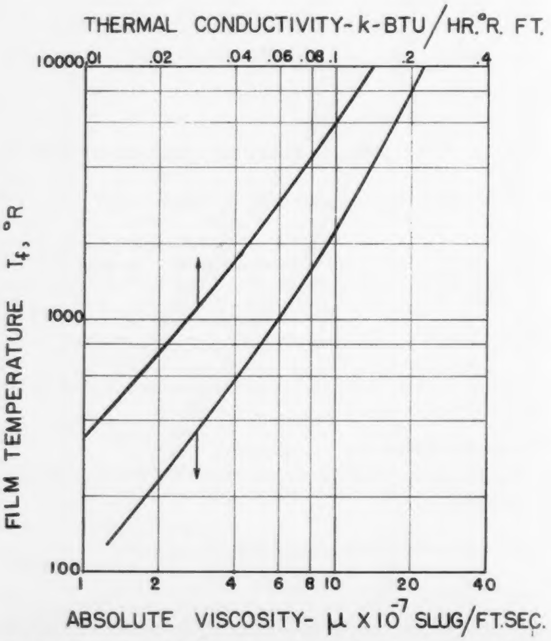

Fig. 3 Viscosity and thermal conductivity as a function of film temperature

(12) $\Delta T_{w_n} = \Delta y\ \zeta_n$
(13) Divide (12) by 2
(14) Repeat (1) through (12) using conditions of ρ, V relative to $y_n - \Delta y/2$ plus T_{w_n} plus $T_{w_n}/2$, yielding $\Delta T_{w_{n_2}}$
(15) Divide (14) by 2
(16) Repeat (1) through (12) using $y_n - \Delta y/2$ and T_{w_n} plus $\Delta T_{w_{n_2}}/2$, yielding $\Delta T_{w_{n_3}}$
(17) Repeat (1) through (12) using $y_n - \Delta y$, $T_{w_n} + \Delta T_{w_{n_3}}$ yielding $\Delta T_{w_{n_4}}$
(18) $\Delta T_{w_n} = 0.1667\ \{\Delta T_{w_{n_1}} + 2\Delta T_{w_{n_2}} + \Delta T_{w_{n_4}} + 2\Delta T_{w_{n_3}}\}$

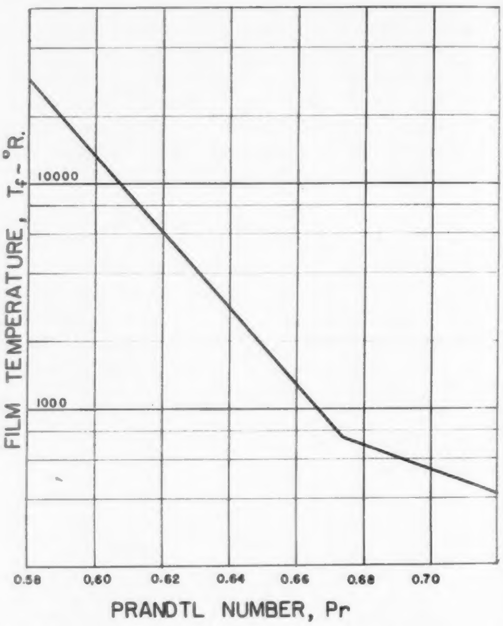

Fig. 4 Prandtl number as a function of film temperature

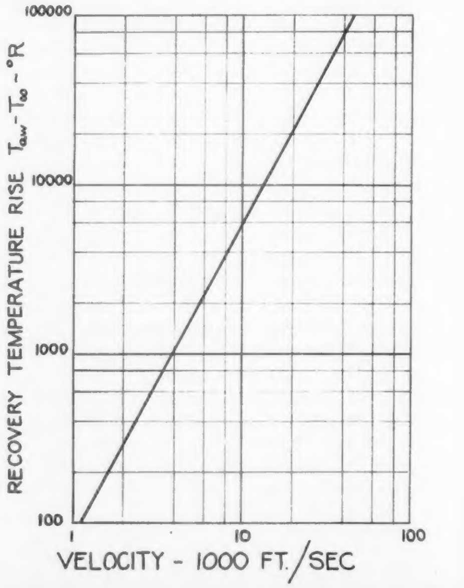

Fig. 5 Recovery temperature rise as a function of vehicle velocity

(*19*) Conditions at start of next interval are

$$y_{n+1} = y_n - \Delta y$$

$$T_{w_{n+1}} = T_{w_n} + \Delta T_{w_n}$$

(*20*) Repeat (*1*) through (*18*) for conditions stated in (*19*).

Conclusion

The method as presented here is simple, requiring only a modest mathematical background and an acquaintance with various digital computer functions. It is readily seen that manipulating the entire re-entry heating problem with a desk calculator would be both tedious and time consuming. Since the method, once programmed, proceeds rapidly toward a solution, it is apparent that a wide range of solutions is obtainable in a relatively short time. Furthermore, if a wide range of parameters is fed into the program, families of temperature history curves can be plotted by an IBM curve plotter with considerable time saving.

The procedure yields skin temperature as a function of altitude. If a plot of temperature vs. time is required, however, it is a simple matter to relate altitude with time from the velocity-altitude computation.

The author believes that, since a complete knowledge of skin temperature is essential to the successful design of a re-entry body, the time saved by resorting to this method justifies its use.

References

1 "Properties of the Standard Atmosphere," Table V, NACA TN 1428, 1947.

2 Newell, H. E., Jr., "High Altitude Rocket Research," Table 16, Academic Press, New York, 1953, pp. 136–137.

3 Ince, E. L., "Ordinary Differential Equations," Dover, New York, 1944.

4 Lo, Hsu, "Determination of Transient Skin Temperature of Conical Bodies During Short-Time, High-Speed Flight," NACA TN 1725, 1948.

5 Gazley, Carl, Jr., "Boundary-Layer Stability and Transition in Subsonic and Supersonic Flow," *Journal of the Aeronautical Sciences*, vol. 20, Jan. 1953, pp. 25–26.

6 "Principles of Operation Type 701 and Associated Equipment," International Business Machines Corp.

7. V. Kármán, Th., and Biot, M. A., "Mathematical Methods in Engineering," McGraw-Hill, New York, 1940.

Theoretical Specific Thrust of a Rocket Motor

(*Continued from page 877*)

complete performance profiles (at frozen equilibrium) can be obtained for an almost limitless number of propellant combinations.

Work is presently in progress to extend the number of elements to species of more recent interest. In addition, a generalized solution is being compiled for shifting equilibrium conditions.

Acknowledgment

This paper is based upon a generalized method first conceived by Irving A. Kanarek. The authors gratefully acknowledge his early enthusiasm and development of portions of this technique, without which this more complete execution and exposition would not have progressed so satisfactorily. In addition, many thanks are due Miss Justine Weiher for her extensive and careful work in reviewing and tabulating the data.

References

1 Sutton, George P., "Rocket Propulsion Elements," John Wiley and Sons, New York, 1949.

2 Huff, Vearl N., Gordon, Sanford, and Morrell, Virginia E., "General Method and Thermodynamic Tables for Computation of Equilibrium Composition and Temperature of Chemical Reactions," NACA Report 1037, 1951.

Jet Propulsion News

Alfred J. Zaehringer, American Rocket Company, *Associate Editor*

Japan Launches First Military Missile

On July 24, at Ojoji Proving Grounds in northeastern Japan, Self-Defense Forces launched Japan's first post-war military missile (see pictures), a solid propellant rocket designated TMA-O-AC. Despite failure of two of the nine test missiles, Defense Agency officials were impressed, feel the firings produced valuable data for the design of future guided missiles.

In this initial performance, TMA-O-AC developed almost 1000-lb thrust, reached a speed of 671 mph, an altitude of 13,000 ft. Range was a little over three miles. Other vital statistics: length, about 5 ft; diameter, 3.15 in.; fuel weight, 5.06 lb; instrument weight, 4.4 lb; gross weight, 33 lb; launching angle 70–80 deg, launcher release speed, about 671 mph. Sides of the rocket opened automatically for parachute release of recording instruments.

Essentially, TMA-O-AC is a modified version of Hideo Itokawa's (Institute of Industrial Science, University of Tokyo) "Baby" experimental rocket and, like the "Baby," is manufactured by Fuji Precision Machinery Co.

A second military rocket, larger than the TMA-O-AC, is already on its way. Designated TMB, it will be produced by Shin Mitsubishi Heavy Industries. Test firing of this new and larger rocket is scheduled to take place any day now.

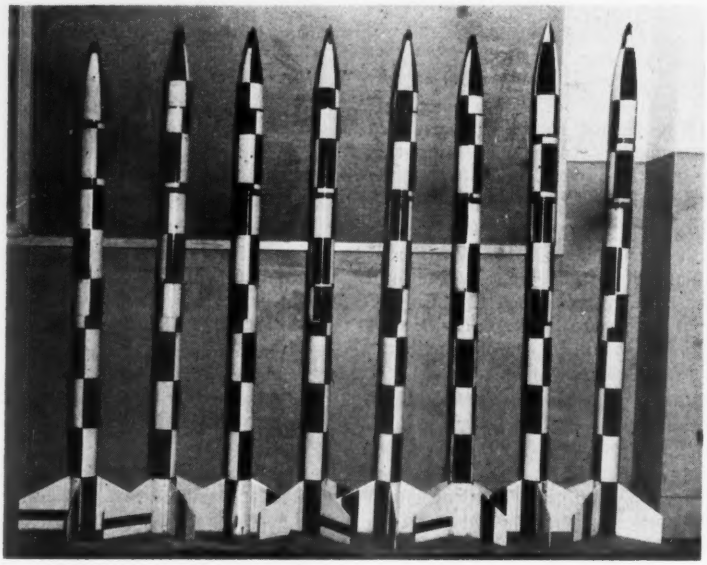

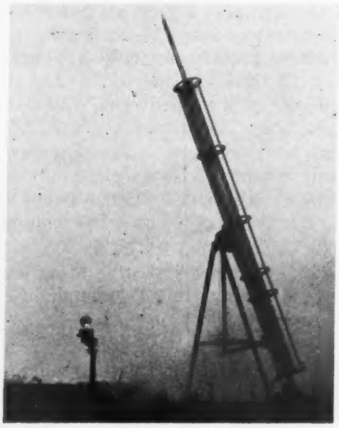

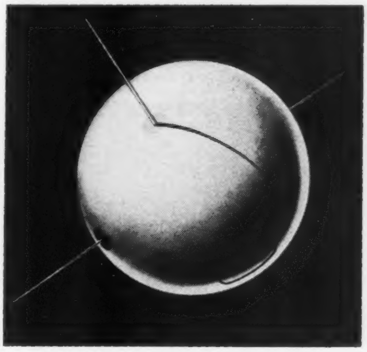

SATELLITE: First step to the moon

Moon-Glow

AT THE opening session of Massachusetts Institute of Technology's recent seminar on Satellites and Orbital Vehicles, Donald H. Menzel, director of the Harvard Observatory, predicted interplanetary travel will take place within the next decade. First step on this journey, said Dr. Menzel, will be the launching of man-made satellites scheduled for the upcoming International Geophysical Year.

Later, in Detroit, satellite fabricator Brooks & Perkins, Inc., added more details. A hollow magnesium sphere, according to B & P, the first satellite vehicle will be smooth and mirror-bright. Each half will be drawn from a single sheet of magnesium alloy. The skin will be one-fiftieth of an inch thick, have four antennas protruding from its surface. The sphere will be 20 in. in diameter, weigh about 4 lb, carry 17 lb to 18 lb of closely packed recording and telemetering equipment.

Inside, in addition to the electronic equipment, there will be strengthening pieces, battery supports, instrument attachment brackets, antenna supports and built-in pressure chambers. Most of these will also be made of magnesium, some being gold-plated as well. Screws will secure the skin to the bracing.

Launching of the first satellite will take place some time after July 1, 1957, from Cape Canaveral. The vehicle will circle the earth at 18,000 mph in what Naval Research Laboratory scientists expect will be an elliptical orbit ranging in altitude from 200 to 800 miles. No one knows how long the satellite will remain in space; predictions range from a few hours to months. When the vehicle slows and starts to fall back into the denser upper air, experts figure it will disintegrate in flames like a meteor.

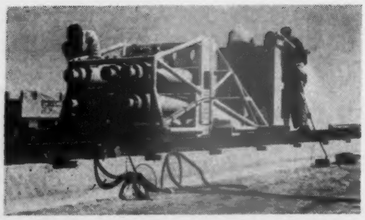
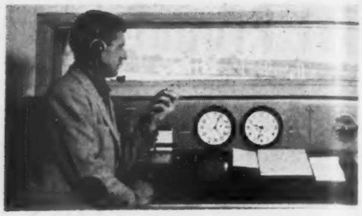

Atop mesa, test sled, readied for supersonic rocket run, takes off, passes control blockhouse, and...

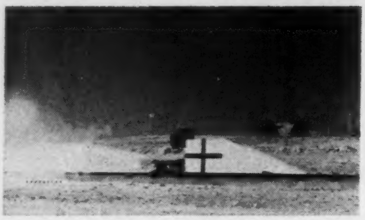

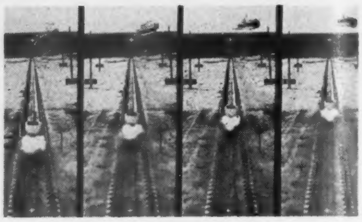

...heads down 12,000-ft track. Hydraulic arrestor and water brake stop sled; dummy hurls over mesa.

SMART: Fast Track and No Speed Limit

NOW in full operation, SMART (Supersonic Military Air Research Track) is the newest addition to military's high speed rocket test tracks. Located near Zion Park (Utah), SMART serves as a research center for problems on high speed ejection, bailouts, and survival equipment.

Unlike other test tracks at Edwards, Inyokern, and Holloman, SMART is set atop a 1500-ft-high mesa, ends its 12,000-ft run just short of the mesa's edge. At the end of a run, test items can be hurled over the edge of the cliff, thus achieving more realistic results.

Test runs have already topped Mach 1.25, are expected to reach Mach 2 before the year is out. Both liquid and solid propellant rockets are used as power plants. Among rockets used so far—individually and in combination—have been HVAR'S with burning time of 0.86 sec, 5KS-4500's, 224B-1's with burning time of 4.6 sec, T-50's with 2.5-sec burning time, and LOKI's with 0.8-sec burning time.

Sleds generally pack six to twelve rockets and are built in two sections: a forward test vehicle and a rocket pusher sled in the rear. The forward test sled carries escape devices and is ejected over the cliff. The rocket sled, however, is stopped—with deceleration force up to 20 g—by a water brake, retro-firing rockets, and an arrestor similar to squeezer piston system in freight yards.

MISSILES

• Navy plans to spend $24 million on conversion of two merchant ships into experimental craft designed to launch Jupiter missile.

• Army has completed construction of its $12 million static firing test stand at Redstone Arsenal. The largest facility of its kind in the U. S., and possibly the world, the unit is built of reinforced concrete, has walls 4 ft thick, stands 145 ft high, and extends 20 ft underground, connecting by tunnel to an observation and control blockhouse 1000 ft away. Capable of testing intermediate range ballistic missiles, the stand is now ready for use, says the Army.

• Air Force F-89H Scorpion (see photo) caries three Falcon guided missiles and twenty-one 2.75-in. rockets in each of its two big wing-tip pods, can fire them selectively.

• One of the new guided-missile frigates authorized for construction in fiscal year 1956 will be named USS King in honor of the late Fleet Admiral Ernest J. King. It will be equipped with the Terrier missile.

• International Congress of Rockets and Guided Missiles will be held in Paris Dec. 3–8.

• As a preliminary to its part in next year's IGY program, U. S. will launch eight rockets this month and next from its newly completed site near Fort Churchill on Hudson Bay in Canada.

• Data on the Petrel air-to-surface missile, released by Navy Bureau of Ordnance, reveal essentially a winged Mark 13 torpedo powered by a J-44 turbojet engine delivering 1000-lb thrust. Other details: 24-ft length, 2-ft diam, 13-ft wingspan. The Fairchild missile is launched from a plane outside the range of enemy antiaircraft and is guided to the target by an active homing system.

• Rascal guidance system is being developed by Federal Telecommunications Lab, Nutley, N. J.

• New firm in the antimissile development race is Waltham Lab. Another is Sylvania Electric Products. The Sylvania project, with Rome Air Development Center, involves detection of intercontinental ballistic missiles. Waltham work is under Army Ordnance and involves not only detection but a complete "anti" system.

• Navaho missile, now under test at Patrick AFB, Fla., is presently using J-40 turbojets, later will use two Wright ramjets. Successful test firings have been reported.

• Jupiter A is the new name for the 200-mile Redstone missile. Jupiter C is the designation for the 1500-mile IRBM. Although not mentioned, Jupiter B may be designation for an all-solid propellant version.

• ASP is the name of the Navy's solid propellant research rocket. ASP has already hit an altitude of 30 miles. Metal parts were made by Horning-Cooper of Monrovia, Calif., while propellant was produced by Grand Central Rocket Co. The single stage rocket hit a speed of 3500 mph, used the same propellant combination that will be used in stage 3 of the Vanguard vehicle. Used for gathering cosmic ray and weather data, projectile is 12 ft long, $6^1/_2$ in. in diameter.

• M-15 rockets made by Phillips Petroleum use ammonium nitrate, carbon black, and synthetic rubber, operate over a temperature range of −75 F to 170 F.

• The X-17, a 3-stage ballistic research missile developed by Lockheed as a hypersonic test vehicle, uses solid propellant motors.

• Of the 25 SM-64's flown, 20 have been equipped with landing gear for recovery.

• Test flights of the subsonic air-to-ground missile, Crossbow, assembled by Radioplane, are now under way.

• Intermediate range Thor, now designated WS-315A is scheduled for first firing in 1957.

• Reaction Motors will build Titan rocket engine under subcontract from Aerojet. RMI, meanwhile, has privately financed a static test stand that can hold a 0.5 million-lb-thrust rocket in a vertical position and 0.2 million-lb in horizontal position.

• Range of Bomarc missile, now 200 miles, is expected to reach 300. Main production is at Seattle Boeing plant, but Wichita will be the ultimate home of the ground-to-air missile.

• Effect of rain on nose cones at Mach 2 were simulated in recent rocket sled runs at Edwards AFB, Calif. Sled used twelve 11,000-lb-thrust rockets burning for 2.2 sec, 3.9 sec, and 4.4 sec.

• New center for studying missile countermeasures will be built by Army at White Sands.

• Trimethyl aluminum is the new hypergolic (with air or oxygen) material produced by Rocky Mountain Research, Inc. (Denver, Colo.). A liquid, it has been used as an igniter for a solid-fuel ramjet burning aluminum.

• Curtiss-Wright Corp., now in control of Studebaker-Packard, recently took the wraps off its 80-sq mile development site at Quehanna, Pa., for work on atomic propulsion of missiles, revealed, among other facilities, test stands capable of handling 100,000-lb-thrust engines.

• Dart, new antitank missile unveiled by Army Ordnance (see photo), looks like a larger version of the French SS-10 rocket. Both are wire-controlled, solid propellant rockets launched from ground vehicles. Dart was designed by Aerophysics (a subsidiary of Studebaker-Packard). Production will be by Utica-Bend Corp. (another subsidiary) at Utica, Mich., under a $16 million contract.

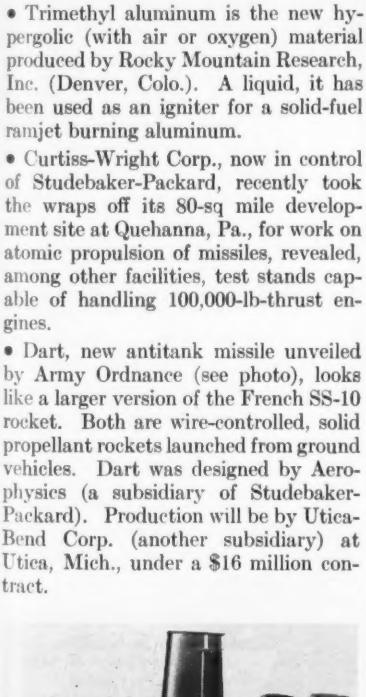

• Falcon missile is now operational on the Scorpion F-89H. In recent gunnery tests, Falcon was seen to run a 90-deg dog leg on its air-to-air mission. Falcon is also slated for operational use with F-102.

• Dan sounding rocket consists of a Nike booster plus a Deacon second stage. This rocket combination, already tested by NACA at Wallops Island, is slated for additional trials at White Sands. Dan will be used for research in the 70–100 mile region during the IGY.

AIRCRAFT

• On August 15, Colonel Horace A. Haynes, Air Research and Development Command, received the Mackay Trophy for his record 822.135 mph run in a F-100C jet at last year's Thompson Trophy Meet. Six days later, Commander Robert W. Windsor, Patuxent River Naval Air Center, bettered Col. Haynes' record by 193.293 mph in this year's Thompson Trophy Meet. Cmdr. Windsor flew a Chance Vought F8U Crusader.

• A new electronic guiding and timing system developed by Minneapolis-Honeywell Regulator Co., claims the company, will enable jet fighters and fighter-bombers to deliver atomic bombs and escape blast effects through an acrobatic maneuver known as LABS (low altitude bombing system.)

• McDonnell's XV-1 convertiplane unofficially exceeded the speed record for helicopters when it reached 200 mph recently.

• Republic Aviation Corp. has developed a twin system of airplane control similar to power steering in automobiles for high speed jet aircraft.

• Another record was broken when Korean ace Capt. Manuel J. Fernandez, flying a F-100C, won the Bendix air race on Sept. 1 with an average time of 666.661 mph. The old record, set by Capt. Edward F. Kenny in 1954, was 616.208 mph.

• Navy's new supersonic jet fighter, the Douglas X-F5D (see photo), will be armed with bombs, rockets, and missiles.

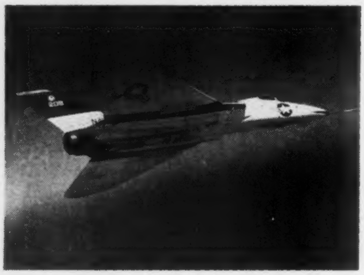

• Designed specifically for helicopter use, the Lycoming T53 gas turbine engine has completed its 50-hr preliminary flight rating test, says maker Lycoming Division, Avco Manufacturing Corp.

• Powered by a Bristol Orpheus turbojet, Italy's new lightweight tactical fighter, Fiat G.91 (see photo), successfully completed it first flight test, will now go through an operational tryout for NATO.

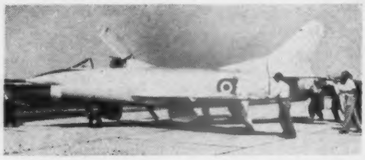

• In the first multiple refueling operation conducted from a seaplane, a Convair R3Y-2 Tradewind transport recently refueled four Navy jet fighters in mid-air (see photo).

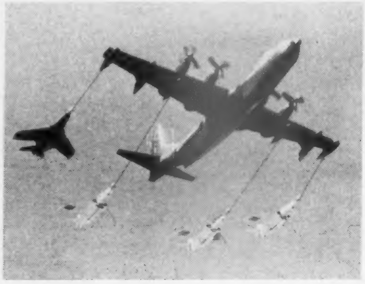

• Strategic Air Command is getting its first supersonic fighters in the form of McDonnell's F-101 Voodoo.

• McDonnell's missile-carrying F3H-2M Demon (see photo) was publicly displayed for the first time during the recent National Aircraft Show in Oklahoma.

• An Air Force Douglas B-66 jet bomber recently flew 2690 miles from Hawaii to California averaging better than 600 mph.

• Air India International has ordered three Boeing 707 jet transports for use on its long-range air routes. First delivery is slated for Jan. 1960.

• Two Army H-21C Workhorse helicopters, single-engine craft, will be adapted for twin General Electric T-58 gas turbines by Vertol Aircraft Corp. under an $1,800,000 government contract.

• A pilotless World War II F6F Hellcat drone, after breaking radio control from Pt. Mugu Missile Test Station, managed to elude two rocket-firing F89D jet chasers for more than two hours, finally ran out of fuel and crashed harmlessly in an empty field.

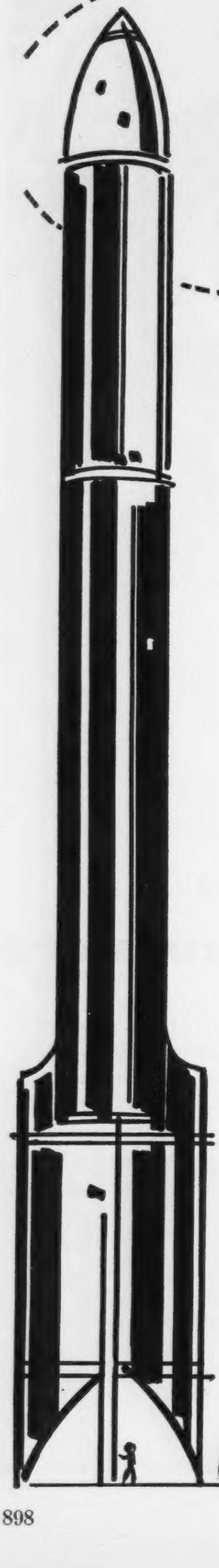

GOVERNMENT

• In its current Employment Opportunities bulletin, Navy Department's Bureau of Ordnance (Washington 25, D.C.) lists a number of openings for aircraft and missile personnel.

• Acting Secretary of the Navy Thomas S. Gates, Jr., recently presented K. T. Keller with the Distinguished Public Service Award in recognition of his service to the Naval Establishment as Director of Guided Missiles, Office of the Secretary of Defense.

• Another award by the Navy, Meritorious Civilian Service Award, recently went to Alexander Satin, chief engineer in the Air Branch of the Naval Sciences Division, Office of Naval Research, for his "leadership in initiating and coordinating a comprehensive research program in aerodynamics, structures, power plants, instruments, experimental airplanes, helicopters and other techniques and equipment used in naval air warfare."

• In a cooperative measure with National Advisory Committee for Aeronautics, Department of Defense will assign officers (from all the services) with degrees in engineering or the physical sciences to duty with NACA. Purpose is to supply NACA with technical and scientific personnel and at the same time provide active duty scientific training for selected military officers.

COMPANIES

• Elgin National Watch Co. (Elgin, Ill.) has signed a contract with Eclipse Pioneer Div. of Bendix Aviation Corp. (Teterboro, N.J.) under which Elgin will supply high precision gear trains and major assemblies for Bendix air data computers designed for jet aircraft.

• Sorenson & Co. (Stanford, Conn.) has merged with Beta Electric Corp. (New York). Both firms make electronic components used in guided missiles.

• Minneapolis-Honeywell Regulator Co. will build a $4 million plant near St. Petersburg, Fla., for development and production of inertial guidance systems.

• Sperry Rand Corp. will spend $2 million on the first unit of a new aviation electronics plant to be located on a 480-acre plant site, 15 miles north of Phoenix, Ariz.

• Pastushin Aviation Corp. (Los Angeles) has received a $1,864,000 Navy contract for manufacture of Mark 88 supersonic steel practice bombs.

• Electronic Engineering Co. (Los Angeles) will supply timing and data processing equipment for the Air Force Missile Test Center at Cocoa, Fla., under a new $800,000 government contract.

• Raymond Rosen Engineering Products, Inc. (Philadelphia), manufacturer of telemetering equipment, has

changed its corporate name to Tele-Dynamics, Inc.

• American Bosch Arma Corp. is moving its headquarters from Garden City, N.Y., to Hempstead, N.Y., as part of its new over-all expansion and modernization program. In another move, the firm recently acquired the government-owned Studebaker-Packard plant in Chicago and established a new division to help handle its growing government commitments in the aircraft and missile fields.

• North American Aviation, Inc., is building a 140,000 sq ft facility in Van Nuys, Calif., to house manufacturing, purchasing, and warehousing operations of its Atomics International division. Scheduled for occupancy in April 1957, the new building will double the company's present plant area.

• Parker Appliance Co. (Cleveland) has appointed Rocket Components Co. (Denver) as distributor for its synthetic rubber O-rings.

• Warren Wire Co. (Pownal, Vt.) is opening a branch manufacturing plant in Alhambra, Calif., for production of aircraft and missile cables.

• Consolidated Diesel Electric Corp. of Canada, Ltd., has established administrative and production headquarters in Rexdale, Ontario, to manufacture and assemble ground support equipment for jet and rocket aircraft.

• Baldwin-Lima-Hamilton Corp.'s Electronics and Instruments Div. has moved into its new $3 million plant in Waltham, Mass.

• Consolidated Avionics Corp. recently acquired 5500 sq ft of new office and plant space in Westbury, L.I., N.Y.

• Aerojet-General Corp. (Azusa, Calif.) has organized a Large Solid Rocket Advisory Committee to counsel A-G on its large solid rocket programs. Members of the committee are Bruce H. Sage (chairman), Theodore von Kármán, H. J. Stewart, C. C. Ross, R. H. Sabersky, B. L. Dorman, and A. L. Antonio.

• American Broadcasting–Paramount Theatres, Inc., and Western Union Telegraph Co. have purchased a 25% interest each in Wind Tunnel Instrument Co., Inc. (Newton, Mass.).

• Gordon Enterprises (North Hollywood, Calif.) has received a USAF contract to build a giant camera for Air Force Flight Test Center at Edwards Air Force Base. Camera will be 25 ft long, weigh 5 tons, and use a 30-in. lens.

• Solar Aircraft Co. will add 117,000 sq ft to its Wakonda jet engine components plant in Des Moines, Iowa.

INSTITUTIONS

• Engineering technician enrollments and graduates for 1955–56 show an increase over the previous year, but fall far short of present needs, concludes Technical Institute division of the American Society for Engineering Education in its new annual survey.

• Western Reserve University will initiate literature searching tests using specially designed automatic equipment for project sponsors.

• Designated MARS, University of Detroit Research Institute of Science and Engineering's new missile and rocket section will do research in liquid and solid propellants, ramjets, and related fields. Headed by Donald J. Kenney of the chemistry department, MARS will use production and test facilities of American Rocket Co. (Wyandotte), set up a 23-acre test site west of Detroit.

• The British Interplanetary Society (London) will introduce shortly a new, general interest magazine tagged "Spaceflight."

• Polytechnic Institute of Brooklyn is offering a new evening course on supersonic aeronautics, "Limit Analysis of Structures," this fall at its Long Island graduate teaching center at Mineola High School.

FOREIGN

Australia: Maralinga, the rocket-range extension to Britain's atomic proving grounds of Woomera, is nearing completion, will serve as a key center for development of medium-range supersonic missiles.

England: Existence of four new British ramjet engines was recently disclosed. Designated BRJ.2, BRJ.4, Thor B.T.1, and Thor B.T.2, the engines are produced by Bristol Aeroplane Co.

A production contract—the first for a British ramjet missile—has been placed for a Thor-powered missile. No thrust figures are available for any of the engines; but the Thor-powered missile, already tested in England and Australia, is reportedly capable of high supersonic speeds and 100% reliability. Four booster rockets were used to bring the ramjet up to operating speed.

• Raven, solid propellant rocket which the British hope will hit the 100-mile altitude mark, is a 25-ft-long, 17-in.-diam single-stage rocket that develops about 11,500-lb thrust for 30 sec. Propellant is British-developed, low cost, low burning rate, ammonium nitrate composite propellant. Raven is launched in an 80-ft-long launching tower.

• Beta rocket engine with two chambers will power the Fairey VTO aircraft. Beta engine can be swivelled.

• Gamma rocket motor has variable thrust. Three programs are available: 8000-lb thrust for takeoff, 800-lb for cruise, and 2000-lb for combat. Gamma also has two barrels.

• Armstrong-Whitworth Aircraft will

build a $2.8 facility at Whitley for research on high speed aircraft and guided missiles.

• Kerosene-burning NRJ-1 is another ramjet that is being tested by the British. Napier-built engine is boosted by eight solid propellant rockets, is 20 ft long, and has a diameter of 18 in. British claim engine has gone higher than any other ramjet.

• British Screamer rocket engine puts out 8000-lb thrust at sea level and increases to 9500-lb at 40,000 ft. Made by Armstrong Siddeley, the motor burns liquid oxygen and hydrocarbon. The engine has a diameter of 28 in., is 78 in. long, and weighs 470 lb. Screamer is used for auxiliary aircraft propulsion.

• Napier Scorpion NSC-1, also using liquid propellants, is now being tested by the British in the Canberra jet bomber.

Canada: Sparrow air-to-air missile will be produced under a $10–$11 million allocation. Original Canadian ATA missile, Velvet Glove, will be discontinued despite $24 million development cost.

Russia: American intelligence sources believe Soviets will have a working nuclear-armed ICBM within five years. Redstone Arsenal spokesman figures that Russia already has flown a ballistic missile over 800 miles.

Japan: U. S. Office of Naval Research has given go-ahead to negotiations between Kellett Aircraft Corp. and Japan concerning purchase of Kellett's rocket-powered "Stable Mabel" helicopters (JET PROPULSION, July, p. 583) in connection with Japanese National Defense Agency's plan for formation of helicopter squadrons.

• Official testing of J3-1 turbojet is about to get underway. Designed and built by Japanese Jet Engine Co., engine is rated at 2650-lb thrust.

RESEARCH & DEVELOPMENT

• Curtiss-Wright Corp. has established a new Turbomotor Division in Princeton, N. J. This division will design and develop advanced propulsion systems in the low and medium power categories for aircraft, helicopters, missiles, and drones.

• Ford Motor Co.'s Pilot Gas Turbine Laboratory (Dearborn, Mich.) is using closed-circuit TV (see photo) to provide remote observation of engine performance in hazardous areas.

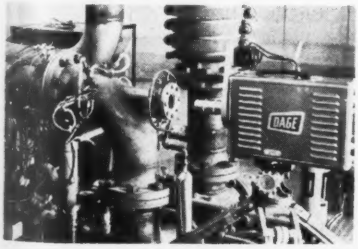

• American Machine & Foundry Co.'s Mechanics Research Dept. and Frankford Arsenal's Pitman-Dunn Laboratories are jointly studying potential applications for cartridge-actuated devices.

• Fischer & Porter Co. recently dedicated its new fluids calibration laboratory. Called "The Allan P. Colburn Memorial Flow Laboratory," the facility is located in Hatboro, Pa.

• Wright Air Development Center, investigating the phenomenon of sonic shock waves, has assigned one phase of this study to Armour Research Foundation.

• Using automatically opening and closing steel bottles in the nose cones of two Aerobee rockets, Army Signal Corps scientists at White Sands Proving Grounds recently collected 48 quarts of pure air from the upper (75 miles) atmosphere. The samples were sent to University of Michigan and Max Planck Institute for Chemistry (Mainz, Germany) where, says the Army, they will be used to help unravel some of the basic mysteries of space flight.

• Another problem of space flight, the handling of human wastes in a tightly sealed space ship, was recently assigned to New York University scientists and engineers by the Air Force. A major factor here is conservation of total mass; weight and bulk of material in the ship must be kept at a minimum. The answer, suggests NYU, may lie in processing the wastes so that they could be partly reused for fuel or to help grow dietary supplements.

• Riding in an open gondola suspended from a Skyhook plastic balloon, two Naval observers reached 40,000 ft, were able to photograph jet aircraft vapor trails at short range. This was one phase of Project Stratolab to conduct research from a manned "space" laboratory attached to a plastic balloon. For research at higher altitudes, observers will use a special pressurized spherical aluminum gondola carried aloft by General Mills, Inc.'s giant plastic Stratolab balloons.

• At its new Parma (Ohio) basic research laboratories, National Carbon Co., a division of Union Carbide and Carbon Corp., will study the problems of jet aircraft flying above 60,000 ft where there is little atmosphere for cooling and all engines "run hot."

• Flame Ceramics, a method of coating metals and other substances with ceramic materials, makes it possible to cover rockets and missiles with a coating that will protect the undercoat from high temperatures, claims developer Armour Research Foundation.

• An experimental French-made Renault auto powered by a gas turbine recently hit 191.2 mph at Bonneville Salt Flats, Utah.

• Lockheed's Missile Systems Division started moving personnel into its new $4 million research laboratory in Palo Alto (Calif.) last month. The division also disclosed plans for use of a new high speed computer in solving some problems involved in the development of the ICBM. Designated Univac Scientific 1103A, the computer, says Lockheed, is the only machine in the world versatile enough to interrupt one complex problem to solve a new, high priority problem while retaining all work on the first for subsequent solution.

• American Bosch Arma Corp. (Garden City, N.Y.) is working on the development of an inertial guidance system for the Air Force ICBM program.

• Lear, Inc., has opened a new research and development facility for aircraft and missile instrumentation work in Santa Monica, Calif.

• Kellett Aircraft Corp. (Merchantville, N.J.) has been awarded three government research and development contracts: two concern design of helicopter stabilizing systems; the other, development of a "proprotor" or combination forward-thrust propeller and vertical-lift rotor.

• A. D. Little is studying the use of hydrogen peroxide and phosphorous as chemical tracking aids for missiles under a $40,005 Holloman Air Development Center contract.

• Production and testing of large solid propellant rocket engines is being investigated in a $95,485 study program for Redstone Arsenal by Ralph M. Parsons Co., Los Angeles.

• Aeroballistics Research Dept. of Naval Ordnance Laboratory has fired test missiles the size of golf balls in a hypervelocity gun at a speed of 7000 mph. Purpose is to simulate high speed effects on full-scale missiles and satellites. Gun is loaded with pressurized helium, heated by high pressure combustion of hydrogen and oxygen.

• McDonnell Aircraft Corp., St. Louis, Mo., is using a novel method of simulating high temperatures on missiles. System uses radiant heat (quartz lamps and reflectors), generates temperatures from 1000 F to 1500 F.

• In tests at the University of Utah, bullets have been fired at over 2 miles per sec. The group eventually hopes to hit over 5 miles per sec by an electrically triggered hydrogen explosion. Tests are conducted in concrete tunnels near Salt Lake City.

• American Machine & Foundry Co. (New York) has established an Advanced Research Dept. at Alexandria, Va., as part of its Defense Products Group to provide high level research and development work for industry and government.

Sixth Symposium on Combustion: A Résumé

WALTER T. OLSON[1]

FROM Aug. 19–24, 670 scientists and engineers of 13 nations assembled at Yale University for the Sixth Symposium on Combustion. Of particular interest was the active participation throughout the meeting of V. N. Kondratiev, L. N. Khitrin, and L. I. Sedov, all of the Academy of Sciences, USSR.

The technical program, including three round table discussions and 117 papers, was formally opened by Reuben A. Holden, secretary of Yale University, and Bernard Lewis, president of the Combustion Institute.

Next, a round table of representatives of seven nations, chairmanned by Walter T. Olson, NACA, discussed "Future Problems in Combustion Research." Top among these problems, as foreseen by panel members, was the need for greater knowledge on such subjects as the transition from detonation to deflagration, the ignition of fire-damp by explosives, the relation of impact sensitivity of explosives to their interior structure, initiation and propagation mechanisms, structure and properties of detonation waves, the kinetics of carbon monoxide combustion and hydrocarbon combustion, preflame reactions, turbulent flames, the partition of energy and the concentrations of species in flames, the physics and chemistry of the flame front, preparation of reactants for combustion, oscillations in high through-put combustors, mechanisms of both low and high temperature oxidation, turbulent combustion, how combustion oscillations are driven, and states and rates in chemistry at high temperatures and in short times.

Eight papers, headed by an invited paper from J. O. Hirschfelder, University of Wisconsin, and the second round table discussion dealt with fast, high temperature reactions wherein departure of species and energy from conventional equilibrium presents a problem. The round table, chairmanned by AVCO's Arthur Kantrowitz discussed methods of attack on high speed reactions. Sampling and analysis, mass spectrography, and shock tube and spectra were suggested for analysis of flames and detonations; simpler studies of the "parts" of a reaction by flash photolysis, by atomic flames, and by molecular beams were also proposed.

The structure and propagation of laminar flames was the theme for the next 32 papers, including invited papers by Theodore von Kármán and Robert M. Fristrom, Johns Hopkins University. Effort continues to be made to simplify or to solve the equations for laminar flame propagation both for the general case and for specific examples. The flame is treated as a one-dimensional flow problem; equations of conservation of mass and energy are written. In general, the several papers on this problem used the so-called steady state assumption for the flame; that is, reactions of intermediates are very rapid compared to the over-all reaction. Other papers were concerned with the effect of environment on flame speed, with the spectra and their implications to reaction kinetics for particular flames, with carbon formation, and with decomposition flames of nitrite esters.

Five papers were on turbulent flames, both diffusion and premixed.

Flame stabilization in fast streams was discussed in eight contributed papers and in the third round table. There was agreement that ignition of unburned gases by burned gases in the stabilizer wake constitutes the flameholding mechanism for premixed gases. For volatile fuel sprays, the effect of vaporization on the temperature and composition of the pilot flame must be considered. Jets and vortices also received attention as flameholders.

A variety of experimental techniques pertinent to combustion, headed by an invited paper on pyrometry of high velocity gases by I. Warshawsky, NACA, occupied another of the sessions.

In still other sessions there were six papers on flammability, ignition, and quenching of flames; four papers on combustion oscillations; eight papers on the combustion of explosives and solid propellants; and seven papers on evaporation and combustion of droplets and sprays. This last session was headed by an invited paper summarizing the combustion of fuel sprays by Seiichiro Kumagai, University of Tokyo, and also featured a panel discussion of droplet and spray combustion.

Progress in the field of solid fuels was ably reviewed by A. A. Orning, Carnegie Tech., who summarized eight papers contributed on the subject and interpolated some of his own observations. These papers dealt with the combustion of pulverized coal, with combustion in a solid bed, and with the mechanisms of burning solid carbon, or coke.

The remainder of the papers, concerned with applications of combustion, included four on fire extinguishing, three on chemical syntheses, three on reciprocating engines, two on rocket propellants, and five on combustion in gas turbines. This last was the topic of a lively panel discussion. Several of the authors were in agreement that, under certain circumstances widely applying, chemical reaction rates pro-

[1] Chief, Fuels and Combustion Research Div., Lewis Flight Propulsion Laboratory, NACA.

vide the slow, or limiting, step to the over-all combustion process in gas turbines. Correlation of combustion efficiency with operating parameters results. The importance of the fuel preparation step, however, was also stressed.

Speaking at the Institute banquet, Dr. Lewis, president of the Combustion Institute, expressed concern at the low ratio of fundamental research leading to a conceptual understanding of combustion to applied, or empirical, research. To increase this ratio, he recommended that colleges and universities organize curricula in combustion science.

At the business meeting, the Institute announced its new quarterly publication, *Combustion and Flame*, the Journal of the Combustion Institute. First issue will be published March 1957. Subscription price: $16/year.

In another announcement, the British section invited the Institute to hold its Seventh Symposium in England in 1958.

The proceedings of the Sixth Symposium will be published in identical format with previous publications of symposia held in 1948, 1952, and 1954. These volumes have come to be essential reference works in the field. Copies may be ordered from the Combustion Institute, Union Trust Building, Pittsburgh 19, Pa.

ARS News

ARS Sets Committees

At the semi-annual meeting last June (JET PROPULSION, July), ARS Board of Directors decided to set up a series of technical committees. Chairmen (see below) were chosen and confirmed last July, and the committees are now in operation.

Six in all, the committees' main purpose, ARS President Noah Davis points out, will be to cater to the growing specialized interests of members. The six committees now formed, for example, will deal with the following fields: liquid rockets, solid rockets, ramjets, instrumentation and guidance, propellants and combustion, and space flight.

Another important function of the committees will be the programming of national meetings and the selection of reviewers. In addition, says Dr. Davis, committee operation will provide increased continuity in carrying out SOCIETY functions. Although chairmen will be appointed for only one-year terms, they will be automatically followed in office by their vice-chairmen who in turn will probably be succeeded by experienced committee members.

(Continued on page 910)

Chairmen of the New ARS Technical Committees

Solid Rockets: William L. Rogers was born in Pendleton, Oregon, March 19, 1921.

At 21, with a B.S. in mechanical engineering from California Institute of Technology, he went to work for Northrop Aircraft Corp. doing layout design on aircraft. He left Northrop and joined Aerojet in 1942. Here, he headed a group which designed, among other solid propellant rockets, the 14AS-1000 JATO motor, the 2.2KS-11,000 booster, the 2.5KS-18,000 booster, the 2.2KS-33,000 booster, and the 15KS-1000 JATO. In 1952, he became assistant general manager of Aerojet, a position he still holds.

An active ARS member, Mr. Rogers served on Board of Directors, Southern California Section, in 1954. He is also a member of the Institute of Aeronautical Sciences and Tau Beta Pi, national engineering honorary society.

Ramjets: Brooks T. Morris, executive engineer, Powerplants, Marquardt Aircraft Co., has been engaged in air-breathing, nonrotating jet engine development work since 1944.

From 1952 to 1955, he was principally concerned—as chief project engineer—with development of ramjet engines for the IM-99 Bomarc. Prior to joining Marquardt in 1949, Mr. Morris worked in the aircraft research and development divisions of Willys-Overland and General Tire and Rubber Co. as power plant group engineer for missile propulsion studies. Before this, 1943 to 1946, he worked on regeneratively cooled liquid propellant motors at Aerojet Engineering Co.

A graduate of Stanford University (A.B. '34; C.E. '38), he has been a member of ARS since 1948. He is also a member of IAS, Sigma Xi, Tau Beta Pi, Phi Beta Kappa, and AAAS.

Propellants & Combustion: John F. Tormey was born in Oneida, N.Y., December 12, 1919.

A graduate chemical engineer (Notre Dame, B.S. '41; MIT, M.S. '43), he served three years in the Navy attached to the Bureau of Ordnance, where he was assigned to varous phases of torpedo research, development, and test.

In 1946, Mr. Tormey joined North American Aviation as a research engineer in the Aerophysics Dept. He was promoted to supervisor of the Propellants Unit in the Research Group at Santa Susana in 1950, and in 1954 took over his present position as group leader of Research and Special Projects at Rocketdyne's Propulsion Field Laboratory at Santa Susana.

He is currently active in the American Chemical Society and in the Southern California Section of ARS.

Liquid Rockets: Lt. Col. Edward N. Hall, USAF, was born in New York City in 1914.

Supervisor of propulsion, Western Development Division Headquarters, Air Research and Development Command, Col. Hall headed an Air Force group which evaluated German propulsion developments after World War II. From 1950 to 1954, he worked on pulsejets, ramjets, and rockets at Wright Field's Power Plant Laboratory.

In 1955, Col. Hall received the Robert H. Goddard Memorial Award from ARS for his "outstanding contribution to the development of liquid propellant rockets."

Col. Hall is a graduate of City College of New York (B.S., engineering, '35; professional degree in chemical engineering, '36) and Cal. Tech. (master's degree, aeronautical engineering, '48).

Space Flight: Krafft A. Ehricke, born in Berlin, Germany, in 1917, came to this country at the end of World War II.

Schooled in Germany, he studied aerodynamics at Charlottenburg Institute of Technology. From 1942 to 1945, he worked in the power plant section of the Peenemunde Rocket Development Center. After arriving in the U.S., he worked first as a jet propulsion specialist at Fort Bliss, Texas, and then at the Guided Missile Development Group at Redstone Arsenal where he was chief of the gas dynamics section. From here, Mr. Ehricke went to work for Bell Aircraft.

Two years later, in 1954, he joined Convair as a design specialist in the guided missile development group. He is now chief of pre-design and systems analysis in Convair-Astronautics.

An active ARS member, Mr. Ehricke is president of the San Diego Section.

Instrumentation & Guidance: John J Burke, presently head of the Guidance and Electronics Division of California Institute of Technology's Jet Propulsion Laboratory, has 12 years of experience in electronics behind him.

A graduate of Cal Tech (B.S. and M.S in electrical engineering), Mr. Burke worked first as an instructor in electrical engineering at University of Houston. He later joined Hughes Aircraft as a research engineer and then JPL in the same capacity. At JPL, he participated in the development of this country's first production guided ballistic missile, the Corporal.

Moreover, he is now engineering vice-president of Hallamore Electronics Co., a division of Siegler Corp.

He is a member of ARS, Institute of Radio Engineers, Tau Beta Pi, Sigma Xi, and American Ordnance Association.

The number and selection of committee members will be up to the individual chairmen. But in making up their committees, explains Dr. Davis, chairmen will aim for recognized leaders in their fields, a balance among industry, university and government representatives as well as a geographical balance.

ARS Adds Six

SINCE last February, AMERICAN ROCKET SOCIETY has added six new members to its corporate roster, boosted the over-all corporate figure to 78. Latest additions are:

• Cooper Development Corp. Formerly known as Horning-Cooper, Inc., the firm, located in Monrovia, Calif., is active in missile design and fabrication as well as the design of systems and instrumentation. Its newest product is the ASP (Atmospheric Sounding Projectile), a high altitude, high speed (Mach 5 or better), solid propellant rocket which was developed and built by the company in less than five months.

Designated by Cooper as corporate representatives to ARS: Clifford D. Cooper, president; Orin E. Harvey, director of administration; E. B. Williams, director of engineering; C. M Zimney, chief engineer; A. L. Pittinger, director of research.

• Kelsey-Hayes Wheel Co. A Detroit firm, Kelsey-Hayes is involved in the design, development and manufacture of gear box assemblies, turbine wheel assemblies, nozzle box assemblies and servomechanisms.

The company selected the following personnel as corporate representatives: Leslie G. Taylor, director of defense sales; Frank E. Hoffman, West Coast manager of sales and engineering; W. R. Alexander, chief engineer, Speco Div.; R. R. MacGregor, chief aircraft process engineer; C. P. Meredith, general manager, Speco Div.

(*Continued on page 912*)

Annual Meeting Coming Up

NEXT month, November 26–30, AMERICAN ROCKET SOCIETY will hold its 11th Annual Meeting at the Henry Hudson Hotel in New York City.

Rear Admiral James Russell, chief of the Navy's Bureau of Aeronautics, will be the featured speaker at the Honors Night Dinner.

On the technical side, the program will offer a number of interesting sessions ranging in scope from Space Law and Sociology to Atomization and Sprays. Two sessions that promise to have wide audience appeal are High Altitude Sounding Rockets I and II. Both of these sessions will be under the direction of Homer E. Newell, Jr., Naval Research Laboratory. Among the presentations in the two sessions will be papers on Aerobee-Hi, two-stage solid propellant sounding rockets, Iris and Arcon rockets, future solid propellant rockets, ASP, balloon- and aircraft-launched rockets, and foreign rockets.

Two classified symposia on Project Vanguard will undoubtedly create high audience interest also. The first symposium, under Chairman Milton Rosen of the Naval Research Laboratory and technical director of Project Vanguard, will deal with propulsion of the satellite. The second symposium will be directed by Chairman James Bridger, head of Vehicle Branch, Project Vanguard, and will be devoted to guidance.

There will be other sessions and symposia on solid propellants, high temperature materials, combustion, liquid propellant rockets, instrumentation and guidance, and space flight.

Complete program will be published in the November issue of JET PROPULSION.

RESERVATIONS FOR DINNER AND LUNCHEONS

Nov. 27—SECTION LUNCHEON $4.50 —No. tickets...... Amt. $.............

Nov. 29—HONORS NIGHT DINNER $8.50* —No. tickets...... Amt. $.............

Total......$.............

* Deduct 50c if reservations are received before Nov. 15, 1956.
All prices include gratuities. Tables seat ten. Make checks payable to American Rocket Society (500 5th Ave., New York 36, N. Y.)

Information for Honors Night Dinner Seating List

Name..............................

Address............................

Company Name......................

Name of Guests (including ladies)..........

....

I have arranged / would like to sit with..............

Names received after Nov. 15 will not appear on seating list.

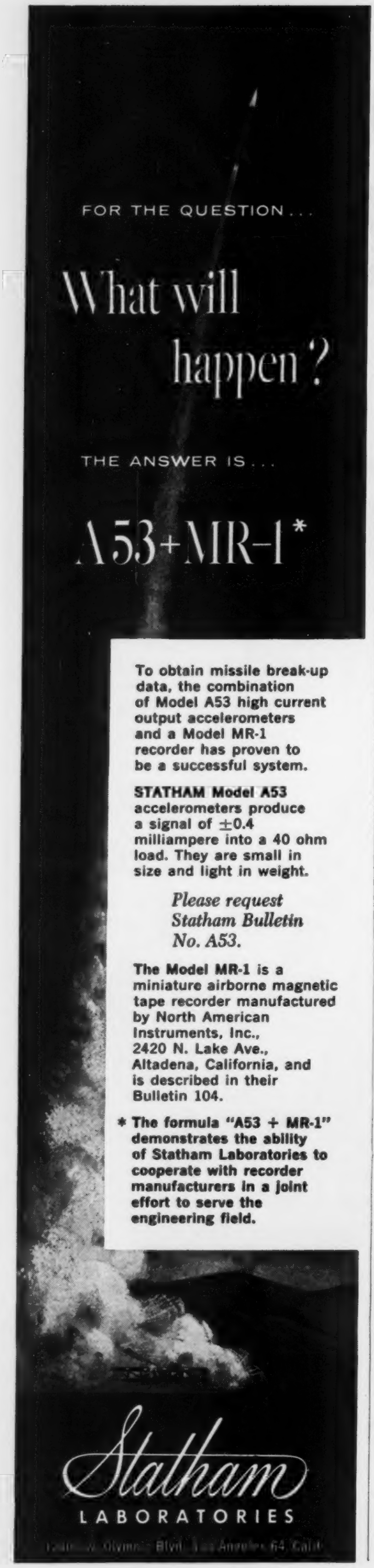

• The Ralph M. Parsons Co. Located in Los Angeles, Parsons is active in research and development of electronic and electromechanical components for missiles, the design and construction of missile facilities, such as test stands and ranges, ground control stations, and instrumentation. The company also carries out technical studies and complete design of facilities for the production of high energy fuels. In April, Atomic Energy Commission entered into a contract with the company for architect-engineering of new flight engine test facilities to be built in the Aircraft Nuclear Propulsion area of the National Reactor Testing Station.

Corporate representatives: C. W. Brandt, Hilton C. Smith, E. C. Lee, H. H. Denlinger, and W. M. Parsons.

• Research and Advanced Development Div., Avco Manufacturing Corp. At present, this Avco division, centered at Stratford, Conn., is engaged in specialized research on shock tubes as well as classified missile research and development for the Department of Defense.

Representing the division in ARS: Jack A. Kyger, project director; Arthur Kantrowitz, director, Avco Research Laboratory; Mac C. Adams, deputy director, Avco Research Laboratory; Abraham Kahane, aerodynamics section chief; Immanuel Lichtenstein, technical assistant to vice-president of research.

• Sperry Gyroscope Co., Div. of Sperry Rand Corp. Active in almost all phases of guided missile development and manufacture, Sperry Gyroscope (Great Neck, N.Y.) is directly concerned with instrumentation, flight controls, engine instruments and controls, drone and unmanned aircraft controls, inertial navigation devices, gyroscopics, servomechanisms, and computing mechanisms.

Selected by Sperry as corporate representatives: M. D. Lockwood, engineering director for surface armament; W. L. Barrow, vice-president for research and development; H. Harris, engineering director of air armament; P. Halpert, chief engineer, Aeronautical Equipment Div.; W. Mieher, chief engineer, Special Missile Systems Div.

• Texas Metal & Manufacturing Co., Inc. (Dallas). Engaged in missile work since 1951, the company, under prime contract to Wright Air Development Center and Redstone Arsenal, has developed oxidizer and fuel servicing systems and equipment for rocket applications.

Representing Texas Metal & Manufacturing are: Henry I. McGee, president; George C. Kershaw, vice-president; Carroll L. Bell, project engineer; E. C. Sindelar, project engineer; Robert J. Smith, Jr., design study engineer.

Operation Clarification

In our coverage of the June meeting of the American Rocket Society (Jet Propulsion, July 1956, p. 587), we described Albert Gail's (Cornell Aeronautical Lab.) ramprop as "essentially a 120-ft-long ramjet." This should have read: "essentially a 120-ft-long ramjet-

San Diego Served

At a dinner meeting held last July, ARS Director Howard S. Seifert presented the San Diego Section with its national charter. Grouped about the document (above, l. to r.) are officers of the new Section: Larmon L. Jirsa, director; Louis F. Muller, Jr., secretary; Krafft A. Ehricke, president; Jack D. Clothier, vice-president; Eugene C. Sims, treasurer; Thomas R. Kochis, director. Hans R. Friedrich, a director, fills out the Section's official complement.

As part of the presentation ceremonies, ARS Director George Sutton discussed "Guided Missiles, Past, Present, and Future." Over 400 members, wives and friends attended.

driven propeller." But just to make certain there is no room left for confusion, we quote directly from Mr. Gail's own summary of his paper, "The Ramprop, a Supersonic Jet-Driven Propeller."

"The ramprop is a propulsion system consisting of rotor blades driven with supersonic speed by ramjets or ramrockets at the blade tips. The structural and aerodynamic problems of ramprops are analyzed and a suitable design is proposed [in his paper, ARS Prepr. 296-56]. The ramprop is found to be a very promising power plant for large convertible aircraft capable of vertical take-off and descent, transonic cruising flight, and useful load capacity corresponding to conventional transport aircraft."

ARS Meetings Calendar

Nov. 26–29: ARS Annual Meeting, Henry Hudson Hotel, New York. Honors Night Dinner on Nov. 29. Speaker: Rear Admiral James S. Russell, chief, Bureau of Aeronautics.

—1957—

March 18–20: ARS Spring Meeting, Hotel Statler, Washington, D. C.

June 9–13: ARS Semi-Annual Meeting, Hotel Sir Francis Drake, San Francisco.

Aug. 25–28: ARS–Northwestern Technological Institute Gas Dynamics Symposium, Northwestern University, Evanston, Ill.

Dec. 2–6: ARS Annual Meeting, New York.

New Patents

George F. McLaughlin, *Contributor*

Jet power plant for aircraft (2,744,381). Paul E. Geisel, Philadelphia, assignor to Arsene N. Lucian, Llanerch, Pa.

Means positioned adjacent to the downstream end of a shroud pipe for diverting outwardly from the axis of the air stream at least some of the stream forming air.

Single burner turbojet engine (2,748,563). Dominik Viktor, Newark, N. J.

Air induction vanes extending spirally around the inner surface of a rearwardly tapered air inlet funnel within a cylindrical barrel.

Intermittent combustion gas turbine engine (2,748,564). R. H. Marchal, F. G. Paris, J. Bertin, and L. A. J. Bauger, Vanves, France, assignors to Société Nationale d'Étude et de Construction de Moteurs d'Aviation.

Velocity-absorbing turbine operated by kinetic energy of gas impulses. A power producing device expands the gas supplied from the exhaust manifold.

Oscillating fuel control for ramjets (2,748,565). Louis S. Billman and Arthur Angelos, Glastonbury, Conn., assignors to United Aircraft Corp.

Method for maintaining maximum thrust and burner pressure by regulating fuel flow in accordance with a fuel increasing and decreasing curve. Fuel flow is increased along the positive slope of the curve when burner pressure drops due to lean fuel-air ratio.

Compound gas-turbine engine with low-pressure compressor and turbine by-pass (2,748,566). A. H. Fletcher, Derby, England, assignor to Rolls-Royce, Ltd.

Working fluid duct having a low pressure compressor, high pressure compressor, combustion equipment, high pressure turbine, power turbine, and low pressure turbine, respectively, in flow series.

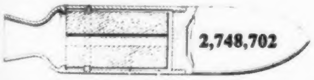

Rocket (2,748,702). Winslow A. Sawyer, E. Braintree, Mass., assignor to the U. S. Army.

Projectile in which a split ring embraces the propellant grain near one end. The other end of the grain is maintained in spaced relation with the combustion chamber in all dimensions.

Rocket type launching carriage for ordnance missile (2,748,703). Wilbur H. Goss and David A. Washburn, Silver Spring, Md., assignors to the U. S. Navy.

Plurality of rockets to provide auxiliary thrust for missiles. Pivots at rear end of rocket allow forward end to swing out of the way when released. Rockets disengage from the casing and are left behind.

Gas turbine engines (2,749,023). G. M. Lewis, Bristol, England, assignor to The Bristol Aeroplane Co., Ltd.

Starting is effected by use of a nozzle directing compressed air on a ring of blades on the compressor rotor. Starting blades are positioned out of the path of movement of the working medium.

Compressors (2,749,025), Edward A. Stalker, Bay City, Mich.

Stages of rotor and stator blades each having a sharp trailing end and a circular arc nose. Blades of downstream stages have larger nose radii than those on the upstream side.

Fusible link jet motor control (2,749,705). Robert P. Haviland, Scotia, N. Y., assignor to General Electric Co.

Multistage jet propelled vehicle with a heat-fusible element downstream from the second-stage motor for interrupting the electrical circuit of the first control system. The circuit must be closed in order for the first stage to operate.

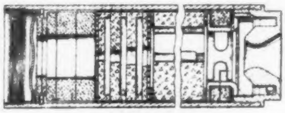

2,750,887

Motor mechanism for missiles (2,750,887). Stanley J. Marcus, China Lake, Calif.

Solid propellant stop member prevents closing valve for discharging gases from the combustion chamber. Propellant charge is formed of slow burning and fast burning grains, the latter designed to be consumed at about the time the stop member is consumed.

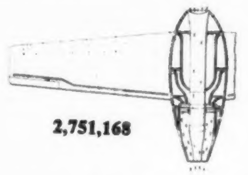

Boundary layer induction system for aircraft (2,751,168). Edward A. Stalker, Bay City, Mich.

Intake openings over the wing surface provide inward flow of air over the wing. Only about 25 per cent of the boundary layer air through intake openings produces laminar flow and low drag.

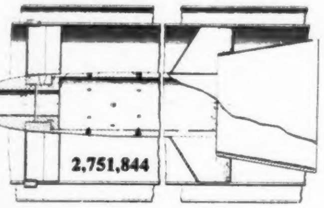

Ignition flare (2,751,844). Harold W. Bixby, Encino, Calif., assignor to the U. S. Navy.

Ramjet-type aerial missile with flare holder in the combustion chamber of the tailpipe. Holder expands and contracts independently of the missile, preventing warping of parts under intense heat during combustion.

Airplane de-icing apparatus (2,751,170), John P. Feltman, Brooklyn, N. Y.

Air introduced to gas captured from the exhaust of a turbojet engine lowers the gas temperature and directs the mixture to portions of the plane to be de-iced.

Deicing apparatus for jet engines (2,750,734). Leonard P. Leigh, Los Angeles, Calif.

Control of the supply of hot air to the inlet duct by means of a member responsive to either positive or negative actuating pressure.

Fuel regulator responsive to combustion chamber pressure (2,750,741). Charles K. Leeper, Cambridge, Mass., assignor to United Aircraft Corp.

Rate of fuel flow systematically varied above a zero value. A valve, movable in timed relation with fuel flow variation, is actuated by sensing pressure in the burner.

Latch mechanism for a rocket launcher (2,751,818). Mitchell E. Bonnett, Havre de Grace, Md., assignor to the U. S. Army.

Parallelogram link having a vane pivotable from a position clear of the exhaust blast from the rocket being fired.

Mechanism for cooling a combustion chamber in propulsion apparatus and for feeding combustion liquids thereto (2,749,706). Robert H. Goddard, deceased, by Esther C. Goddard, executrix, Worcester, Mass., assignor one-half to The Daniel and Florence Guggenheim Foundation.

A jacket space and spray-cooled space are formed by inwardly projecting end walls for the closed end of the chamber. Liquid oxidizer is fed to the jacket space and into the spray-cooled space. A cooling film of liquid fuel is directed against the wall at the closed end of the chamber.

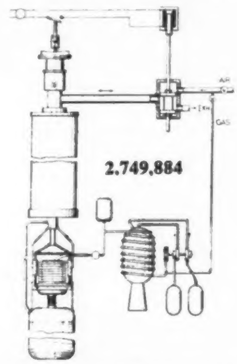

Pressure-operated feeding apparatus for combustion liquids in an internal combustion chamber (2,749,884). Robert H. Goddard, deceased, by Esther C. Goddard, executrix, Worcester, Mass., assignor one-half to The Daniel and Florence Guggenheim Foundation.

Liquid is supplied under low pressure to the space within a closed casing containing a bellows, Gaseous fluid under high pressure to the interior of the bellows depresses the lower end of the bellows, closing off the liquid supply.

Out of the Past

When rocket pioneer Dr. Robert H. Goddard died on August 10, 1945, he left extensive notes on his experiments. As a result, his many inventions continue to become part of present-day rocket development through new patents issued to his estate by the U. S. Patent Office (see above).

EDITOR'S NOTE: The patents listed above were selected from recent issues of the Official Gazette of the U. S. Patent Office. Printed copies of patents may be obtained at a cost of 25 cents each, from the Commissioner of Patents, Washington 25, D. C.

New Equipment and Processes

Equipment

Electrical, Electronic

Lead Zirconate Pressure Transducer. Model LC-33 is stable, has a range up to 1000 psi, response of 1–80,000 cps for sensing sound or shock waves produced by explosions, passing missiles, noise, etc. Atlantic Research Corp., 901 N. Columbus, Alexandria, Va. (photo).

Proximity Transducer Systems. For counting, detecting metals, control, or indicating rate of travel or distance. Electro Products Laboratories, 4501 N. Ravenswood, Chicago 40, Ill.

Tantalum Capacitors. Series TW "Tan-O-Mite" are ultra-small (0.095–1/8" diam, 1/4–1/2" long) and cover range of 0.02–30 mfd. Ohmite Manufacturing Co., 3625 Howard St., Stokie, Ill.

High-Frequency Force Transducer. Type 9326 cells have capacity of 20,000 lb, response of 1900 cps. In solid propellant motor static tests, measured full thrust in 3 microsec. Baldwin-Lima-Hamilton Corp., Philadelphia 42, Pa. (photo).

Thermistor Heat Detector Cells. Bolometers in the 1–12 micron range. Three models available. Servo Corporation of America, 20–20 Jericho Turnpike, New Hyde Park, L. I., N. Y.

Resistant Pressure Transducer. Stands temperatures up to 500 F, pressures up to 1500 psi with a life of 1000 hours exposure to red or white fuming nitric acids. Rahm Instruments, Inc., 237 Lafayette St., New York 12, N. Y. (photo).

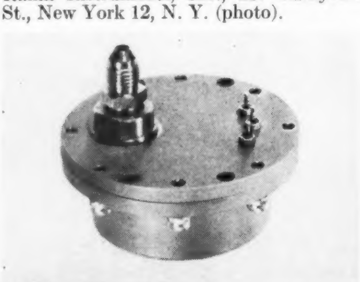

Silicon Power Rectifiers. Features negligible current leak for airborne applications with 250 ma-50 amp forward current. Components Division, Federal Telephone and Radio Co., 100 Kingsland Road, Clifton, N. J.

Rate Gyro. Model 36129 is oil-filled, withstands 100 g, provides rate signals up to 70 v. **High-Temperature Potentiometer.** Rated to 200 C, Model 875T carries 2 w at 150 C. G. M. Giannini & Co., 918 E. Green St., Pasadena 1, Calif.

Analog-Digital Converters. Available in count range to 543,288. Long life. Norden-Ketay Corp., 99 Park Ave., New York, N. Y.

High-Temperature Potentiometers. Operation to 225 C. Single and multi-turn types. Fairchild Controls Corp., Components Div., 225 Park Ave., Hicksville, L. I., N. Y.

Analog-to-Digital Converter. For long distance transmission of data representing voltage, current, and power. Long distance accuracy of less than 1%. Bendix Pacific Division, 11600 Sherman Way, North Hollywood, Calif.

High-Temperature Pressure Pickup. Type 4-136 operates continuously up to 600 F. Available in gage and differential types. Consolidated Electrodynamics Corp., 300 North Sierra Madre Villa, Pasadena, Calif.

Mechanical

Metering Valves. For gases and liquids to 6000 psi, −100 to 500 F operating range. Aluminum, brass, or stainless steel. Robbins Aviation, 1735 W. Florence, Los Angeles 47, Calif.

New Seal. Pneu-Trol Quad Rings seal from 0 to 5000 psi, use silicone rubber. Minnesota Rubber & Gasket Co., 3630 Wooddale Ave., Minneapolis 16, Minn. (photo).

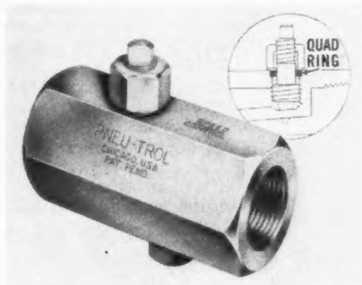

Explosive Valve. Normally closed, opens in 2 millisec. Operating pressure of 5000 psi, back pressure seal of 4500 psi. Sensitivity to shock is nil. Weighs 6 oz (photo). **Multiple Wire Thermocouple Gland.** Entrance of 1,2,4,6, or 8 wires from vacuum to 20,000 psi seals. Glands operate at −300 to 1850 F. Conax Corp., 7811 Sheridan Drive, Buffalo 21, N. Y.

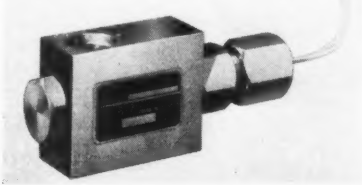

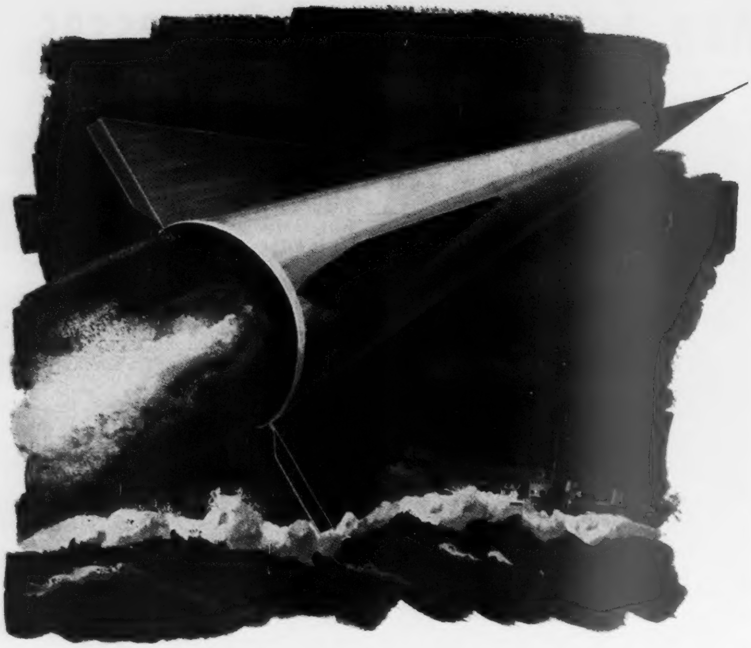

Preload Indicating Washer. Accuracy of plus or minus 10% permits loading to 80% of bolt yield strength. Standard Pressed Steel Co., Jenkintown, Pa.

Swaging Tools. Made of 4130 chrome-moly steel, rated at 125,000 psi minimum tensile. U. S. Engineering Co., 521 Commercial St., Glendale 3, Calif.

Breakaway Couplings. Ball lock stands severe vibration. High pressure units to 3000 psi. Standard sizes of $^1/_4$" up. Eastern Aircraft Products Corp., River St., Orange, N. J.

Test

Caliputer. Pocket-sized, combines slide rule, vernier caliper, and depth gage. Caliputer, P. O. Box 586, Rancho Santa Fe, Calif.

Explosion Chamber. For simulation of explosions of various magnitudes and pressures at altitudes up to 80,000 ft. Tenney Engineering, Inc., 1090 Springfield Road, Union, N. J.

Servo-Graphic Recorder. No. 22700 is direct writing on 5" wide chart. Full scale pen travels is $2^1/_2$ sec. 100 mv full scale. Rectilinear trace. Weighs about 15 lb. C. H. Stoelting Co., 424 N. Homan Ave., Chicago 24, Ill.

Pocket-Size Calculator. Weighs 8 oz, is hand-operated. Adds, subtracts, multiplies, divides, squares, cubes, extracts square roots. Capacity: 8×6×11 places. Contina Ltd., Vaduz, Liechtenstein.

Centrifuge. Hycon Vari-G can test up to 500 g. Speed reached in 150 millisec. Hycon Mfg. Co., 2961 E. Colorado St., Pasadena 8, Calif. (photo).

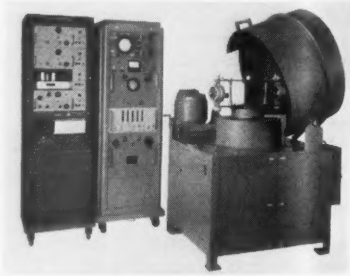

Electrodynamic Recorder. Model GA 1023 has frequency range to 200 cycles; 20 ma rms for full-scale deflection produces rectilinear traces. Direct-writing pen. E. A. Massa, Massa Laboratories, Inc., Hingham, Mass.

Oscillograph Record Camera. For single frame recordings, Model 352 automatically advances film frames in rapid sequence at random, or at synchronized, intervals. **Wide-Band Preamplifier.** Model 342 permits investigation of low level signals with any oscillograph. Allen B. DuMont Laboratories, 750 Bloomfield Ave., Clifton, N. J.

Fully Automatic Film Processing. F-310 is portable, self-feeding, and fast 16-mm processor. **Paper Drier.** F-306 dries 1000 eight by ten prints per hour or 15 ft per min. **Film Processor.** Designed for trailers and shipboard use. Fairchild Camera & Instrument Corp., Robbins Lane, Syosset, Long Island, N. Y.

Inertial Mass Flowmeter. Of Ni-Span C, can handle liquids with specific gravities of 0.6–1.2 and viscosities of 0.2 to 24 centipoise, moving 0–15 lb per sec (overload rate 100 lb per sec) at temp of −67 to 250 F. Weight is 6 lb. H. A. Wilson Co., Union, N. J.

High Temperature Accelerometer. Glennite KAHT-310 will measure shock and vibration at temp to 300 F without cooling. Frequency range of 10–2000 cps and acceleration range up to 300 g. Gulton Mfg. Co., 212 Durham Ave., Metuchen, N. J.

Multi-Environment Test Chamber. Model D-102A has 12-cu ft stainless steel inner chamber. Uses dry ice. Ranges of −100 to 400 F. Mantec, Inc., 126 Maryland St., El Segundo, Calif.

Portable Tape Transports. For magnetic tape data recording under adverse missile, jet environmental conditions. Davies Laboratories, 4705 Queensbury Rd., Riverdale, Md.

Low-Temperature Chamber. Temperature range of −100 to 220 F, 8×8×10 ft interior has auxiliary working doors. Tenney Engineering, Inc., 1090 Springfield Rd., Union, N. J. (photo).

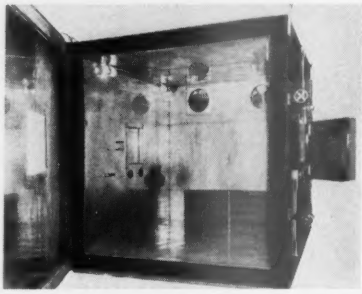

Materials

Heat Resistant Stainless Steel. Several alloys are available as castings material. Empire Steel Castings, Inc., Reading, Pa.

Lithium. Metal is furnished in form of castings 8 in. long and $1^1/_2$ in. diam. Special grade contains maximum sodium content of 0.02% Maywood Chemical Works, Maywood, N. J.

Porcelain Enameled Aluminum Foil. Available in 24-in.-wide coils 300 ft long. Various finishes and thicknesses resist thermal shock and feature dielectric of 500 v per mil. Alliance Ware, Inc., Alliance, Ohio.

Silicone Rubber Insulated Wire. For temp to 500 F. Continental Wire Corp., Wallingford, Conn.

Ceramic. Heat-shock resistant up to 2500 F. Grade HT-2 is available as bar, flats, rod, or rounds ready for machining. Technion Design & Mfg. Co., Inc., 262 Mott St., New York, 12, N. Y.

Structural Adhesive. Metalbond 302 for metal-to-metal and sandwich bonding. Narmco Resins & Coatings Co., 600 Victoria St., Costa Mesa, Calif. (photo).

Silicone Aluminum Paint. H-170 also available in blue, red, gold. Temp to 1700 F. Air dries. Speco, Inc., 7308 Associate Ave., Cleveland 9, Ohio.

Acid-Proof Mortar. Silicate-type Corlok resists nitric and other concentrated acids at temp to 1900 F. Pennsylvania Salt Mfg. Co., 3 Penn Center Plaza, Philadelphia 2, Pa.

Acid Mittens. Gauntlet or short style with index finger can be used in fuming nitric acids and 100% sulfuric acid. Surety Rubber Co., Carrollton, Ohio.

Silicone Cloth Coat. SE-701 works at temp of −120 to 700 F and is useful for hot air ducts, etc. Good solvent resistance. General Electric Co., Silicone Products Dept., Waterford, N. Y.

Chemlon. Teflon is available in rod, tubing, sheet, and tape form. Crane Packing Co., 6400 Oakton St., Morton Grove, Ill.

Teflon Spaghetti. Available in wire sizes #8 through #26 and has an operating range of −320 F to 555 F. **Teflon Tape.** Polypenco tape comes 2, 5, and 10 mil thick, has dielectric of 400–500 v/mil. Polymer Corp. of Penna., 125 North Fourth St., Reading, Pa.

Teflon Felt. Kelon-T impregnated comes $^1/_{16}$ in., $^1/_8$ in., and $^1/_4$ in. thick. Shamban Engineering Co., 11617 W. Jefferson Blvd., Culver City, Calif.

Polyurethane Prepolymer. ZL-239 for foams with high water absorbency values (1200%). **Partial Prepolymer.** ZL-222 is diisocyanate and polyester for foam processing. **Polyester.** ZL-219 for producing polyurethane foams. Thiokol Chemical Corp., 780 N. Clinton, Trenton 7, N. J.

Chemical Cloth. Herculite combines vinyl and rayon to form resistant, tough fabric. Herculite Protective Fabrics, Inc., 140 Little St., Belleville, N. J. (photo).

Hydrazine and Hydrazine Hydrate. Available as free base, 100% hydrate, 85% hydrate, and 65–75% technical solution of hydrate. Many salts also offered. Fairmount Chemical Co., 136 Liberty St., New York 6, N. Y.

Fibreglas Pressure Bottles. Light, strong, noncorrosive, and shatterproof construction. Capacities of 50–3200 cu in. Walter Kidde & Co., Inc., Aviation Div., Belleville 9, N. J.

Lithium Hydride. Available in drum quantities as crystalline lumps or under nitrogen in jars as powder. Maywood Chemical Works, Maywood, N. J.

Silicone Paint. Alumicone withstands 1500 F temperatures. Atech, Inc., 3840 Lagrange St., Toledo 12, Ohio.

ENGINEERS...
LOOK TEN YEARS AHEAD!

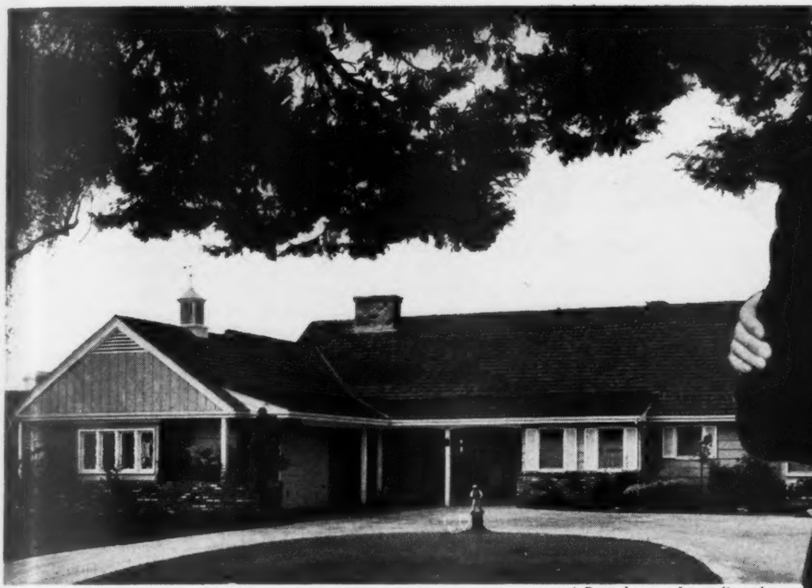

A Douglas engineer lives here

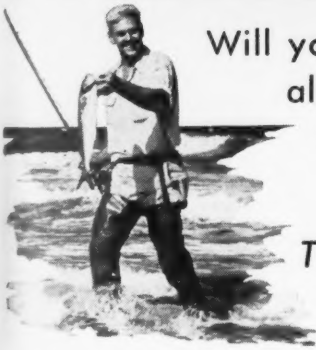

Will your income and location allow you to live in a home like this...spend your leisure time like this?

They can...if you start your career now at Douglas!

Take that ten year ahead look. There's a fine career opportunity in the engineering field you like best waiting for you at Douglas.

And what about the Douglas Aircraft Company? It's the biggest, most successful, most stable unit in one of the fastest growing industries in the world. It has giant military contracts involving some of the most exciting projects ever conceived...yet its commercial business is greater than that of any other aviation company.

The Douglas Company's size and variety mean that you'll be in the work you like best—side by side with the men who have engineered the finest aircraft and missiles on the American scene today. And you'll have every prospect that ten years from now you'll be where you want to be career-wise, money-wise and location-wise.

For further information about opportunities with Douglas at Santa Monica, El Segundo and Long Beach, California and Tulsa, Oklahoma, write today to:

DOUGLAS AIRCRAFT COMPANY, INC.
C. C. LaVene, 3000 Ocean Park Blvd.
Santa Monica, California

DOUGLAS **First in Aviation**

Book Reviews

Ali Bulent Cambel, Northwestern University, *Associate Editor*

Reflections of a Physicist, by P. W. Bridgman, Philosophical Library, New York, 1955, 2nd enlarged edit., 576 + xiv pp.

Reviewed by L. A. DuBridge
California Institute of Technology

This second edition of P. W. Bridgman's collected nontechnical writings is identical to the first edition published in 1950 except that ten additional papers have been added. All but three of the thirty-two papers have been published previously in other journals and many of them were originally papers or speeches presented before such organizations as the American Academy of Arts and Sciences, The American Physical Society, the American Association for the Advancement of Science, etc.

Although the book is described as a collection of Dr. Bridgman's nontechnical writings, many of the papers discuss fundamental scientific subjects. Rather than presenting results of Dr. Bridgman's own scientific work, they describe his point of view toward science, his philosophy of science, and his attempts to elucidate the attitudes which physicists and other scientists must take toward their subjects in view of the radical changes which the Twentieth Century has brought in the fundamental nature of many scientific conceptions.

Professor Bridgman, who won a Nobel Prize in Physics for his brilliant and original investigations in the field of high-pressure phenomena, has also contributed immeasurably to the way in which physicists and other scientists think and speak about scientific matters. It was the revolutionary impact of relativity and quantum mechanics on physical thought which forced physicists to re-examine from the experimental point of view the nature of physical terms and concepts. Bridgman then evolved what he terms "the operational point of view" which, simply stated, means merely examining every definition, every statement, every concept, from the point of view of the actual physical or conceptual operations by which the term is defined or the statement tested. Einstein's theories had demanded that physicists redefine such fundamental concepts as length, mass, energy, and time. Quantum mechanics required similar redefinitions of basic concepts of identity, location, and predictability. Bridgman proposed that all physical concepts be clearly stated in terms of specific operations, and stated that one should expect to encounter difficulties as the range of our experience broadens unless such operational definitions are evolved and adhered to.

A definitive treatise on this subject was published by Bridgman under the title "The Logic of Modern Physics" in 1926. The present volume is a series of more or less disconnected essays on the subject of the operational point of view and examples of its application.

The first nine essays are treatments of general topics; the next eight take up specific scientific situations, such as the law of cause and effect, statistical mechanics and the second law of thermodynamics, the time scale, etc. Essays 18 through 26 discuss social problems in which Bridgman has attempted to apply also his operational methods, while the last group of essays concern the relation of physicists to society in the postwar world.

It is difficult to attempt to summarize or to review this collection of essays. Some are of considerable importance and lasting value; others are after-dinner speeches whose timeliness has already passed. In reading the various essays one is frequently forced to refer back to the date it was written in order to understand the "coordinate system" in which it should be judged. The world was not the same in 1952 as in 1932!

Needless to day, in writing on social questions Dr. Bridgman will not command as much agreement as when writing with admitted authority on questions of science and scientific philosophy. Nevertheless, his papers are always thought-provoking. Every young scientist should read Chapter 21 on "Scientists and Social Responsibility" in which he discourses most illuminatingly on the impossibility of a scientist, before he makes a measurement in the laboratory, being required to consider the possible social implications of any information he is about to uncover. Bridgman says, "If I personally had to see to it that only beneficent uses were made of my discoveries, I should have to spend my life oscillating between some kind of a forecasting bureau to find what might be the use made of my discoveries and lobbying in Washington to procure the passage of special legislation to control the uses. In neither of these activities do I have any competence, so that my life would be embittered and my scientific productivity cease."

One of the most delightful of the essays is Chapter 22 on "Science and Freedom" adapted from the talk which he gave at a dinner on the occasion of his award of the Nobel Prize in Physics in December 1946. In this paper he outlines his methods of working in the laboratory, the necessity which he found for working only with small groups, for working with his own hands, having plenty of time for leisure and reflection, and being as free as possible from administrative chores. Too few physics laboratories are like that any more, but there are many individuals who could work far more creatively if such conditions could be restored.

Protective Coatings for Metals, by D. M. Burns and W. W. Bradley, Reinhold Publishing Corp., New York, 1955, 2nd edit., 643 pp. $12.

Reviewed by Hiram Brown
Solar Aircraft Company

This is a very comprehensive book on the subject. It discusses in detail both metallic and chemical coatings. The method of accomplishing the desired coating, the properties of the respective coatings, and the various methods of testing them are adequately covered from both the technical and the practical point of view. Particular—and warranted—stress is given to surface cleanliness and preparation prior to coating.

Among the more common metal coatings discussed are aluminum, tin, lead, cadmium, silver, gold, nickel, chromium, and copper. The coating methods for metals are discussed under the following classifications: hot dipping, spraying, electrodeposition, chemical deposition, cladding, and cementation. In most cases hot dipping and cementation lead to diffusion of the coating into the base metal and the formation of alloy layers which differ from either coating or parent metal. Where diffusion occurs, the layers do not merge gradually but change abruptly. Hot dip coatings are usually thicker than other types of metallic coatings. Thick layers tend to be brittle. Electro-deposited coatings do not result in diffusion. Electro-deposited coats are more uniform in thickness than hot dip coatings, less porous than sprayed coatings, and of higher purity than either.

Surface defects and appearance of coatings, such as porosity, ripples, chatter marks, and mottling, are described and the significance explained. This should be of particular interest to those concerned with visual appearance as an indication of quality or process control.

It is pointed out that simple or flat parts are much easier to coat by any of the processes than are intricate shapes of the same material. This is due to the low throwing power of most electrolytic baths, and poor accessibility of certain areas during spraying or dipping.

Several unusual applications for metallic coatings are discussed. For example, chromized low alloy steel is equal in corrosion resistance to a 30 per cent chromium stainless steel. Electroplating with copper can be done to shield certain areas during carburization. Aluminum coatings are used to lend resistance to corrosion, galling, and abrasion. The use of coatings for temporary use includes such subjects as oil and greases for rust prevention, and plastic coatings which can be stripped or peeled from the part whenever desired. There are also special coatings effected by chemical conversion of the metal surface, such as anodizing, phosphating, chromating, and the black oxide type of coating. A small amount of discussion is given on the use of ceramic and cermet coatings for high temperature use. Use of coatings are discussed in the fields of aircraft, automobile, household appliances, boilers, and oil field piping. Cathodic protection—in addition to coatings—is found useful for applications in soils or salt water where electrolysis can occur.

For discussion purposes, organic coatings are divided into three classes: paints, enamels, and lacquers. The

primary difference is due to the carrier employed. The chemistry of organic coatings is discussed in detail, including the drying action. The use of pigments is also included.

Numerous methods for testing coatings are discussed in detail and evaluated. These methods include corrosion tests, salt spray, humidity, adherence, ductility, thickness of coating, weight of coating, ability to withstand bending, magnetic and electronic gages, metallographic, and physical tests such as abrasion. Many of these tests are practical tests which are actually used extensively by quality control groups.

Some Fundamentals of Combustion, Gas Turbine Series, Vol. 2, by D. B. Spalding, Academic Press, Inc., and Butterworths Scientific Publications, 1955, 250 pp. $7.50.

Reviewed by Robert A. Gross
Fairchild Engine Division

This book is written for the engineer who is concerned with the design of combustion equipment. The author presents the elements of the fundamental phenomena that make up the complex process of combustion, and attempts to draw together in one book the important disciplines which should underlie the design and intelligent development of combustion chambers.

The text first reviews some elements of thermodynamics, fluid flow, and heat and mass transfer. This review covers pertinent fundamentals in 81 pages sprinkled with diagrams, equations, and some numerical examples. The author then treats heat and mass transfer with chemical reaction (67 pages), chemical effects in combustion (76 pages), and engineering implications (15 pages). A pleasant mixture of differential equations, physical models, approximate solutions, and experimental results is presented. The burning of solid fuels, combustion of metals, and surface catalytic combustion are some unusual topics which are briefly touched upon. Combustion in premixed gases, laminar and turbulent flame propagation, flame stabilization, and ignition are some of the more conventional topics briefly discussed.

Although the text aims at fundamentals, the differential equations employed are, unfortunately, often introduced without derivation and quite frequently left naked, i.e., no solutions are presented. Many simple examples, often drawn from the author's own work, attempt to show the influence and interaction of the different phyšical phenomena. Of particular merit is the section on mass transport with chemical reaction.

The author has left out some items which certainly are of interest to combustion engineers. Such subjects as combustion in supersonic flow (detonation), combustion in nonsteady flow (screech, etc.), and ignition time delays have largely been ignored. There is little attempt to filter and unify the fairly extensive list of references.

There are very few places where an engineer can find a single treatment that introduces him to the elements of combustion theory. This book helps fill that gap.

DOW

Dow high temperature magnesium alloys have excellent fabrication characteristics

Lightweight structural metals with high strength, stiffness and elasticity at elevated temperatures! A new group of Dow magnesium alloys offers a great combination of these properties without the fabricating difficulties normally experienced with other high temperature materials.

Specially developed for use in airframes, missile and engine structures, the new alloys are already making weight reductions possible for several manufacturers. These alloys show advantages at temperatures up to 700°F. Limited test data on properties up to 800°F. are available for some of them.

FABRICATION: Fabrication characteristics are equal to those of standard magnesium alloys.

WELDABILITY: 95 to 100% weld efficiency at elevated temperatures.

FORMABILITY: Single deep draws can be easily accomplished.

MACHINABILITY: Best machining characteristics of any structural metal.

One of the new alloys is magnesium-thorium composition HK31A. It is now available in rolled form from stock. Castings and sheet in mill quantities are also readily available. A companion alloy for extruded shapes and forgings will soon be in production.

For more information about the new high temperature magnesium alloys, contact your nearest Dow Sales Office or write to THE DOW CHEMICAL COMPANY, Magnesium Sales Department MA 362MM, Midland, Michigan.

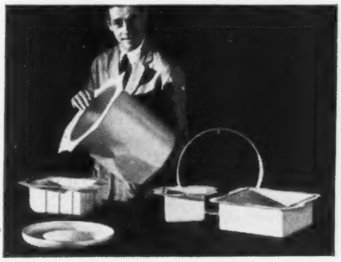

EASILY FORMED. These HK31A parts were drawn using production dies and processes for standard magnesium alloys. The parts retained a higher percentage of original properties than standard alloys.

you can depend on DOW MAGNESIUM DOW

Technical Literature Digest

M. H. Smith, ***Associate Editor,*** **and M. H. Fisher,** ***Contributor***
The James Forrestal Research Center, Princeton University

Jet Propulsion Engines

Efficiency and Pressure Loss in the Combustors of Jet Engines and Combustion Turbines, by Maurice Roy, *Zeitschr. Flugwiss.*, vol. 4, May–June 1956, pp. 190–194 (in French).

Propulsion. Section B. Research and Development Trends. The Future in Ram-Jets, Jet Engine Compressor Problems in High Speed Flight. Gas Turbines for Aircraft (Table), *Aviation Age*, vol. 25, June 1956, pp. B-3–B-21.

Guided-Missile Propulsion, by T. J. Keating, *Aeron. Engng. Rev.*, vol. 15, June 1956, pp. 67–70.

Some Linear Dynamics of Two-Spool Turbo-Jet Engines, by David Novik, *NACA TN* 3274, June 1956, 35 pp.

Free-Jet Performance of 16-Inch Ram-Jet Engine with Several Fuels, by Fred A. Wilcox, *NACA RM* E50I06, Oct. 31, 1950, 23 pp. (Declassified from Confidential, *NACA Research Abstracts* no. 101, May 25, 1956, p. 9.)

Analysis and Experimental Observation of Pressure Losses in Ram-Jet Combustion Chambers, by William H. Sterbentz, *NACA RM* E9H19, Nov. 4, 1949, 22 pp. (Declassified from Confidential, *NACA Research Abstracts* no. 101, May 25, 1956, p. 9).

Free-Flight Performance of 16-Inch-Diameter Supersonic Ram-Jet Units. I. Four Units Designed for Combustion Chamber Inlet Mach Number of 0.12 at Free Stream Mach Number of 1.6 (Units A-2, A-3, A-4, and A-5), by William W. Carlton and Wesley E. Messing, *NACA RM* E9F22, Sept. 22, 1949, 52 pp. (Declassified from Confidential, *NACA Research Abstracts* no. 101, May 25, 1956, p. 8.)

Performance of a Ram-Jet-Type Combustor with Flame Holders Immersed in the Combustion Zone, by Roland Breitwieser, *NACA RM* E8F21, Nov. 1, 1948, 47 pp. (Declassified from Confidential, *NACA Research Abstracts* no. 101, May 25, 1956, p. 8.)

Investigation of Effects of Movable Exhaust-Nozzle Plug on Operational Performance of 20-Inch Ram Jet, by William H. Sterbentz and Fred A. Wilcox, *NACA RM* E8D22, July 27, 1948, 32 pp. (Declassified from Confidential, *NACA Research Abstracts* no. 101, May 25, 1956, p 8.)

Flight Investigation of a 20-Inch Steady-Flow Ram Jet, by John H. Disher, *NACA RM* no. E7I05a, Jan. 14, 1948, 29 pp. (Declassified from Confidential, *NACA Research Abstracts* no. 101, May 25, 1956, p. 8.)

Initial Flight Investigation of a Twin-Engine Supersonic Ram Jet, by Maxime A. Faget and H. Rudolph Dettwyler, *NACA RM* L50H10, Sept. 15, 1950, 28 pp. (Declassified from Confidential, *NACA Research Abstracts* no. 101, May 25, 1956, p. 12.)

Experimental Investigation of Pressure Fluctuations in 3.6-Inch Ram Jet at Mach Number 1.92, by James F. Connors and Albert H. Schroeder, *NACA RM* E9H12, Oct. 13, 1949, 20 pp. (Declassified from Confidential, *NACA Research Abstracts* no. 101, May 25, 1956, p. 9.)

Investigation of Internal Regenerative Fuel-Heating System for 20-Inch Ram Jet, by Sol Baker and Eugene Perchonok, *NACA RM* E9F20, Sept. 1, 1949, 22 pp. (Declassified from Confidential, *NACA Research Abstracts* no. 101, May 25, 1956, p. 8.)

Ramjet-Turbojet Powerplants Can Extend Flight Regime, by Joseph Friedman, *Aero Digest*, vol. 72, June 1956, pp. 30–32.

Turbine Disks for Jet Propulsion Units, Part I, by A. E. Johnson, *Aircr. Engng.*, vol. 28, June 1956, pp. 187–195.

Analytical Evaluation of Effect of Equivalence Ratio, Inlet-Air Temperature, and Combustion Pressure on Performance of Several Possible Ram-Jet Fuels, by Leonard K. Tower, and Benson E. Gammon, *NACA RM* E53G14, Sept. 1953, 59 pp. (Declassified from Confidential, *NACA Research Abstracts* no. 102, June 22, 1956, p. 17.)

Rocket Propulsion Engines

Demonstration of Reliability in Liquid Propellant Rocket Motors, by A. G. Thatcher and H. A. Barton, *Inst. Aeron. Sci. Prepr.* 588, Jan. 1956, 16 pp.

Approximate Analysis of Rocket Nozzle Scale and Dynamic Effects, by Franklin P. Durham, *Colorado Univ. Rep.* 5, Oct. 1954–April 1955, 45 pp.

Some Aspects of Guided Missile Power-Plant Reliability Requirements, by H. A. Eubank, C. C. Ross, and R. C. Stiff, *Aerojet-General Corp.*, 1955, 19 pp. (ASTIA AD- 74,360.)

Tables for Determining the Pressure and Temperature of the Reservoir of a High-Low Pressure Gun or a Rocket Motor, by W. Boyle and H. Flatt, *Aberdeen Proving Ground Ballistic Res. Labs., Rep.* 772, *Supplement*, Aug. 1955, 55 pp.

Reminiscences of German Rocketry, by Wernher von Braun, *J. Brit. Interplan. Soc.*, vol. 15, May–June 1956, pp. 125–145.

Combustion Chambers for Rocket Engines, by A. D. Baxter, *J. Brit. Interplan. Soc.*, vol. 15, May–June 1956, pp. 146–163.

Investigation of Rocket Engines for the Direct Measurement of Exhuast Jet Velocities, by Loren E. Bollinger and Rudolph Edse, *Wright Air Dev. Center Tech. Rep.* 54–269, March 1956, 73 pp.

Heat Transfer and Fluid Flow

Preliminary Investigation of Effects of Combustion in Ram Jet on Performance of Supersonic Diffusers. I. Shock Diffuser with Triple-Shock Projecting Cone, by J. F. Connors and A. H. Schroeder, *NACA RM* E8F15, Sept. 15, 1948, 18 pp. (Declassified from Confidential, *NACA Research Abstracts* no. 102, June 22, 1956, p. 14.)

Survey of Information on Two-Dimensional Cascades, by Max J. Schilhansl, Report on Gas Turbine Technology, Brown University, *Wright Air Dev. Center Tech. Rep.* WADC 54–322, March 1955, 168 pp.

Problems and Results in the Investigation of Cascades, by H. Schlichting (translated from *Zeitschr. Flugwiss.*, vol. 1, 1953, pp. 109–122), *Gt. Brit. Tech. Info. Bur. Trans.* TIB/T4538, Nov. 1955, 23 pp.

Feasibility Study of the 1200°F, J-1 4" x 4" Quickly Variable Nozzle for Ram Jet Addition to the Engine Test Facility, Vol. II. Final Report. *Sandberg-Serrell Corp. Rep.* R247–6; AEDC TR-563, Feb. 11, 1956, 372 pp.

Experimental and Theoretical Investigation of Rotating-Stall Characteristics of Single-Stage Axial-Flow Compressor with Hub-Tip Ratio of 0.76, by Robert W. Graham and Vasily D. Prian, *NACA RM* E53I09, Nov. 1953, 34 pp. (Declassified from Confidential, *NACA Research Abstracts* no. 102, June 22, 1956, p. 17.)

Combustion

Investigation of Limits of Flame Stability of Disk Flame Holders in a Free Stream, by Gustave G. Kutzko, *Wright Air Dev. Center Tech. Rep.* 55–134, April 1956, 12 pp.

A Study of the Fundamentals of Combustion, by E. F. Searight, R. T. Ellington, R. E. Peak, and S. A. Weil, Final Report, *Inst. Gas Technology*, May 1955, 28 pp.

Significance of Quenching by Ports in Burning Velocity Measurements by Bunsen Burner Methods, by J. M. Singer and Joseph Grumer, *Project Squid Tech. Rep.* Bu M-14-P, March 1956, 3 pp.

A Flat Flame Burner and Its Characteristics as Applied to Theoretical Studies, by J. W. Jenkins, *Princeton Univ. Chem. Kinetics Proj. TN* 23, Sept. 1955, 48 pp.

The Application of Radiation Techniques to Engine Combustion Studies, by William G. Agnew, *Gen. Motors Engng. J.*, vol. 3, May–June 1956, pp. 14–20.

Isothermal Decomposition of Explosives, by M. A. Cook and M. Taylor Abegg, *Indust. Engng. Chem.*, vol. 48, June 1956, pp. 1090–1095.

Rate of the Reaction: $H+O_3 \rightarrow OH+O_2$. An Analysis of a Product Emitter Flame, by David Garvin and John D. McKinley, *J. Chem. Phys.*, vol. 24, June 1956, p. 1256.

Final Report from May 1, 1952 – June 30, 1955 (Research on Flame Temperatures), by N. Ginsburg, *Syracuse Univ. Inst. Indust. Res.*, Oct. 30, 1955, 44 pp.

Mechanism and Flame Speed for Hydrazine Decomposition, by Mitchell Gilbert and David Altman, *Calif. Inst. Tech. Jet Propulsion Lab. Prog. Rep.* 20-278 June 1955, 6 pp.

Thermal Decomposition of Nitrogen Dioxide, by W. A. Rosser, Jr., and Henry Wise, *J. Chem. Phys.*, vol. 24, Feb. 1956, p. 493.

The Thermodynamic Properties of Carbon Dioxide Up to 1000°C. and 1400 Bars. II. Various Energies, Isochoric Heat Capacity and Joule-Thompson Coefficient, by Dona Price, *Naval Ord. Lab. Rep., Navord* 4086, Aug. 11, 1955, 26 pp.

The Solution of the Equations for a Steady-State, Low Velocity Flame by Means of Relaxation Methods, by Thomas F. Schatzki, *Univ. of Wisconsin Naval Res. Lab., CM*-853, Sept. 14, 1955, 135 pp.

A Comparison of Combustion Modes in Intermittent Jet Engines, by D. F. Pangburn, *Rensselaer Polytech. Inst. TR* AE 5504, Dec. 1, 1955, 1 vol.

The Application of Probability Theory to Explosive-Ignition Phenomena, by Ran-

som B. Parlin and J. Calvin Giddings, *Utah Univ. TR* 17, Sept. 30, 1955, 18 pp.

The Performance Testing of Aircraft Gas Turbine Combustion Chambers Under Altitude Conditions, by P. Martin and M. V. Herbert, *Gt. Brit., Nat. Gas Turbine Estab. Mem.* M. 231, Nov. 1954, 24 pp.

Flame Speeds in Hydrazine Vapour at Low Pressures, by A. R. Hall, *Gt. Brit., Royal Aircr. Estab. TN* RPD 129, Sept. 1955, 12 pp.

Fundamental Principles of Flammability and Ignition, by Bernard Lewis and Guenther von Elbe, *Combustion and Explosives Res. Inc.*, Aug. 31, 1955, 11 pp.

Burning Rate Studies. Part 2. Measurement of the Consumption Rate of Nitroparaffin Fuels with Nitric Acid, and the Effect of Varying the Viscosity of These Systems, by Harry Williams, A. Greenville Whittaker, and P. M. Rust, *Naval Ord. Lab. Rep., Navord* 1999, Pt. 2, March 31, 1955, 48 pp. (*Naval Ord. Test Station,* NOTS 1085).

Non-Steady Behavior of a Simplified Model of Solid Propellant Burning, by Leon Green, Jr., *Aerojet-General Corp. TN*-15, Nov. 1955, 20 pp. (*AF Off. Sci. Res., TN* 55–475).

The Role of Quenching in the Reactions of Oxidation and Decomposition of Methane at High Temperatures and Extremely High Pressures, by Y. N. Ryabinin, A. M. Markevitch, and I. I. Tamm, *Cornell Univ. Dept. of Chem.*, 1956, 5 pp. (translated from *Akad. Nauk., SSSR, Doklady,* vol. 94, no. 6, 1954).

The Thermal Decomposition of Ethane, by Robert E. Varnerin and John S. Dooling, *Catholic Univ. Amer. TN* 8, Nov. 1955, 12 pp. (*AF Off. Sci. Res. TN* 55-408).

Flame Speed Measurements by the Flame Kernel Method, by H. L. Olsen and E. L. Gayhart, *Johns Hopkins Univ. Appl. Phys. Lab., CM*-855, Nov. 1955, 30 pp.

The Chemical Steady State in HBr Flames. I. Diffusion Neglected, by Mitchell Gilbert and David Altman, *Calif. Inst. Tech. Jet Propulsion Lab. Prog. Rep.* 20-276, June 1955, 17 pp.

The Chemical State in HBr Flames. II. Effect of Diffusion on the HBr Flame, by Mitchell Gilbert and David Altman, *Calif. Inst. Tech. Jet Propulsion Lab. Prog. Rep.* 20-277, June 1955, 31 pp.

NO_2 Sensitization of H_2-O_2 Mixtures, by W. Rosser and H. Wise, *Calif. Inst. Tech. Jet Propulsion Lab. Mem.* 20-117, Dec. 1955, 4 pp.

The Mechanism of the Homogeneous Thermal Reaction Between Ethylene and Deuterium, by Robert E. Varnerin and John S. Dooling, *Catholic Univ. Amer. TN* 7, Oct. 1955, 17 pp. (*AF Off. Sci. Res. TN* 55-407).

Mass Spectrometric Investigation of the Hydrogen-Oxygen Reactions, by K. U. Ingold and W. A. Bruce, *J. Chem. Phys.*, vol. 24, Feb. 1956, pp. 360–364.

Report on Thermodynamics, by Norman F. Ramsey, Jr., *Ordnance,* vol. 110, April 1956, pp. 898–900.

Special Study of Mixtures of Normal Hexane and Air. IV. Study of Ignition Delay and Kinetics of Oxidation, by E. Freling, *Inst. Francais du Petrole, Rev. et Ann. Combustibles Liquides,* no. 12, 1955, pp. 1543–1610 (in French).

Effect of Burner-Tip Temperature on Flashback of Turbulent Hydrogen-Oxygen Flames, by Loren E. Bollinger and Rudolph Edse, *Indust. Engng. Chem.*, vol. 48, April 1956, pp. 802–807.

Index to Advertisers

...Giannini AC output, inductive pickoff accelerometers are specified

Giannini AC output, inductive pickoff accelerometers provide the precise accuracy and consistent reliability demanded by today's high speed, high altitude aircraft and missiles.

Supplementing the wide range of Giannini potentiometer output accelerometers, the Series 24611 are ideal for accelerometer applications requiring superlative performance in the most critical airborne guidance and control systems. Through virtually frictionless inertial mass suspension, the magnetically damped Series 24611 Accelerometers offer extreme sensitivity and low threshold; and, as in all Giannini products, RELIABILITY is their distinguishing feature.

WHERE RELIABILITY COUNTS, the Series 24611 is the criterion for accurate, consistently reliable AC measurement of linear acceleration.

For further information, write for Bulletin 24611.

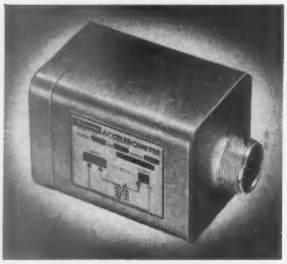

Specifications:

RANGES... ± 0.25g to ± 10.0g

THRESHOLD SENSITIVITY ... as low as 10^{-4}g

AC OUTPUT... to 20v/g

REPEATABILITY ... better than 0.1%

DAMPING ... magnetic, no coulomb friction so that response follows faithfully that of a second order resonant system.

Giannini

Engineering positions are open for career-minded young men at several locations—write for details.

sales offices | ***NEW YORK 1, N.Y.,*** *Empire State Bldg., CHickering 4-4700*
CHICAGO, Ill., *8 So. Michigan Ave., ANdover 3-5272* • ***PASADENA, Calif.,*** *918 E. Green St., RYan 1-7152*

G. M. GIANNINI & CO., INC. • 918 EAST GREEN STREET • PASADENA, CALIFORNIA

JET PROPULSION

Journal of the

AMERICAN ROCKET SOCIETY

Rocketry . . . Jet Propulsion Sciences . . . Astronautics

VOL. 26 OCTOBER 1956 NO. 10, PART 2

(In Two Parts)

Second Annual Supplement on

GUIDED MISSILE EQUIPMENT

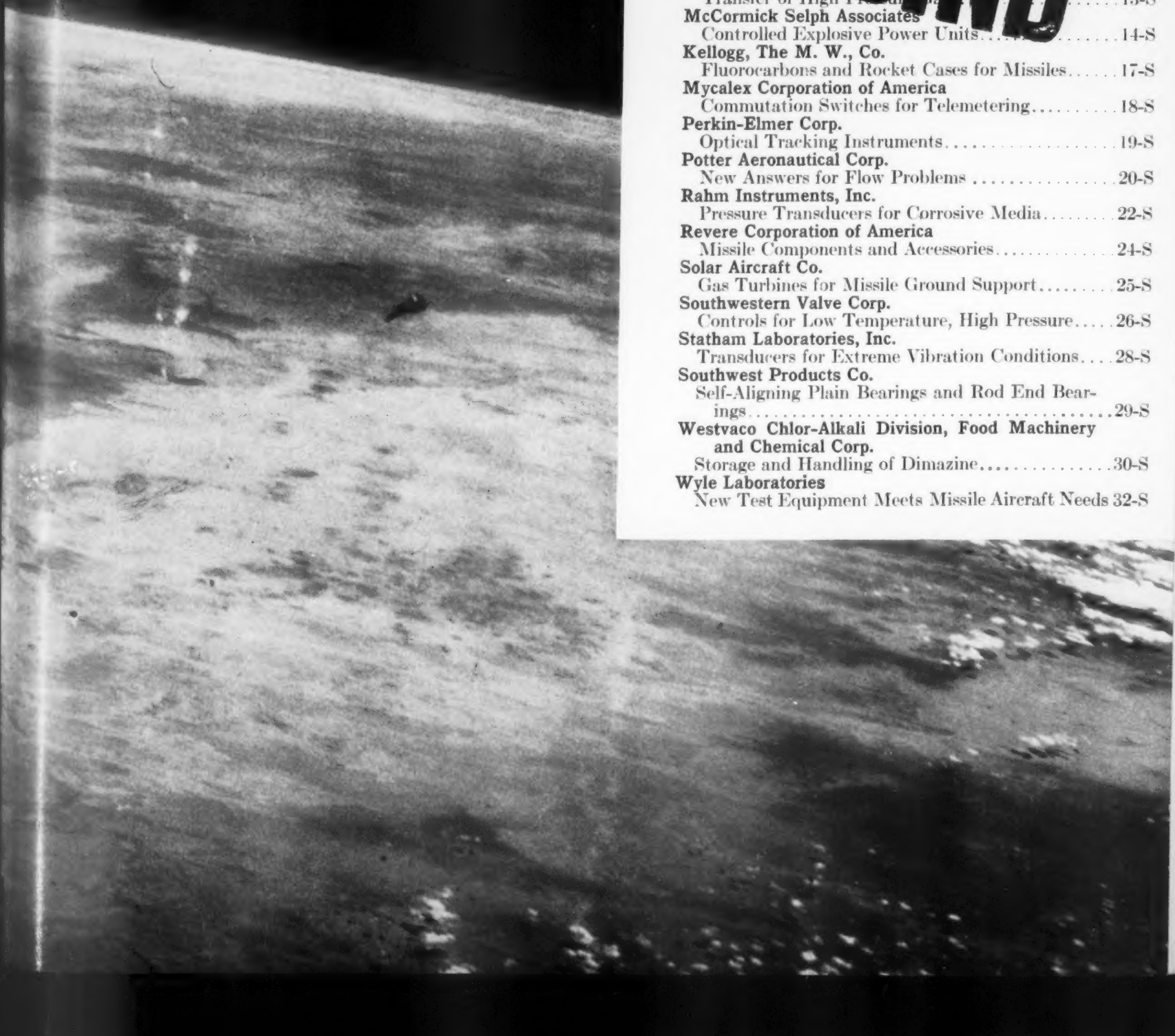

Las
vited
produc
sile E
losoph
ARs
techni
help t
comple
would
now u
pany
with
and pe
supple
This
the ex
once a
tors''

Octo

GUIDED MISSILE EQUIPMENT

A JET PROPULSION SUPPLEMENT
OCTOBER 1956

JET PROPULSION Starts a Habit . . . .

Last September, JET PROPULSION invited industry to "editorialize" about its products in the First Annual Guided Missile Equipment Supplement. The philosophy behind the experiment was this: ARS Members have a need for detailed technical information on new products to help them in their work. Publishing this *complete* information in our regular issues would require more editorial space than is now available. The solution: Let a company write its own new product copy—with graphs, flow charts, photos, etc.—and *pay* for the space in a special annual supplement.

This reasoning was, apparently, sound; the experiment proved a success. So we once again asked our "contributing editors" in industry to prepare copy for the Second Annual Guided Missile Equipment Supplement. This time, however, there were some snags in the arrangement.

We were, for example, guilty of underestimating the amount of time required to compose these articles or, in some cases, to get them cleared through security channels. It's probably a sign of the times that no less than 18 companies said they wanted to be in this year but "couldn't possibly meet the deadline." One prime missile contractor said that 120 days were needed, regretted not being able to submit an article, "as we feel the supplement is an excellent publication which has done much to stimulate interest in the field of guided missiles."

At any rate, the GME Supplement has aroused enough praise of this sort to warrant making it a part of the JET PROPULSION advertising program. It will continue as an annual (along with the Annual Supplement on Careers in the Rocket and Missile Industry*). As presently planned, the next GME Supplement will appear November 1957, and the deadline for copy is hereby announced: September 20, 1957. We promise to announce full details next May.

---

*Also comprised of industry-authored articles, the Careers Supplement gets a special distribution to colleges and this year, if practical, to selected high schools. It will be published in February 1957. Copy (following JET PROPULSION Supplement style) is due December 21, 1956.

Published by the American Rocket Society, 500 Fifth Ave., New York 36, N. Y.

Rocketry and Related Fields

WALTER H. WINNARD, JR.

District Sales Manager, Aerojet-General Corporation, Azusa, Calif.

THE high performance demands, minimum space requirements, and extreme operating conditions of missile systems require a variety of components designed and developed for the particular missile system. The Aerojet-General Corporation, with plants at Azusa and Sacramento, Calif., is America's leading industrial organization devoted to research, development, and manufacture of rocket engines and related devices. Aerojet has long operated as a component manufacturer for missile systems prime contractors.

Founded in 1942, the growth of Aerojet has been that of the rocket propulsion field itself. Over 60 million dollars has been invested in facilities, which include 120 different firing positions for testing hardware ranging from small igniters to rocket engines of one million pounds thrust. The test facilities, techniques, and capacities are second to none. Over 8000 are employed at the Azusa and Sacramento plants.

The reliability requirements of missile equipment are more severe than in almost any other application. In many areas, conventional methods of Quality Control do not provide the degree of reliability that must be assured; and the new or expanded techniques that must be applied continually challenge Aerojet's Quality Control organization. Under the system that has proved most successful at Aerojet-General, close coordination is maintained among Engineering, Production, and Quality Control functions. Quality begins with the basic design, and is engineered and built into the product from this point forward.

Large solid propellant rocket

Rocket Engines

Aerojet's rockets for guided and unguided missiles vary in thrust from a few pounds to over 100,000 lb, and in duration from a few seconds to over thirty minutes. Their application includes use as boosters and prime power plants for missiles.

The diversity and scope of programs successfully completed at Aerojet have resulted in technical competence which can be acquired only through extensive and continued work with a variety of rockets. This successful development experience with a variety of solid and liquid propellant rocket types is more useful than the limited experience with one rocket type and one fuel or oxidizer.

A variety of rocket engines are qualified items in production, i.e., shelf items, while others are in development status.

On the basis of all solid propellant rockets produced by this company on which field firing data are available, 99.91 per cent reliability has been achieved. Over 7000 acceptance test firings have been made on one type, and not one critical defect was observed.

Architect-Engineer Services

The Architect-Engineer Division was organized in response to a demand and to fill a need for specialized architect-engineer services in the field of rocket propulsion. To date, services have been provided for specialized facilities valued in excess of 200 million dollars. Full-time qualified engineering staffs are active and available in the fields of civil, mechanical, electrical, architectural, and process engineering, chemical engineering, instrumentation, and specifications.

Field Service

Supporting services are provided to insure success of Aerojet-General products in the field. Some of these services are: periodic and special field service, resident representation for sustained support, operational support for initial test programs, and training courses for user personnel indoctrination. Field Service Manuals are provided for clarity and assurance of operational acceptability of the system.

Servicing and Checkout Equipment

Portable servicing equipment has been developed for handling fuels and corrosive liquids. These units have self-contained electrical power units to provide power for an electrically driven reciprocating pump capable of delivering fluid in either direction.

Checkout equipment is designed to check rocket components for leaks, pressure ratings, electrical system continuity, individual component timing, and over-all system time sequencing functioning. A self-contained pressure-energy source is provided.

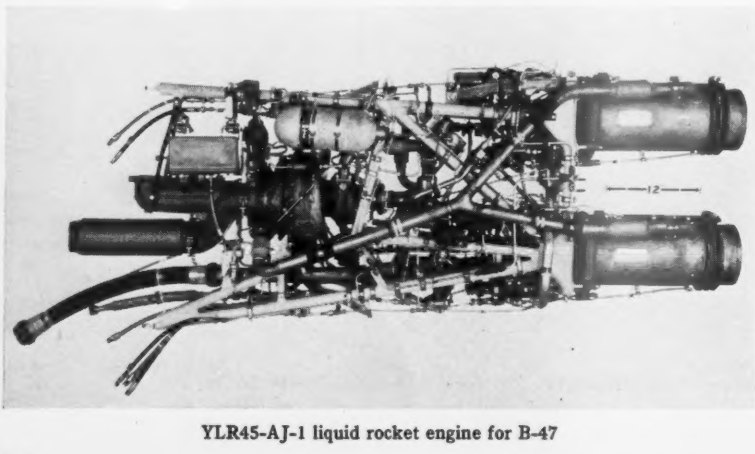

YLR45-AJ-1 liquid rocket engine for B-47

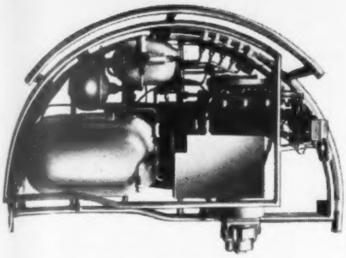

Auxiliary power supply

Auxiliary Power Units

Auxiliary power units are a necessary adjunct to virtually every high speed, high altitude vehicle, and the design, development, and production of such units comprise an important phase of Aerojet's activities.

The requirements for intermittent electrical and hydraulic power in manned and unmanned vehicles long ago exceeded the delivery abilities of conventional sources. Batteries and accumulators, to meet performance needs, often require exorbitant weight and space allotments. The compactness of APU's makes their use mandatory in such installations. Both the one-shot systems, used in early vehicles, and more recent APU's have been shown to be completely adequate and truly reliable "power packages," without which present and future high speed flight would be virtually impossible.

Aerojet has long been successfully engaged in APU work. Yet the work cannot be considered static in any sense. As each new project begins, it has been our experience that the specifications are progressively more severe. Voltages must be maintained within 1 per cent and output frequencies held to within ± 1/4 per cent under wide variations in electrical load. Weight reductions are always required and space too is at a premium.

To achieve the specification requirements, design ingenuity is taxed to extremes. Turbine rotational speeds up to 80,000–90,000 rpm are common. Ambient-pressure conditions from sea level to 65,000 ft and operating temperatures from −65 F to those imposed by supersonic flight are everyday problems. To meet these and other stringent requirements, continuing design and development efforts with new configurations and new products will insure that Aerojet remains in the forefront of this challenging field.

Homing set

Infrared Devices

Aerojet-General's Electronics and Guidance Division now leads the field in manufacture of IR devices for various applications. This highly qualified group is supplying production IR hardware, successfully culminating twelve years of research and development exclusively devoted to IR. These devices are characterized by:

- Passivity (do not betray their presence)
- Superior performance and reliability
- Compactness and light weight
- Low cost

Pressure Switches

Designed primarily for use on rocket combustion chambers, these items are finding widespread use throughout rocket and missile systems as a result of their rugged and reliable operation. Some of the design features are:

- Withstand extremely large overpressures. As an example, a 20-psi switch is not affected by a 4000-psi overpressure.
- Withstand extremely high rates of pressure rise. Tests have been made with rates exceeding 1 million psi per sec without affecting the switch.
- Accurate switch settings can be maintained over broad temperature ranges, and vibration does not affect the switch.
- Highly corrosive fluids can be used with this unit.

Gas Pressure Regulators

Regulators specifically designed for rocket and missile applications have been developed by Aerojet-General. Features of these regulators include:

- Satisfactory operation in missile, aircraft, and rocket environments.
- Accurate outlet pressure regulation, with extremely wide variations in inlet pressure.
- Regulators integrated with other air system components have been developed. Other applications for which our regulators have been used include shutoff valves, overboard dump valves, burst diaphragms, check valves, and relief valves.

Control Valves

A very wide selection of rocket propellant control valves have been developed at Aerojet, and it is within our capability to develop any type of rocket feed system control component.

Aeromarker

The Aeromarker is a device emitting an eye-catching flash of light, instantaneously developing a dense smoke puff of sizable proportions that lingers for minutes; this puff is radar-reflective and, under certain conditions, attractive to infrared seekers. These units are primarily used for visual acquisition or tracking of targets, missiles, or aircraft traveling at high speeds and altitudes ranging above 60,000 ft. Visibility ranges in excess of 50 miles are obtainable, depending on the size of the unit utilized.

Explosive-Actuated Mechanisms

Aerojet's explosive bolts, releases, and latches, made to individual specifications, are intended for applications such as guided missile flight termination and recovery, emergency stores release from aircraft, etc.

Conventional Warheads

Aerojet's Explosive Ordnance staff has contributed to the advancement of current shaped charge and controlled fragmentation systems.

Several new warhead fabrication techniques have been developed at Aerojet-General whereby parasitic weight of components is greatly decreased without loss of efficiency. In turn, explosive efficiency is increased by the application of techniques of explosive loading for maximum density.

Aerocutter

The name "Aerocutter" designates a family of explosively actuated devices designed to cut (1) bundles of electrical wiring, (2) fuel, air, or gas tubing, and (3) tow or control cables. These units are used primarily as a means of flight or thrust termination and as an aid in missile recovery.

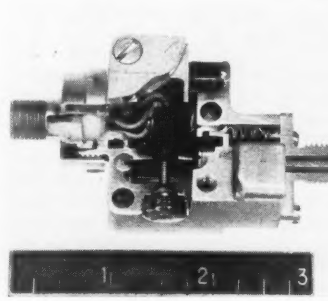

Pressure switch

Guided Missile Destructors

These are designed to contain an amount of high explosive which, when initiated through a self-contained safety and arming mechanism, breaks the missile apart, thereby terminating flight. Destructors are needed for two main purposes: (1) To terminate flight in the event of guidance failure in order to protect populated or test areas from erratic and uncontrolled missile flights; and (2) to render the missile aerodynamically unstable to aid in the recovery of on-board instrumentation.

Conclusion

Aerojet's decentralized organization, with ten operating divisions, offers excellent prospects for engineers, chemists, physicists, and mathematicians with an eye toward an active, challenging future and an interest in intriguing activity.

The Dynamic Unbalance Test Installation

JAMES B. KENDRICK

Project Engineer, Aerophysics Development Corporation
(A Curtiss-Wright Corporation Subsidiary), Santa Barbara, Calif.

THE necessity for adequate test equipment capable of the dynamic balancing of missile and rocket equipment, such as rocket motors, rotating launchers, flywheels, and turbo machines, has always presented designers with problems of test machine simplicity, size, and application. Aerophysics has recently solved this problem through the design and development of a simple vertical balancing machine capable of the dynamic balancing of equipment up to 5000-lb weight, 20,000-lb thrust, up to 36 in. diam, over-all lengths of 10 ft, and rotating speeds of 10,000 rpm. Dynamic unbalance may be measured on a spinning rocket motor, firing or not firing.

The problem of dynamic balancing is one of bringing into coincidence the mass centerline and geometric centerline of a rotating mass. The unbalance is determined by measuring the amplitude and phase of motion of the freely suspended rotating mass. Weights for correction can then be applied in any two corrective planes if it is necessary.

At a speed of 1000 rpm, a 200-lb rotor approximately 50 in. long has been balanced to an accuracy of approximately one-millionth of a radian. Displacement pickups on the test stand have measured displacement to an accuracy of within 0.000050 in. This corresponds to a weight correction of only $^1/_{16}$ oz or 0.004 lb.

The test stand consists of a rigid outer frame, and a stiff lightweight inner frame mounted on two or more flexure rods or cables. These flexure rods serve as vertical supports for the inner frame but do not constrain the lateral or pitching motion of the frame. Adjustments are provided for varying the lengths and attachment points of the flexure rods. In this way the natural frequency of the inner frame can be modified, as desired, to provide optimum response amplitudes. The adjustments will depend on the rotational speed of the equipment mounted in the inner frame. The freely suspended inner frame permits the resolution and recording of extremely minute amplitudes which are due to small amounts of unbalance in the rotating mass.

The outer frame is stiff and comparatively heavy in order to minimize external disturbances to the balancing machine and to provide a fixed frame of reference for measurement. Rigid stops are provided in all directions for safety, convenience of operation, and protection of the flexure rods. The stops may be adjusted, as necessary, to allow motion within the measuring range of the pickups.

Instrumentation is provided for measuring displacements in two correction planes and a phase angle (angular location of unbalance) at the various rotational speeds. The displacement and phase

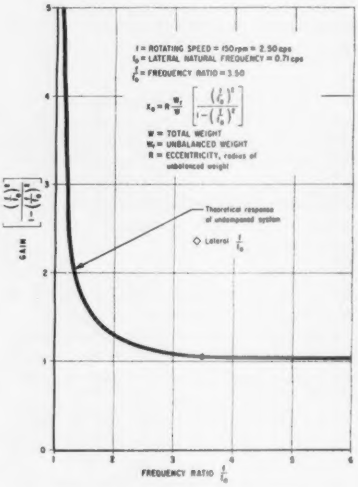

Frequency response curve

angle can be recorded, in addition to location, on an oscillograph record. The displacement pickups are self-contained and include a calibration micrometer. Amplitudes from 0.000050 in. to 0.020 in. or more can be determined using the same pickup. The displacement accuracy of 0.000050 in. corresponds to one-millionth of a radian or one-fifth of a second of arc in a 50-in. spacing of pickups. The displacement pickups are designed to allow an inner frame travel of $^1/_4$ in. without damage to the instrument.

Location of the unbalance position is obtained by using a transducer arrangement. The output of this arrangement is recorded on the oscillograph alongside the displacement record. The location of the maximum displacement point on the periphery may then be determined. This point can be determined within ± 5 deg. The oscillograph record will then include the phase angle and two displacement records.

The alignment specifications for a light-weight motor required the dynamic spin axis to coincide with the geometric spin axis within 0.0003 radian. The empty weight of the rocket motor is approximately 50 lb and will be rotated at 150 rpm or 2.5 rps. At this low rotational speed a lateral natural frequency of 0.50 to 0.75 cps is desirable to assure reproducible measurements of unbalance. If the flexure rods or cables are approximately 20 in. long, the lateral natural frequency f_0 will be

$$f_0 = \frac{1}{2\pi}\sqrt{\frac{g}{l}} = \frac{1}{2\pi}\sqrt{\frac{32.2}{1.66}} = 0.71 \text{ cps}$$

which is within the desired range.

Unbalance in a rotating body is gener-

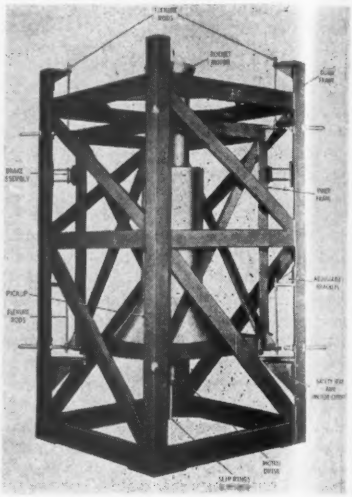

ally measured in ounce-inches. For example, a rotor weighing 62.5 lb (1000 oz) whose mass center is displaced 0.001 in. from the rotational axis, is 1 oz-in. out of balance. This would be an angular unbalance of $0.001/50 = 0.00002$ radian. A malalignment of 0.0003 radian is then comparable to a 0.015-in. displacement of the motor in a 50-in. length. Considering an empty rotor weight of only 50 lb, then unbalance will be

$$(0.015)(50 \times 16) = 12 \text{ oz-in.}$$

Considering the total weight of the test stand inner frame, including the rotor at 800 lb = 12,800 oz, then the displacement will be

$$x_0 = \frac{RW_r}{W} = \frac{12}{12{,}800} = 0.001 \text{ in. for a gain of 1}$$

Thus, a half amplitude displacement measure of 0.001 in. on the test stand would correspond to a malalignment between the dynamic spin axis and the geometrical axis of 0.0003 radian for the empty rotor. Conversely, the displacement measurement times the weight, equals the amount of unbalance.

In order to apply corrective balance weights, it is of course necessary to measure the phase angle between an index point and the maximum displacement of the mass. The accuracy of the balancing operation will be primarily dependent upon the accuracy of the displacement pickups, as well as the phase angle measurements. Proper selection of pickups for maximum sensitivity in the operating range will insure best results.

It is believed that many other useful applications may be found for the present design, which has a wide flexibility for accommodating bodies of various weights, thrust, diameter, length, and rpm.

Temperature and Pressure Sensing Systems

T. M. STICKNEY

Aero Research Instrument Company, Inc.
315 No. Aberdeen Street, Chicago 7, Ill.

IT HAS been found that the design of a good pressure or temperature sensing system requires more than choosing a sensing probe which has good internal performance and reproducibility. The external effects of the probe on its environment and the effects of the environment on the performance of the probe must always be considered. In fact, a good job usually requires complete knowledge of the flow pattern, flow boundaries, boundary layer thickness, Mach number range, pressure range, and temperature range. The design, development, and manufacture of individual probes, rakes, and complete integrated sensing systems have been the specialty of the Aero Research Instrument Company, Inc., for the past three years. ARi has also performed wind tunnel tests and calibrations on a contract basis and has developed instrument wind tunnels for other agencies. A typical example of the latter is a wind tunnel now under construction designed to operate at total temperatures to 4800 R and up to Mach 1.0 at static pressures from $^1/_5$ to 2 atmospheres. This is probably the highest temperature, continuous flow wind tunnel in existence.

Associated products include swaged MgO ultra-high temperature conduit, hot wire anemometer equipment, and subminiature thermocouple reference junctions.

Following is a discussion of several probes of interest to those in the missile field.

T-1305 Aircraft Total Temperature Probe

A small, rugged, and highly accurate total temperature probe has been developed for use on missiles and operational aircraft. This probe, either boom or strut mounted, can be obtained with a choice of resistance elements or thermocouple elements. Resistance elements can be either precision wire wound with operating ranges up to 1000 F or of the thermistor type. Thermocouple elements are available for operation to temperatures of 2800 F and generally show a faster response to temperature changes. Five volt output can be realized from thermocouple elements through the use of small electronic and magnetic amplifiers and a new ARi subminiature cold junction compensator.

Employing the double stagnation principle, the T-1305 has very high recovery (Fig. 1) and negligible radiation and conduction errors. Data also indicate a low time constant signifying rapid response to temperature changes. Probes of this type show complete insensitivity to 20 degree angle of attack.

HS-1063 Aircraft Pitot Static Probe

An electrically heated supersonic pitot static probe designed to meet U. S. Air Force MA-1 specifications is a recent addition to the ARi line of standard products. The probe weighs less than $1^3/_4$ lb and has an ice removal time of less than $1^1/_2$ min. When properly positioned relative to the aircraft, the static pressure error will be less than 1 per cent in the 0 to 3.0 Mach number range except in the vicinity of sonic flow. Moisture problems are virtually eliminated since all orifices are self-draining.

T-1306 "Lox" Probe

A most useful probe for measurements in liquid oxygen, the T-1306 has a rod type thermistor sensing element and a swaged MgO pressure-tight support. Tests indicate that a particular probe will repeat its resistance reading at −183 C well within 1 per cent. A typical calibration performed at ARi is shown in Fig. 2. A calibration curve is supplied with each probe, and each probe is given a series of immersions prior to calibration to stabilize the thermistor element.

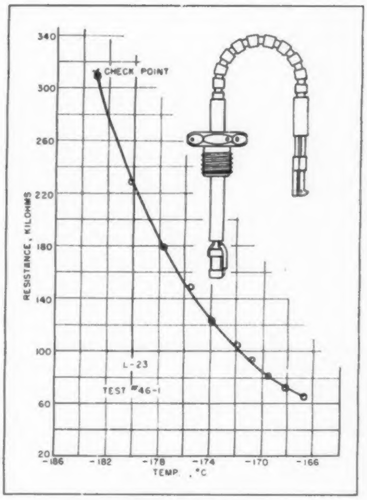

Fig. 2 T-1306 "LOX" probe

T-1006 Uncooled High Temperature Probe

Accurate measurement of total temperatures up to 3000 F is possible through the use of Aero model T-1006-2 aspirated high temperature probe. Preliminary tests indicate a life of about 20 hours at 2900 F without cooling. Tailpipe temperatures up to 2000 F can be measured with the T-1006-1 which is made from less critical materials. Recovery error for the T-1006 probe is less than $^3/_4$ per cent of total temperature, and time constant values usually range from 0.6 to 0.8 sec. Recovery and time response are constant over large ranges of Mach number and ambient pressure. The thermocouple element size and location are such that negligible radiation and conduction errors exist.

T-1105 Water-Cooled Probe

This exposed junction probe is designed for continuous service at temperatures above 3000 F. Corrections for conduction error resulting from the forced cooling are made, using a base temperature measured by two auxiliary thermocouples. Radiation corrections require knowledge of the approximate duct wall temperature. Complete instructions and a calibration curve for recovery are supplied, so that the only other parameters necessary to correct the indicated reading are Mach number and ambient pressure at the probe. Tests in afterburners indicate that accuracies better than 2 per cent are possible after corrections have been applied.

Information regarding small pressure and temperature probes can be obtained by inquiring for our new catalog.

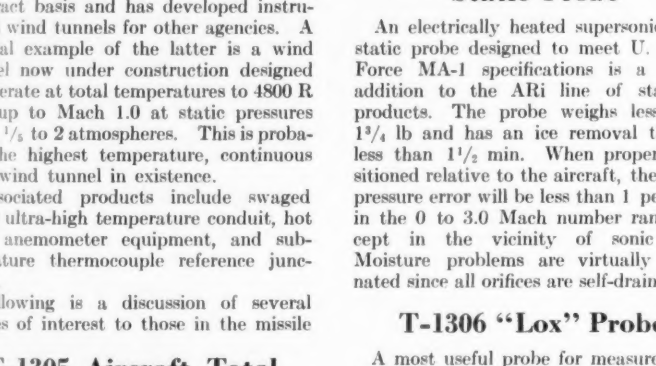

Fig. 1 T-1305 aircraft total temperature probe

High-Speed Digital Data Processing

WILLIAM KNEEN

Technical Services Department
Consolidated Electrodynamics Corporation
300 N. Sierra Madre Villa, Pasadena, Calif.

THE vast quantities of data required by missile and other large-scale test programs have made automatic data processing a necessity. Entire development projects can be stalled while mountains of raw test data wait to be reduced. Today, CEC's MilliSADIC Systems—the most widely used high-speed, analog-to-digital data processing systems—are busy breaking bottlenecks in critical projects all over the country. They are not only saving man-hours and consequently dollars, but they are also shortening the elapsed time between actual tests and the availability of data at engine test facilities, missile telemetering stations, and data processing centers. Aerojet-General, AVRO Aircraft Ltd., Eglin AFB, General Electric, Lockheed (Marietta), NOL (Corona), and Marquardt Aircraft are all using MilliSADIC Systems.

Although custom-engineered for each data processing application, MilliSADIC Systems achieve economy—and unusual dependability—through the use of standardized component modules. They may be readily expanded or adapted to new test demand. Both input and output characteristics are compatible with standard data acquisition, recording, and processing instruments, and CEC's Systems Division can supply integrated MilliSADIC Systems, complete from transducer to computer input.

Inputs

MilliSADIC Systems accept inputs in the form of (1) analog voltages, (2) pulse durations, and (3) pulse trains. With the incorporation of suitable analog-signal-conditioning equipment, a wide range of analog-voltage input levels may be handled. MilliSADIC Systems are well adapted to reduction of data recorded in analog form on magnetic tape.

Outputs

In general, within the capabilities of the analog-to-digital converter or commutator (1500 samples per sec single channel, 400 samples per sec commutated) the speed of the readout device or other receiving device is the limiting factor in determining system speed. Buffer magnetic tape storage allows high input sampling rates with comparatively low-speed output devices. Output may be in the form of punched paper tape, punched cards, or may be fed to an electronic digital computer via digital magnetic tape.

The Converter

The heart of the MilliSADIC data-processing system, the analog-to-digital converter, accomplishes its task in essentially three simultaneous operations. These are: (1) analog to pulse-duration conversion, (2) pulse-duration to pulse-train conversion, and (3) the counting of pulses in the train.

The analog-to-pulse-width converter utilizes a Miller integrator circuit (linear sweep circuit), two "multiar" comparison circuits, two bi-stable multivibrators, and an "AND" gate. The linearly decreasing sawtooth sweep voltage is first compared with a zero reference and then with the analog in question. The time duration between zero comparison and analog comparison is proportional to the value of the analog signal.

Pulse-duration to pulse-train conversion is accomplished as follows: Agreement of the sweep voltage with zero reference starts a local oscillator, whose frequency is 2.5 megacycles, and agreement with the analog stops the oscillator. The pulse duration has thereby measured off a number of cycles proportional to the original analog value (or original pulse duration). Pulse-shaping circuitry follows the local oscillator.

The resulting pulse trains (or pulse trains supplied as input) are counted by a high-speed three-decade counter. The accumulated count of the pulse train represents the digital value of the input signal. Prior to each such count accumulation, the counter is reset to zero. The three-decade counter operates on a binary-coded-decimal basis, with a standard 1-2-4-8 weight for the four flip-flops in each decade.

At a fixed interval after the start of each digitization, the count standing in the counter is transferred to a three-decade register where it is stored until read out in a serial manner to the subsequent system equipment. The accuracy of conversion from converter input to digital output is within one part in one thousand. System error from commutator input to digital output will then be less than 0.25 per cent of full scale. These specified accuracies will be realized for 99.9 percent of the data processed.

MilliSADIC Units

D-C Amplifier

The amplifier raises input signals having a full-scale level as low as plus 0.5 volt to the −100 volt level required by the converter. The amplifier has sufficient band width to amplify the 400-cps square-wave train generated by the commutator, and the highest-frequency components usable on a single-channel basis.

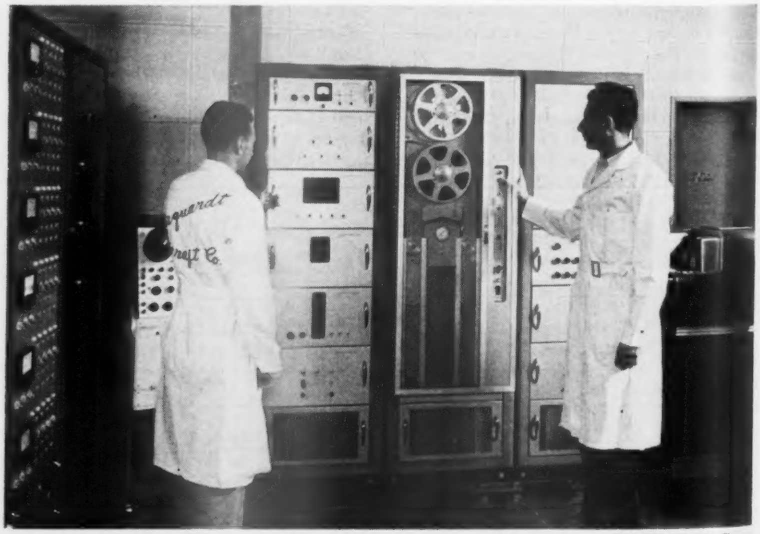

Custom-designed for Marquardt Aircraft Company's specific needs, a MilliSADIC System helps engineers evaluate ramjet engine performance

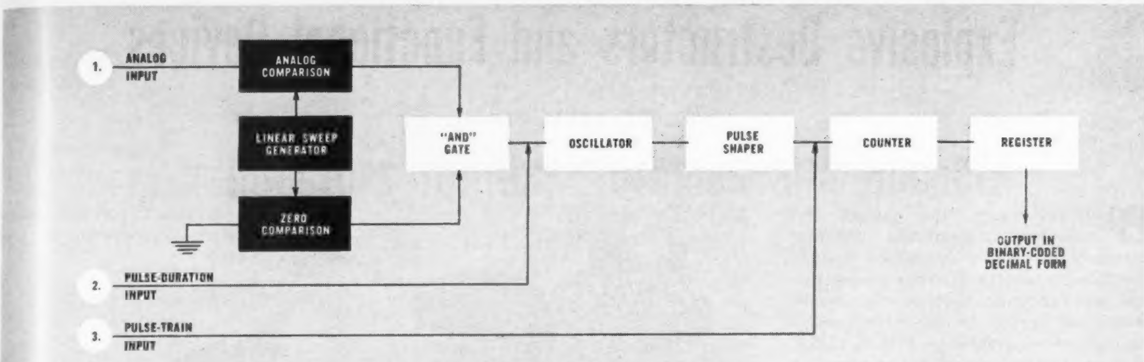

BLOCK DIAGRAM OF MilliSADIC CONVERTER

Control Unit

The control unit provides signals causing the various required operations to occur in the correct time sequence. System control may be completely self-synchronous and control the speed of operation, or it may be controlled by an external signal.

Time Accumulator

The Time Accumulator counts pulses from an internal or external timing source. The time at which the first sample in each data group was taken is thereby provided. Addition of the Time Accumulator to the basic system provides relative time identification of when samples are taken. A modified Time Accumulator, the MilliSADIC Time Decoder, will accept binary-coded-decimal time information supplied by the DataTape system, Consolidated's magnetic-tape data-acquisition system.

Commutator

Addition of the Commutator and a Digital Tape Storage Unit to the basic system will permit the sampling of up to 100 channels at a rate of 400 channels per sec. Input level equals plus $^1/_2$-volt full scale. The high-speed commutator utilizes an electronically controlled relay matrix. Commutation capacities may be expanded in groups of 100 channels.

Digital Tape Storage Unit

The Digital Tape Storage Unit allows data to be taken at one speed and read out at another. This unit permits the actual sampling rate to be as much as 60 times faster than the system output speed.

By recording at one speed and playing back at a slower speed, the rate of sample occurrence may be brought within the limitations imposed by readout devices.

Storage Register

Essentially, the Storage Register is a tape-to-card converter, converting data from the "time-series" form in which it occurred, to "time-parallel" form for insertion onto punched cards. The input to the unit is serially occurring digits, each of which is represented in binary-coded-decimal form. The 1-2-4-8 weights comprising the code appear on four inputs simultaneously.

The Storage Register has the capacity for storing two groups of IBM cards of data and time. Each group consists of 20 three-digit data samples and six digits of time. The remaining 14 columns of each card may be used for fixed constants which may be selected on the front panel of the Storage Register.

A combination of magnetic-drum storage and relay storage is used. While any card of data is being read into the drum storage (in time series), the preceding card of data is being read out of the drum to the relay storage and from there to the punch.

If system output is to be directly into an electronic digital computer the Storage Register may be bypassed. Tape generated by the Digital Magnetic Tape Storage Unit is in the format of the Datatron computer and may be played back on the Auxiliary Tape Unit of such a computer adapted for operation with MilliSADIC. Another tape unit offers an input path into an IBM 704 computer with only slight modifications to the 704. Tape generated by the Digital Tape Storage Unit is played back on this unit.

Additional system modules performing functions not described here may be provided as required. For example, an editing unit capable of controlling the selective digitization of inputs from analog magnetic tape records is available. Through the use of this unit, it is possible to eliminate the processing of redundant data.

Another example of a system module which may be provided is a preamplifier having a limited bandwidth. In commutated systems this preamplifier provides filtering of input circuits when required, as well as the required input sensitivity for low-level signals.

Construction

MilliSADIC modules other than the Tape Storage Unit are drawer-slide-mounted units and are constructed with all heat-producing components mounted toward the center. A center gap continues in line through all drawers in a cabinet, creating in effect a "chimney" for the blower. In addition to heat dissipation, this construction has the advantage of making all wiring and small components easily accessible from the sides of each drawer.

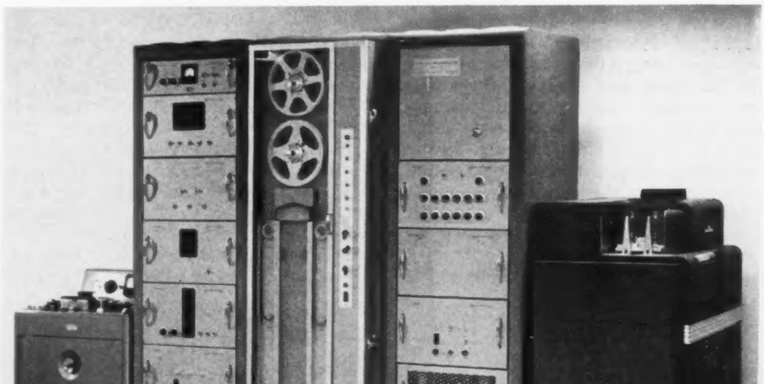

A MilliSADIC System is used by the Missile Evaluation Department at the Naval Ordnance Laboratory, Corona (NOLC), to reduce telemetering data

Explosive Destructors and Functional Devices

E. WILLIAM PLACE

Manager, Missile Products Division, Beckman & Whitley, Inc., San Carlos 12, Calif.

BESIDES having the obvious but unusual manufacturing facilities necessary to serve the specialized needs of the missile industry in explosive destructors and functional devices, Beckman & Whitley is capable of full environmental testing under specification MIL-E-5272A, or more stringent specifications where required.

Extensions of this include the construction of simulated structures for design proof explosive tests, and the rather unique ability to conduct vibration, shock, JAN fuze jolt and jumble, high and low temperature, humidity, and acceleration tests on fully loaded units.

In five years background in this field, Beckman & Whitley products have seen service on practically every major missile.

Explosive Destructors

Possible variations in design of explosive destructors are practically infinite when the special problems of configuration and location in the missile are, as they must be, taken into account. However, from a functional standpoint, Beckman & Whitley destructors can be classified as those armed by: (1) lanyard, (2) shock, (3) electrical command pulses, (4) acceleration integration, and (5) other miscellaneous parameters such as heat, altitude, etc. Charge types include: (1) Primacord, (2) canister (integral and remote), and (3) shaped charge (integral and remote).

In all units, proved, stable military explosives are used for safety in handling and dependability in use. Built-in time delays up to ten seconds can be provided, and where fault-free operation is required under conditions of power failure, units are self-powered by integral batteries.

One feature common to all destructors is that of detonator-safe initiation. A basic safe/arm device is illustrated in Fig. 1. This unit stands between the priming circuit and the charge and functions in such a way as to assure that closing of the priming circuit will not fire the destructor as long as it has not been placed in the armed position by removal of the lanyard pin. Effectiveness of the unit can be seen from the photo.

The foregoing functions are elaborated and refined in the unit illustrated in Fig. 2.

Fig. 2. Remotely commanded electrically armed destructor with telemetering and safety circuits included

Here is shown an integral canister type with remote electrical arming and telemetering features. A rotary solenoid takes the place of the spring drive to rotate the detonator charges into alignment between the primers and the boosters, these functions being applied in dual parallel in most designs to insure infallibility.

Added circuitry in this unit provides switching so that separate pushbuttons are used for arming and disarming. Further circuitry returns a telemetered signal to the command position for indication of either safe or armed position, and short-circuits the primers when the unit is in safe position.

Fig. 3 illustrates a destructor with still greater functional sophistication and one in which a high degree of destructive capability is packaged into a remarkably small volume. This is an acceleration-integration armed unit with an integral shaped charge. In the top view, the aperture of the shaped charge can be seen; the installation plate which forms a section of the skin of the vehicle is at the upper rear. At bottom is the arming mechanism. The objective of this destructor is to perforate the nose of a rocket engine and at the same time separate structural parts of the missile under arming conditions which would assure that the vehicle was not only in flight but had reached a certain specified distance from the launcher before actuation could be possible. The mechanism shown permits arming only after the proper number of g's have been applied in the correct direction and sustained for a long enough time to permit the associated clockwork escapement to pass through its cycle.

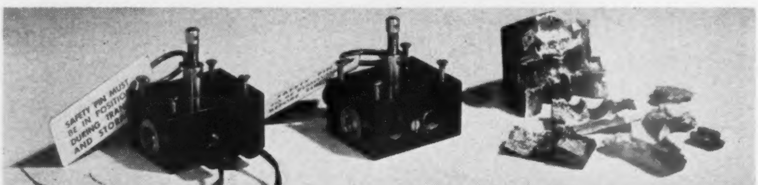

Fig. 1. Safe/arm unit for destructor and device: left, intact; center, after firing in safe position; right, after firing in armed position

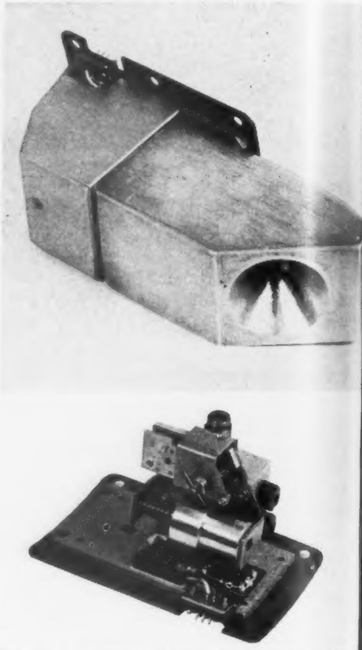

Fig. 3. Shaped charge destructor with acceleration-integration arming mechanism

Functional Devices

Considering space, weight, and cost, one-shot functions can be most efficiently driven by explosive action as contrasted to hydraulic, pneumatic, or electric methods. There are a half a dozen or so major types of functional devices which have been produced by the Beckman & Whitley group. These include: guillotine choppers; electrical components such as disconnects and relays; pullers, thrusters, and rotators, including releases, pistons, etc; frangible bolts; injectors; and valves.

A typical guillotine cutter is this Primacord-actuated type (Fig. 4). Units have been produced large and powerful enough to cut $2^1/_2$-in.-diam air-to-air refueling hose.

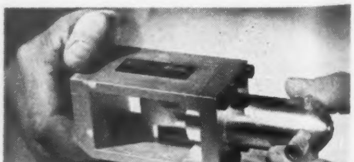

Fig. 4. Guillotine chopper for severing combination bundles of fuel and hydraulic lines, electrical cables, etc.

Fuel Injectors for Gas Turbines and Rockets

H. F. ROTHWELL

Vice-President, Engineering
Delavan Manufacturing Co., West Des Moines, Iowa

A battery of test stands used to test and calibrate jet aircraft engine nozzles

SINCE the termination of World War II, development of reaction engines for aircraft has been intensive enough to bring significant advances in the techniques of fuel injection. Particularly in the case of gas turbines, enough work has been done to evolve fuel injector types which have been adequate for present needs. Experience has established injector types which seem to have the best prospect of success with more demanding needs of the future. The more stringent requirements are the outgrowth of the need for more power.

Designs of liquid fuel injectors for both rockets and jet engines represent as much variety as the engines in which they are used. Each is designed specifically for its intended purpose. Advancement of the art, improved materials of construction, improved liquid propellants, and innovations in engine development will almost certainly result in progressively more exacting requirements for future propellant injectors. In rockets the trend toward controlled flight, prolonged use of power, and manned rocket-powered craft will inevitably emphasize the need for modulated propellant injection in future engines.

It seems probable that some of the techniques of fuel injection employed in aircraft gas turbine may lend themselves, with appropriate revisions, to the more advanced form of rocket propulsion. Basic requirements common to fuel injectors for gas turbines of the present and propellant injectors for rockets of the future are:

1 Wide range of fuel input rate to accommodate varying demands of thrust from take-off to high altitude cruise.

2 Precise metering of propellant input rate to minimize the cumulative effect of variables in fuel system components which affect flow rate.

3 Dependability under the full range of expected operating conditions.

4 Durability. Even in expendable rocket applications, the injectors must withstand the rigors of considerable performance testing in the engine.

5 Simplicity of design, construction, and control.

6 Minimum weight and volume.

7 Design which will minimize malfunctioning from corrosion or deposits resulting from distillation or decomposition of residual liquids.

8 Spray droplet patternation to provide optimum combustion in the space available.

9 Freedom from internal or external leakage due to thermal expansion or other causes.

It is anticipated that rocket engines of the future will introduce a list of problem requirements peculiar to themselves. Among these may be:

1 Higher temperature operation. Rocket range varies as the square of specific impulse. Higher combustion chamber temperature and pressure increase specific impulse. The urge for improvement will no doubt lead to the development of improved propellants and materials of construction which will respectively produce and permit a higher temperature environment for the injector.

2 The propellant materials, together with elevated temperatures, may result in unique problems of corrosion resistance versus the necessity for machinability, hardenability, etc., of parts which must be manufactured to close dimensional limits.

3 In the case of bipropellants, and particularly those which are hypergolic, the necessity for external mixing and the absolute avoidance of internal leaks will be imperative.

4 Future higher energy propellants may evolve special problems of mixing and spray droplet patternation in relation to combustion efficiency. With this will go the necessity for more specialized study of droplet size and patternation.

5 Unforeseen innovations in engine design may possibly introduce the need for complementary innovations in injector design, control, and principles of operation.

Perhaps the most important asset which can be borrowed from aircraft gas turbine injector experience is the availability of highly specialized engineering organizations accustomed to satisfying the fuel injection requirements of an exacting and rapidly advancing industry. Facility for design and development is brought to a state of high efficiency through continuous intensified activity along those lines. The approach and the philosophy of development are similar in both jet and rocket propulsion; only the details may be different.

Experience has taught the wisdom of anticipating problems in advance. With an early start toward their solution and the application of adequate engineering manpower, the results are likely to be available when needed.

Instruments and Test Equipment

RALPH E. BROWN
Vice-President and Chief Engineer
Genisco, Incorporated, 2233 Federal Ave., Los Angeles 64, Calif.

Test Equipment

G-Accelerators

GENISCO G-Accelerators provide a quick, accurate means of subjecting electronic or mechanical components and assemblies to g forces similar to those encountered in actual operation.

All models were designed to provide extremely simple operation, necessary accuracy, and to perform for long periods with only routine maintenance. They are suitable for both precise laboratory testing and large-quantity, production-line test programs. Modifications in the basic machines or accessories to meet particular requirements will be given prompt attention by Genisco engineers. Write, outlining your specific needs.

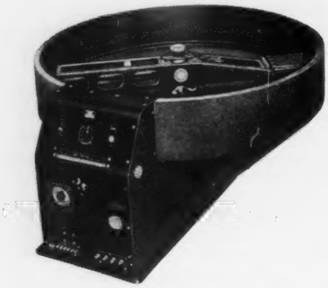

Model B78—Used primarily for testing relays, switches, tubes, etc., and for calibrating and evaluating accelerometers.

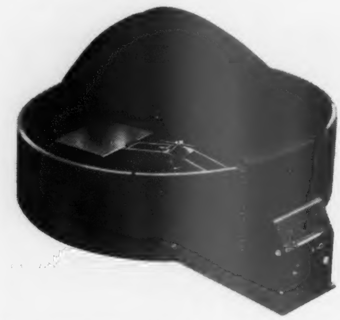

Model C159—The 100 lb weight capacity of this larger machine permits testing of system packages or sub-assembly components of missiles or aircraft.

Model D184—A high speed machine for testing accelerometers and other small instruments under high g forces.

Model E185—(Not illustrated.) Accommodates two complete mechanical or electronic packages weighing up to 300 lb each. Has automatic dynamic balancing system.

Accessories add to testing convenience
Accessories for Genisco G-Accelerators include an optical system, air system, additional slip ring systems, special mounting stand, strobe system, access doorway and deep tubs to accommodate tall test objects, closed-circuit television system for the E185.

Specifications for Genisco G-Accelerators

		Model B78	Model C159	Model D184	Model E185
g range		0.02 to 110 g	0.03 to 75 g	1 to 800 g	0.02 to 65 g[1]
rpm range		5 to 420 rpm	5 to 280 rpm	50 to 1650 rpm	10 to 180 rpm
Radius of gyration		19″ to 24″	22″ to 46″	1″ to 12″	40″ to 80″ maximum
Weight capacity		25 lb	100 lb each end of boom	6-1/2 lb objects 2–5 lb objects	300 lb each end of boom
Centrifugal capacity		1200 g lb	2000 g lb	1000 g lb	30,000 g lb
Accuracies: Performance (basic machine)	Wow	0.5% maximum above 10 rpm	0.5% maximum above 10 rpm	0.5% maximum above 50 rpm	0.5% maximum
	Drift	0.1% maximum above 10 rpm	0.1% maximum above 10 rpm	0.2% maximum above 50 rpm	0.5% maximum
Accuracies: speed measuring devices	Tachometer	within 1% above 30 rpm	within 1% above 30 rpm	within 1% above 200 rpm	within 1% above 30 rpm
	Timer & counter	0.5%	0.5%	0.1% at any speed setting (pulser & electronic counter)	0.1% at any speed setting (pulser & electronic counter)
	Strobe	0.1%, or within accuracy of line frequency[2]	0.1%, or within accuracy of line frequency[2]	0.1%, or within accuracy of line frequency	not used
Max. test object size		8″ × 8″ × 8″	24″ × 24″ × 18″	6″ × 6″ × 6″	30″ × 28″ × 27″
Vibration isolation		0.03 g up to 500 cps	0.03 g up to 500 cps	0.03 g up to 500 cps	0.01 g maximum in any plane
Motor		1-hp, 220/440 v, 60-cps, 3-phase	1-hp, 220/440 v, 60-cps, 3-phase	1-hp, 220/440 v, 60-cps, 3-phase	15 hp, 440 v, 60-cps, 3-phase
Dimensions:	Length	65″	105″	42″	requires compartment 16′ diam × 7′ high; a recess in the floor 5′ in diam × 3′ 6″ deep may be required
	Width	56″	96″	31-1/2″	
	Height	32″	50″	88-1/2″ maximum	
Shipping weight		850 lb	2760 lb	1400 lb	5900 lb

[1] Range to 100 g is available with larger power supply.
[2] Optional equipment.

Rate-of-Turn Tables

Rate-Of-Turn Table, Model C181—An extremely precise machine for calibrating and evaluating rate gyroscopes, or for low g force testing and calibrating purposes. It is rugged, simple to operate, and built to operate continuously for long periods with only minimum maintenance.

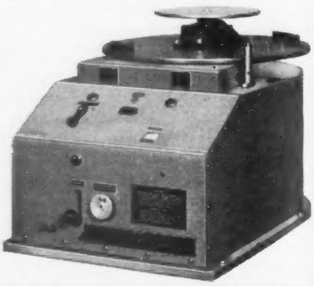

Genisco Rate-of-Turn Table, Model C181, with Sub-Range Adapter mounted on main turntable.

Specifications:

Range: Infinitely variable from 0.01 deg per sec to 1200 deg per sec.
Turntable capacity: 100 lb.
Electrical noise levels: Leads are individually shielded and of instrumentation quality. Noise levels in standard rings are approximately −60 db or better.
Constancy of angular velocity: Within 0.1 per cent, including errors due to wow and drift, at any rate setting.
Vibration acceleration: Not to exceed ±0.015 g at frequencies up to 500 cps.
Accuracy of rate settings:
By use of drum scale: Within 1.0 per cent of actual rate.
By use of tuning fork strobe: Within 0.01 per cent.

Accessories for the Rate-of-Turn Table, Model C181, include a precision Strobe System, Sub-Range Adapter, mounting stands.

Rate-of-Turn Table, Models G347 and S347—A small, relatively inexpensive machine for rapid calibration and evaluation of rate gyroscopes. The Model G347 has an infinitely variable range of 1 to 600 deg per sec; the Model S347 is infinitely variable from 0.1 to 60 deg per sec. A unique-disc-integrator drive system provides smooth and constant rotation of the turntable over full range. Additional features include maximum portability, simple foolproof operation, and virtual immunity to operational abuse. The machine incorporates 18 slip rings and an integral stroboscopic system.

Specifications:

Range: 1 to 60 deg per sec (Model S347); 1 to 600 deg per sec (Model G347).
Turntable capacity: 25 lb.
Electrical noise levels: High quality slip rings provide for transmission of low-level signals with negligible electrical noise.
Constancy of angular velocity: Within 1/2 per cent, including errors due to wow, drift, and flutter at any rate setting.
Vibration acceleration: Not to exceed ±0.015 g at frequencies up to 500 cps.
Accuracy of indicated rate settings: Accuracy of setting and repeatability better than 1 1/2 per cent.
Accuracy of strobe rate settings: Better than 0.1 per cent.
Weight: 60 lb.

Table tilts 90 deg—The machine can be operated with the axis of table rotation at any angle between the horizontal and vertical. This feature of inclinability can be used to produce fractional sinusoidal functions of acceleration of gravity as well as to compensate for earth rotation.

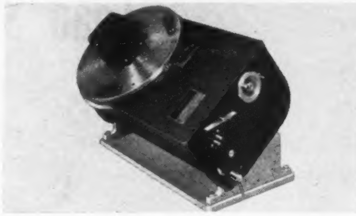

Instruments

Genisco's primary specialization in instrument manufacturing is potentiometer-type accelerometers for guided missile, aircraft, and fire-control system application. Many Genisco instruments are currently being used on missiles in large-scale production.

The success of Genisco instruments is due largely to two factors: design competence and skilled technical artisans. Unusually clean potentiometer windings, double-contact precious-metal brushes, and precisely set brush pressures result in extremely low noise levels. All instruments are hermetically encapsulated to provide complete isolation from external environmental contaminants.

Accelerometers—These instruments now available in large quantities.

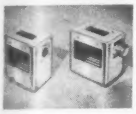

Accelerometer, Model DDL—Magnetically damped, low-range instrument available in ranges from ±1 g to ±30 g. Ultrasensitive models can be supplied with ranges as low as ±0.1 g. Certified to Air Force Spec. MIL-E-5400 and MIL-E-5272A. Especially good where severe shock and vibration accelerations are encountered.

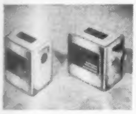

Accelerometer, Model GLH—Magnetically damped, rugged instrument with low natural frequencies for low range. High quantity production assures good price and delivery schedules.

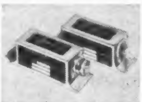

Accelerometer, Model GMO—Miniature, viscous-damped, rugged instrument with ranges from ±2 g to ±30 g. Unbalanced range instruments also available. High natural frequencies.

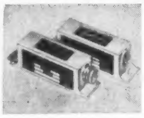

Accelerometer, Model GMT—Basically a Model GMO with internal thermostat-operated heater, assuring maximum environmental stability within the instrument. Damping remains constant with change in ambient temperature.

Analog Digital Converter

The Genisco Analog Digital Converter (ADC) converts variable mechanical positions into unambiguous electrical contact settings of decimal form.

Each standard decade has ten possible positions. A stack of three decades covers a number range from 000 to 999; a stack of four, 0000 to 9999, etc.

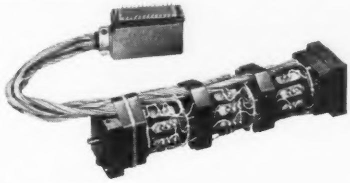

Specifications:

Reliability and long life: 400 × 10^6 number changes without servicing; 96 × 10^3 number changes per minute possible with special adaptor.
No additional relays required: 1 amp dc contact rating. Readout taken at standstill.
Accuracy: Better than one least increment.
Low torque required: A three decade unit has a friction breakout torque of 0.5 oz-in. maximum. Additional decades contribute little additional friction.

General Specifications for Genisco Accelerometers[1]

		DDL	GLH	GMO	GMT
Range		±0.1 to ±8 g [2]	±0.1 to ±8 g [2]	±2 to ±30 g	±2 to ±30 g
Natural frequencies		5 to 14 cps	6 to 16 cps	14 to 52 cps	14 to 52 cps
Linearity		all calibration points within 1% of full scale from the best straight line			
Resolution		proportional to number of turns of potentiometer, generally 0.34% of full scale			
Damping		0.5 to 0.9 of critical	0.6 to 0.9 of critical	0.3 to 2.0 of critical	0.3 to 2.0 of critical
Hysteresis		generally less than 0.5% of full scale output			
Operational life (minimum)		3,000,000 cycles	3,000,000 cycles	2,000,000 cycles	2,000,000 cycles
Potentiometer resistance		2K to 10K	2K to 10K	2K to 15K	2K to 15K
Acceleration Environment[3]	Vibration	MIL-E-5272A, procedure I	8 g at 10 to 55 cps on any axis	10 g on nonsensitive axes; 100% overload on sensitive axis	10 g on nonsensitive axes; 100% overload on sensitive axis
	Steady-state	50 g on nonsensitive axes; 100% overload on sensitive axis	40 g on nonsensitive axes; 100% overload on sensitive axis	40 g on nonsensitive axes; 100% overload on sensitive axis	40 g on nonsensitive axes; 100% overload on sensitive axis
	Shock	MIL-E-5272A, procedure II	40 g for 11 msec on nonsensitive axes; 100% overload on sensitive axis	50 g for 7 msec on nonsensitive axes; 100% overload on sensitive axis	50 g for 7 msec on nonsensitive axes; 100% overload on sensitive axis
Operational temp range		−65 F to + 275 F	−65 F to + 185 F	−10 F to + 185 F	−65 F to + 200 F
Connections		glass hermetically sealed header or cannon receptacle			
Finish		standard finish is gold plate; other finishes and paints optional			
Weight (approx.)		40 oz	2 to 2 1/2 lb	8 oz	10 oz
Brush contact resistance		equivalent contact resistance less than 100 ohms at 0.1 ma brush current			

[1] Exact specifications for particular instrument applications will be submitted upon request.
[2] Ranges to ±30 g with reduced damping.
[3] Higher ranges better in regard to environmental conditions.

Lead Sulfide Photosensitive Resistor

STANLEY H. DUFFIELD

Development Engineer, Apparatus and Optical Division
Eastman Kodak Company, Rochester, N. Y.

FOR missile instrumentation and sensing applications, there are unique advantages in the simplicity of the Kodak Ektron Detector, a photosensitive resistor.

The Kodak Ektron Detector utilizes the peculiar electrical properties of lead sulfide. Normally formed on a 0.30-in.-thick glass blank, it consists of a rectangular deposit of lead sulfide and gold electrodes deposited at the edges of the sensitive area. Complex, exact arrays and mosaics of such resistors can be produced. The basic unit is overcoated with plastic for protection. Kodak Ektron Detectors are rugged and can be very small.

Although they respond to x-ray radiation down to a few Ångstroms in wavelength, their useful photosensitivity is usually considered to range from 0.25 micron (2500 Ångstroms) to 3.5 microns (35,000 Ångstroms). In the visible region, the detector responds to a 2500 K tungsten light source about the same as a red-sensitive gas-filled phototube of comparable sensitive area under comparable conditions. Though the detector competes with phototubes and photomultipliers when exposed to tungsten light, it reaches maximum sensitivity at a wavelength of about 2 microns in the infrared region. Operating at room temperature at 2 microns, the Kodak Ektron Detector gives hundreds of times the response of a good laboratory bolometer. At −40 C, its sensitivity at 2 microns increases about 25 times. The cell's response to "chopped" or pulsed light sources is usable from steady illumination to as high as 10,000 radiation pulses per sec.

In addition to their exceptional spectra response, Kodak Ektron Detectors are characterized by high signal-to-noise ratio, time constants in the range of 400 to 1000 microsec under normal conditions, dark resistance of 0.2 to 0.8 megohm for any square cell, and a negative coefficient of resistance. In a uniform radiation field, the signal-to-noise ratio at a given voltage varies directly with the square root of the cell area. Since the most interesting properties of these photoresistors are associated with infrared response, investigations have been chiefly in the wavelength region from 1 to 3 microns. Use of geometry is made to obtain a desired dark-resistance value. Choice of cell configurations ranges over an extended scale of resistance values.

Because of the permissible variety in cell geometry, high-impedance detectors need not be long, narrow units, but may be "folded" into compact rectangular patterns. Fig. 1 depicts three detectors of the same over-all size but with impedances of (a) 0.002 megohm, (b) 0.2 megohm, and (c) 20 megohms, respectively. The solid black areas indicate electrodes; shaded areas, the sensitive area; and clear areas, the clear glass base. Because of the generation of rasters which conform to the cell pattern, the folded rectangular patterns do not lend themselves directly to being scanned.

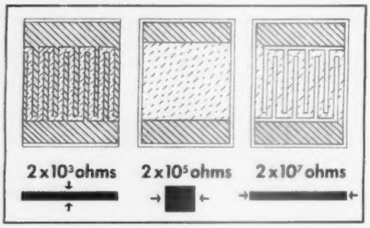

Fig. 1

Cooling the Kodak Ektron Detector causes a rapid increase of signal and resistance relative to the increase in noise. This results in a rapid increase in the signal-to-noise ratio and a corresponding decrease in the required incident radiation to produce a signal equal to noise (noise-equivalent power). One outstanding characteristic of the detector is its absence of mechanical microphonics.

Cooling also brings about a change in the usable spectral range. An upward shift in long-wavelength response at low temperatures extends the range of the detector markedly. To assure maximum wavelength sensitivity, the cell must be isolated from extraneous infrared radiation emitted by surrounding objects at room temperature, since this background illumination may mask the signal.

Kodak Ektron Detectors have a negative temperature coefficient of resistance in the order of 4 per cent per degree centigrade. Therefore, serious mismatch may result from large temperature changes. In employing cooled cells, mismatch can be minimized by using a second cell as the load resistor for the signal cell. Both should be similarly cooled, but the load resistor cell should be shielded from the signal radiation. Eastman Kodak Company fabricates paired detectors as a single unit for this purpose.

The 400 to 1000-microsec time constant of the photo-resistor at room temperature shows a batch-to-batch deviation. It appears to be an undetermined function of the deposition process, which is primarily aimed toward material having maximum signal-output characteristics. The time constant, and hence frequency response, may be altered by changing the temperature of the detector. Response to radiation chopped at frequencies over a range of temperatures has been determined. For every increase in temperature, there is a decrease in signal amplitude. This decrease grows less marked and occurs at higher chopping frequencies as temperature levels rise. The signal, expressed in decibels, becomes lower as temperature becomes higher. Available data suggest a boundary condition wherein the response, while being reduced in amplitude, is, at least, more and more independent of frequency.

The response of a Kodak Ektron Detector compared with several phototubes when exposed to a 2500 K source furnishing 67 microlumens per square centimeter at the receiver is shown in Table 1. A 1-megohm load and 90-volt supply were used, and the size and shape of the detector were equal to the projected area of the photocathode of the tubes.

In general, Kodak Ektron Detectors prove most successful for applications which utilize one or more of the following characteristics:

1 Their unique spectral response.

2 Their high signal-to-noise ratio when exposed to infrared radiation.

3 Their small size and over-all ruggedness.

4 Their availability in complex and exact arrays and mosaics.

A booklet giving more detailed information on Kodak Ektron Detectors is available from Eastman Kodak Company, Military and Special Products Sales Division, Rochester 4, N. Y.

Table 1

Kodak Wratten Filter No.→ Color→	None	47B Blue	61 Green	29 Red	87C (Infrared-transmitting)	18A (Ultraviolet-transmitting
	Relative signal with no long-wave cutoff (open to 2.7 microns)					
Ektron Detector	1000	1000	1000	1000	1000	1000
925 (Red vac.)	48	37	37	48	26	22
930 (Red gas)	382	263	266	366	175	354
929 (Blue vac.)	37	3	7	1	1	29

Transfer of High Pressure Gas

RICHARD L. HAYMAN

President, Haskel Engineering and Supply Co., Glendale, Calif.

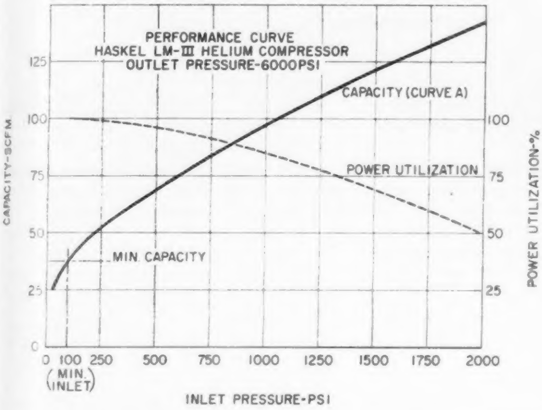

Fig. 1 **Typical performance curves for three-stage booster**

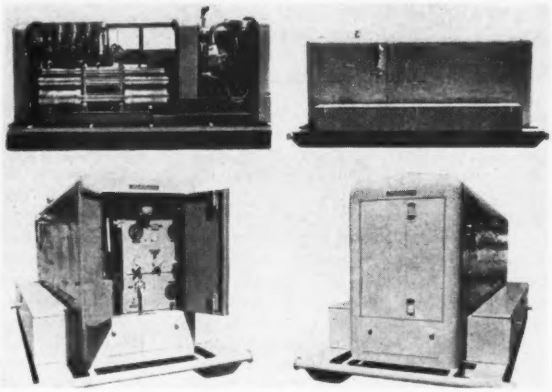

Fig. 2 Haskel Model LM-III Helium Compressor with diesel engine drive and a three-stage, double acting, hydraulic driven compressor; unit is completely equipped for tactical uses

THE use of liquid fuel rocket engines has created a necessity for high pressure inert gas of the utmost purity to be used for pumping the oxidizer within the missile. To meet this requirement, engineers of Haskel Engineering & Supply Co., at Glendale, Calif., have developed a series of booster compressors with a variety of capacities and pressure ranges. These multistage compressors feature:

- Operation without lubrication to minimize contamination of the gas.
- Outlet pressures to 10,000 psi, average capacities from 1 SCFM to over 65 SCFM, inlet pressures as low as 50 psig.
- Operation at full inlet pressure for maximum average capacity from the booster.
- Hydraulic drive for lightweight, compact installation.
- Stationary and portable versions with electric or engine prime mover.

These compressors are particularly valuable when used in conjunction with a blow-down system to supply the high pressure gas to the missiles or related test programs. Such a system uses a high pressure gas storage vessel as a source for the gas. The difference in pressure in this vessel and the desired system pressure is usually great enough to make possible extremely high flow rates. In many cases where the pressure required is relatively low, it is feasible to work directly from commercial bottles at pressures of approximately 2200 psi. However, with the advent of higher pressure requirements in missile and test systems, the pressure in commercial bottles is no longer high enough to supply the final pressure necessary for the high pressure differential required for high flow rates. It then becomes necessary to transfer gas from commercial bottles to receivers that can hold higher gas pressures.

The high pressure receiver size and maximum pressure are functions of the end use requirements, and once these parameters are established the requirements for the entire transfer system can be outlined as follows:

1 Time to fill the receiver to maximum operating pressure when the receiver is initially at zero pressure.

2 Time to fill the receiver to maximum operating pressure when receiver pressure has been reduced to a minimum usable pressure.

3 Total supply volume that must be available to accomplish either items 1 or 2 above when working to certain minimum supply pressures.

The minimum supply pressure of item 3, the time requirements of either 1 or 2, and the maximum operating pressure in the receiver will determine the requirements for the booster compressor.

A careful evaluation of minimum inlet pressure to the booster compressor is warranted to insure that the best compromise is obtained between booster cost and the savings in gas, by reducing the pressure in the supply bottles to a minimum.

From the above requirements, the booster compressor requirements for a transfer system can be approximated thus:

The supply volume required to bring the receiver to operating pressure from a given initial and final supply pressure is

$$1. \quad Vs = \frac{PV_r}{P_1 - P_f} \quad \text{SCF}$$

The equalization pressure when an empty receiver is first opened up to the supply gas is

$$2. \quad Pe = \frac{P_1 V_s}{V_s - V_r} \quad \text{psia}$$

The average capacity required of the compressor to bring the receiver from equalization pressure (2) to operating pressure is

$$3. \quad Qe = \frac{V_r(P - Pe)}{Te} \quad \text{SCFM}$$

And if the capacity is to be based on the time required to bring the high pressure receiver up to pressure from some other pressure than the equalization pressure, the capacity will then be given by

$$4. \quad Qx = \frac{V_r(P - Px)}{Tx} \quad \text{SCFM}$$

The hydraulic drive arrangement used in the Haskel booster compressors is especially suited to meet the various different performance requirements of systems such as outlined above. This hydraulic drive, especially in multistage compressors, proves exceedingly desirable by providing a high average capacity when working from a source such as bottles where inlet pressure will vary over a wide range. This average capacity will be over twice the minimum capacity obtained when working at the minimum inlet and is a distinct advantage over other methods of boosting gas pressures. This can be pointed out by reference to Fig. 1 which shows performance curves for a 3-stage booster in SCFM when compressing gas from 100 psi to 6000 psi. From curve A it can be seen that the output from the booster rises sharply as inlet pressure becomes greater than the 100 psi minimum requirement. When inlet pressure has increased to 2000 psi (the approximate pressure available from commercial bottles), the output has increased to over 300 per cent of the minimum output. Also at this point power utilization is still relatively high despite high inlet pressure.

Vs = supply volume, SCF
Vr = receiver volume, ft^3
P = max. receiver pressure, psi
Pe = equalization pressure, psi
P_1 = initial supply pressure, psi
P_f = final supply pressure, psi

Controlled Explosive Power Units

FRANK W. LaHAYE

Vice-President, McCormick Selph Associates
Hollister, Calif.

ONE requirement basic to all airborne systems and components states that the functions to be performed shall be accomplished by units having the minimum weight and bulk. This item is of particular importance with respect to those devices which are required to perform work such as operating generators, pressurizing hydraulic systems, releasing external stores, and starting engines. One of the most efficient methods developed to date for performing these functions utilizes controlled explosive power as a prime mover. McCormick Selph Associates of Hollister, Calif., have concentrated their efforts on the design, test, and production of such devices. Four specific product lines now manufactured and stocked are:

1 Gas generators.
2 Pressure squibs.
3 Igniters.
4 Explosive bolts.

Each of the above products has been developed and chosen on the basis of broad experience in the field of explosive ordnance. As a result, a standard line of explosive actuated products is now available. These stock items may be obtained in a variety of explosive loads and electrical impulse sensitivities. Due to the rapid expansion of the field of application for this type of unit, a continuing development program is maintained and a design and development group has been established to handle all nonstandard applications.

Explosives, when properly harnessed, have certain prime advantages over any other energy source. These are:

1 The highest energy/storage ratio of any power source enabling the packaging of tremendous power in a minimum space and weight.

2 A reliability factor that approaches 100 per cent when properly packaged and produced.

3 A tremendous diversity of applications.

The availability of "packaged power" in the form of explosive cartridges on both a standard and special item basis is of prime interest to the aircraft and missile industry. Detailed information on the four product lines mentioned above is given in subsequent paragraphs.

Gas Generators

The gas generator is a device for creating a known amount of gas at predictable pressures and temperatures for a given time.

The gas generator is used to provide power for the following basic operations:

1 Operate turbines.
2 Pressurize fluids and systems.
3 Actuate pistons and expandable rings.
4 Ignite liquid propellants.

Some current applications in which gas generators are used are as follows:

1 Ejection systems for personnel and cargo.
2 Emergency accumulator power.
3 Missile electrical generation systems.
4 Bag inflation for flotation or impact.
5 Hydraulic pump actuation.
6 Emergency pressure for braking systems.
7 Gyroscope power.

The gas generator is essentially a small rocket engine and consists of the following items. A squib, igniter, solid propellant charge, pressure controlling nozzle, container, electrical connector and attachment system for connecting the gas generator to the unit for which it is providing power. Fig. 1 shows six types of gas generators chosen to illustrate a selection of sizes and types available.

Fig. 2 shows a cross-section view of the gas generator shown at the top center of Fig. 1. Starting at the left side of the drawing the first part consists of the AN-type electrical connector which is shown with the safety shorting clip in place across the terminals. The next item is the insulating pressure seal through which the electrical connections enter the container. Next is the bridge wire which is heated by the application of electrical current to initiate the explosive primer which surrounds it. The ignition of the primer by electrical heating then starts the burning of the igniter charge which, in this instance, consists of two mechanically and chemically different loads. The first of these loads consists of a booster charge which is a packed individual grain powder pressed directly on top of the primer. The second load is a single tubular pellet which surrounds both the primer and the booster charge. An aluminum disk is used as a closure seal over this entire assembly. The parts previously described are those which comprise the integrated igniter unit which contains the squib and the ignition material. The hermetic sealing of this assembly eliminates the possibility of contamination and insures the highest possible reliability in operation. With the ignition of the booster charge, the gas pressure ruptures the closure and expands into the cavity containing the solid propellant as a cloud of separately burning pellets. Simultaneously, the second igniter load starts burning on the inner surface of the pellet and injects a sustained stream of high temperature gases and solid burning particles into the cavity.

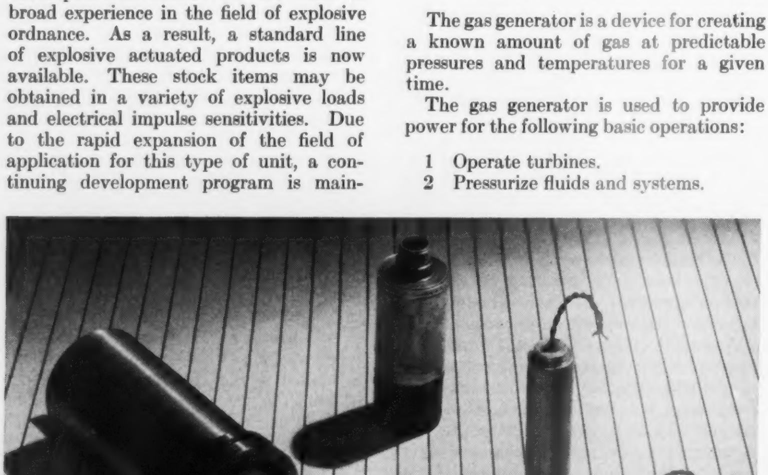

Fig. 1 Typical gas generators shown with 1-in. background spacing

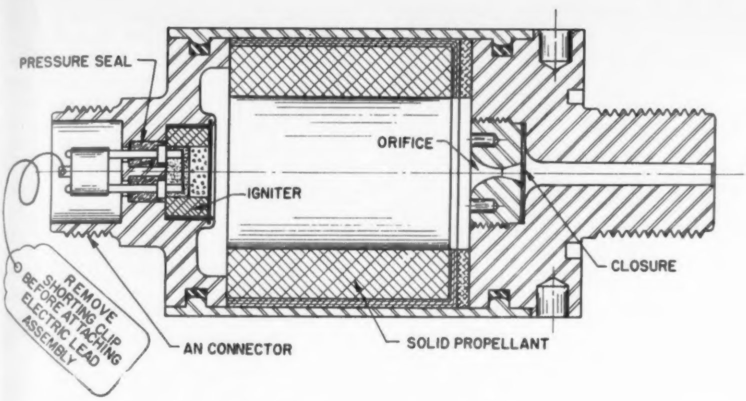

Fig. 2 Gas generator cross section

In this dual action the booster charge initiates ignition of the propellant and the tubular pellet sustains it, thereby providing superior low temperature ignition.

During propellant ignition the temperature and pressure in the cavity rise until the hermetic closure located at the right side of the outlet orifice ruptures, allowing the gas to escape through the duct in the threaded section. This outlet is a critical orifice and will control the escape pressure of the gas within narrow limits until the main charge is practically exhausted.

Installation of the gas generator into its associated system is accomplished by threading it in place with the aid of a standard spanner wrench which fits in the holes provided on the container body. After the mechanical installation the only remaining item is to remove the shorting clip, make the electrical connection, and the unit is ready to deliver its packaged power.

When considering the application of gas generators to the solution of any problem, the following points should be kept in mind:

1 They are highly efficient and can be readily tailored to provide precisely the total power and power rate required.

2 The generator itself has no moving parts and is insensitive to acceleration, vibration, and other mechanical phenomena.

3 Both composite and double base propellants are available and loads may be selected to give a wide range of characteristics with regard to storage and operating temperature ranges, shelf life, horsepower output, burning time, and operating pressures.

4 Cost in production, weight and cube are low in relation to unit of power produced.

5 The units are simple to integrate and install in system.

One interesting characteristic of gas generator performance is shown in Fig. 3. This figure shows four typical pressure time curves for different types of gas generator propellants and configurations. The step curve on this chart is typical of the type of pressure-time response which could be used to drive a turbine for producing electrical energy. The initial high pressure plateau would compensate for the starting mechanical and electrical inertia of the system and the subsequent lower pressure level would continue to drive the system at the most efficient power expenditure.

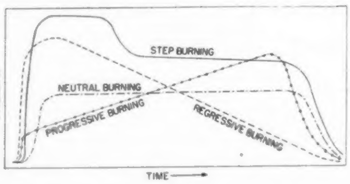

Fig. 3 Typical P-T characteristics

The following is a table of typical performance and specification characteristics for representative gas generators.

Pressure tolerance	±7% at constant temperature
hp output	0.01 to 150
Temperature range	−65 F to +165 F
Operating time	1/2 to 120 sec
P-T characteristics	see Fig. 3
Output pressure	15 to 25,000 psi
Storage life	up to 5 years

The following outline states the information required for the evaluation of a gas generator powered system and for the detail design of the generator. It should be used as a guide when requesting information or preparing specifications on this type of equipment.

1 Type, volume, density, and rate of fluid to be moved.
2 Volume of system before and after operation.
3 Mass flow rate of gas for turbine applications.
4 Pressure and temperature limits of system.
5 Desired pressure or force and opposing pressure or force.
6 Sketch of system to be powered by gas generator.
7 Operating temperature range desired.

Pressure Squib

By definition, a pressure squib is a hermetically sealed mechanical assembly capable of being threaded into an associated system and containing an electrical connector, a bridge wire, a sensitive priming charge, and a main charge.

A typical family of pressure squibs is shown in Fig. 4. There are two basic applications for this item. The first of these is as a self-contained power source for moving pistons or accomplishing other mechanical actuation. In this application the pressure squib is acting as a small gas generator but one having operating times in the microsecond to one-half second range. The second usage is as an initiator for the ignition of larger charges in the manner discussed in the sections on gas generators and igniters.

The McCormick Selph integrated squib design offers definite advantages over previously available types for both of the applications given above. The first of these is the unitized screw-in feature which permits the ready insertion of the unit into pretapped systems. The second is in the variety of operating parameters available in any single size case. The form factor of the squib container permits bridge wire sensitivity to be tailored to individual requirements by variation in wire length, diameter, and material. It similarly allows output pressure, temperature, and functioning time to be modified by changes in type, amount and grain size of both primer and main charge. Therefore, the same squib case may be used for a power source or initiator having a wide range of outputs.

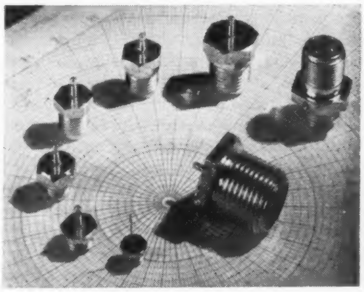

Fig. 4 Representative pressure squibs

Igniters

An igniter is an intermediate device which is initiated by a squib and which in turn ignites another charge. Igniters are used for the ignition of both solid and liquid propellants and are produced in a variety of packages as evidenced by Fig. 5. Due to the intimate relationship between the igniter and the physical configuration and chemical properties of the system in which it is used, the igniter package design is almost wholly controlled by external requirements. Therefore, igniters may be packaged in any number of form factors and materials, including frangible, metal, plastic, and pressed explosive containers. In every case, however, the igniter composition and package are designed and produced in the form having the highest initiation efficiency.

Specific factors effecting igniter design are as follows:

1 Required pressures and temperatures for ignition of the main propellant.
2 Type and geometry of the main

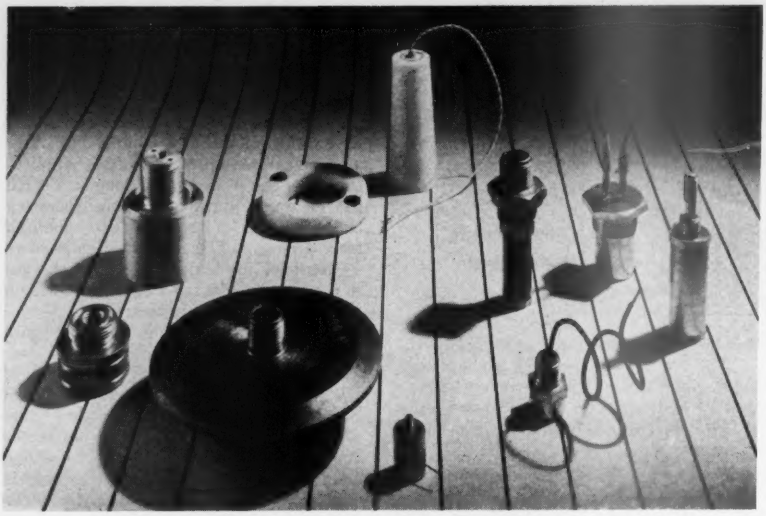

Fig. 5 Current model igniters shown against 1-in. background spacing

propellant (i.e., liquid or solid, end or internal burning).
3 Functioning time.
4 Installation requirements (i.e., head nozzle, fixed or frangible).

Igniters are essentially unique devices requiring new designs for each application if maximum efficiencies are to be achieved. Considerable experience in this field, however, has indicated that igniter design problems logically separate into well-defined families. Therefore, an organization having the requisite background can solve many problems by adaptation of previous models rather than attacking each new problem from a development standpoint. This latter approach should be explored for each igniter requirement and used, if possible, in order to effect the maximum savings in time and money consistent with adequate performance.

Explosive Bolt

Practically any standard bolt can be converted to an explosive bolt by machining it to take an explosive charge. This is accomplished by drilling a concentric hole in the center of the bolt and installing the explosive and firing train. The purpose of this is to provide a component capable of performing the normal bolt holding function with the additional capability of being broken at a predetermined point by an electrically actuated command.

Until recently all explosive bolts were based on the same principle as the pressure squibs previously described. A firing train and main charge were used to build up pressure in a sealed chamber in the bolt center. When the pressure in the chamber exceeded the ultimate tensile stress of the thinnest section of the bolt, the bolt separated. The point of separation was controlled by machining a notch into the outside diameter of the bolt to provide a point of stress concentration. This type of design was reasonably satisfactory as a separation device but did suffer from several major disadvantages. These are:

1 The pressure actuation principle requires a seal for the firing train that has a large safety factor above the pressure required for tensile failure at the weakened section. Any leakage could result in a severe pressure reduction in the chamber and failure to separate.

2 A separate machining operation is necessary for cutting the stress concentration groove and a pre-torquing operation is required in order to assure a clean separation at the groove.

3 To insure separation reliability it is necessary to use thin wall sections at the point of failure. Therefore, when large masses are to be structurally supported, the diameter of the bolt must be excessively increased in order to obtain sufficient total cross section to withstand the required stress.

4 The amount of charge, and therefore the degree of pressure that can be produced, is a partial function of the size of bolt used.

These shortcomings have recently been overcome by a new explosive bolt design as shown in Fig. 6. The new design consists of two major sections, the first of which is the bolt body and the second the explosive cartridge. This two-piece construction enables the bolt proper to be installed at any convenient time and the explosive cartridge to be installed just prior to use. The second principal difference is even more important. The new firing train has a high explosive main charge rather than a slower burning gas producing type. When initiated, this produces a high order detonation and creates a shock wave in the metal of the bolt assembly. This shock wave progresses longitudinally through the bolt until it reaches the section containing the bottom of the bored hole. At this point a stress concentration occurs which exceeds the ultimate stress of the bolt section and results in a clean fracture and positive separation.

The advantages of the new bolt are summarized below:

1 It is not subject to failure because of gas leakage.

2 The proper high explosive charge selection results in uniform reproducible bolt failure.

3 The unit is not sensitive to pressure or temperature as is the case with pressure actuated devices.

4 The explosive cartridge may be installed after the bolt is attached to the structure.

5 The use of high explosive permits smaller charges, smaller chambers, and results in thicker wall sections for a given bolt diameter than is the case with pressure-type units. This allows larger tensile loads to be handled for identical sizes of bolt and improves the efficiency of the high explosive type since the shock wave technique is enhanced rather than impaired by an increase in wall thickness.

Summary

In an article of this type it is not possible to discuss more than a few representative types and applications of the explosive cartridges designed and manufactured by McCormick Selph Associates. Detailed technical data sheets are available upon request for standard items. New devices and techniques are under constant development and the submission of any problems lending themselves to solution through the use of explosive cartridges will be welcomed.

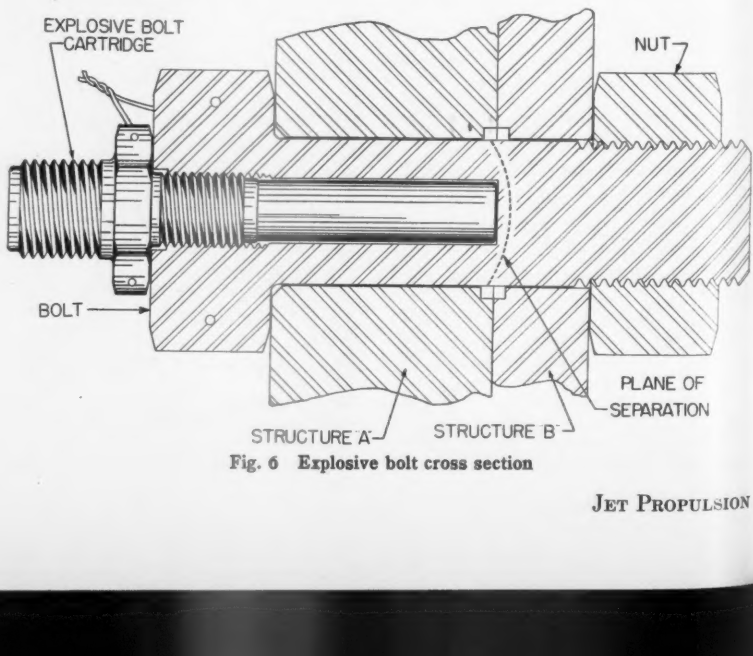

Fig. 6 Explosive bolt cross section

Fluorocarbons and Rocket Cases for Missiles

FRANCIS J. HONN and K. DEXTER MILLER, JR.

The M. W. Kellogg Company, Jersey City 3, N. J.

HIGH temperatures and unusually corrosive chemicals are two problems with which the engineer must deal in selecting materials for missiles and missile launching equipment. These problems become especially acute where electrical insulation, gaskets, tubing, diaphragms, lubricants, and protective coatings are concerned, since these items are normally made from organic polymers severely limited in thermal stability and/or chemical resistance.

Fluorocarbons, that is, organic materials containing a substantial proportion of fluorine bonded to carbon, often provide an effective answer to both problems simultaneously. The great strength of the C—F bond, together with the extra stability imparted by fluorine to adjacent C—C bonds, is responsible for the heat resistance of fluorocarbons, permitting effective operation in the range 300–600 F. The fluorine atoms surrounding the molecular backbone are also responsible for resistance to chemical attack, vapor permeability, and solvent swelling. Since fluorine is the most electronegative element, carbon bonded to fluorine is already in its most highly "oxidized" state—hence, the great stability of fluorocarbons toward oxygen, ozone, oxidant-propellants, and atmospheric deterioration. Hydrocarbon fuel resistance, too, is an inherent property of fluorocarbons, arising from favorable solubility parameters and a high degree of polymer crystallinity.

KEL-F[1] Fluorocarbons

At Kellogg, we have based much of our fluorocarbon research on chlorotrifluoroethylene ($CF_2{=}CFCl$), versatile starting material in which the chemical inertness and thermal stability of fluorine are tempered with the tractibility of chlorine. KEL-F 270 and 300 resins are hard, high melting thermoplastics which can be molded by compression, injection, extrusion, and transfer methods. Zero moisture absorption, low dielectric loss, high dielectric strength, and mechanical toughness, together with the properties described above, make these polymers an excellent choice for electronic missile components. A closely related product, KEL-F 500 resin, has been especially designed to resist embrittlement during heat aging or radiation exposure. It is ideal for hookup wire insulation, spaghetti tubing, and other thin wall extrusions or moldings.

Fluorine Diversified

Research on chlorotrifluoroethylene has branched out in three directions involving modifications in (1) physical form, (2) molecular size, and (3) molecular structure. Physically, KEL-F 300 resin has been reduced in particle size to form KEL-F NW-25-TR and N-2 dispersions. These formulations are sprayed or dipped and fused at 480–500 F to provide protective coatings resistant to the attack and penetration of acids, alkalies, and oxidants. Thanks to the chlorine in the polymer, these coatings are truly continuous and pinhole-free. Vessels as large as 5000-gal tank trailers have been successfully coated and operated. The normally "antisticking" KEL-F 300 resin is bonded to metal with a fluorocarbon-thermosetting resin primer, PN-25.

Another physical form of KEL-F 300 resin for corrosion service is KEL-F Plastic laminate. This combination of plastic facing and glass cloth backing is cemented to metal, wood, and ceramics with conventional adhesives. Complex surfaces are covered by hot-forming, and seams between adjacent sheets closed tightly by thermal pulse sealing.

Purposely limiting the molecular size of chlorotrifluoroethylene polymers results in a series of oils, waxes, and greases having the general formula $Cl{-}(CF_2{-}CFCl)_x{-}Cl$. These products retain the thermal stability and resistance to acids, alkalies, oxidants, and halogens characteristic of high molecular weight resin, yet act as efficient lubricants for compressors, plug cocks, and valve stems. Because of their high density, selected waxes are efficient flotation fluids for gyros.

Molecular structure has been altered by copolymerization of chlorotrifluoroethylene with other fluorocarbons, notably vinylidene fluoride ($CF_2{=}CH_2$). Incorporating $-CH_2$ groups converts hard, insoluble polychlorotrifluoroethylene to ketone-ester soluble resins (KEL-F 800) and elastomers (KEL-F 5500, 3700). Both products are distinguished by extreme resistance to oxidants, fuels, and lubricants. The resin finds use in air-drying lacquers and in the construction of hose and fuel cells for fuming nitric acid and hydrogen peroxide. The elastomers, cured with benzoyl peroxide or hexamethylene diamine carbamate, are serviceable up to 450 F. Both resin and elastomer are available as latexes for casting, dipping, and fabric coating.

Specialty KEL-F products include: (1) KEL-F Acids, efficient surfactants for acidic, oxidizing media for reducing interfacial tension between oxidant fuels and hydrocarbons; and (2) KEL-F Inks, adherent compositions for printing on antisticking surfaces. A silver ink is used to print flexible, electronic circuits on KEL-F film.

In all, there are over forty KEL-F fluorocarbons to help the missile engineer solve the dual problems of heat and chemical resistance.

Steel Rocket Cases

The modern high performance guided missile rocket presents to the designer a surprisingly subtle problem, in the face of its apparent simplicity. The M. W. Kellogg Company, working with the Bureau of Ordnance of the Navy Department and the Allegany Ballistics Laboratory, has for some years been designing and building structural parts for these solid propellant rockets. In our experience, these designs have represented a delicate balancing operation in which structural properties, precision machining, and cost of production are weighed to find the best compromise.

The importance of weight needs no explanation, nor does the emphasis on cost of production, in an increasingly competitive market. Precision machining becomes essential in many missile applications to provide interchangeability and accuracy of alignment in flight.

From the mechanical engineering standpoint, the rocket case is a pressure vessel in which the pressure of combustion exerts tension forces on the containing walls. These forces are usually dominant but are complicated by thermal shock, high temperatures, and gas erosion which enter into the picture in one way or another. The most interesting part of the design problem lies in the provision of a low and uniform factor of safety in all parts. The stress analyst is called upon here to use his arts and imagination to the fullest. The industrial engineer and manufacturing personnel find also an interesting challenge: they must produce a large vessel accurately, rapidly, and with little margin for error. They must combine the facilities of a large erecting shop, a precision machine shop capable of producing substantial quantities of units, yet flexible enough to permit rapid introduction of changes.

The design goals and standards in this field are continually broadening as the general knowledge of rocketry increases; the solid propellant rocket now stands on the threshold of an era of great progress. With new and better techniques of case manufacture, it may challenge the liquid propellant rocket in the very fields where the latter's sway has been unchallenged.

---

[1] Registered trademark of The M. W. Kellogg Company for its fluorocarbon products.

Commutation Switches for Telemetering

J. H. DUBOIS

Vice-President—Engineering, Mycalex Corporation of America, Clifton, N. J.

THE Mycalex Model TM-55 Series Type CP-299 Commutation Switch with Supramica® 555 commutator plates consists of a motor-driven switch with two rings of contacts of the "make-before-break" type. In a typical application, the function of the information ring is to sample intelligence from instrumentation transducers in prearranged sequence; and the function of the calibration ring is to sample calibration voltage.

The switch is a precision assembly, designed and built to exacting standards to assure long operating life and trouble-free service, with low noise level and total reliability.

The Supramica 555 ceramoplastic commutator plates are masterpieces of precision molding, combining dimensional accuracy with functional efficiency which cannot be duplicated in any other insulating material. The plates operate with unparalleled efficiency because of their accurate and stable construction, complete freedom from contact looseness, ability to withstand shock and vibration, and thermal endurance as high as 950 F. Because Supramica 555 has a coefficient to thermal expansion similar to that of metals, a very tight bond to insert contacts is obtained. Tolerances remain constant under severe operating conditions. Under normal circumstances, it is impossible for contacts to loosen and cause signal noise or loss of control.

In the standard CP-299 assembly, all gating contacts in the information ring are connected together and to one pin of a standard AN connector; each information contact, master contact, and the wiper arm is connected to individual pins of the connector. In the calibration ring, all gating contacts are connected together and to one pin of the connector; all calibration contacts are connected together and to one pin of the connector; the master contact and the wiper arm are each connected to an individual pin.

Some modification of the contact arrangement is possible, but is limited by the capacity of the standard AN connector. If other circuitry is required, special adaptations will be considered.

Each type of switch is designed for the desired sampling, and built for the function it is to perform and the conditions under which it is to operate. The operation of Mycalex Model TM 55 Series commutation switches in telemetry emphasizes the essential characteristics of switches for the transmission of low level signals. Transducers with peak output as low as 10 mv can be sampled without the use of preamplifiers, and with previously unattainable low noise levels. Every new Mycalex Model TM 55 Series switch should start as a prototype, with a full and complete series of field tests under actual operating conditions before production models are designed. In many cases, methods, models, and procedures developed in the prototype stage can be incorporated advantageously into the final production, with savings of time and expense.

Designers are invited to visit Mycalex Electronics Corporation to discuss specifications, and to observe the type of signaling being achieved.

Specifications

Electrical	Input	Power	115 ± 5 volts ac 380 to 520 cps Single phase
		Signal	The signal input is the output of the sampled transducers
	Output	Speed	Nominal speed with rated input at 400 cps, 115 volts, is 5 rps ± 0.5
		Noise	Not to exceed 1 per cent
Duty cycle	12 deg of rotation, apportioned information contact 50% minimum; gating contact 15% minimum; overlaping or make time 5%; master contact 277.5 ± 10%		
Environment	Temperature	−65 F to 160 F	
	Humidity	95% ± 5% with condensation at room temperature for 24 hr ± 1/2 hr. One hour warm-up for drying	
	Altitude	Sea level to 75,000 ft	
	Vibration	10 to 57 cps at 0.06 in. double amplitude, 57 to 500 cps at 10 g	
	Shock	15 g, 11 ± 1 millisec duration	
	Life	Minimum 100 hr without cleaning, servicing, or adjustments	
Physical	Size	2 5/8 × 2 5/8 × 5 5/8 plus extension with connector	
	Weight	Under 3 lb	
	Mounting	Four tapped holes in base	

Supramica Ceramoplastics

Supramica ceramoplastic, manufactured from the highest quality electrical glass and Synthamica synthetic mica, are high-frequency, high-temperature electrical insulators with an unusual combination of dielectric and physical properties. They are extensively used in the manufacture of electrical and electronic components, radomes, and other devices subjected to extreme operating conditions.

Supramica ceramoplastics offer these advantages of special significance in aviation and jet propulsion:

- Total, permanent dimensional stability
- Imperviousness to moisture and humidity
- Thermal coefficient of expansion equal to that of steel
- High continuous operating temperature
- Resistance to thermal shock and cycling
- Radiation resistance

Supramica® ceramoplastics, Mycalex® glass-bonded mica, and Synthamica mica are manufactured exclusively by Mycalex Corporation of America.

Optical Tracking Instruments

THOMAS P. FAHY

Director of Engineering, Engineering and Optical Division
Perkin-Elmer Corporation, Norwalk, Conn.

As GUIDED missiles and rockets are developed, tested, improved, and retested, the tracking equipment which records their trajectory through space must undergo the same pattern of change and improvement. This equipment is highly specialized and its design requires an intimate knowledge of three fields: optics, electronics, and mechanics.

At the Perkin-Elmer Corporation we have brought together a group of engineers skilled in all three of these basic and important fields. As a group they have developed astronomical telescopes, advanced bombsights, periscopes, long focal length telephoto lenses, servo and computor control systems. Working from this background, this group has, in recent years, made significant contributions to the guided missile and rocket programs of the United States and several other NATO countries.

We would like to describe for you some of the optical tracking instruments already produced or under development by Perkin-Elmer—both at our home plant in Norwalk, Conn., and at our subsidiary Bodenseewerk plant in Ueberlingen, West Germany.

ROTI—Mark I

ROTI-Recording Optical Tracking Instrument was developed to meet two prime needs: to provide an optical tracking instrument which could measure the position of a moving object in space and time with a greater accuracy than has been obtainable; and to provide a system with greater adaptability for different missions (missile problems) than those which had existed before.

ROTI is a twin telescope arranged with one telescope over the other and mounted on a movable platform. The upper telescope is a Newtonian type with a variable focal length from 100 to 500 in. in steps of 100 in. The lower telescope is a modified Schmidt type, variable from 50 to 100 in. in steps of 25 in. Both telescopes have a 16-in. aperture. Both have auxiliary power change optics mounted on turret arrangement, color filters, and neutral density filters. Both are highly corrected anastigmatic systems.

ROTI provides a versatility not found in other instruments. It affords a wide-field telescope for observing a missile launching at close range and a long focal length (long range) telescope for watching the missile in flight or on impact.

To make a permanent record for data reduction, 2 synchronous-type 70 mm cameras with frame rates up to 100 per sec will be mounted at the secondary focus of the telescopes after the power change elements. Both telescopic combinations can be used simultaneously in one mission; for example, one with black and white film, the other with color. A third camera will photograph the azimuth and elevation dial readings. Four types of data appear on film: the picture of the missile, the azimuth angle, the elevation angle, and a time code signal measured from zero time when the missile was launched.

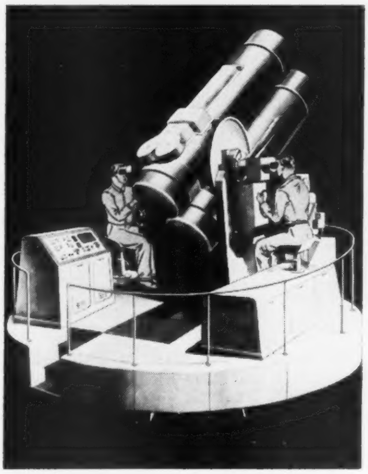

Recording optical tracking instrument

Both ROTI Mark I and Mark II (see above) are capable of tracking smoothly at an extremely wide range of tracking rates. Both have a "stiff stick" control which operates an aided tracking system.

ROTI—Mark II

ROTI Mark II may be used at focal lengths of from 100 to 500 in. in 100-in. steps. There is an input from radar range data for automatic focusing. Since photographs must be made under varying atmospheric conditions, exposure is also automatically controlled.

Because of its size, ROTI Mark II requires a permanent installation. For optimum performance it is protected by an air-conditioned astrodome especially designed by Perkin-Elmer for the purpose.

"TPR"

A third instrument which bears a close relationship to the two ROTI's is "TPR" (Telescopic Photographic Recorder). It has the fundamental difference that it is designed to be portable. The TPR telescope has a 24-in. aperture and focal lengths of 100, 200, and 300 in.

The camera telescope is mounted on a modified 90 mm M2A1 gun mount with auxiliary power supplies and supplementary equipment contained in a separate trailer.

The unit can be operated by one or two operators. Provision is made for both remote and aided tracking operation.

Kth55 Cine Theodolite

Bodenseewerk-Perkin-Elmer's most recent cine theodolite, type Kth55, is the result of 30 years' experience in theodolite design. It embodies a number of improvements that increase its range, accuracy, and general usefulness for optical tracking problems.

Among the new features of type Kth55 are the following:

1 In the Master Station, the pulse generator is controlled by means of a quartz stabilized oscillator which permits a factor of two increase in over-all accuracy.

2 Provision is made for one-man or two-man operation.

3 A new series of lenses (for the Kth55 and other similar instruments) has been developed by Perkin-Elmer to increase the range of the instrument. Designs are available in focal lengths of 40 cm (refracting), 60 cm, 48 in., and 60 in. (catadioptric). With a type Kth55 installation, objects moving in space at angular rates up to 60 deg per second may be photographed and tracked accurately.

Automatic Alignment Devices

Perkin-Elmer has recently developed several automatic alignment devices. High resolution angular alignment can be achieved by this electro-optical sensor. These units also provide for the monitoring of the aligned object with an output signal to close the loop.

✦ ✦ ✦

Perkin-Elmer is a diversified, growing young company. If you are a physicist or engineer and would like to grow with us, send us your résumé.

New Answers for Flow Problems

R. W. SCHOOLEY

Product Development Director, Potter Aeronautical Corporation, Route 22, Union, N. J.

ALTHOUGH it is now widely adopted for general industrial use where high precision in flow measurement or control is critical, the Pottermeter was originally developed specifically for the rocket industry and is still regarded as the standard instrument for measuring the flow of liquid fuel and oxidizers. As a matter of historical interest, some of the first Potter Flow Sensing Elements built to the present design were used by Reaction Motors, Inc., in the Viking rocket program; and similar units were used by Bell Aircraft in the oxygen tank balancing system of the famous X-1.

Recent developments in the design of Potter Sensing Elements and associated equipment have further extended their usefulness in the jet engine and rocket fields. This report attempts to list some of the more important advances for the benefit of those interested in flow measurement, air speed measurement, tachometry, and the telemetering of these variables.

New Flow Sensors

The Potter Flow Sensing Element, which has long been familiar to those engaged in research, development, and production testing in the rocket and aircraft engine fields, is now available in a greater number of sizes, ranging from the new 1/8-in. unit which has a minimum capacity of 0.05 gpm, to the 8-in. element which will handle over 5000 gpm. New materials of construction and new machining techniques now make possible the accurate metering of halogen compounds such as HCl, and also permit operation at temperatures up to 450 F with no special precautions for cooling the pick-up coil.

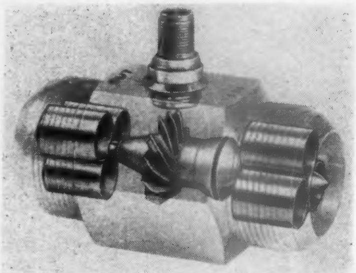

Fig. 1. Phantom view of Potter Flow Sensing Element

Special Elements

In addition to standard units, special elements can also be fabricated to customers' specifications to solve difficult installation problems. Specialized requirements in rocket research have brought about the development of two new Potter Flow Sensors both of which employ the familiar "floating rotor" principle.

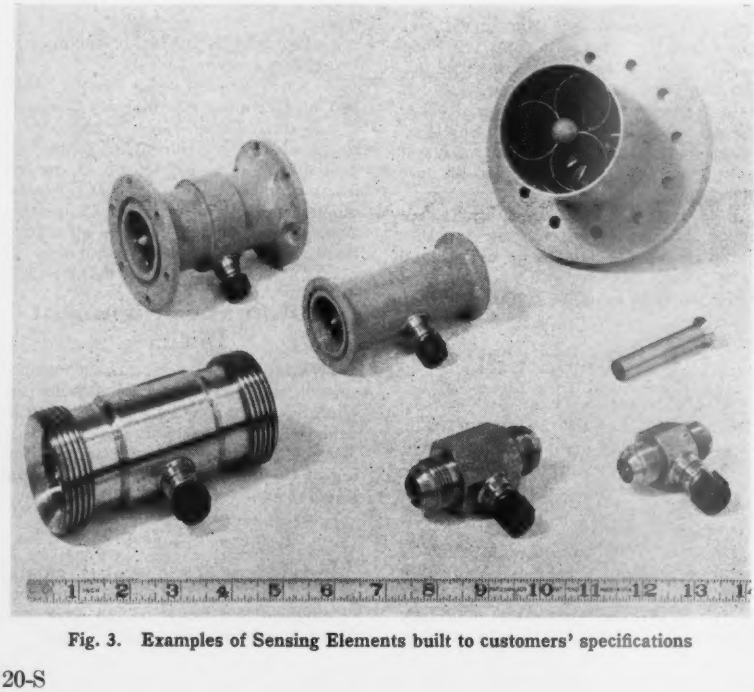

Fig. 3. Examples of Sensing Elements built to customers' specifications

High Frequency Units

The need for higher response speeds for transient flow measurement has necessitated the use of flow sensors having substantially higher output frequencies than can be obtained with the conventional hub-mounted magnet. Through the use of a reluctance coil pickup, it is possible to obtain output frequencies as high as 3000 cps.

In addition to improved performance with high speed instrumentation, the higher cycles-per-gallon constant of this unit gives considerably more accurate readings of flow rate when used with an EPUT meter.

A unit having special magnetic shielding is also now available for use in locations where an appreciable amount of magnetic interference is encountered.

Producing the same frequency output signal as the conventional Potter unit for measuring either flow rate or total, noise generation is minimized and dependability increased.

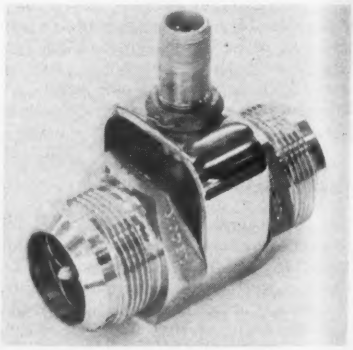

Fig. 2. Lo-Hum Flow Sensing Element

Ratio Control

Since the output of the Potter Flow Sensing Element is inherently linear with respect to flow over a wide range of operation, the applicability of this type element to ratio control applications has long been realized. A total fuel total oxidant ratio control system, operating on a digital basis, has been devised for obtaining the maximum total impulse from a rocket engine through the control of the ratio of fuel and oxidizer from the supply tanks to the combustion chamber. The system does not accumulate error due to short-time disturbances, since it has a memory dating from the instant combustion is started. Tests have shown that this system is easily capable of maintaining a preset ratio within 1/2 per cent.

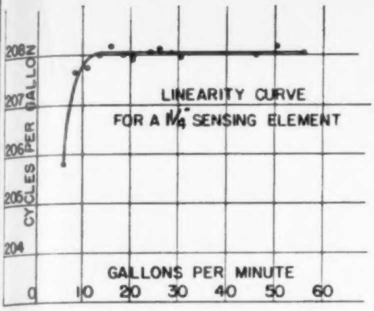

Fig. 4 Linearity curve for a $1^1/_4$-in. Sensing Element

Air Speed Indicator

Operating with high accuracy at subsonic and supersonic airspeeds, a new primary sensing element now undergoing field tests produces an a-c voltage whose frequency is directly proportional to airspeed. This signal can be read as air-speed or it can be compared with the output signal from a Potter flow sensor measuring fuel consumption in order to obtain a reading directly in air-miles per gallon. Because of the high accuracy obtained, the new device is expected to find acceptance as a wind tunnel standard as well as for flight applications.

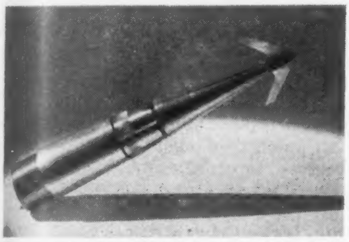

Fig. 5 Sensing Head for Airspeed Indicator

Mass Flowmeter

The need for separate sampling and for density measurement in order to obtain a reading in terms of mass flow is now eliminated through the new Potter Density Detector Unit. Employing an eccentrically mounted, totally submerged displacer, the unit produces a resistance change which is directly proportional to fluid density over a range from 0.6 to 0.9. This is transmitted, as a correction signal, directly to the flow indicating instrument which automatically indicates flow in lb per hr or other mass units. The Density Detector Unit can be added easily to existing systems.

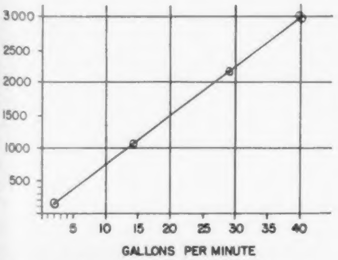

Fig. 6 High frequency Flow Sensor

Total Flow Measurement

Reading of total flow with high accuracy is accomplished through the use of an electronic counter to totalize the output pulses of the sensing element. The Model 21 Totalizer, an all-purpose electronic counter, operates from an input signal as low as 10 millivolts at output frequencies to 1 kc. The indicated total is multiplied by a constant conversion factor to obtain the actual flow in volumetric units.

The Model 25 Flow Digitizer also available for direct reading of total flow has the same operating characteristics as the Model 21, except that it includes a push-button computer which automatically converts the total number of input pulses to a direct reading of total flow.

Wide-Range Precision Flow Indicator

Flow measurement with extremely high accuracy over a wide range of operation is now possible through the use of a multichannel frequency converter which is mounted directly inside the case of an analog or digital type indicating potentiometer. This permits a single instrument to be used with a number of sensing elements graduated progressively. Switching can be either manual or automatic, and provision is made for the automatic actuation of control valves to direct the flow through the proper sensing element.

Potter laboratory-type frequency converters used in flowmeter and tachometer systems, have also been improved through recent design modifications to permit their use in multiple-element systems. Other new modifications have improved linearity, stability, and tube life.

Fig. 7 Model 21 Electronic Counter—for total flow indication—registers up to 99,999,999 pulses at frequencies to 1 kc

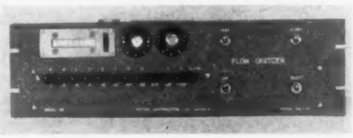

Fig. 8 Model 25 Flow Digitizer—preset to automatically compute total flow

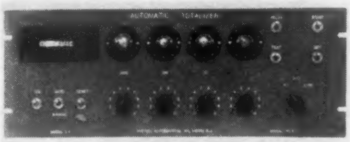

Fig. 9 Model 24 Automatic Totalizer—preset to control flow automatically

Information and Specifications

When writing or phoning for literature, please state title and number.

Pottermeters. General information Specification Sheet S-1.

Pottermeter. Mounting dimensions Specification Sheet S-2.

Flow Rate Indicators. Analog-type with indicating dial; also recording and controlling. Data Sheet 10.3-5a.

Flow Rate Indicator. Digital with null-balance servo system. Specification Sheet L-5.

Flow Rate Indicator—Tachometer. Portable frequency converters measure Pottermeter output or rpm to 190,000; used with milliammeter or electronic potentiometer Specification Sheet L-1.

Flow Rate Indicator and Totalizer. Airborne Specification Sheet AF-1.

Electronic Totalizer. Specification Sheet L-2.

Computing Electronic Totalizer. Specification Sheet L-3.

Predetermining Totalizer. Specification Sheet L-4.

Engine and Afterburner Flow Summating System. Report SY-1.

Four Engine Flow Indicator and Summating System. Report SY-4.

Density Detector and Indicator; Mass Flowmeter System. Report 27.

Methods of Flow Measurement. Article R-1.

Transient Response of Turbine Type Flowmeter. Article R-2.

Measuring Rocket Fuels. Article R-3.

Fig. 10 Model 31 Total Flow Converter—operates electromagnetic counter to indicate total flow

Fig. 11 Precision Digital Flow Rate Read-Out System

Pressure Transducers for Corrosive Media

GEORGE T. SENSENEY

Vice-President—Engineering
Rahm Instruments, Inc.
237 Lafayette St., New York 12, N. Y.

THE development of liquid propellant rocket engines has required in-flight measurement of tank pressures involving corrosive oxidants, such as fuming nitric acids and hydrogen peroxide, and fuels similar to hydrazine and its derivatives.

Heretofore various barrier configurations were devised to prevent direct contact of the active media with the elastic element; this type of system was employed in both bourdon tube and diaphragm designs with only fair success.

1 The most common of the barrier systems is the oil-filled transducer, so arranged that the corrosive liquids or gases impinged on a nonmetallic diaphragm which then effected the transmission of pressure changes through the oil barrier to the elastic member. From a purely mechanical point of view this approach required that the barrier diaphragm be thin enough so as not to impart a nonlinear addition to the spring system. Porosity of the barrier diaphragm, even in the most carefully selected materials, often permitted enough contamination of the oil-filled space so that decomposition of the hydraulic fluid and subsequent corrosion of the internal parts caused serious error if not complete failure. It should be noted that Teflon diaphragms were in general considered to be unsatisfactory because of the porosity of thin sheets of this material. Polyethylene and certain fluorinated hydrocarbons such as Kel-F were found to be satisfactory in most respects; in considering any organic barrier material, the effects of temperature extremes are sometimes more important considerations than corrosion resistance.

The effects of temperature in the range from −55 C to 200 C can be disastrous in a fluid-filled instrument; they simply will not function. Volumetric changes in the transmission fluids, whether silicones, natural oils, etc., are as high as 20 per cent over the temperature range involved. The expansion or contraction of the fluid barriers when coupled with marked changes in compliance of the barrier diaphragm rendered the instruments inoperative for the purposes of any valid measurement.

2 The alternative to introducing a barrier cell closed at one end with a compliant synthetic diaphragm as mentioned above involves the insertion of a fluid-filled tube open at one end to the corrosive medium and connected directly to the instrument case, also containing barrier fluid. Certain inert fluorinated oils of the Fluorlube type, or similar, are satisfactory if they can be contained in the piping arrangement ahead of the instrument. Such a pipe should be fairly long in relation to its diameter to prevent by-passing or mixing of the active medium with barrier fluid. Any such pipe arrangements result in poor rise time characteristics, and there is always the danger that environmental vibration and/or acceleration will eject barrier fluid from the pipe. It should be noted that satisfactory test stand arrangements have been constructed utilizing a fluid barrier of the type just described wherein the elimination of a nonmetallic diaphragm to contain the oil body resulted in good temperature performance.

3 There are other types of pressure transducing instruments, such as those involving a bonded strain gage, which can be applied to the surface of a pipe or pressure vessel to obtain accurate measurements. All of these devices necessitate the use of ancillary equipment whose weight and space requirements are prohibitive in most flight and missile instrumentation. The possibility of failure in such equipment is many times that of the potentiometer instrument.

In connection with the Earth Satellite Program, Rahm Instruments, Inc., was asked to consider the design and manufacture of a series of potentiometer-type pressure transducers with electrical output proportional to pressure input, most of the units being required for use with corrosive media. An analysis of the transducer requirements of the telemetering program indicated that the main consideration would be material selection, and that while some modification of the transducer sensing mechanism might be in order it seemed that the existing electromechanical linkage concept was adequate to meet the dynamic performance required. Materials of construction became the focal point of effort since direct contact of oxidants and fuels with the sensing element was considered to be essential, particularly if the afore-mentioned fluid pressure transmission difficulties were to be avoided.

In connection with the selection of elastic sensing members, it became apparent that only certain of the 300 series stainless steels provided any hope in terms of corrosion resistant properties. Though the stainless steels, such as type 316 alloy, exhibit poor temperature stability in that their moduli of elasticity vary with temperature more widely than isoelastic alloys, such as Ni Span C, they were selected because of their chemical properties. Also, it should be noted that the hysteresis errors inherent in stainless steel diaphragm shells is higher than either Ni Span C or beryllium copper. The problem, in terms of elastic element selection, was reduced to the question of a satisfactory method of joining the capsules or bourdon tubes of stainless steel to the necessary pipe fittings and closures.

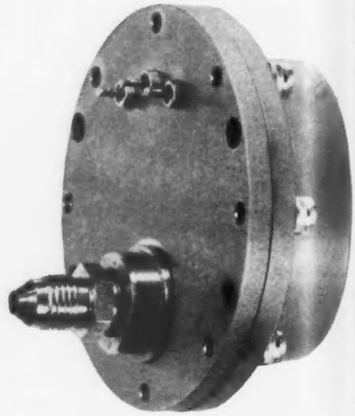

Fig. 1 High pressure fail-safe pressure transducers for corrosive media (0.75 actual size)

(A) The modulus of elasticity change with temperature, and the resultant rate change, was partially compensated for in the bourdon tube configuration (Fig. 1) by using a rate resistor; in the diaphragm-type instruments the modulus change error was corrected by use of a bimetallic spring element.

(B) The hysteresis errors were materially reduced by providing a greater amplification in the potentiometer movement, thus avoiding the excessive displacements which had previously been required of the bourdon tubes; actually the greater hysteresis errors were encountered in the bourdon tube instruments in the range of 1000 lb and over.

(C) The problem of joining a stainless steel 316 alloy bourdon tube to an appropriate pipe connection, as well as providing an adequate closure for the tube, presented a serious problem. Brazing or soldering of any kind was ruled out for reasons of poor corrosion resistance of such joints. A first approximation of the problem resulted in an all mechanical assembly involving a captive tapered plug and socket on each end of the bourdon tube. This required that a shaped, threaded protuberance be formed as part of the basic tube element. This proved to to be a very difficult problem particularly with the alloy in question. Effective closure and sealing was achieved, but the relatively massive end fittings resulted in poor vibration performance. Though instru-

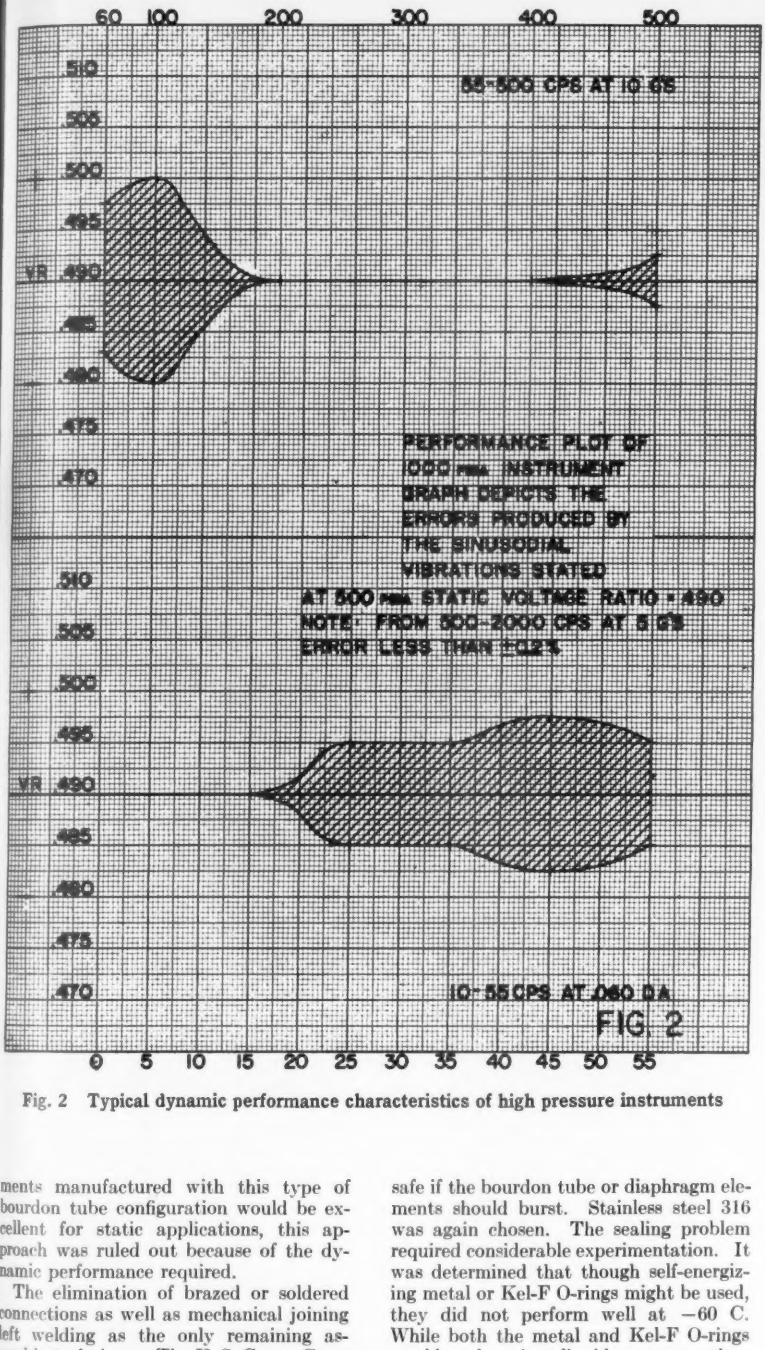

Fig. 2 **Typical dynamic performance characteristics of high pressure instruments**

ments manufactured with this type of bourdon tube configuration would be excellent for static applications, this approach was ruled out because of the dynamic performance required.

The elimination of brazed or soldered connections as well as mechanical joining left welding as the only remaining assembly technique. The U. S. Gauge Company of Sellersville, Pa., extended the maximum cooperation in developing a welding technique for stainless 316 bourdon tubes for use with corrosive materials. The welding was achieved with special nickel chrome alloys in a mechanically driven jig which prevented spot burning of the tube at any point. Subsequent extensive testing at Rahm Instruments, Inc., has proved that this technique produces a tube assembly which, after being passivated, yields dependable service after hundreds of hours of exposure to acids.

An important requirement of the development program for the Vanguard project was that the instruments be fail-safe if the bourdon tube or diaphragm elements should burst. Stainless steel 316 was again chosen. The sealing problem required considerable experimentation. It was determined that though self-energizing metal or Kel-F O-rings might be used, they did not perform well at −60 C. While both the metal and Kel-F O-rings would seal against liquid pressures, they did not satisfactorily seal against gas at low temperature. Ultimately a silicone rubber O-ring upon which a Kel-F sheath had been drawn solved the problem; this type of O-ring configuration withstood the corrosive media throughout the range of pressure and temperature required.

The dynamic specification of the instruments for Vanguard were fairly nominal and the vibration and steady-state acceleration characteristics of the instruments are detailed by the appended graph (Fig. 2). In addition, a tabulation of average linearity, hysteresis, and temperature errors are included in Table 1. Fig. 3 illustrates the general configuration

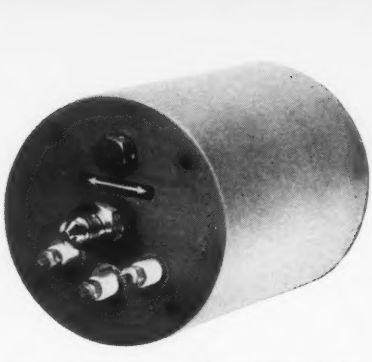

Fig. 3 Low pressure fail-safe transducers for corrosive media (0.75 actual size)

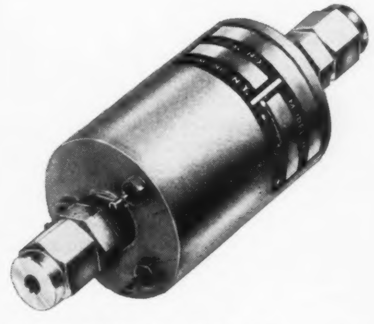

Fig. 4 Miniaturized units for noncorrosive applications (0.75 actual size)

of the all-stainless steel hermetically sealed unit for ranges up to 50 psia. This capsular-type instrument permitted the admission of concentrated peroxide directly into the sensing element.

In addition to the instruments designed and manufactured for corrosive applications, Rahm Instruments, Inc., is currently providing a series of small absolute and differential units typified by the unit shown in Fig. 4. It is anticipated that these small units will be available in configurations and internal structures suitable for use with corrosive media.

Table 1 Typical linearity, temperature, and steady acceleration characteristics of high pressure units

	Voltage Ratio				
psia	At +25 C pressure increasing	At +25 C pressure decreasing	At −54 C	At + 71 C	During Accel.[1]
0	0.025	0.030	0.028	0.016	0.025
100	0.257	0.265	0.255	0.247	0.262
200	0.490	0.491	0.485	0.484	0.499
300	0.724	0.725	0.715	0.719	0.730
400	0.948	0.948	0.928	0.955	0.955

[1] Steady state acceleration of 10 g applied in best dynamic axis.

Missile Components and Accessories

J. LEO RAESLER

Engineering Manager, Revere Corporation of America, Wallingford, Conn.

FOR many years Revere Corporation of America has manufactured Fuel System Components, High Temperature Lead Wire and Thermocouple Wire, Heat and Airflow Products, and Electronic Weighing Equipment for aircraft and industrial applications. Revere has applied many of these products to missiles. They include: light weight special purpose flowmeters, thermocouples, probes and harnesses, liquid oxygen level switches, electronic weighing systems, gravimetric fuel meters, hermetically sealed relays, and high temperature wires.

Below is a description of equipment particularly applicable to missiles.

Liquid Oxygen Float Switch

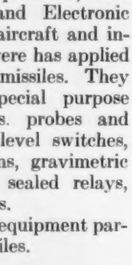

L-Ox switch.

Revere F-70630 L-Ox Switch indicates or controls liquid oxygen level in missiles. The unit utilizes a magnetically operated hermetically sealed Revere GLASWITCH[1] as the contact element, permitting safe use in explosive atmospheres. All materials used in this switch are insensitive to liquid oxygen and are not subject to impact deterioration. Operates through −320 F to +300 F. Contact rating is 0.5 amp inductive at 28 v dc. Available in SPST and SPDT. Standard AND 10057 end fittings. Other models available for liquid nitrogen and liquid fuels.

Fuel Meter Reads Directly in Pounds

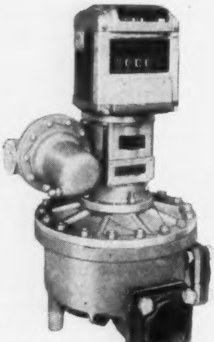

Gravimetric fuel meter

This new Revere Gravimetric Meter eliminates specific gravity sampling of fuels and gallons-to-pounds computations. It measures fuel delivered to missile directly in pounds.

The Gravimetric Meter automatically compensates for changes in density ranging from 5.4 to 7.4 lb per gal caused by changes in temperature or type of fuel. Accurate to 0.5 per cent of total delivery. Flow range is 250 to 2200 ppm at density of 7.4 ppg; 250 to 1600 ppm at 5.4 ppg. Other flow and density ranges available.

Fast-Response Relay with Hermetically Sealed Contacts

The F-70334-1 relay makes contact in less than 2 millisec and is immune to contact contamination and mechanical bugs. Recommended for use in explosive atmospheres. Called the GLASWITCH Relay, model shown consists of four SPST hermetically sealed Revere GLASWITCHES magnetically operated, providing four Form A or B contacts per relay.

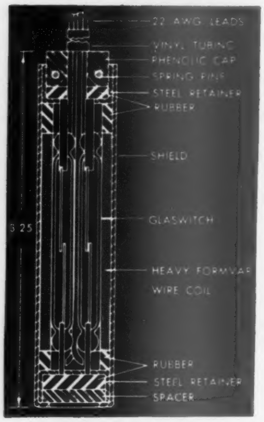

Diagram of Glaswitch relay

Switches and actuating coil are mounted in shock-resistant material and enclosed in a steel housing for magnetic shielding and protection. Relays can be stacked in any combination. Number of contacts, mounting, and plug-in arrangements to suit application. Contact rating: 0.5 amp inductive or resistive load at 28 v dc. Coil rating: 480 milliwatts. Send for Bulletin No. 1061.

(*Magnified view*)

Permacode®—Teflon[2] Striped to the Wire

PERMACODE is a Teflon-insulated hook-up wire with striping that goes right down to the conductor. The colors are good for the life of the wire; they are not obscured or removed by abrasion or heat. Coding is available in a wide variety of combinations of single or multiple stripes selected from fifteen basic solid colors. The insulation quality is unaffected by the striping process.

PERMACODE is good for continuous operation from −90 C to +210 C. Strips clean. Doesn't shrink when soldered. Available with either solid or stranded silverplated copper conductors. Shielding and jacketing can be furnished. Sizes: 28 to 16 gage in 0.010-in. wall (600 v) and 0.015-in. (1000 v) thicknesses. Conforms to MIL-W-16878, Types E and EE.

Remote Weighing

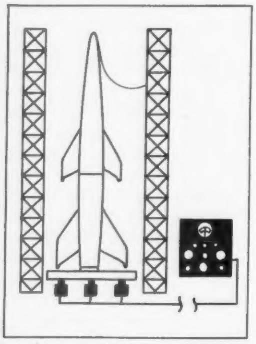

Missile weighted by load cells

Revere's Cox and Stevens Division manufactures an electronic scale configuration for missile launching platforms and for other weighing operations. Newly developed multicolumn, hermetically sealed load cells are combined with ruggedized, high response, self-balancing instrumentation, making it possible to read remotely the final weight of the missile prior to control adjustment and launching. Readout can be by dial scale, printed ticket, digital display or punched tape. Equipment meets the accuracy and stability requirements of missile designers.

[1] Revere trademark.
[2] E. I. du Pont trademark.

Gas Turbines for Missile Ground Support

ERWIN O. A. NAUMANN

Chief of Advanced Studies
Solar Aircraft Company
San Diego 12, Calif.

HANDLING, testing, and launching of guided missiles require a multitude of services which are external to the missile proper. Specific requirements for such ground support equipment are dictated by the operational concept of the missile system and the detail design of the missile. In general, hydraulic, electric, mechanical, and pneumatic power are needed at the site of operation for erecting and aligning, fueling, calibration, checkout, and launching. The proper selection of the prime movers for such services is of great importance, considering the safety, reliability, quality, and control requirements. In addition, depending on the operational concepts, emphasis may be placed on such items as versatility, transportability, self-sufficiency, and logistics. Considering these, the advantage of using gas turbine prime movers is definitely indicated. The lightweight, compact engines are capable of using a wide variety of fuels and are easy to integrate with the driven components, such as pumps, compressors, and generators.

Solar Aircraft Company has designed and is manufacturing a variety of gas turbine driven power units for diverse applications. Solar combines them in complete packages for ground, shipboard, and airborne electric generator sets, space heaters, smoke generators, air bleed power supplies, and pumps. The present production units use as the prime movers the 50-hp Mars and the 500-hp Jupiter engines.

The Mars engine weighs approximately 100 lb, which includes the gearbox and the accessories, and its dimensions are 23 in. in height, 17 in. in width, and 23 in. in length. It develops 50 bhp at a speed of 40,000 rpm, or 42 ppm bleed air with a bleed air pressure of 18.3 psig. Air mass flow, pressure ratio, and fuel consumption are 2.7 pps, 2.5:1, and 2.2 lb/bhp × hr, respectively.

The Jupiter engine weighs approximately 990 lb, including gearbox and accessories; its dimensions are 42 in. by 32 in. by 91 in. It develops up to 520 bhp at 20,000 rpm, or 150 ppm bleed air with a pressure of 45 psig. Air mass flow, pressure ratio, and fuel consumption are 9 pps, 4.6:1, and 0.92 lb/bhp × hr, respectively.

Both engines are designed for operation over a temperature range from −65 F to +130 F. They operate on all commonly used fuels, such as gasoline, jet engine fuel, diesel fuel, and kerosene. Complete protection against overspeed, overtemperature, and loss of oil pressure is provided.

Construction of both engines is simple and compact. The Mars engine employs a single-stage centrifugal compressor, single elbow combustor, and a single-stage radial inflow turbine. Turbine and compressor are mounted back-to-back on the same shaft. The Jupiter engine employs a ten-stage axial compressor, single combustor, and a three-stage axial turbine. For constant speed application, the three stages are coupled together, whereas for variable speed application the third stage of the turbine is not connected to the gas producer section but mounted on a separate power take-off shaft. Both engines have completely automatic electrical start systems, and power is available in less than one minute even at extreme low temperatures. Preheating is not required.

The Mars engine is also available with a hand-crank starting system; the Jupiter engine is adaptable for pneumatic or fuel-air starting systems.

Standard speed control systems for both engines incorporate a droop-type governor with 5 per cent droop from no load to full load and steady-state speed variation of ±0.5 per cent. The system is adaptable for isochronous governing and parallel operation when used for generator set applications.

Other types and sizes of gas turbine prime movers are presently in development to satisfy power requirements different from those of the described units.

It is important that proper and timely consideration be given to the ground support requirements for guided missiles systems so that *optimization* of the system be achieved, and an effective research tool or weapon be developed. The gas turbine prime mover should play a more important role in this concept in the future, due to its inherent characteristics and flexibility for integration into such a complex system.

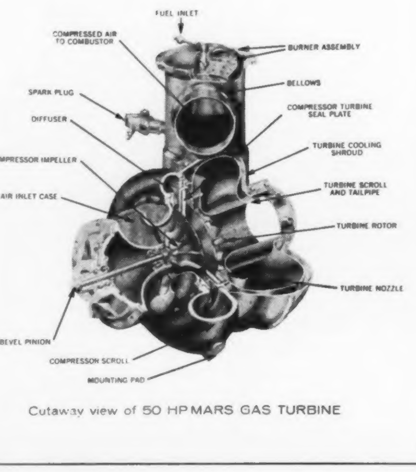

Cutaway view of 50 HP MARS GAS TURBINE

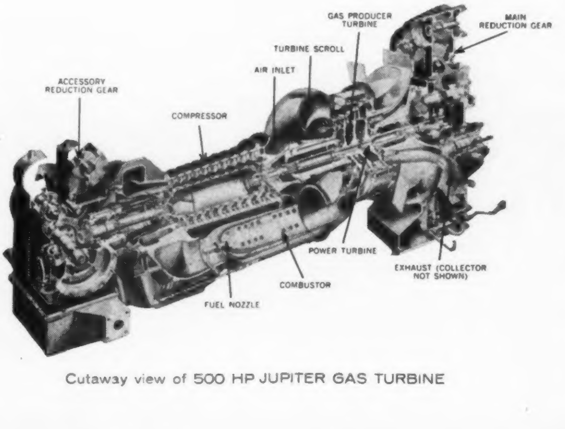

Cutaway view of 500 HP JUPITER GAS TURBINE

Controls for Low Temperature, High Pressure

ROBERT L. SCHALLER

President, Southwestern Valve Corporation
Box 179, Santa Ana, Calif.

SINCE its inception, Southwestern Valve Corporation has devoted its facilities and manpower to the research, development, and manufacture of controls for use in the missile field. Such items as pneumatic or solenoid actuated valves, regulators, reliefs, and checks, have found wide acceptance for both airborne and ground support equipment.

Management by engineers, and an engineering department willing to accept challenging projects, have resulted in the development of many interesting controls for such fluids as liquid oxygen, helium, and other inert gases: nitric acid, 90 per cent hydrogen peroxide, air, water, JP fuels, alcohol, etc. Operating temperatures normally fall within the range of −325 F to +350 F, pressure ranges from zero to 6000 psi; the allowable leakage rate is zero.

Even though minimum mass seems to be of extreme importance in the design of airborne controls, the basic engineering problems are coincidental to those of ground support equipment. The major problems are those of reliability, performance, simplicity, versatility, storage, sales appeal, and conformance to military or commercial standards.

Reliability and performance are usually grouped together and are considered to be of paramount importance to the design engineer. Since a great deal of our work has been in the low temperature, high pressure field, our designs reflect the philosophy of minimum moving parts or seals. The use of dissimilar metals has been avoided wherever possible to minimize galvanic action and avoid problems due to varying coefficients of thermal expansion. The problem of producing units with repetitive characteristics has become more and more important so that many of our valves must be timed within a maximum of 5 millisec of each other. Performance and reliability have always taken preference over cost.

Recognizing that highly skilled personnel may not always service our products, great emphasis has been placed on simplicity of design. Where unusual control problems have been solved through the use of complicated valving design, we have simplified the problems of understanding and servicing by breaking down the units into individual components or subassemblies. In this way the function of the subassemblies is more easily understood and the problem of troubleshooting and testing is more easily resolved.

All controls have versatility to some extent; however, the degree of this characteristic marks the importance of the products. Some specifications are so tightly defined that the resulting control can perform in only one way and usually with a very limited number of fluids. Those of our products designed for universal application have had strong emphasis placed on the following factors:

1 Use of fluids such as inert gases, 90 per cent hydrogen peroxide, liquid oxygen at −300 F, nitric acids, etc.

2 Operating pressure ranges, increasing or decreasing with minimal changes.

3 Broad temperature ranges (−325 F to +350 F) with zero leakage; higher temperature and lower ranges through the use of special seals and seat materials.

4 Programming flows through timing or varying the orifice. All of our pressure actuated valves can be equipped with microswitch devices, and the timing of opening and closing can be programmed. At the same time, a variety of plugs can be supplied to give linear flow characteristics, etc.

5 The valves are designed to cope with overpressurization. All the ground equipment has been designed with a safety factor of four. The airborne equipment usually has a safety factor of two.

6 Versatility of changing one type of control to another so that a pressure actuated valve might be changed into a regulator, hand valve, or vent relief valve. This subject is more fully covered in the next paragraphs.

Serviceability has become of greater importance due to the large influx of inexperienced personnel in the various specialized fields. Minimum weight and volume requirements are considered only if they are consistent with good design or production techniques. External adjustment of seals and springs is given a great deal of consideration. Similarity of products, both externally and internally, has become almost a rule so that many different types of controls look alike and contain many of the same parts. This is possible through the use of control assemblies which can be bolted to the units externally. One of our lines allows a kit conversion from a pressure actuated valve to a vent relief valve, hand valve, or regulator.

With the larger valves from about $1^1/_2$-in. pipe size and upward, a tremendous amount of time is lost in pulling the valve out of the lines in order to properly service them. Servicing of a 6-in. valve, even under an emergency program, can often result in the loss of as much as 18 hr test stand time. Our latest line of valves can reduce this "down time" to a minimum. This is possible because the valve can be completely serviced without removal from the lines. By taking out 8 or 12 bolts the entire valving mechanism (including the seat) can be removed from the line, serviced in a test fixture, and replaced in the line without fear that leakage will result from this reassembly. The method of accomplishing this is unique and merits consideration from test stand designers. (See illustration.)

Storage problems have been approached in the following ways: Wherever possible, corrosion-resistant materials have been used, usually 300 Series stainless steel. Materials requiring plating or chemical treatment have been avoided except on the magnetic steels for solenoids, etc., where chrome plating or Parkerizing has been utilized. The use of "rubber" elastomers where "sets" or "drying out" occurs has been minimized, as has been the use of plastic type elastomers under constant tension or compression which would ultimately result in surface checking or cracking.

Our largest product growth has been experienced through our development of ground support equipment. We are manufacturing and designing equipment for airborne use by West Coast manufacturers and other areas of the United States.

Drawing on the results of our research and development program and our broad experience in the missile field, we feel that our combined line of products offers the missile engineer a control which will meet almost any of his design requirements. For those problems requiring research and development work, our engineering staff and our laboratory (equipped for liquid nitrogen service) are available.

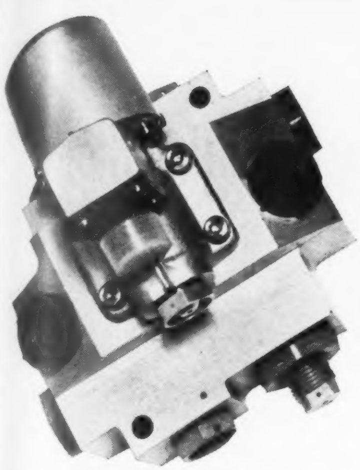

MV527—4 way, 3 position; AND 10050-8, 3000 psi

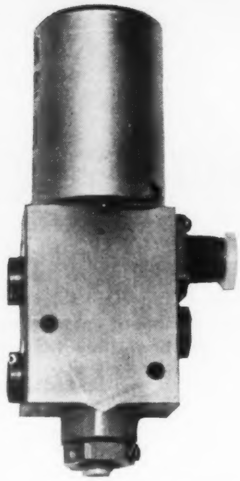

MV543—3 way, 2 position; AND 10050-4, 3000 psi

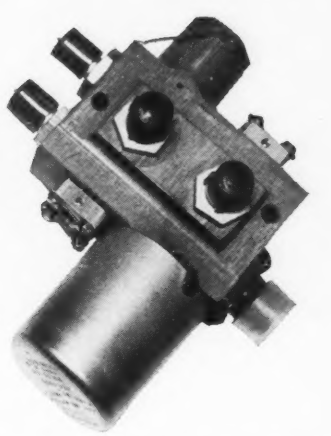

MV500—4 way, 2 position; AND 10050-4, 3000 psi

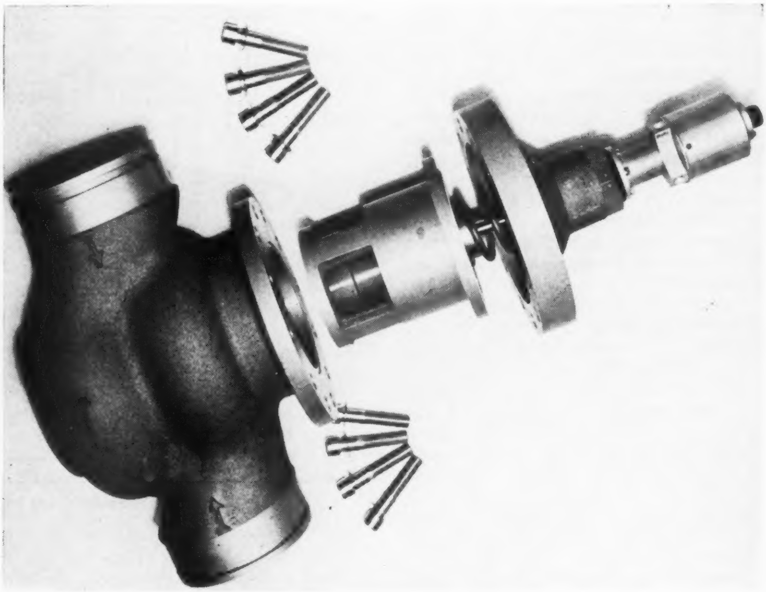

PV500 series—1-in. to 6-in. tube. Lox service, ASA flanges

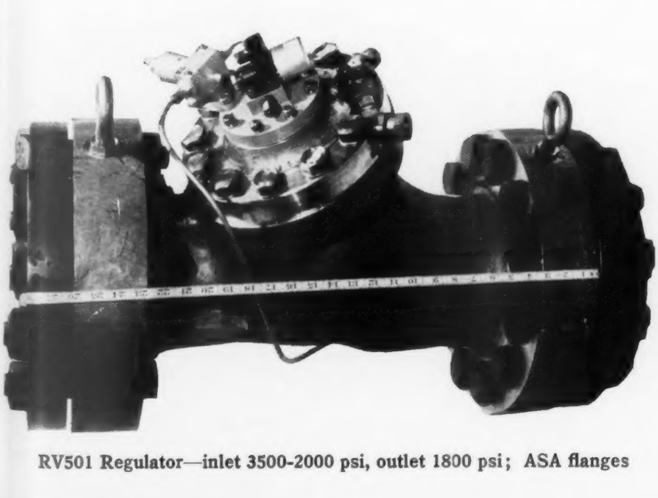

RV501 Regulator—inlet 3500-2000 psi, outlet 1800 psi; ASA flanges

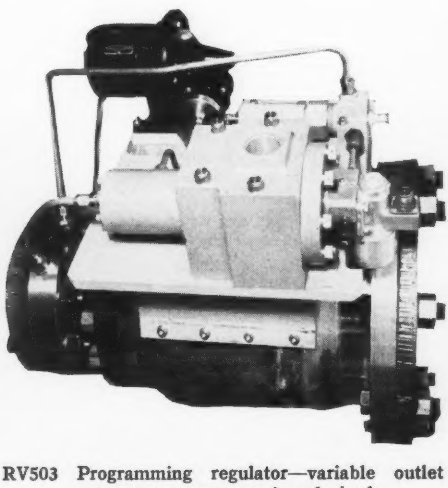

RV503 Programming regulator—variable outlet pressures; programmed as desired

Transducers for Extreme Vibration Conditions

M. DI GIOVANNI

Chief Engineer, Special Projects Division
Statham Laboratories, Inc.
12401 W. Olympic Blvd., Los Angeles 64, Calif.

PRODUCT improvement is the duty of any manufacturer who is a supplier to agencies charged with the responsibility of developing means to safeguard the general welfare. Statham Laboratories pioneered the principle of the unbonded strain gage, and its instruments for dynamic measurements have implemented fundamental work in diverse fields for many years. With a technical staff of physicists and engineers who understand and even anticipate the problems of the research workers in the vanguard, it carries on a continuous program to improve older designs and to introduce new ones. As a consequence, Statham pressure transducers and accelerometers have achieved popular acceptance and wide use.

Each field of scientific exploration has specialized problems in research devices. Repackaging has satisfied many requirements, resulting in a variety of standard designs which emphasize minimum weight and size, resistance to corrosive fluids, temperature control, etc. The basic transducing element itself has been modified to produce either high voltage or high current output, controlled natural frequencies, increased sensitivity, or minimal thermal errors over extended temperature intervals.

During pressure measurements on equipment for missiles and experimental aircraft, vibration is a serious problem. The specifications for instrumentation are customarily established by laboratory evaluation, but vibration conditions are difficult to simulate. Field experience with conventional instruments in extreme vibratory environments produced either inadequate records or damaged transducers. To solve the problem required a rugged transducer of exceedingly high natural frequency and the elimination of cantilevers or linkages which introduce spurious modes.

This challenge has been met by the Statham biradial unbounded strain gage transducer element, shown schematically in Fig. 1. Competitive laboratory qualification tests have proved the superior accuracy, linearity, and stability of Statham biradial pressure transducers. Field experience with these transducers, where vibrations are known to be on the order of 8000 cps at 700 g, has not damaged a single instrument.

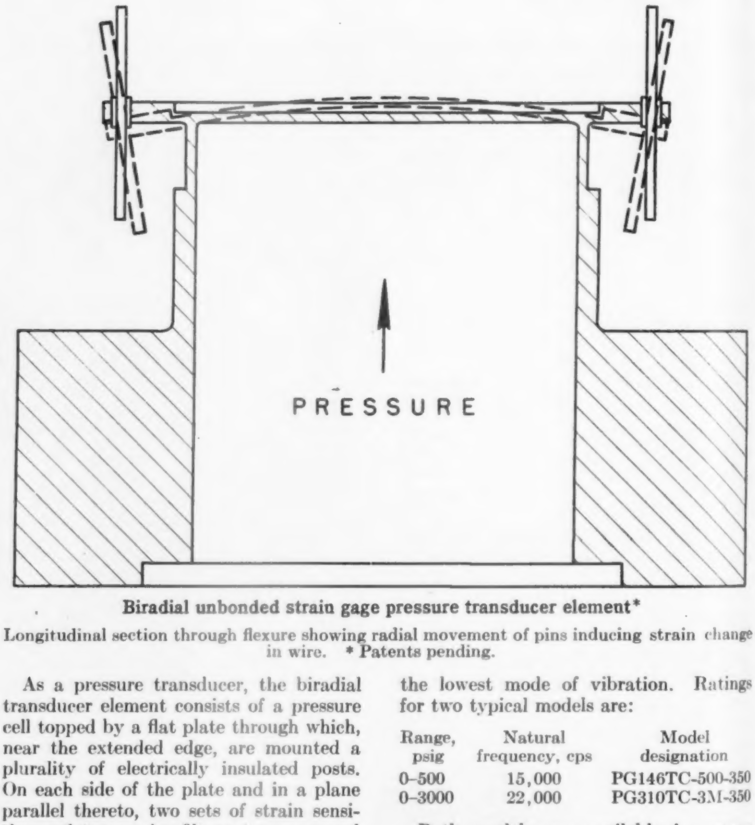

Biradial unbonded strain gage pressure transducer element*

Longitudinal section through flexure showing radial movement of pins inducing strain change in wire. * Patents pending.

As a pressure transducer, the biradial transducer element consists of a pressure cell topped by a flat plate through which, near the extended edge, are mounted a plurality of electrically insulated posts. On each side of the plate and in a plane parallel thereto, two sets of strain sensitive resistance wire filaments are wound around the posts and connected in such manner as to comprise the four arms of a Wheatstone bridge. When pressure is applied, the posts are displaced angularly, altering the electrical balance of the bridge to produce an electrical signal in the output circuit. Pressure transducers containing this new element can be dynamically balanced, since the natural frequencies of the diaphragm plate and its rim are matched.

Pressure transducers incorporating the biradial transducer element are currently in use at a number of test stands for the measurement of gage or absolute pressures in ranges from 0–500 to 0–5000 psi. In catalog descriptions of these instruments, the natural frequency rating is for the lowest mode of vibration. Ratings for two typical models are:

Range, psig	Natural frequency, cps	Model designation
0–500	15,000	PG146TC-500-350
0–3000	22,000	PG310TC-3M-350

Both models are available in ranges from 0–500 to 0–5000 psig. The physical dimensions of the Model PG310TC pressure transducer are $2\frac{3}{4}$ in. long by $1\frac{1}{16}$ in. diam, weight 7 oz, while those of the Model PG146TC pressure transducer are $4\frac{5}{32}$ in. long by $1\frac{5}{8}$ in. diam, weight 26 oz. The letters "TC" in the model designation indicate special electrical temperature compensation to limit the change in sensitivity to 1 per cent per 100 F change, and the shift in zero to the same percentage of full scale over the temperature interval −65 to +250 F.

The advantages of the biradial unbonded strain gage can also be enjoyed in Statham absolute or gage pressure transducers with ranges from 0–15 to 0–10,000 psi.

Self-Aligning Plain Bearings and Rod End Bearings

K. V. HACKMAN

President, Southwest Products Co.
1705 S. Mountain Ave., Duarte, Calif.

SOUTHWEST Products Co. manufactures two kinds of self-aligning bearings. (1) The self-aligning plain bearing, as produced by Southwest, consists of only two pieces, a spherical ball with a hole for a close tolerance bolt or shaft to pass through, and a one-piece outer race which completely surrounds the spherical ball. The latter can be mounted anywhere in a housing where self-alignment is required for a bolt or shaft, generally a nonrotating shaft. (2) The self-aligning rod end bearing is the "Monoball®"[1] plain bearing installed in a housing shaped like an eye bolt as the name implies, and in the end of a rod to engage a bolt fastened to a yoke, crevis, or arm. The "Monoball®" self-aligning is not intended for the antifriction purposes of ball or roller bearings supporting *rotating* or rpm shafts. They have many applications in various sizes in aircraft or similar structure, especially a moving structure subject to deflections, twists, vibrations, and strains.

Southwest Products Co. self-aligning plain bearings have distinctive advantages well recognized by the airplane industry, as follows:

1 There are two prominent types (two-piece construction) self-aligning bearings on the market. The Messerschmitt type is by its design the cutting away of metal on one side of the outer race to introduce or load the ball (which weakens the outer race and the accompanying wider tolerance between ball and race) and results in specific costly defects in airplane applications.

[1] "Monoball®" (Trademark Registered®).

2 Southwest "Monoball®" self-aligning bearing has a greater bearing surface, size for size, than any other bearing; therefore, it bears heavier radial and thrust loads, size for size, than any others on the market today.

3 Southwest "Monoball®" self-aligning bearings, due to know-how, can be made of harder and tougher steels SAE 4130, SAE 52100 (chrome-molybdenum and various stainless steels) than competitive products, an advantage of immense importance in fulfilling the customer's requirements.

4 In many sizes Southwest "Monoball®" self-aligning bearings readily replace the corresponding sizes of many antifriction rod end bearings, where used for the self-aligning feature under vibration. Sales here are on performance, not on price. For these uses it is safe to say Southwest would originally have been specified, if then known, because replacements now are tending steadily to Southwest.

Present-day operating conditions require from the "Monoball®" self-aligning bearings use of a tough metal in the ball and race. Originally the *ball* was made of SAE 52100 *steel* and the *race* of *high strength bronze*. For heavy duty service aircraft the bronze race is no longer used; a tougher metal is now used. Here the use of SAE 4130 steel, "chrome-moly" and stainless, is demanded, which Southwest alone is in a position to supply (in a two-piece bearing) as stated in Point 3 above. Higher temperature operations are also required. Jet propelled aircraft produce temperatures as high as 1000 deg F. These call for heat-treated stainless steel balls and stainless steel races. Only Southwest can supply these bearings in the two-piece construction. The purpose of "Monoball®" self-aligning bearings is to allow the shaft or bolt, which passes through the ball (a close prescribed tolerance between the ball and race) to self-align in any direction without any bending strain on the shaft or bolt, housing or structure, also to allow misalignment in fabrication of component assemblies.

The self-alignment feature is secured by an internal self-aligning design where a single ball operates on an internal spherical surface in the outer race or ring.

1. *Support for Actuating Cylinders*

"Monoball®" self-aligning plain bearings have been applied to the trunnions of hydraulic pneumatic cylinders, also "Monoball®" rod ends being used on the ends of cylinder rods, to take bending deflections without damage to structure. The bearings, both plain and rod end types, take care of the heavy loads during flight and operation on the ground.

2. *Retractable Landing Gear*

There are many joints and levers in the conventional landing gear of aircraft for which the "Monoball®" self-aligning bearing is well adapted. While it has been general practice to use plain bushings or bearings for these joints, it has been found that Southwest "Monoball®" self-aligning bearings enter readily into the design and are being used in increasing quantities, due to high static loads and alignment problems.

3. *Landing Gear Strut. Drag Link Struts*

Due to severe misalignment in these struts, the ordinary plain bushing or bearing does not provide for self-alignment, and is severely strained along with structure deflections. The Southwest "Monoball®" self-aligning bearings are being used in the ends of these struts with no undue strain on the "Monoball®" bearing or structure.

4. *Landing Gear Trunnions—Main*

One typical application: while it is desirable to use antifriction bearings in these locations, the antifriction bearings cannot take care of the high static load condition which must be carried by the bearing throughout the flight period; also, due to the weight of the gear being suspended, heavy shock loads are placed on the bearing in travel through rough air. Due to smaller space requirements and higher allowable loads required by supersonic aircraft, the Southwest "Monoball®" bearings with their higher capacities (loads), small weight, and outside diameter, combine nicely with the present design.

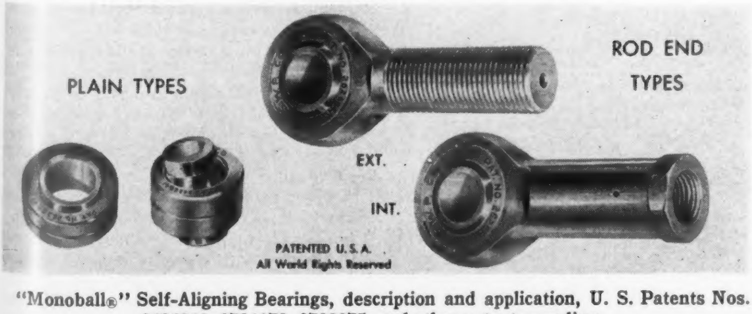

"Monoball®" Self-Aligning Bearings, description and application, U. S. Patents Nos. 2626841, 2724172, 2728975, and other patents pending.

Storage and Handling of Dimazine[1]

WILLIAM B. ROSE

Manager, Development Department, Westvaco Chlor-Alkali Division
Food Machinery and Chemical Corporation, South Charleston 3, W. Va.

THE accelerated interest the rocket industry has shown in Westvaco's unsymmetrical-Dimethylhydrazine as an advanced propellant has been most gratifying.

The industry's need for basic data on the storage and handling of Dimazine has at times taxed our ability to disseminate this information. The following material, prepared by our technical staff, is a primer on loading, storage, and handling of Dimazine. It attempts to answer many of the questions frequently asked. We welcome inquiries on all specific problems, and will be pleased to furnish literature cited in the article.

Background Properties

Dimazine is a clear colorless limpid liquid. Its structural formula is $(CH_3)_2NNH_2$. Chemically, it is an organic base and its reactions are related to those of alkyl amines and substituted hydrazines. It has a rather sharp ammoniacal or fishy odor, characteristic of organic amines. Certain physical data on Dimazine are listed in Table 1.

Dimazine is hygroscopic. In laboratory tests designed to exaggerate this effect, we have observed a pickup of several per cent of water within a twenty-four hour period, although under normal handling and storage conditions, there is no serious problem. It is miscible in all proportions with most common liquids, including water, ethanol, gasoline, and other petroleum products. It is flammable, forming explosive compositions with air over a range of about 2 to 99 volume per cent Dimazine. It flashes (Tag Closed Cup) at about 34 F. Its spontaneous ignition temperature in air at one atmosphere (740 mm Hg) is 480 F. With nitrogen under similar conditions, no ignition occurs up to the top temperature explored of about 750 F.

The critical temperature of Dimazine is about 480 F. It is not shock sensitive, and is thermally stable at temperatures well above its boiling point. Range finding work on high temperature stability carried out by heating small quantities of liquid Dimazine sealed within glass capillaries to successively higher temperatures showed no decomposition during thirty minutes at 550 F, but some carbonization at 700–800 F and a decrease in liquid volume upon cooling to ambient temperature. Inclusion of specimens of nickel and stainless steel in the capillary containers had no obvious effects.

Liquid Dimazine is resistant to air oxidation, but its vapor at ambient temperature reacts slowly with air to form traces of other products. Although we do not consider this of practical significance, nitrogen blanketing of Dimazine eliminates the tendency toward vapor phase oxidation and is probably desirable in view of the broad explosive limits of the vapor.

We have observed no formation of gums or other solids upon sustained storage of Dimazine under proper conditions. It should be noted that carbon dioxide reacts with Dimazine to form a carbonic acid salt and that extended exposure to air or other CO_2-containing gases could lead to eventual precipitation of this material. However, we have deliberately stored partially filled drums of Dimazine without nitrogen flushing for sustained periods, including repeated opening of the drums for sampling, with no evidence of change in quality or other deterioration.

Dimazine may be handled in most common metals. These include mild steel, Types 303, 304, 316, 321, and 347 stainless steel, nickel, and several aluminums, including 2S and 52S. It is recommended on general principles that only clean facilities in good order be employed in the handling and storage of the product. Dimazine is a powerful swelling agent toward many rubber and elastomeric plastic compositions. Teflon,[2] polyethylene, and Garlock 735[3] gaskets are serving well in our facilities and we also have observed that Mylar[2] film and unplasticized Kel-F[4] are highly resistant to Dimazine. Several butyl rubbers, including Stoner BS-55,[5] have also been reported to be satisfactory for Dimazine service.

The use of thermometers, manometers and other instruments, etc., containing mercury, under circumstances that might allow entry of mercury into the Dimazine system, should be avoided.

Table 1 Physical properties of Dimazine

Molecular weight	60.08
Specific gravity	0.795 (60/60 F)
Density	6.64 lb/gal @ 60 F
Coefficient of expansion	0.00074/F (@ 60 F)
Boiling point	146 F
Freezing point	−72 F
Vapor pressure	98 mm @ 60 F
Viscosity	0.586 cps @ 60 F
Flash point (Tag closed cup)	34 F
Specific heat	0.653 Btu/lb/F (@ 60 F)
Heat of formation	−338 Btu/lb
Combustion	14,200 Btu/lb
Fusion (@ FP)	72 Btu/lb
Vaporization (@ BP)	241 Btu/lb
Thermal conductivity (liq.)	0.12 Btu/hr sq/ft-F/ft
Surface tension @ 25 C	0.0019 lb/ft
Refractive index	1.4056 (n^D25 C)
Critical constants	
Temperature	480 F
Pressure	880 psia

Loading and Transfer

In loading Dimazine at our plant, the drums, the Dimazine supply line and storage reservoir, and all other metal equipment involved are electrically grounded for prevention of static accumulation. Local ventilation around the filling nozzle is maintained by means of a small flexible suction line from an exhaust blower set directly over the drum opening, for pulling off all Dimazine vapor escaping from the drum. The operator wears rubber gloves, splash goggles, and a cannister-type respirator, but does not normally wear other protective clothing.

No unusual practices are indicated for the unloading and handling of sealed drums of Dimazine, so long as there has been no leakage or loss of contents. Contact with leakage in either liquid or vapor form should be avoided because of its toxic nature. We recommend that drums of Dimazine be left sealed, just as received, pending need for transfer of their contents.

Before unloading, the drums and other equipment should be electrically grounded. Care should be taken to relieve any pressure that may have developed. Normally there is no pressure beyond that corresponding to an elevation in vapor pressure in the event that the drum is being unloaded at a temperature higher than that at which it was originally filled. Pressure development from this source might normally range up to 3 or 4 psi. The potential hazard is primarily from liquid Dimazine being entrained and blown out by the escaping vapor, if there has been a pressure elevation and if the plug is carelessly and too rapidly removed.

If the drum is to be emptied in a single operation, it is normally unnecessary to maintain a nitrogen atmosphere as the liquid contents flow out, but it should be realized that an explosive mixture will be present in the vapor space of the drum if air is allowed to displace the contents. Neither oxidation nor moisture pickup should be significant under these conditions. The empty drum should be flushed thoroughly with water to remove any remaining small amount of Dimazine.

The most conservative practice for drums being only partially emptied at the

---

[1] (Unsym-Dimethydrazine). Trademark.
[2] du Pont Co., Wilmington, Del.
[3] Garlock Packing Co., Pittsburgh, Pa.
[4] M. W. Kellogg Co., New York, N. Y.
[5] Stoner Rubber Co., Anaheim, Calif.

time of original tapping is the maintenance of an atmosphere of inert gas within the vapor space through flushing with nitrogen as the contents are withdrawn.

It is generally desirable that the receiver into which Dimazine is transferred be flushed with nitrogen if any large vapor volume is to be involved.

Transfer may be through gravity flow, gas pressurization for displacement, or pumping. Dimazine has proved rather difficult to contain because of its attack on most packings and sealants, and local ventilation such as supplementary exhaust intakes should be provided at points of chronic leakage.

Shipping and Storage

Dimazine is presently shipped in single-trip 55-gal ICC Type 17C mild steel drums, 5-gal mild steel containers, and smaller quantities in 1-gal bottles. The drums are fitted with polyethylene gaskets and are nitrogen padded.

We have worked with the Bureau of Explosives and the Interstate Commerce Commission and have secured their approval for rail and motor freight shipments in the containers listed as well as in tank cars when the need arises.

Railway Express shipments are limited to 5 pints (about 3 lb) per case, and up to this amount may also be shipped by air, but only on all-cargo flights. Dimazine shipments require a "red" warning label.

There are no particularly critical limitations on storage environment. Tests have shown Dimazine to be thermally stable at temperatures well above those normally encountered in the atmosphere, and its freezing point is very low. From a practical viewpoint, storage should be maintained comfortably below the boiling point of the material, and our inclination would be to set a limit of perhaps 120 F as a peak temperature for sustained periods. Large quantities should be stored in comparatively isolated areas, and powerful oxidants, such as nitric acid, hydrogen peroxide, etc., should be kept out of the immediate storage area.

We see no sharp limitation on the number of drums that may be stored at a single point, but if major quantities are to be handled, consideration should be given to tank car shipments and storage in bulk. Our studies suggest the use of horizontal cylindrical tanks, maintained under a nitrogen pressure of about 25 psi gage. Mild pressurization, rather than atmospheric breathing, is favored for reduction of losses of Dimazine from periodic fills and withdrawals and from daily changes in ambient temperature.

Fire Safeguards

Dimazine is highly flammable and flashes at a low temperature. Open fires, sources of sparking, etc., should be avoided and all equipment should be electrically grounded. Explosion-proof wiring, lighting, motors, etc., are indicated for areas in which it is to be handled.

We favor the use of large volumes of water fog for combating Dimazine fires. In our tests, liquid Dimazine burned smoothly and cleanly, and was readily extinguished upon dilution with some two or more volumes of water per volume of Dimazine. Much higher Dimazine concentrations in water will support combustion, although flame intensity is progressively weakened as the Dimazine content of the solution is lowered. It will be remembered that Dimazine is miscible with water in all proportions.

Carbon dioxide also is effective in extinguishing Dimazine fires. Chemical foams are not recommended since Dimazine seems to deactivate the foam-forming surfactant and to rapidly destabilize the foam. We observed poor behavior with both standard and alcohol-type foams examined in our laboratory. Carbon tetrachloride is not recommended.

Decontamination and Destruction

Equipment can generally be decontaminated rather simply by thorough flushing with large volumes of water or with dilute acid. It may be conveniently steamed thereafter. It should, of course, be thoroughly dried prior to return to Dimazine service, making sure that no water has been trapped at low points.

Our suggestion for deliberate destruction of comparatively large quantities of Dimazine is by its burning under proper supervision and safeguard. It may also be destroyed chemically by reaction with aqueous sodium hypochlorite (bleach). Small quantities such as minor spills, etc., usually can be disposed of most conveniently through sewering with water.

Toxicity and Protection

Although Dimazine is not sufficiently toxic by any of the three criteria established by the ICC to be rated as a Class B poison, we consider it a hazardous material and recommend care in its handling. The Medical Laboratories of the Army Chemical Center have determined preliminary LC_{50} values of about 125 and 250 ppm for acute inhalation toxicity to mice and to rats, respectively, during a four-hour exposure as detailed in Chemical Corps Medical Laboratories Report 292, by Jacobson, et al. Work we sponsored at the University of Rochester suggests an acute oral LD_{50} of about 360 mg per kg of body weight for rats and, from skin penetration tests on rabbits, that absorption of between 20 and 150 mg per kg causes death. All forms of exposure (inhalation, skin, and oral ingestion) should obviously be avoided. Dimazine is reported to be a respiratory irritant and convulsant. Its strong characteristic odor allows detection of some 10 ppm vapor concentrations in the atmosphere, making it reasonably self-warning. Nevertheless, we recommend the use of adequate ventilation and an ammonia-type cannister mask, as well as goggles and gloves, when handling it under field conditions.

Liquid Dimazine does not cause typical caustic burns or other marked irritation upon extended contact with the skin as do many organic bases. This is perhaps unfortunate, since it is thus not self-warning in this respect. *Care should be taken to promptly remove clothing upon which Dimazine is spilled and to thoroughly water-flush all areas of exposed skin. We would expect to detect early indications of chronic or cumulative injury through routine medical examination of personnel handling the material. (A tentative "Medical Bulletin" prepared for our plant organization and for the local medical profession is available on request.) No adverse effects on personnel have been detected over the extended period in which we have been producing and handling Dimazine.*

Product Quality

Although not directly pertinent to the handling and storage of Dimazine, it is perhaps in order to include a short commentary at this point regarding quality, specifications, and analysis of the product. Our basic recommendations are as listed in Table 2.

Our regular production over the past two years has readily met these specifications.

Redstone Arsenal has prepared a specification for unsymmetrical-Dimethylhydrazine, (Proposed) Military Specification MPD540, of Feb. 24, 1955. Its key requirements are a minimum assay of 98 per cent and no more than 2 per cent water, 2 per cent volatiles, and 0.2 per cent nonvolatiles. Dimazine easily complies with this Redstone specification in all respects. The preliminary data we have seen on an Air Force specification now in preparation suggest that it will be somewhat tighter. We are inclined to favor its more rigorous requirements.

Other Information

We are interested in comparing notes and working with all agencies having a present or potential demand for commercial quantities of Dimazine. We will welcome inquiries regarding pricing, supply, and all other pertinent aspects of the subject.

Table 2 Specifications of Dimazine

Property	Value	Westvaco analytical method
Assay	98 wt % min.	SC 44E-3
Specific gravity @ 25/4 C	0.783 to 0.786	SC 44E-1
Distillation range		SC 44E-4
10% temperature	143 F min.	
90% temperature	148 F max.	
Melting point	−70 F max.	SC 44E-2
Color (light transmittance)	90% min.	SC 44E-8

The information presented in this review, although not guaranteed, is to the best of our knowledge true and accurate. Also, all suggestions with respect to use of this product are made without guarantee since the conditions of use are beyond our control. Nothing herein is to be construed as advertising or authorizing practice of any invention covered by existing patents without license from the owners thereof.

New Test Equipment Meets Missile Aircraft Needs

FRANK S. WYLE

President, Wyle Laboratories, 128 Maryland St., El Segundo, Calif.

Wyle Laboratories Has Nation's First Major Helium Test Facility

BELIEVED to be the only existing facility of its type, Wyle Laboratories now has a group of systems designed to provide and program large flows of helium, liquid nitrogen, air and water—including:

1 High pressure, high volume helium at −300 F to +400 F.

2 9000 gpm liquid flow.

3 Flow rates up to 8 lb per sec nitrogen vapor at 0 to −300 F.

All systems can be used in conjunction with the complete range of natural and induced environments required for qualification tests on components.

View of central instrumentation (below) and control room where expert engineers monitor and record flow, pressure, temperature, and electrical characteristics.

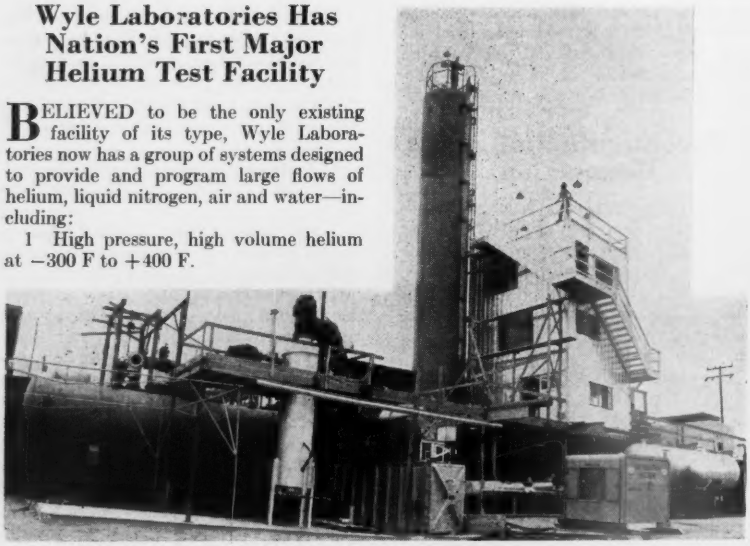

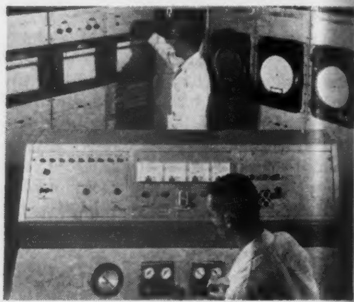

General view (above) of new Wyle high volume flow system. Test facility provides high and low pressure helium flows at 400 F to −300 F, also, extremely high flows of water and low temperature nitrogen vapor. Complete provisions for storage and recovery are included. Control and instrumentation room at right above

Wyle Research Corporation Is Leader in Field of Electrical Qualification

Rated foremost in the field of electrical qualification tests, Wyle Research Corp. has an Instrumentation Branch devoted to evaluation of accelerometers, gyros, synchros, and other precision instruments used in the missile and aircraft industry.

Working with test equipment of maximum accuracy, the Branch has facilities to simulate acceleration, roll, pitch, yaw, temperature, pressure, and other physical environments.

A precision azimuth to provide angular inputs to an accuracy of $1^1/_2$ sec of arc has been added. Newest facility is a Precision Voltage Phase Comparator (see photo) developed for use where output voltage vectors with phase shift must be nulled with high accuracy. Inertial and other transducers with ac output functions are measured with voltage ratio accuracy of two parts per 100,000 and with phase shift determinations of ±0.02 deg.

A complete analysis of test facilities and personnel contributing to Wyle's leadership in the field is available to members of the aircraft and missile industry.

New Hydraulic Concept Provides 100 g Acceleration in Vibrator With 20,000-lb Block-Force

A new principle using electronically actuated hydraulic power amplification is employed in a new vibration testing system rated at 20,000-lb block force.

The "Hydrashaker" is produced and marketed by Wyle Manufacturing Corp. under an exclusive license from Northrop Aircraft, developers of the basic concept.

Wyle engineers applied the principle to provide accelerations to 100 g with 0.4-in. total displacement and 20,000-lb block force with 5–2000 cps useful frequency range.

Only 15 per cent of available force is used to drive Hydrashaker's moving assembly to 100 g, leaving ample force to test missile or aircraft structures and components.

This efficiency contrasts with electrodynamic vibrators which use virtually all available force to operate moving assemblies at 40 g.

Other Hydrashaker advantages: elimination of magnetic field inherent to electrodynamic systems; accurate control of reaction forces encountered in testing resonant structures—control made possible by Hydrashaker's driving power.

Specifications include: 75-hp, motor-driven, 3000-psi hydraulic pump; electronic exciter console with monitoring instrumentation; also available: system to program variable frequencies; provisions for mixed frequency and white noise analysis.

New precision voltage phase comparator

Explosion-Proof Building

Wyle Laboratories has added an explosion-proof building to test high pressure pneumatic components under conditions of acceleration, vibration, and shock. Remote controls operate test equipment.